C.1

NACA

RESEARCH MEMORANDUM

COMPARISON AND EVALUATION OF TWO MODEL TECHNIQUES USED IN PREDICTING BOMB-RELEASE MOTIONS

By Harry W. Carlson, Douglas J. Geier, and John B. Lee

Langley Aeronautical Laboratory
Langley Field, Va.

NATIONAL ADVISORY COMMITTEE
FOR AERONAUTICS

WASHINGTON

December 27, 1957

NATIONAL ADVISORY COMMITTEE FOR AERONAUTICS

RESEARCH MEMORANDUM

COMPARISON AND EVALUATION OF TWO MODEL TECHNIQUES USED IN PREDICTING BOMB-RELEASE MOTIONS

By Harry W. Carlson, Douglas J. Geier, and John B. Lee

SUMMARY

For the purpose of calculating bomb trajectories, forces and moments have been measured on bombs of three fineness ratios in the presence of a swept-wing fighter-bomber configuration at a Mach number of 1.61. Trajectories thus obtained have been compared with those from dynamic model tests and an analysis has been made to determine the source of errors and to suggest improvements in both techniques.

INTRODUCTION

In recent years, considerable research effort has been devoted to the problem of predicting the behavior of bombs released from full-scale aircraft. It has been shown that, for some conditions, a bomb can experience interference forces due to the airplane flow field of sufficient magnitude to cause the bomb to deviate from a normal trajectory and collide with the releasing airplane. Forced ejection has been used to alleviate these difficulties, but it is still important to have an accurate prediction of release paths in order that an ejection system of minimum size can be used and disturbances causing bombing inaccuracies can be minimized.

For release from an open bay, where use of pure theoretical methods would be extremely difficult, if not impossible, two basically different experimental approaches have been used. In one method similarity laws (ref. 1) are applied to wind-tunnel dynamic-model drops. The conditions believed to be the most important in determining the bomb motion are made to meet the similarity relationships exactly, whereas other factors having some influence must necessarily be neglected. The scaled dynamic drops are usually recorded photographically for detailed study. In the second technique, the trajectory of a bomb following release is calculated by a step-by-step application of the equations of motion by using

mapped data of bomb forces in the presence of the airplane. These data are obtained by static measurements in wind-tunnel tests.

Although any direct comparison of full-scale drops at supersonic speeds with either type of model prediction may be lacking, it is still possible to make an evaluation of the methods. Measured force data from models may be used to calculate trajectories for actual drops of dynamically scaled model bombs. It is reasonable to believe that the degree of correlation obtained with dynamic model drops is also a measure of the ability to calculate full-scale drops from force data. If the correlation can be established, the force data can be used in calculating the corresponding full-scale drops in order to evaluate the simple similarity relationships used in the dynamic drop testing (provided the Reynolds number effects can be assumed to be negligible). Evaluations of this nature were made in reference 2. The agreement between the two experimental methods, however, left much to be desired, and the main conclusion was that for both methods the configurations (including the bomb bay) must be duplicated in all possible details.

The present report presents the results of a coordinated investigation which included (1) static force tests in the Langley 4- by 4-foot supersonic pressure tunnel with subsequent drop calculations and (2) model drop tests of identical bombs from the same airplane model in the preflight jet of the Langley Pilotless Aircraft Research Station at Wallops Island, Va. A fighter-bomber airplane model and bombs of three shapes were used in the tests at a Mach number of 1.61. The results are compared and analyzed in the manner suggested in the preceding paragraph.

SYMBOLS

C_{D_b} drag coefficient of bomb, $\frac{\text{Drag}}{qS}$

C_{L_b} lift coefficient of bomb, $\frac{\text{Lift}}{qS}$

C_{m_b} pitching-moment coefficient of bomb, about bomb nose, $\frac{\text{Pitching moment}}{qSl}$

p pressure, lb/sq in. abs

q dynamic pressure, lb/sq ft

S	frontal area of bomb, sq ft
l	length of bomb, in.
x	longitudinal position of bomb midpoint, measured rearward from bomb-bay midpoint, in.
z	vertical position of bomb midpoint, measured downward from fuselage center line, in.
t	time, sec
$\dot{z}$	vertical velocity of bomb center of gravity, ft/sec
α_b	angle of attack of isolated bomb
α_{wf}	angle of attack of wing-fuselage configuration
θ	attitude angle of bomb center line referenced to horizontal, deg
$\dot{\theta}$	angular velocity of bomb, deg/sec
f	fineness ratio of bomb
Δx	incremental distance (horizontal)
Δz	incremental distance (vertical)

Subscript:

0	at instant of release

MODELS AND TESTS

Geometrically identical models were used in the static force tests and dynamic drop tests. Dimensional drawings of the fighter-bomber wing-fuselage configuration are presented in figure 1(a), which also shows the general arrangement for the force tests. Figure 1(b) shows the equipment used in the dynamic model tests. Drawings and photographs of the bomb models and ejectors used are shown in figure 2.

In the force tests the wing fuselage was mounted on a model sting attached to the regular support sting of the Langley 4- by 4-foot supersonic pressure tunnel. The bombs were mounted on a six-component strain-gage balance, which was sting mounted off the tunnel side wall by the

mechanism shown in figure 1(a). Bomb angles of attack of -15° to 15° were provided by this system. A detailed description of the testing equipment and procedures may be found in reference 3.

In the dynamic model drop tests, performed in the preflight jet of the Langley Pilotless Aircraft Research Division Station at Wallops Island, Va., bomb release was accomplished through the use of an ejecting mechanism utilizing hydraulic pressure. Photographic records of the drops were made by use of multiple exposures by a bank of Strobolights. Details of the ejection mechanism, the stroboscopic technique, and a discussion of the similarity relationships used are given in reference 4.

Two streamlined bomb shapes having fineness ratios of 4 and 7, and a bluff bomb (or "spool") shape were tested in these investigations. Both streamlined bombs had fins. Throughout the paper the bombs and ejectors will be identified as in the following table:

Bomb		Ejector		Ejector used with -
Designation	Description	Designation	Shape	
1	Spool shape	A	Basic	Bombs 2 and 3
2	Fineness ratio 4	B	Streamlined	Bomb 2
3	Fineness ratio 7	C	Spool	Bomb 1

The nominal ranges of the angles of attack and positions used in the force tests and a convenient index to the wing-fuselage-ejector-bomb configuration tested are presented in table I.

PRECISION OF DATA

The repeatability or relative accuracies during the force tests are estimated from an inspection of repeat test points, zero shifts, and static deflection calibrations to be as follows:

x, in.	±0.05
z, in.	±0.10
C_{D_b}	±0.01
C_{L_b}	±0.03
C_{m_b}	±0.03
α_b, deg	±0.10

PRESENTATION OF RESULTS

Isolated Bomb Data

Drag, lift, and pitching-moment data for the three bombs are presented in figure 3. The unusual shapes of the isolated data curves for bomb 1 are explained in reference 5. It should be noted that the bomb pitching moment in all cases is referenced about the bomb nose.

Basic Data Plots

Lift, drag, and pitching-moment coefficients for bombs 1, 2, and 3 in the presence of the wing-fuselage combination with no ejector in the bomb bay are presented in figures 4 to 6. The same coefficients for these bombs in presence of the wing-fuselage-ejector configuration are presented in figures 7 to 10.

These basic data are presented in the form of plots of coefficients against z (the vertical distance between the fuselage center line and the bomb midpoint). Data for seven bomb angles of attack are shown. From these data, contour maps of bomb forces and calculations of bomb motions and paths can be made. An evaluation of the effects on bomb forces and moments of an ejector protruding beneath the fuselage can also be made from basic data plots and contour maps. A summary of the test conditions (bomb position and attitude) is given in table I. Figure 11 presents photographs of the dynamic model drops used and discussed in this report. Table II gives the pertinent information for these drops.

Contour maps.- Figures 12 to 18 present contour maps of each coefficient for bombs 1, 2, and 3 in the presence of the wing-fuselage configurations with and without an ejector. The bomb midpoint is the reference point (the point at which the coefficient is plotted) for all contour plots. The bomb, bomb bay, and ejector are shown on each plot to scale. From an inspection of figures 12 and 15 it can be seen that, in general, there is an increase in gradients in the vicinity of the ejector and somewhat of a rearward shift in maximum values of the coefficients due to the presence of an ejector. From figures 16 and 17 it can be seen that there are small changes in magnitude and contour due to changing ejector shape. Where it was necessary to extrapolate data in order to complete the maps, dashed lines are used.

Bomb trajectories.- Figures 19 to 24 present time histories of horizontal and vertical position and attitude angle. The drawings represent the bomb at successive positions along its calculated trajectory at a time interval of 0.002 second. These figures show comparisons between

bomb trajectories obtained from dynamic model tests and bomb drop paths calculated from force tests as in reference 3.

DISCUSSION OF RESULTS

A comparison was made in reference 2 between a forced-ejection model drop and a calculated drop for the same conditions using static force data. The bomb bay used in the force tests did not include a dummy ejector. That comparison is repeated in figure 19(a). Although the trajectory (Δx, Δz) was predicted fairly accurately, the correlation for bomb pitching motion left much to be desired. In addition, it should be realized that a reasonably accurate bomb center-of-gravity trajectory can be predicted without a knowledge of the airplane-induced disturbances, inasmuch as it is largely determined by the bomb weight and isolated bomb drag. It was suggested in reference 1 that the discrepancies were due to the absence of a simulated ejection mechanism in the bomb bay used in the static force tests.

When the force data obtained with the ejector were used, an improved prediction resulted; this prediction is compared in figure 19(b) with drop data reproduced from the preceding figure. In this computed case an ejection velocity of 26 feet per second was used, since it more nearly agrees with the actual release conditions than does the nominal value of 30 feet per second. This change in velocity is responsible for the improved agreement in the vertical displacements.

In order to demonstrate more forcibly the importance of the initial release conditions, figure 20 has been prepared. In part (a) of figure 20, the nominal or preset release conditions (attitude angle, ejection velocity, etc.) were used in the force data calculations and a complete failure to predict the actual pitching motion resulted. However, deflections and play in the release mechanism caused the bomb angle at zero time (as measured by photographs) to be about $1\frac{1}{2}^{\circ}$ instead of the preset 4°. In addition, if the dashed line can be regarded as a reasonable fairing of the experimental data, the bomb has a pitching velocity of considerable magnitude ($-3{,}600^{\circ}$ per second) at that instant. Using that dashed line as the basis for selecting the initial conditions produced the result presented in figure 20(b). Obviously, the angular velocity had been grossly overestimated. Fortunately, in this case, a check run (case 2) was made in which the timing of the Strobolights was out of phase with the timing of case 3. The data from both runs, which have been plotted in part (c) of figure 20, indicate that the repeatability of the dynamic drop tests is very good. However, it is now apparent that a faired curve of a somewhat different character is required to represent the drop data. Use of this dashed curve in obtaining control conditions ($\theta_0 = 1.0^{\circ}$;

$\dot{\theta}_0$ = 1,400° per second) results in a considerable improvement in the ability of the calculative technique to predict the pitching motion.

These results illustrate clearly the need for an accurate evaluation of the actual conditions at the instant of release in order to obtain correlation of the calculations with the photographically recorded ejection tests. It is also evident that this knowledge is essential in determining exactly what full-scale conditions are being simulated. In view of these difficulties, all subsequent calculations will be made from force data measured with a simulated ejector in place and will use initial conditions determined from faired experimental drop curves.

A spool-bomb drop made at low ejection velocity (6.3 ft/sec) is shown in figure 21. The calculative prediction is very good up to 0.016 second after release but is poor after that time.

Figure 22 presents a similar comparison for the fineness-ratio-7 finned bomb ejected with a velocity of 34 feet per second and shows a degree of correlation. As before, the good agreement of the curve with the first four points of the bomb angle plot indicates that the lack of agreement beyond that point may be due to inadequacies in the calculative technique used. Very likely a closer grid of test positions is necessary to obtain a more detailed picture of the rapidly changing interference forces. There are other possible causes of the discrepancies between the two test methods, such as the Reynolds number change and the deletion of higher order terms in the equations of motion given in reference 3.

In one case, shown here in figure 23, a more streamlined ejector was used with bomb 2. The calculated drop compares well with the dynamic model drops for the first 0.012 second. Thereafter the bomb reached an attitude angle of 12° whereas the calculation showed a maximum angle of about 4°. This large difference in pitch amplitude has not been explained. The failure of the calculative technique to predict this effect again is indicative of the aforementioned difficulties. The machine calculations presented in this report are particularly sensitive in this respect, since linear interpolation between test points was used.

The data for the forced ejection model drop of figure 19 have been reproduced in figure 24, where they are compared with calculations using the full-scale conditions which the model drops simulate. A model scale of 1/20 was assumed. Bombs of three different weights have been treated in the three parts of the figure. Corresponding altitudes were chosen so that each case meets the requirements for this type of simulation $\left(\frac{\text{Store density}}{\text{Static pressure}} = \text{Constant}\right)$. The displacements and times now refer to the full-scale cases. The calculations show almost identical curves for each of the drops and agree well with the model drop data. The agreement

for this type of simulation depends on a large ejection velocity in order that the effects of gravity will be minimized. In reference 2 calculated drops were used to illustrate the effect of release velocity on the degree of simulation obtainable. Reynolds number effects have not been considered in these comparisons.

CONCLUDING REMARKS

For the purpose of calculating bomb trajectories, forces and moments have been measured on bombs of three fineness ratios in the presence of a swept-wing fighter-bomber configuration. Trajectories thus obtained have been compared with those obtained in dynamic model tests and an analysis of the results was made.

In both of the model testing techniques it is important that all details of the actual bay be duplicated insofar as possible. In addition, the release mechanism used in the drop tests must be designed to minimize play and deflection during release, and the release conditions must be accurately set or known. The results indicate that the static-force mapping technique requires a more closely spaced grid than was used in these tests.

When the above-mentioned sources of error were eliminated as factors in the correlation (to the extent possible with the existing data), acceptable correlation between the static-force and dynamic-drop techniques was obtained at least during the critical period immediately following release. The results indicate that both techniques are useful for model investigation of release problems and for guidance of full-scale investigations. The ultimate correlation of both methods with full-scale drop tests (which depends on the Reynolds number effects being small or negligible) should be checked as soon as flight data become available.

Langley Aeronautical Laboratory,
National Advisory Committee for Aeronautics,
Langley Field, Va., October 1, 1957.

REFERENCES

1. Sandahl, Carl A., and Faget, Maxime A.: Similitude Relations for Free-Model Wind-Tunnel Studies of Store-Dropping Problems. NACA TN 3907, 1957.

2. Faget, Maxime A., and Carlson, Harry W.: Experimental Techniques for Predicting Store Motions During Release or Ejection. NACA RM L55L20b, 1956.

3. Smith, Norman F., and Carlson, Harry W.: Measurement of Static Forces on Internally Carried Bombs of Three Fineness Ratios in Flow Field of a Swept-Wing Fighter-Bomber Configuration at a Mach Number of 1.61 With Illustrative Drop-Path Calculations. NACA RM L56I18, 1957.

4. Lee, John B., and Carter, Howard S.: An Investigation of Ejection Releases of Submerged and Semisubmerged Dynamically Scaled Stores From a Simulated Bomb Bay of a Fighter-Bomber Airplane at Supersonic Speeds. NACA RM L56I10, 1956.

5. Geier, Douglas J., and Robins, A. Warner: Wind-Tunnel Measurement of Static Forces on Internally Carried Bombs of Two Different Bluff Shapes in the Flow Field of a Swept-Wing Fighter-Bomber Configuration at a Mach Number of 1.6. NACA RM L57A23, 1957.

TABLE I.- INDEX TO WING-FUSELAGE-BOMB CONFIGURATIONS

AND POSITIONS USED IN THE FORCE TEST

Bomb	Ejector	α_b, deg	x, in.	z-range, in.	Basic data figure
2	A	0, ±5, ±10, ±15	-1.5, -0.5, 1, 3, 6	0 to 10	8
2	B	0, ±5, ±10, ±15	-1.5, -0.5, 1, 3, 6	0 to 10	9
3	A	0, ±5, ±10, ±15	-1.65, -0.15, 1.85, 3.85	0 to 10	10
1	C	0, ±5, ±10, ±15	-1.5, -0.37, 0.50, 2, 4, 6, 8	0 to 10	7
2	None	0, ±5, ±10, ±15	-2.55, -1.05, 0.7, 2.95, 5.95	0 to 6	5
3	None	0, ±5, ±10, ±15	-1.65, -0.05, 1.85, 3.85	0 to 10	6
1	None	0, ±5, ±10, ±15	-1.05, 2.95, 6.95, 8.95, 10.95	0 to 6	4

TABLE II.- INITIAL CONDITIONS OF DYNAMIC DROPS

Case	Bomb	Weight, lb	Moment of inertia, lb-in.^{2}	Center-of-gravity location, percent length	q_0, lb/sq ft	θ_0, deg		$\dot{z}_0$, ft/sec	
						Nominal	Actual	Nominal	Actual
1	1	1.80	1.870	35.0	3869.2	4.0	2.1	11.25	6.3
2	1	.410	.418	35.0	3869.2	4.0	-.4	30.0	31.5
3	1	.409	.420	35.0	3869.2	4.0	1.5°	30.0	33.4
4	2	.4173	.592	50.0	3622.0	4.0	4.0	30.0	26.0
5	2	.4240	.595	50.0	3714.7	4.0	2.3	30.0	30.8
6	3	.419	1.175	50.0	3942.24	-2.0	-2.0	30.0	34.0

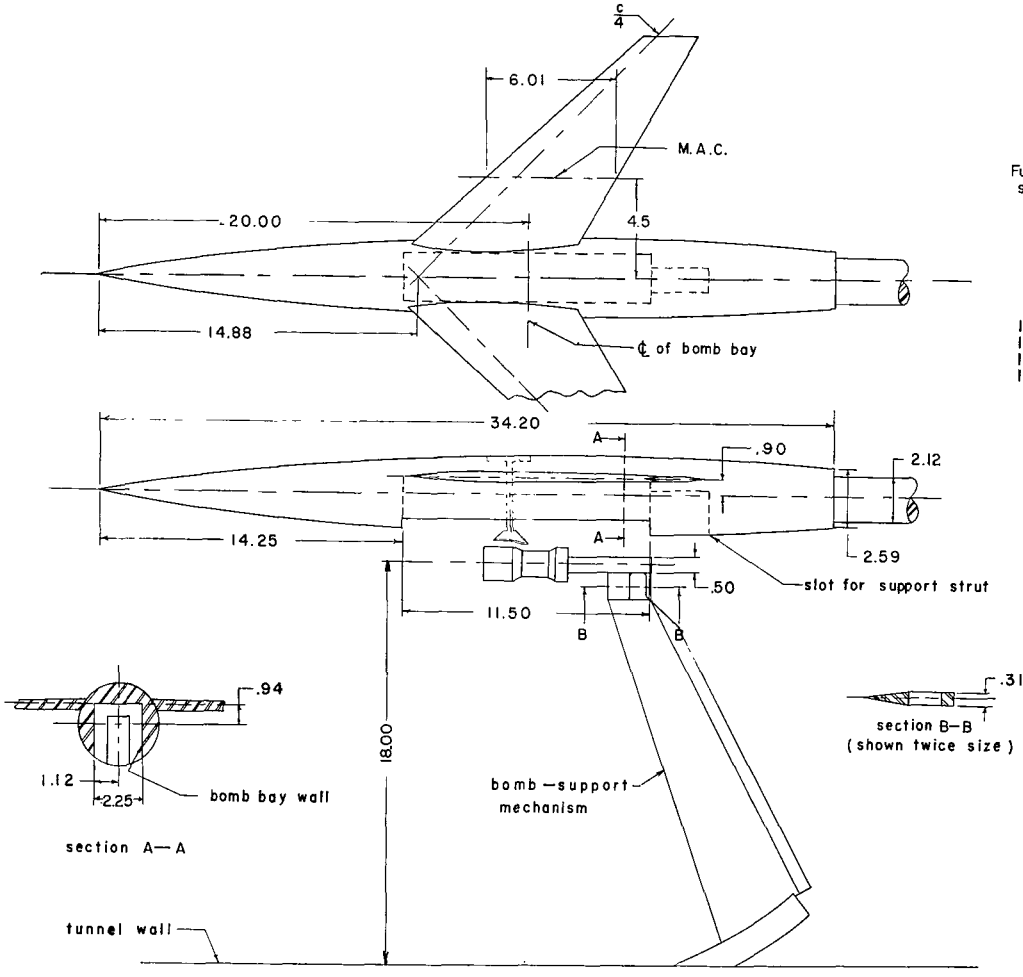

Design Fuselage Coordinates

Fuselage station	R	Fuselage station	R
0	0	17.200	1.744
1.562	0.411	18.762	1.777
3.128	0.672	20.324	1.795
4.690	0.884	21.886	1.800
6.252	1.063	24.233	1.779
7.818	1.217	25.795	1.748
9.381	1.349	27.361	1.702
10.943	1.461	28.923	1.641
13.290	1.597	30.485	1.564
14.852	1.667	32.052	1.471
15.633	1.697	34.200	1.298

Wing Data

Wing span	21.918
Sweep $\frac{c}{4}$	45°
Aspect ratio	4
Taper ratio	0.3
℄ chord	8.430
Tip chord	2.529
M. A. C.	6.010
Section	NACA 65A006

(a) Model setup for static force tests.

Figure 1.- Layout of models, wing dimensions, and fuselage coordinates. All dimensions are in inches.

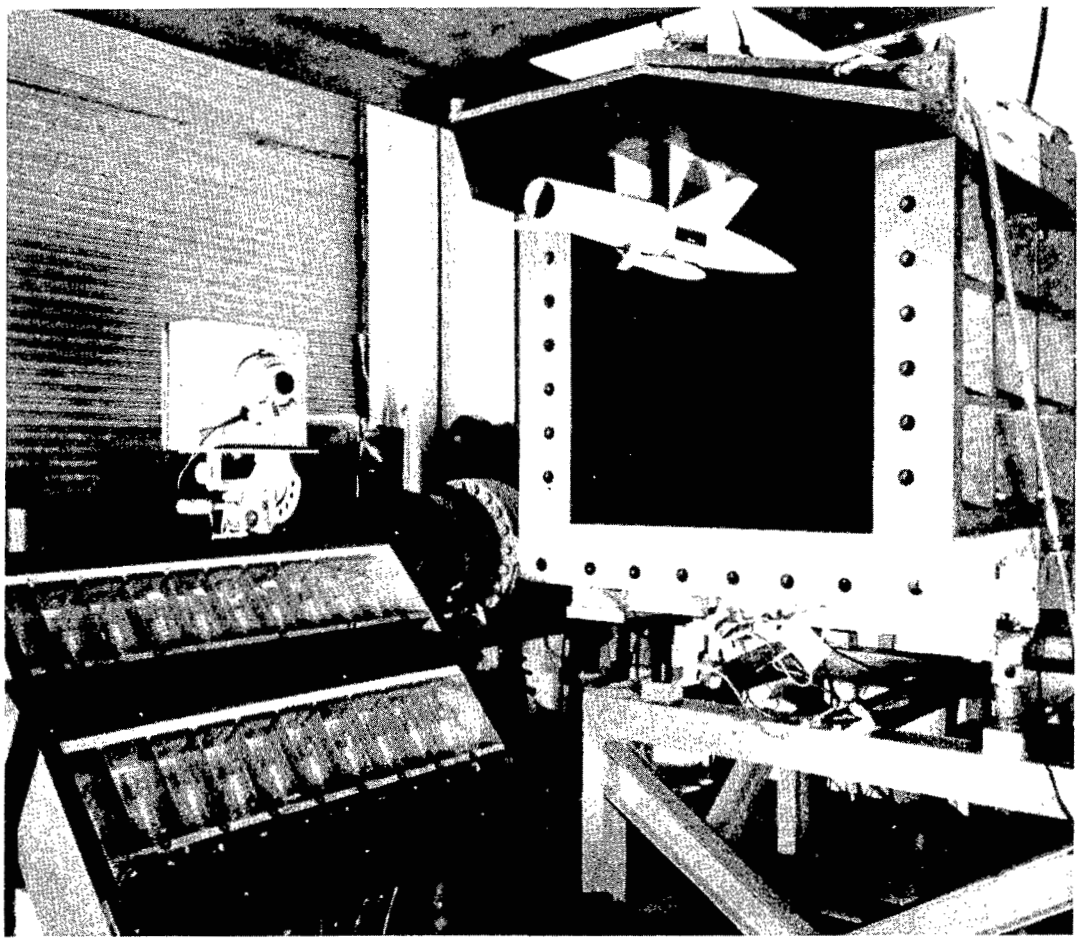

L-57-1647

(b) Equipment setup for dynamic model tests. Strobolights at bottom left. Wing-fuselage model is same as that in figure 1(a).

Figure 1.- Concluded.

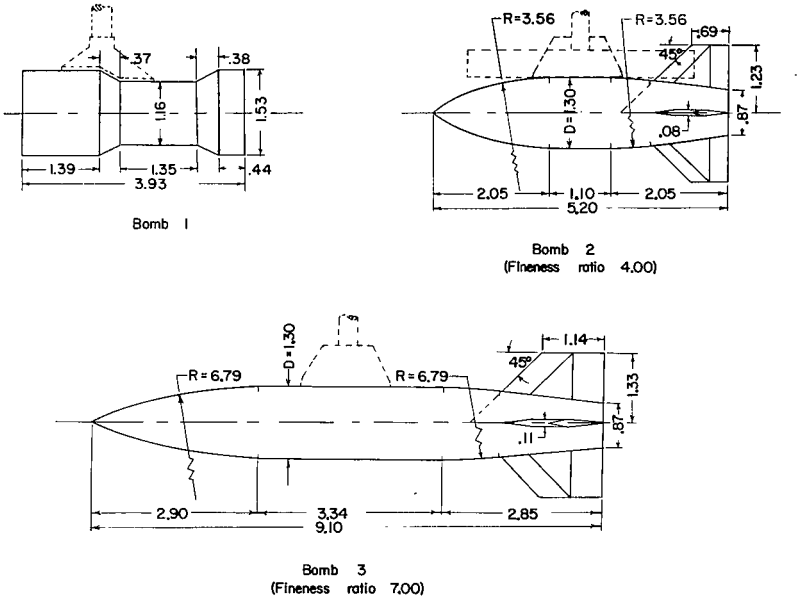

(a) Bombs. (Ejector position shown.)

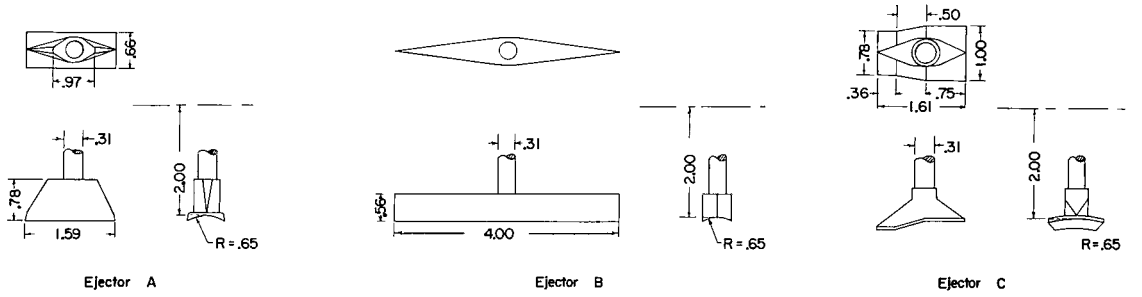

(b) Bomb ejectors.

Figure 2.- Details of models. All dimensions are in inches.

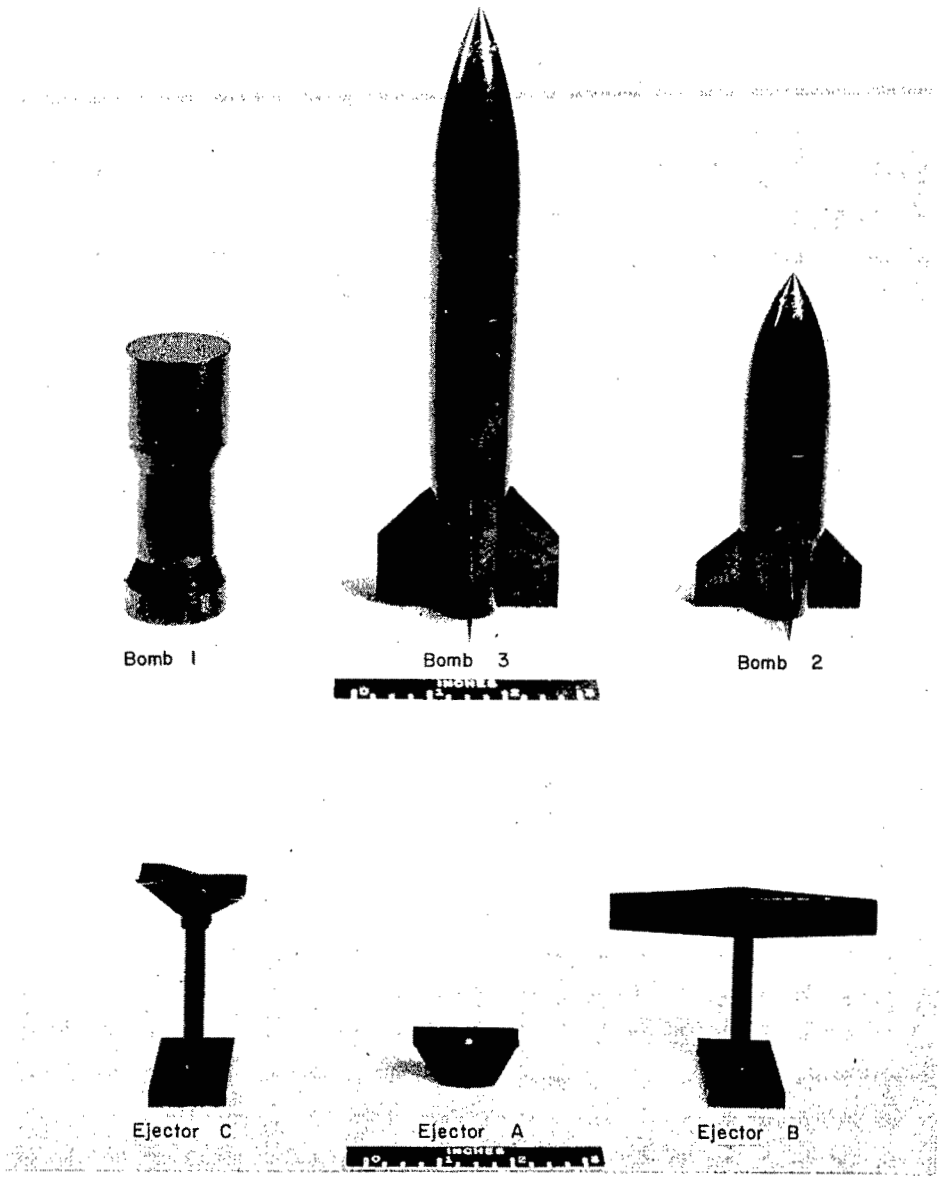

(c) Photograph of models. L-57-1646

Figure 2.- Concluded.

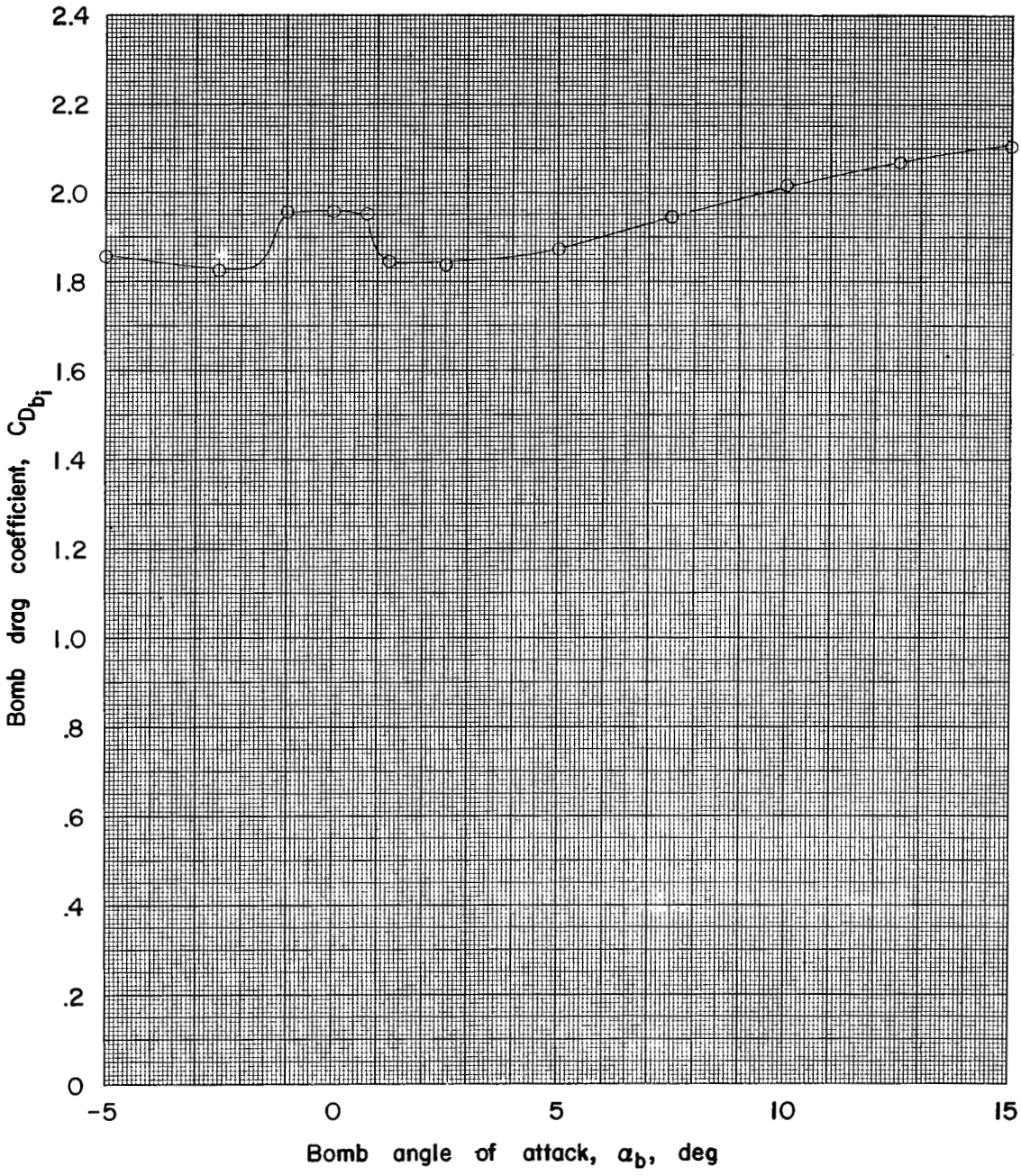

(a) Bomb 1.

Figure 3.- Aerodynamic characteristics of the isolated bombs.

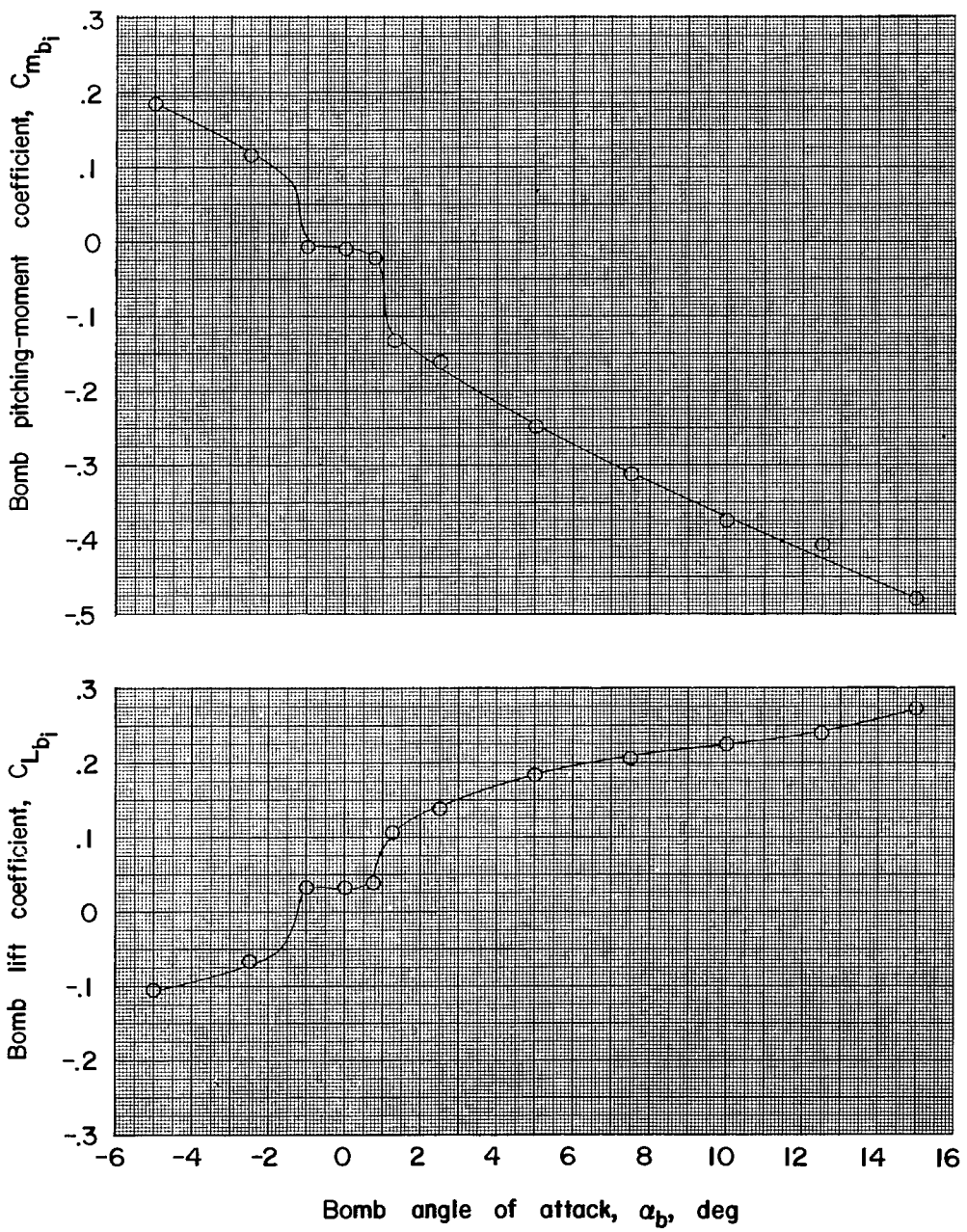

(a) Concluded.

Figure 3.- Continued.

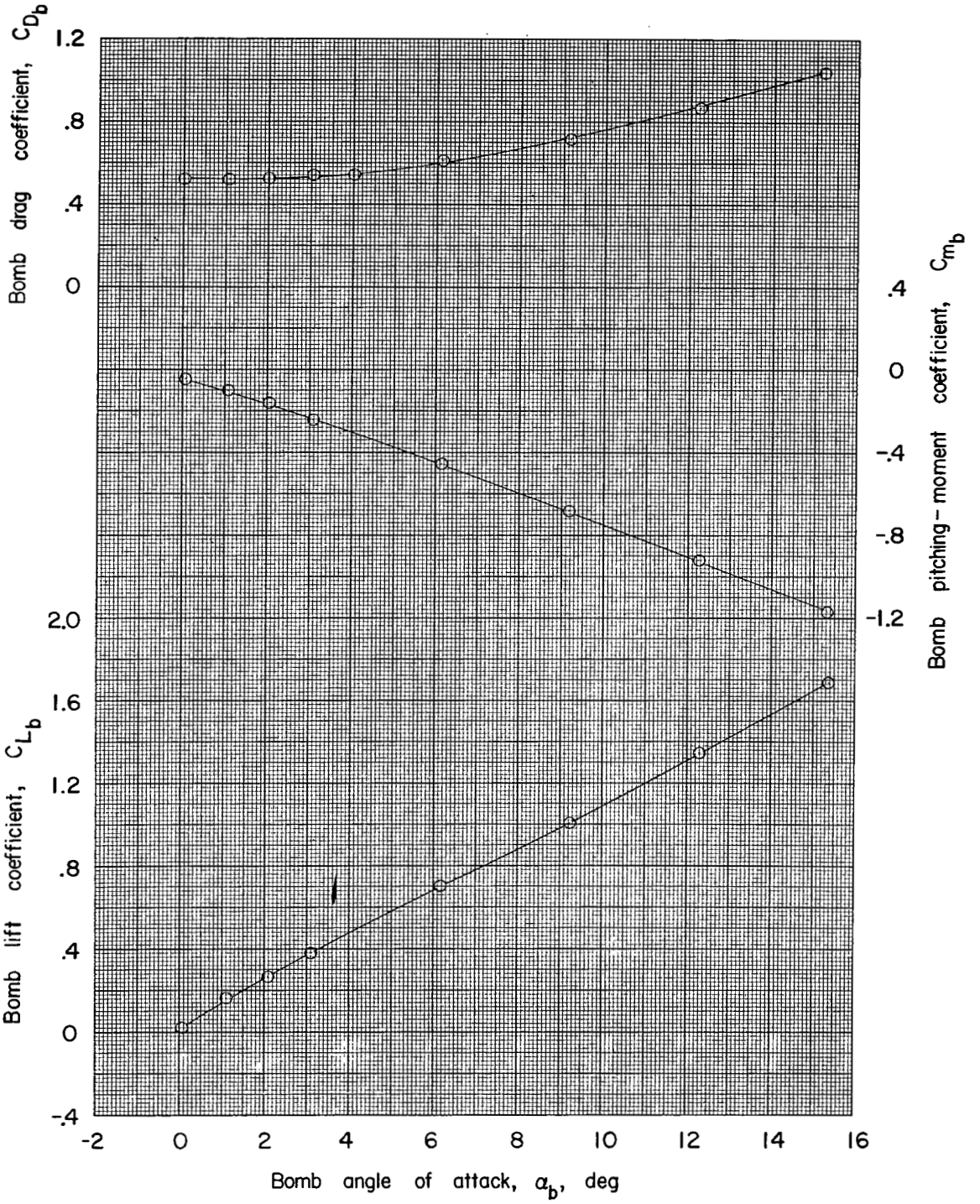

(b) Bomb 2.

Figure 3.- Continued.

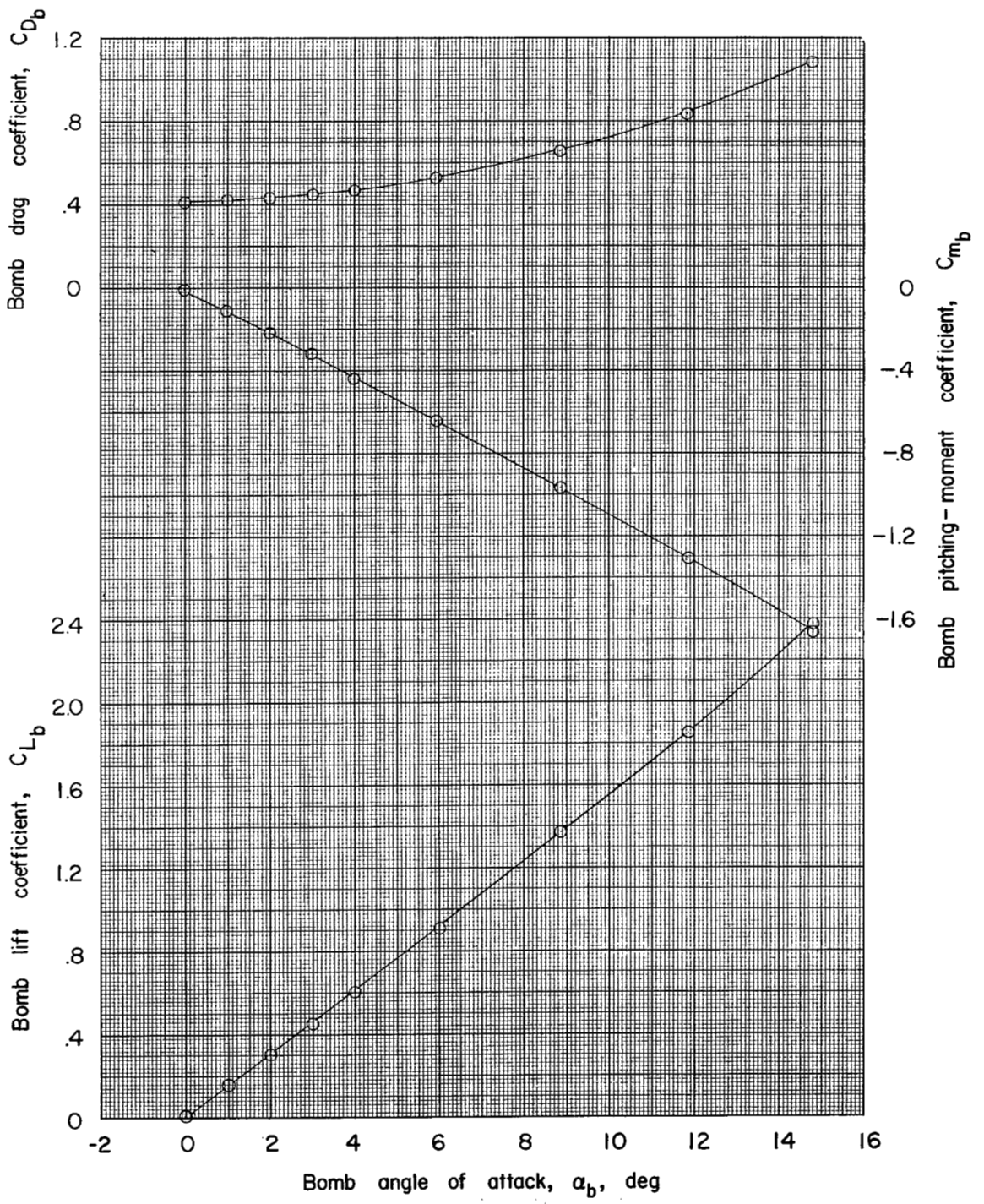

(c) Bomb 3.

Figure 3.- Concluded.

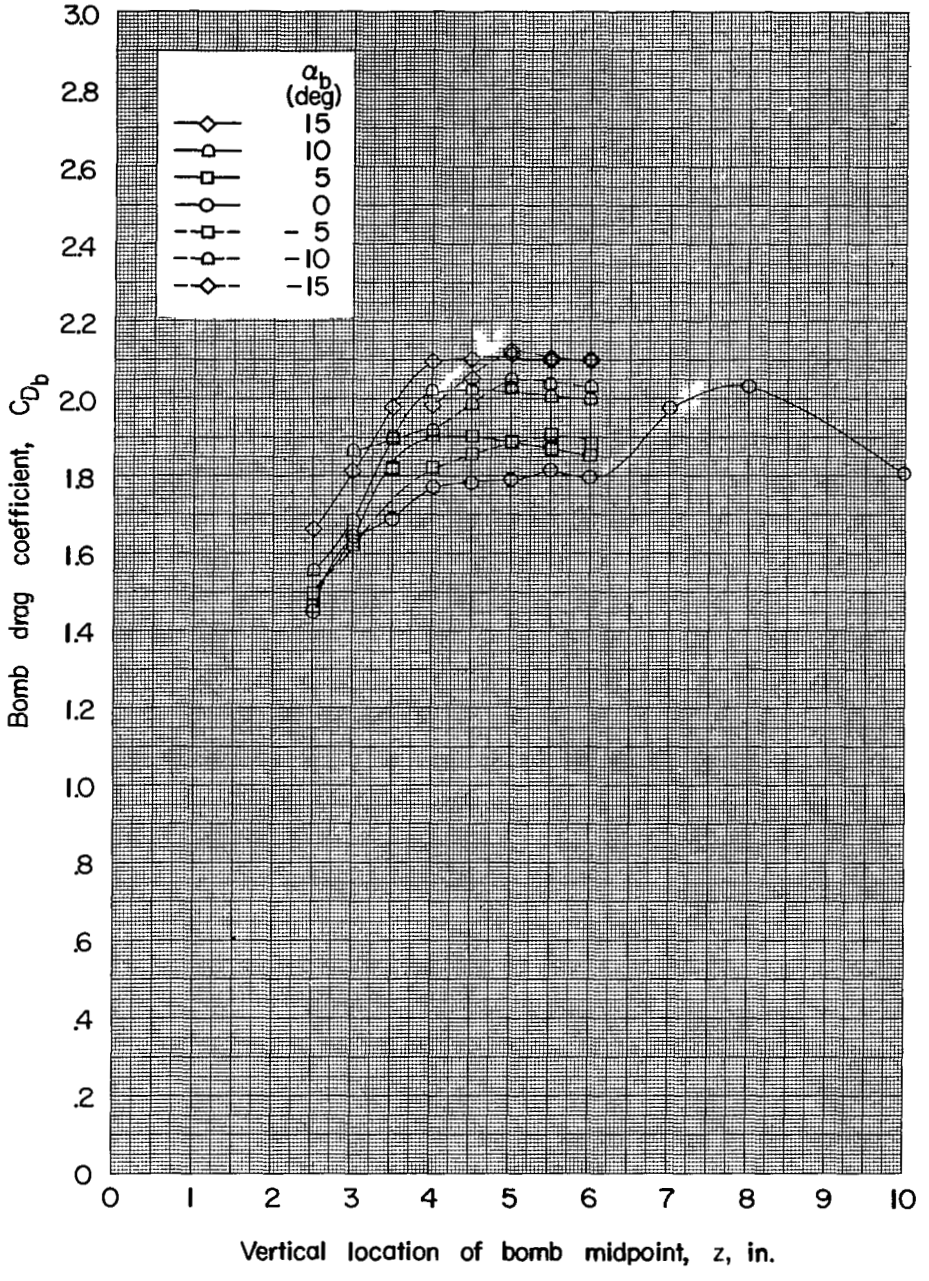

(a) x = -1.05 inches.

Figure 4.- Force and moment data for bomb 1 in presence of the wing-fuselage combination without ejector. $\alpha_{wf} = 4^{\circ}$.

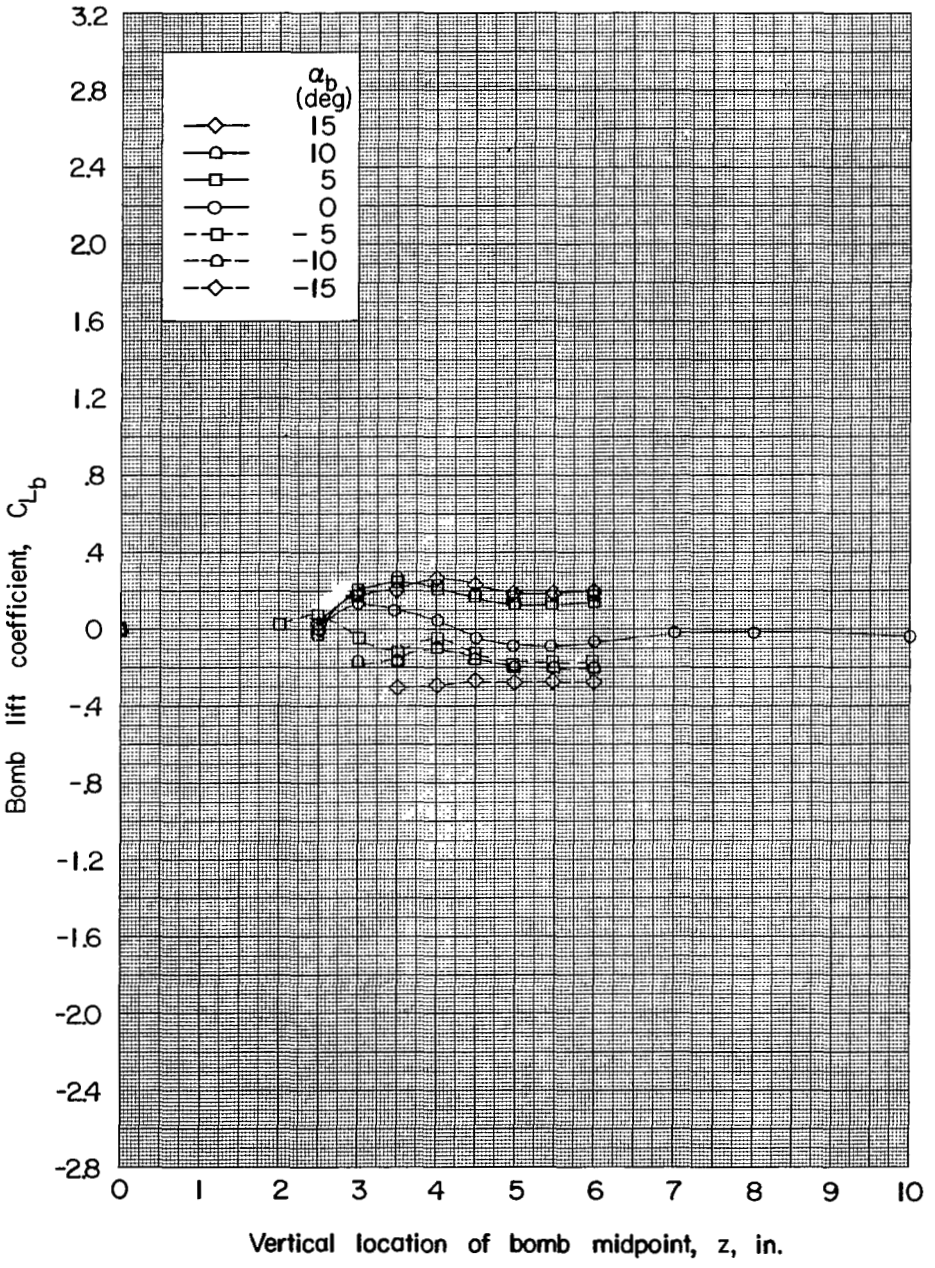

(a) Continued.

Figure 4.- Continued.

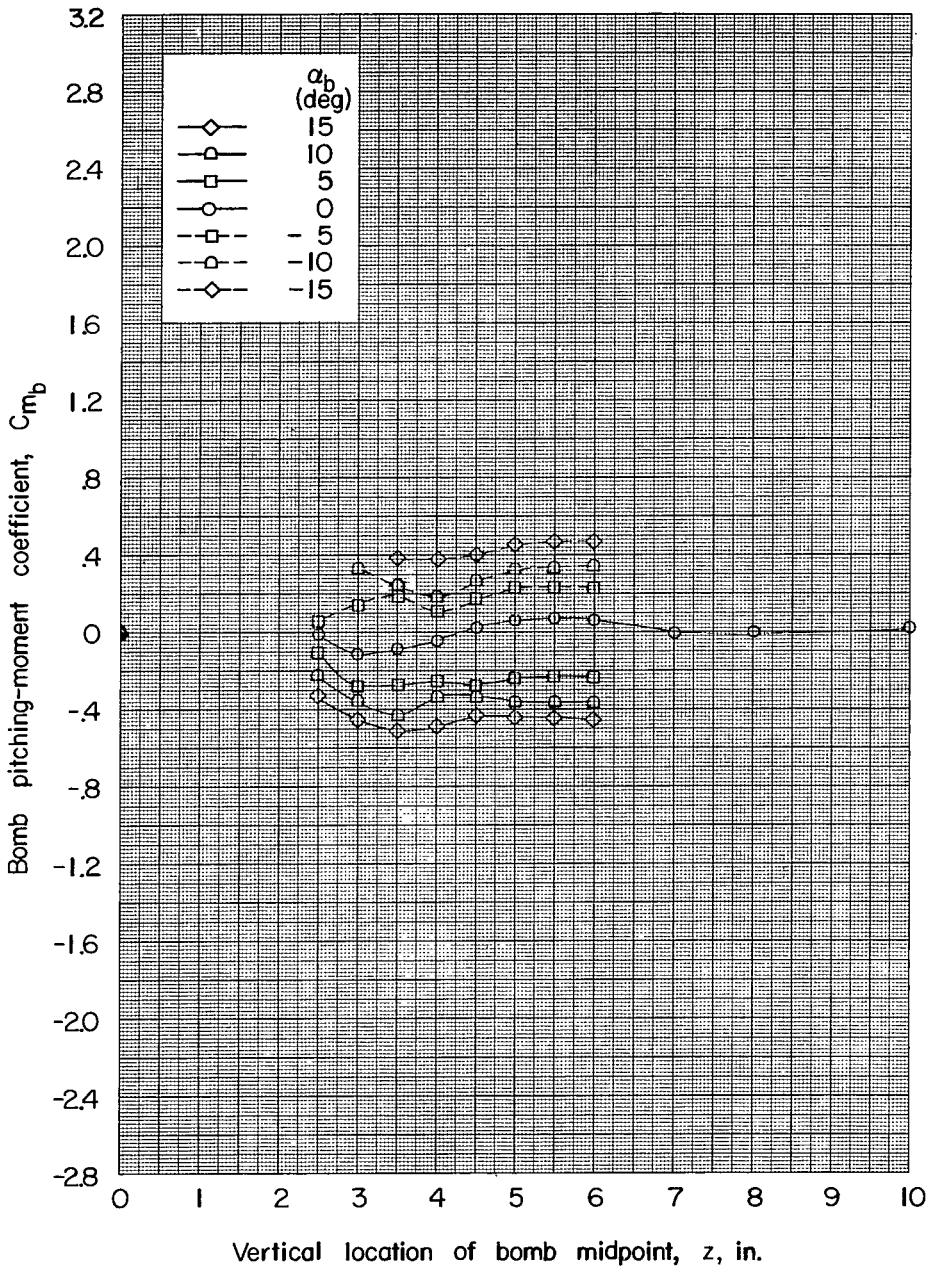

(a) Concluded.

Figure 4.- Continued.

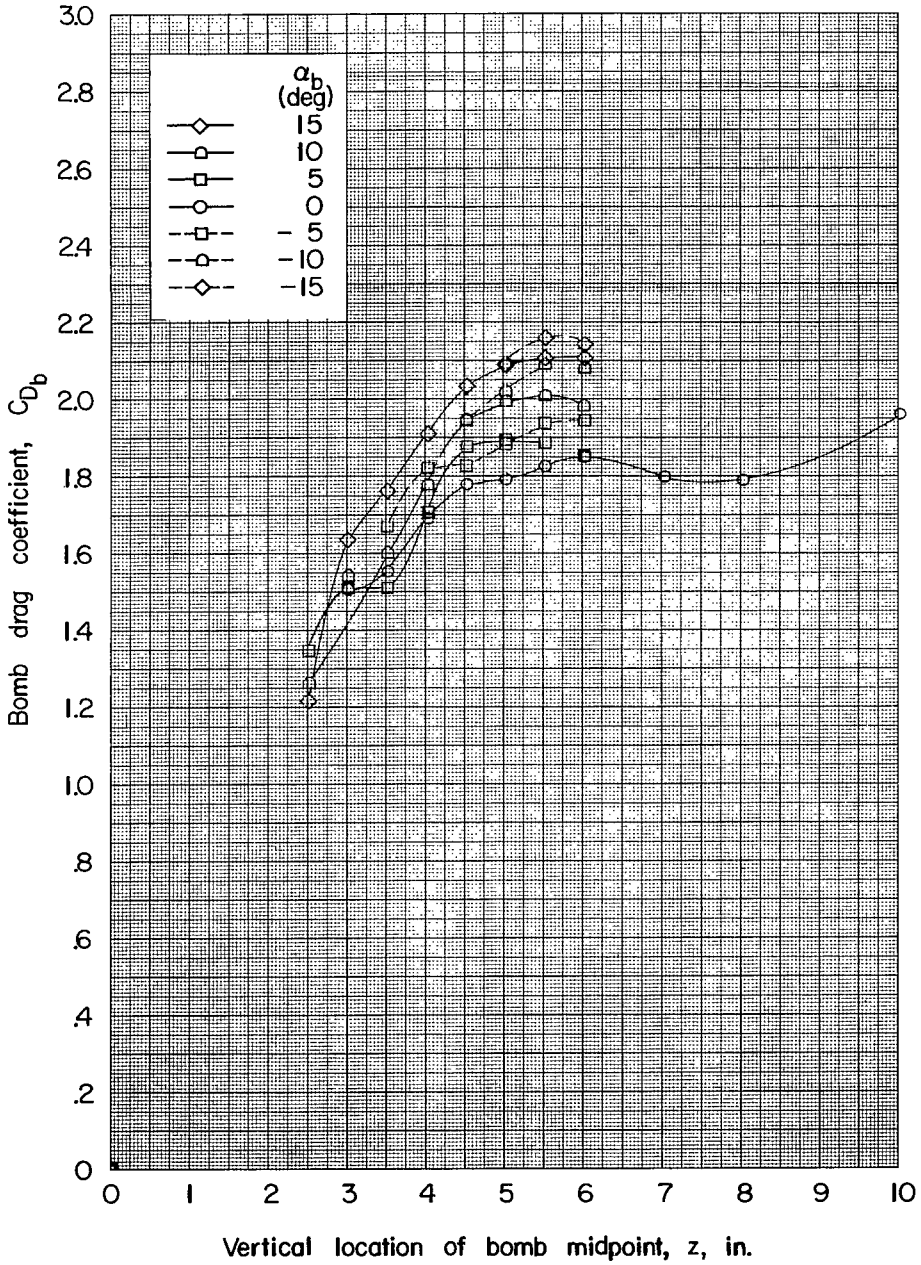

(b) x = 2.95 inches.

Figure 4.- Continued.

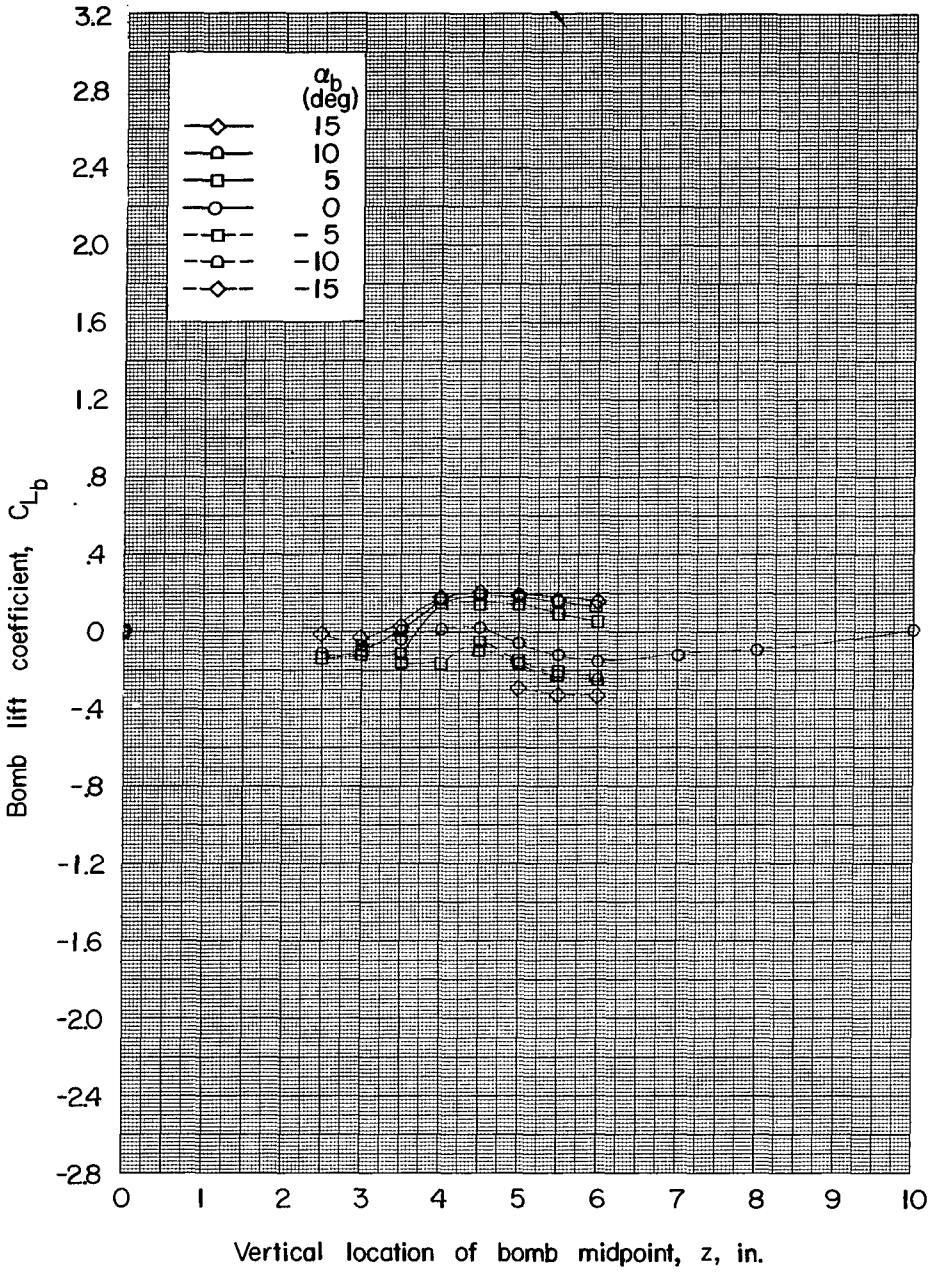

(b) Continued.

Figure 4.- Continued.

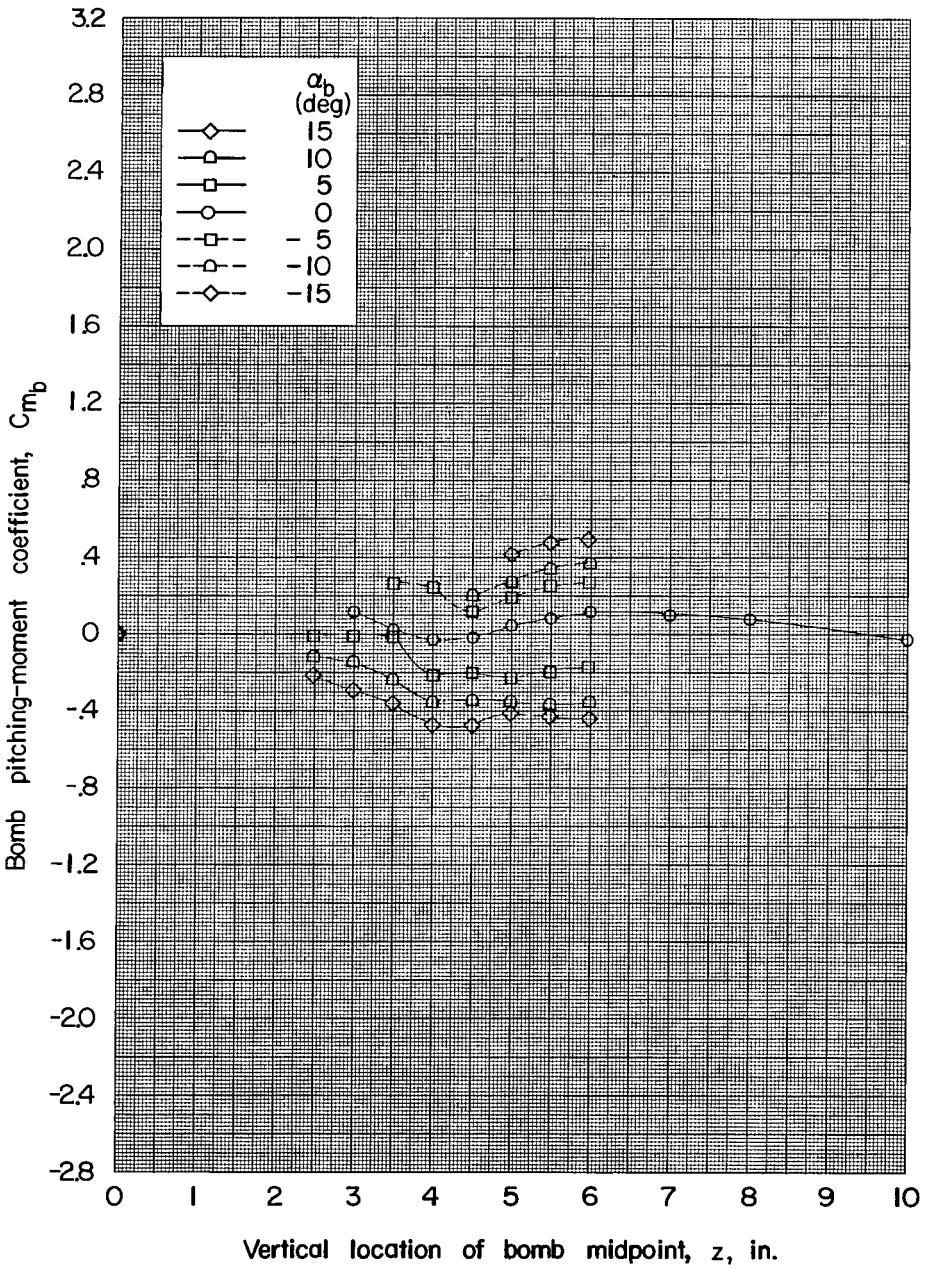

(b) Concluded.

Figure 4.- Continued.

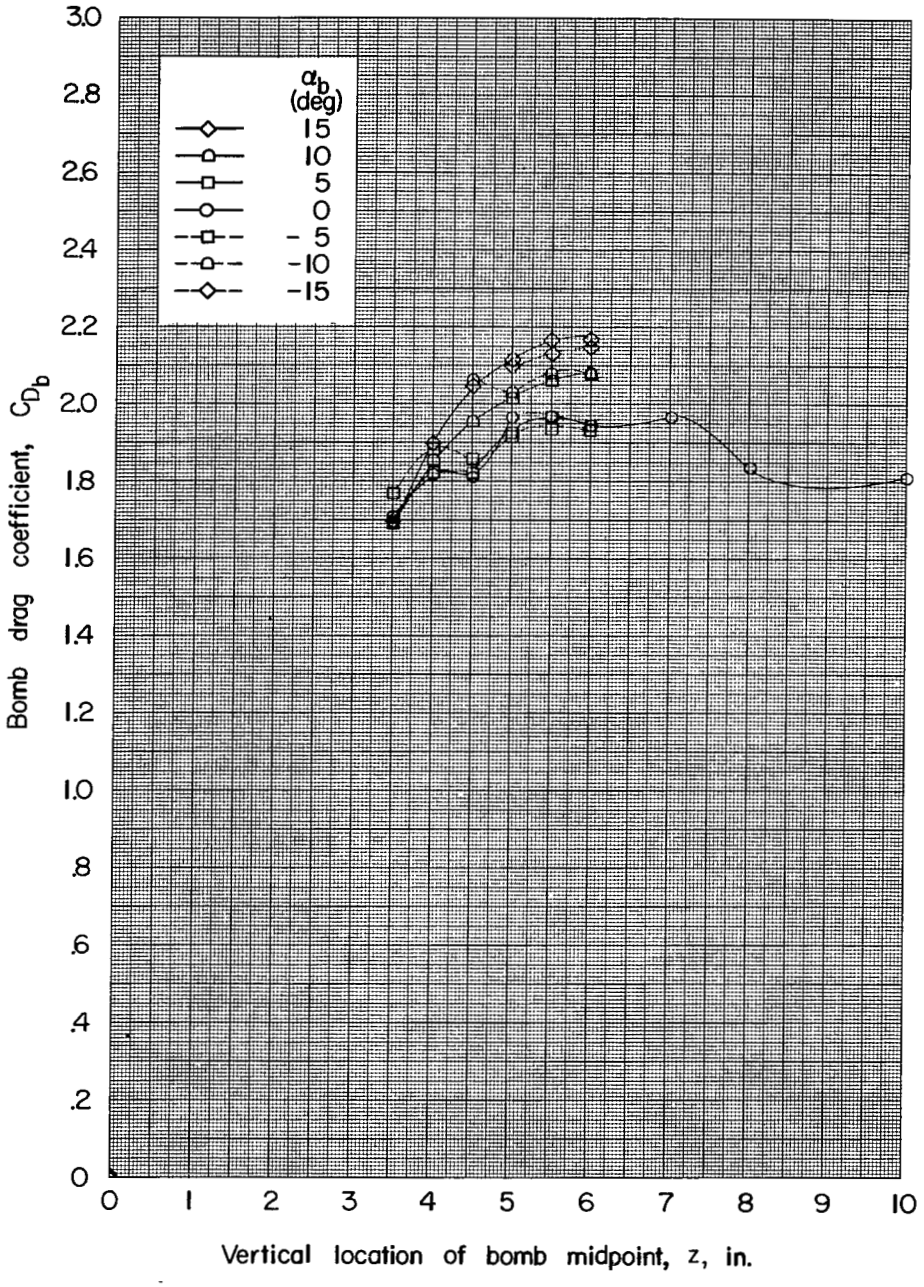

(c) x = 6.95 inches.

Figure 4.- Continued.

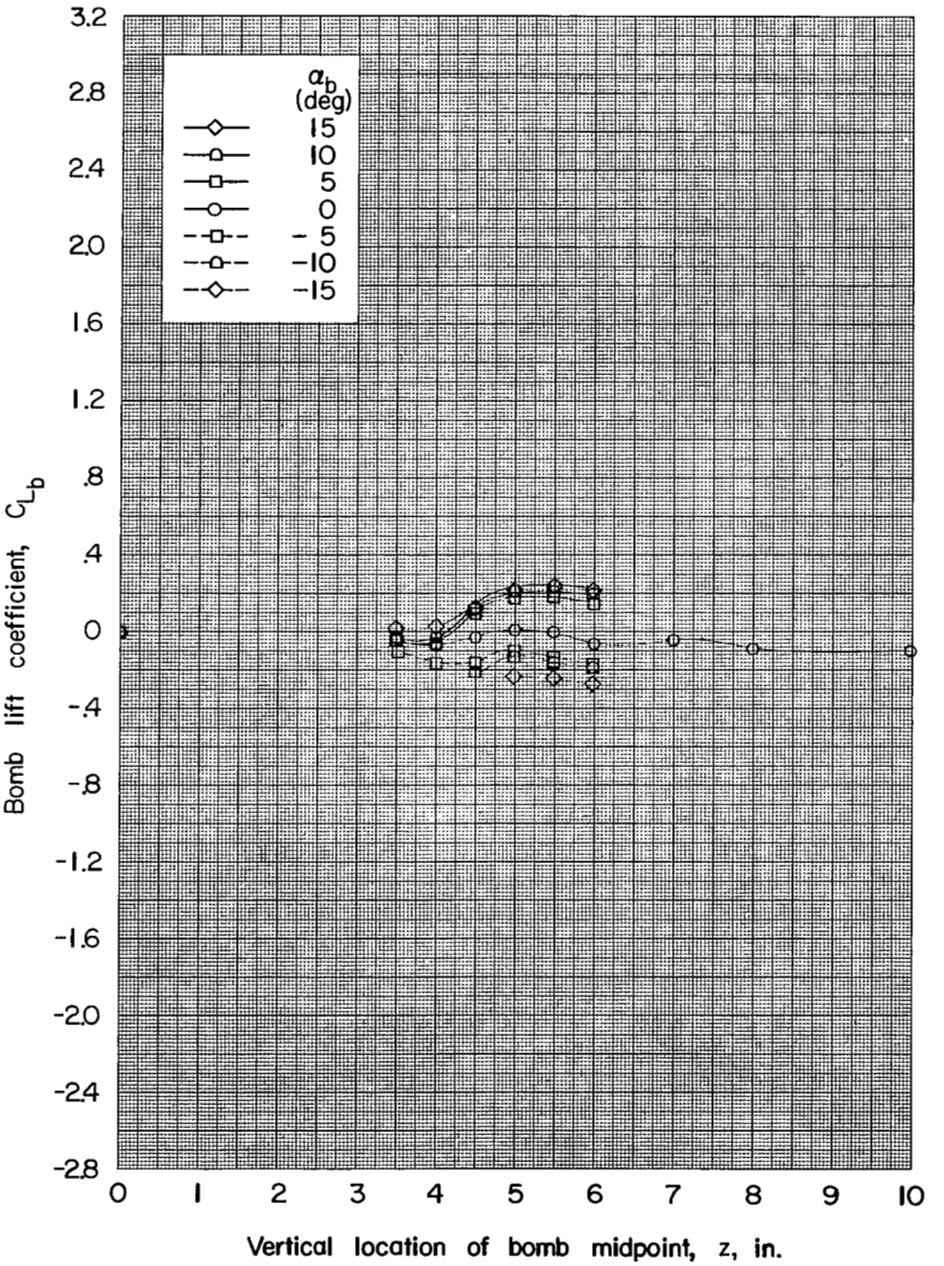

(c) Continued.

Figure 4.- Continued.

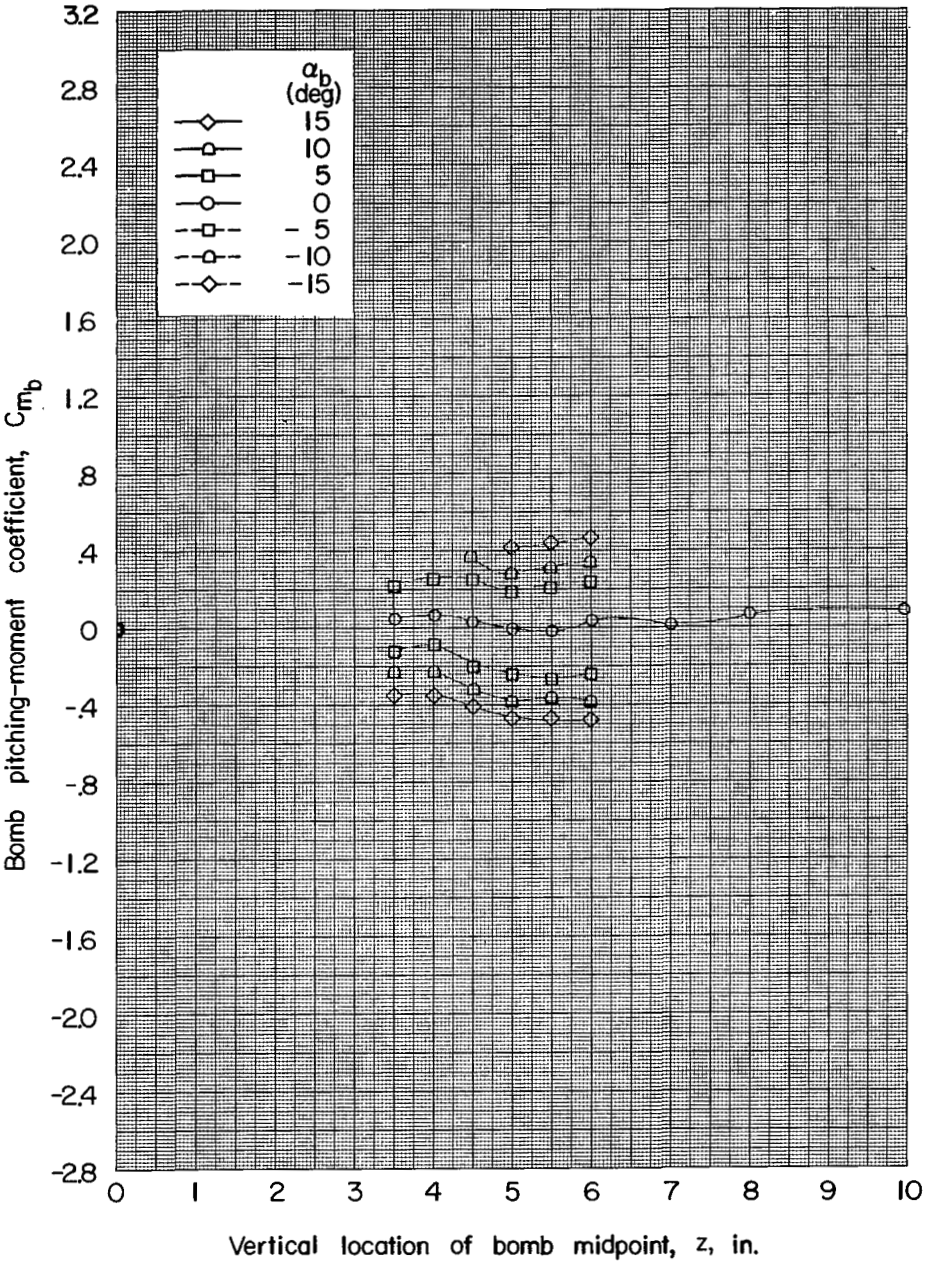

(c) Concluded.

Figure 4.- Continued.

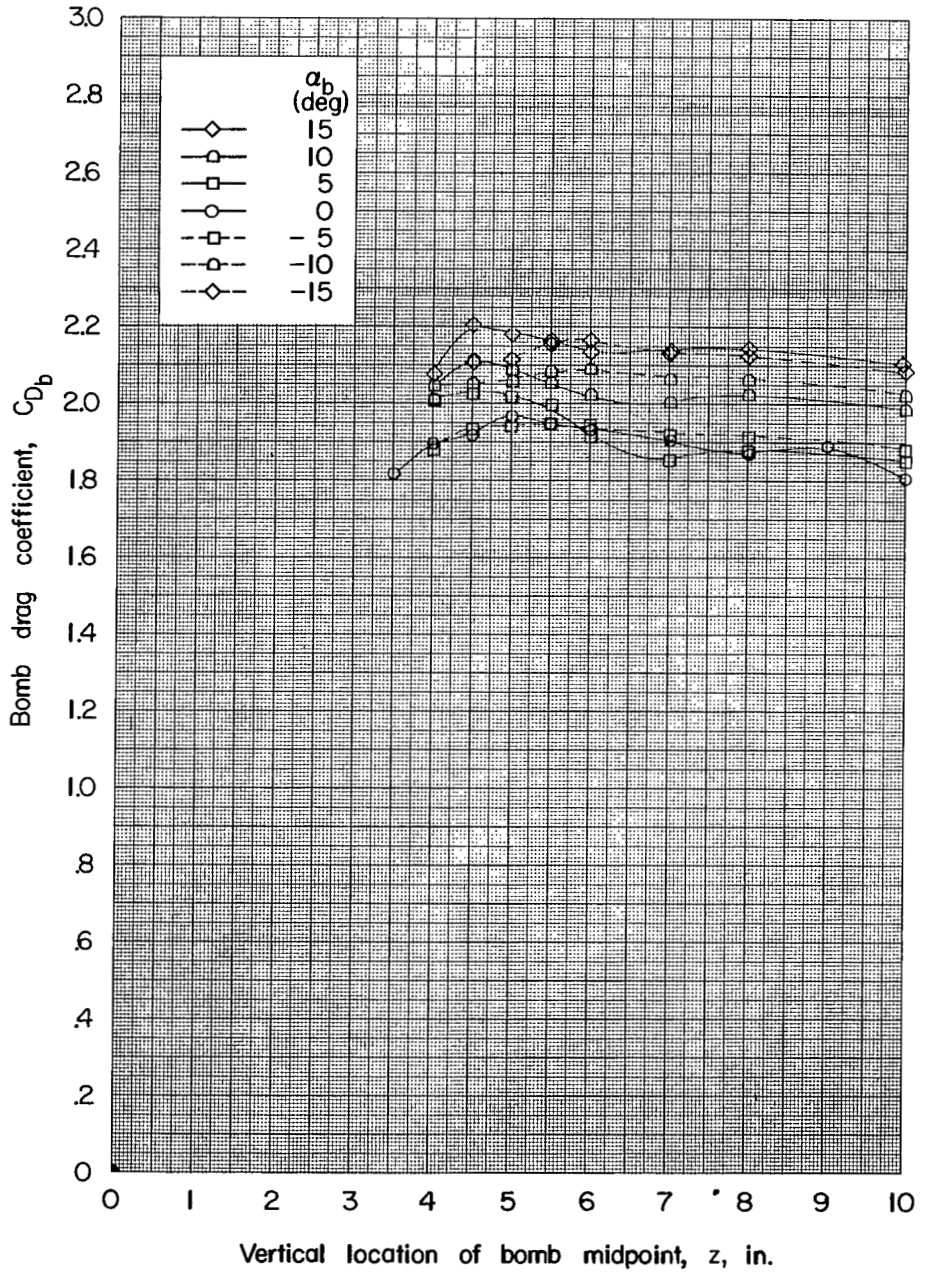

(d) x = 8.95 inches.

Figure 4.- Continued.

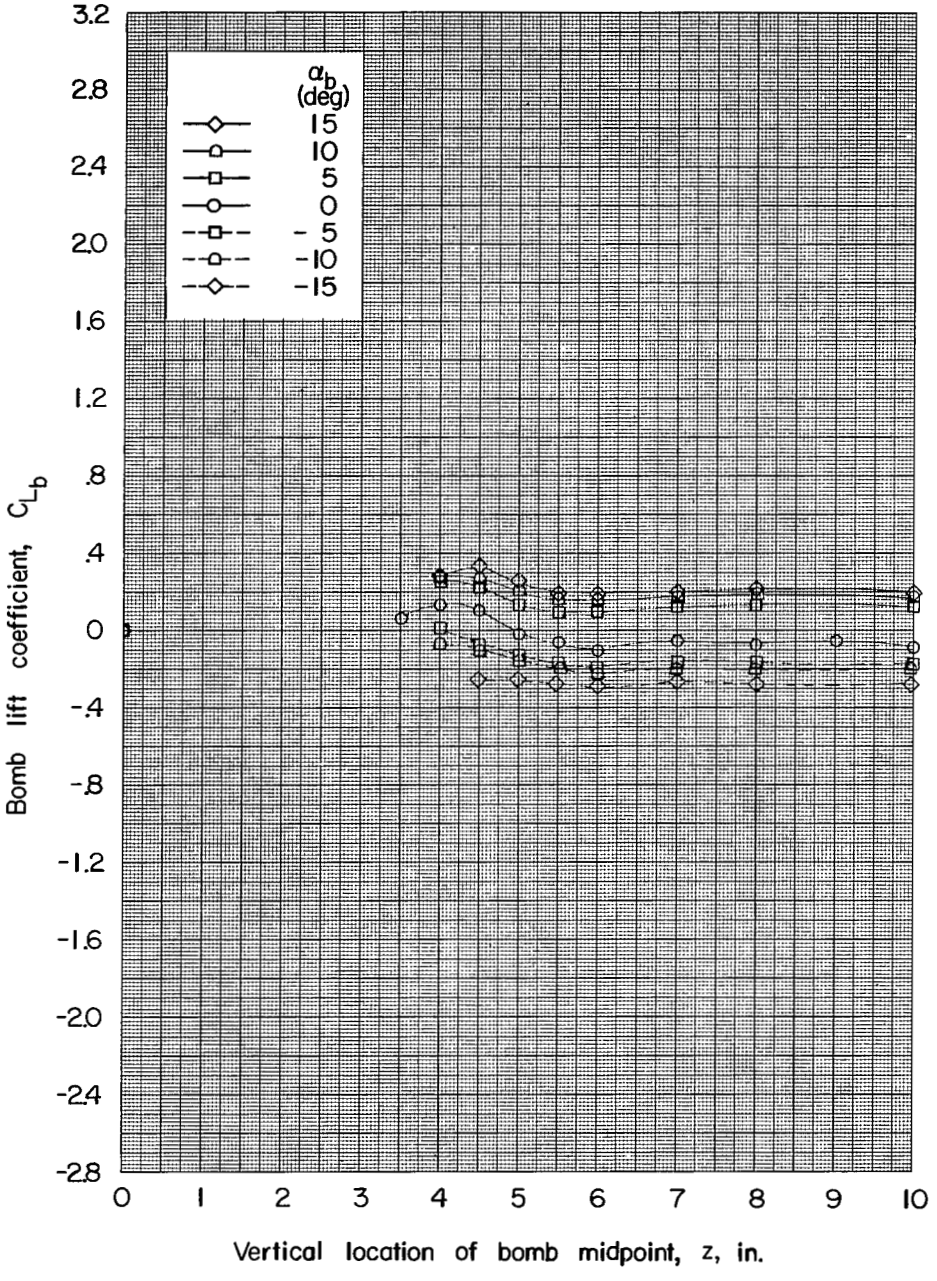

(d) Continued.

Figure 4.- Continued.

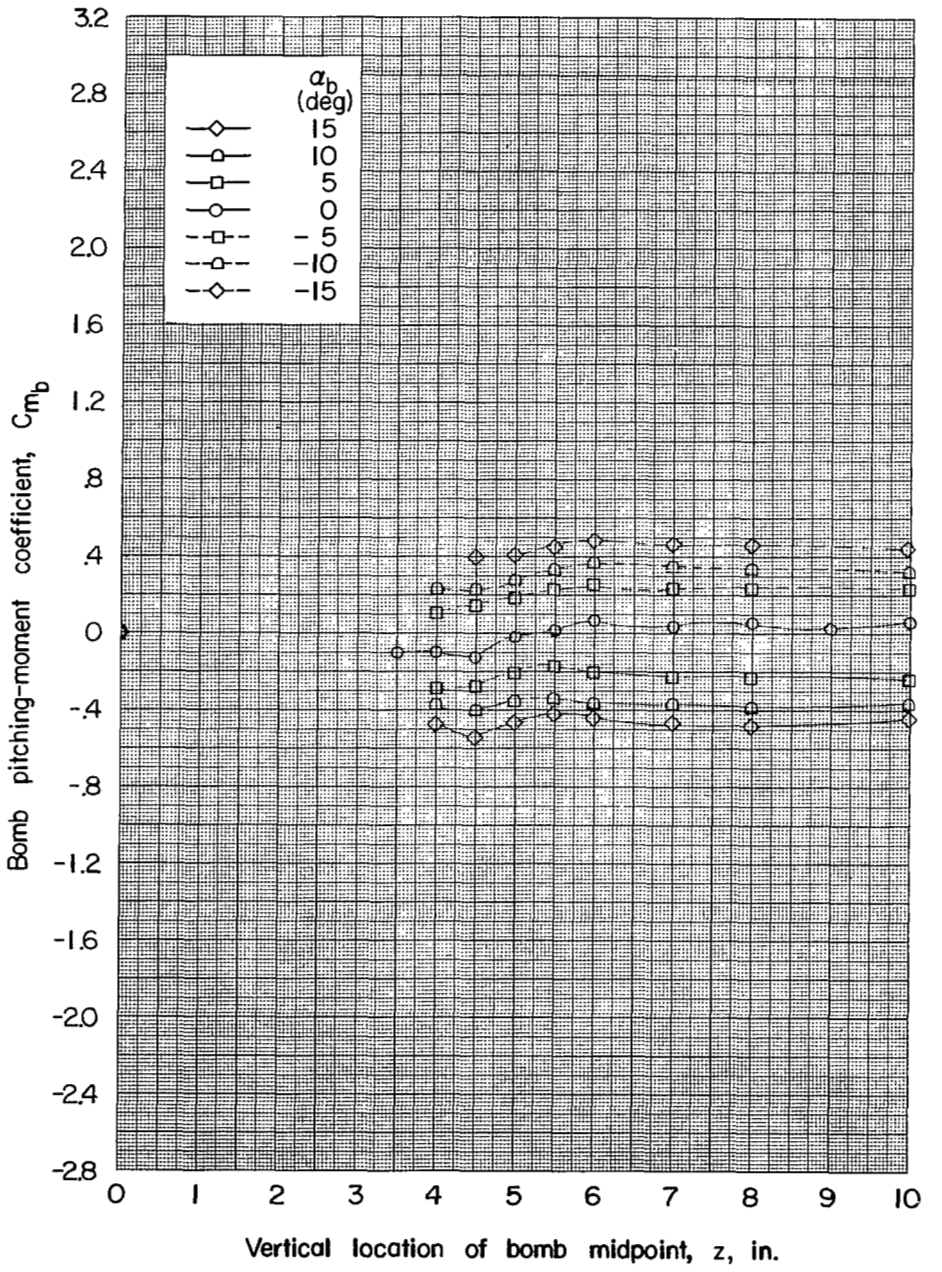

(d) Concluded.

Figure 4.- Continued.

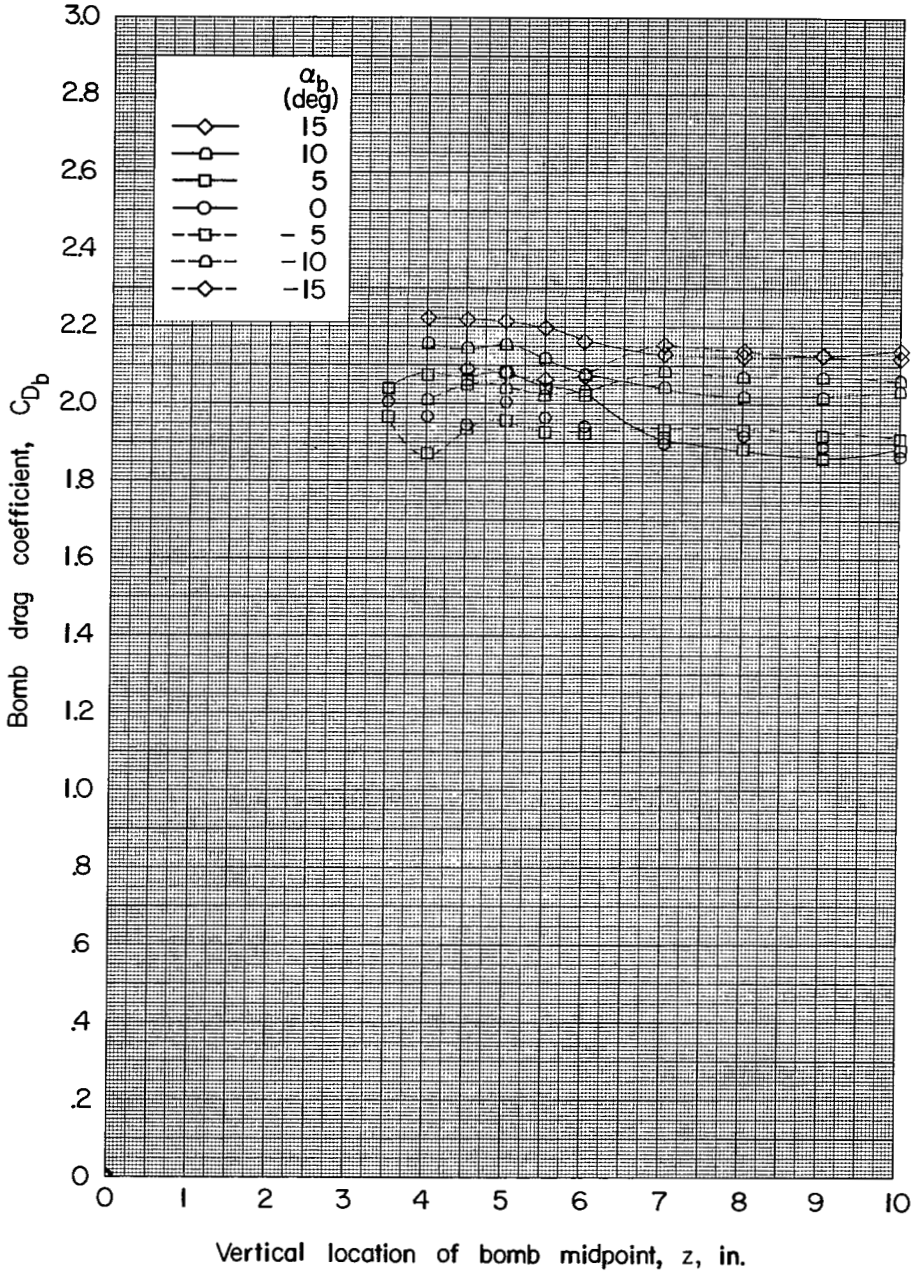

(e) x = 10.95 inches.

Figure 4.- Continued.

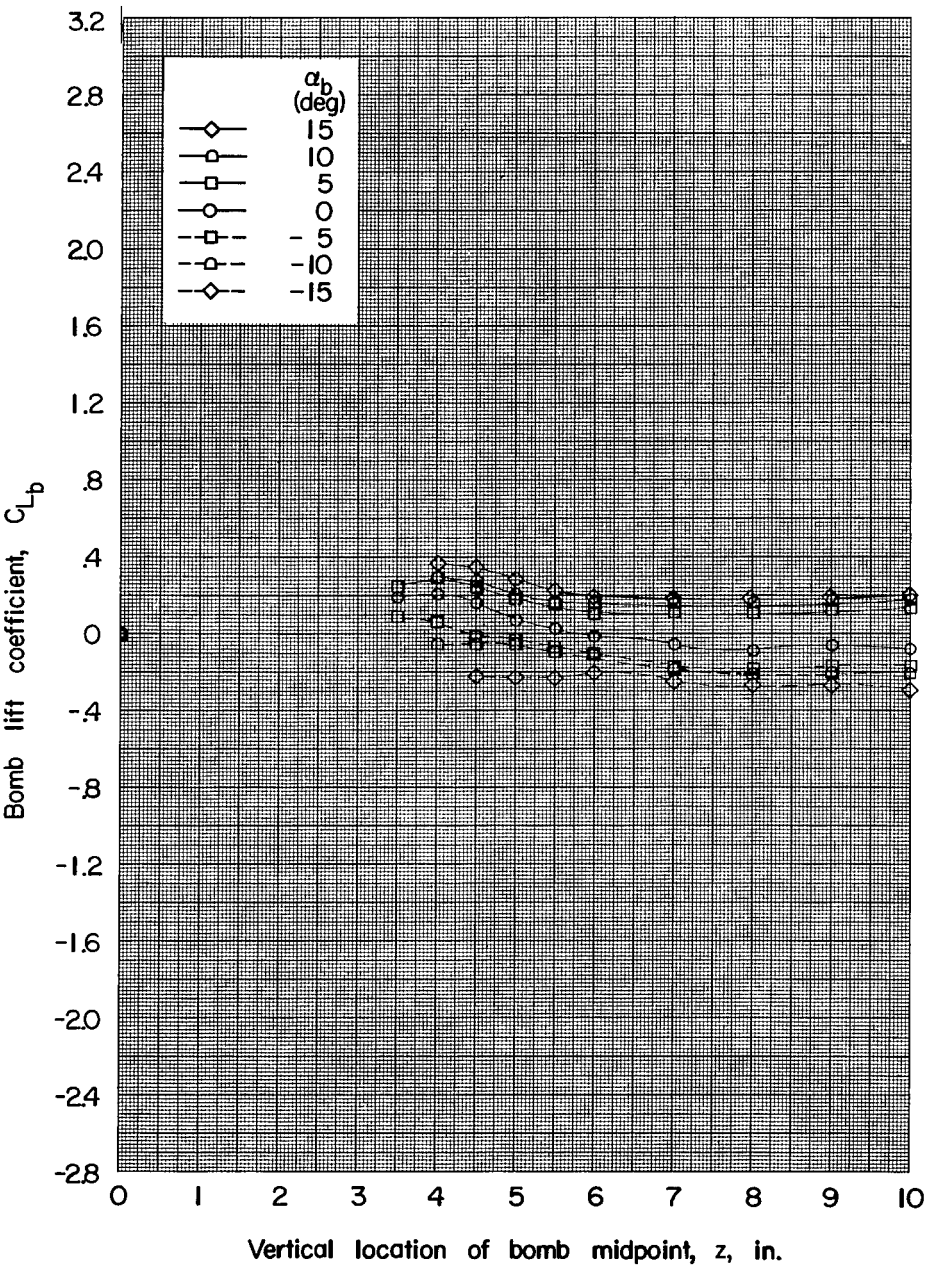

(e) Continued.

Figure 4.- Continued.

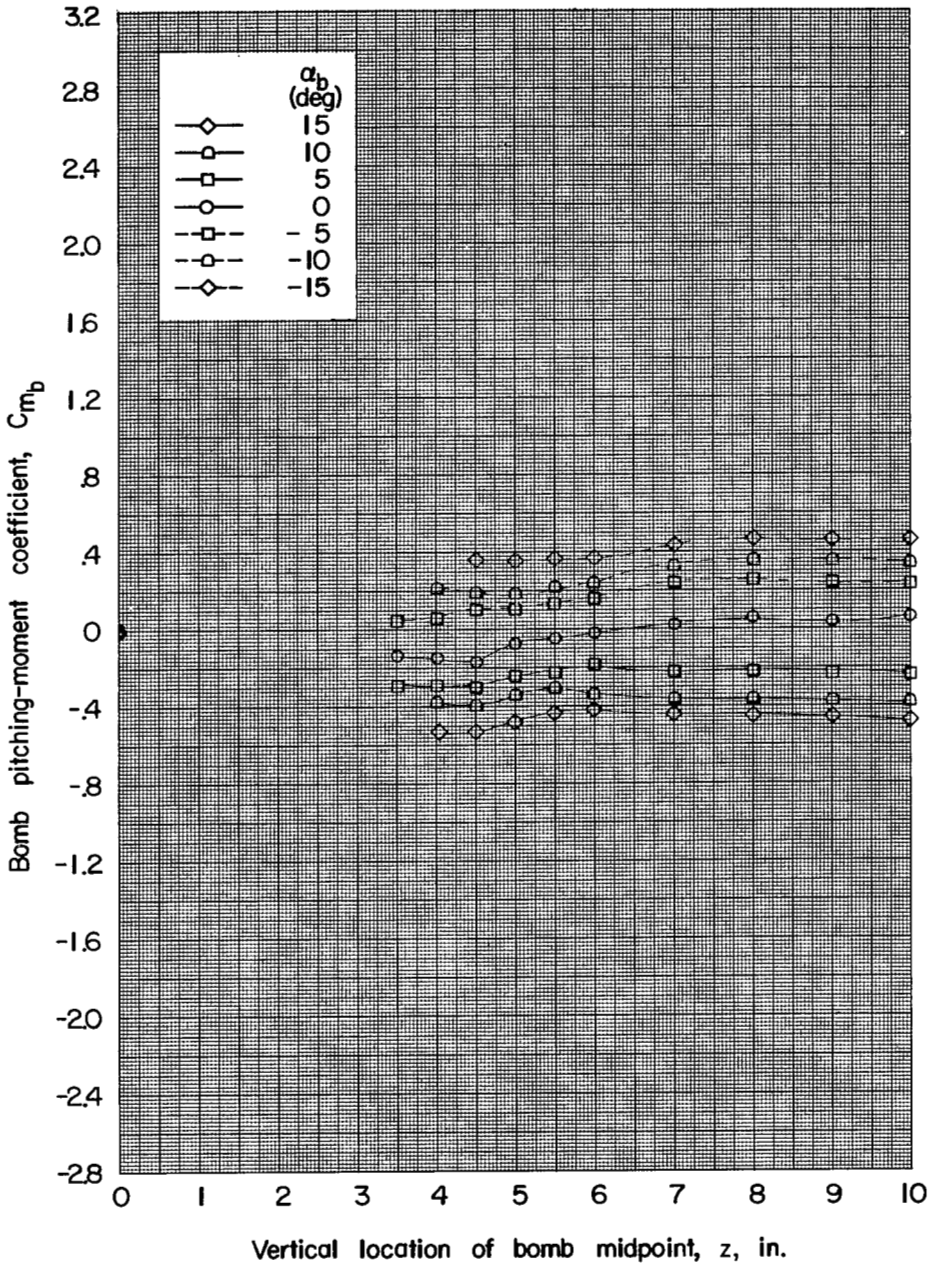

(e) Concluded.

Figure 4.- Concluded.

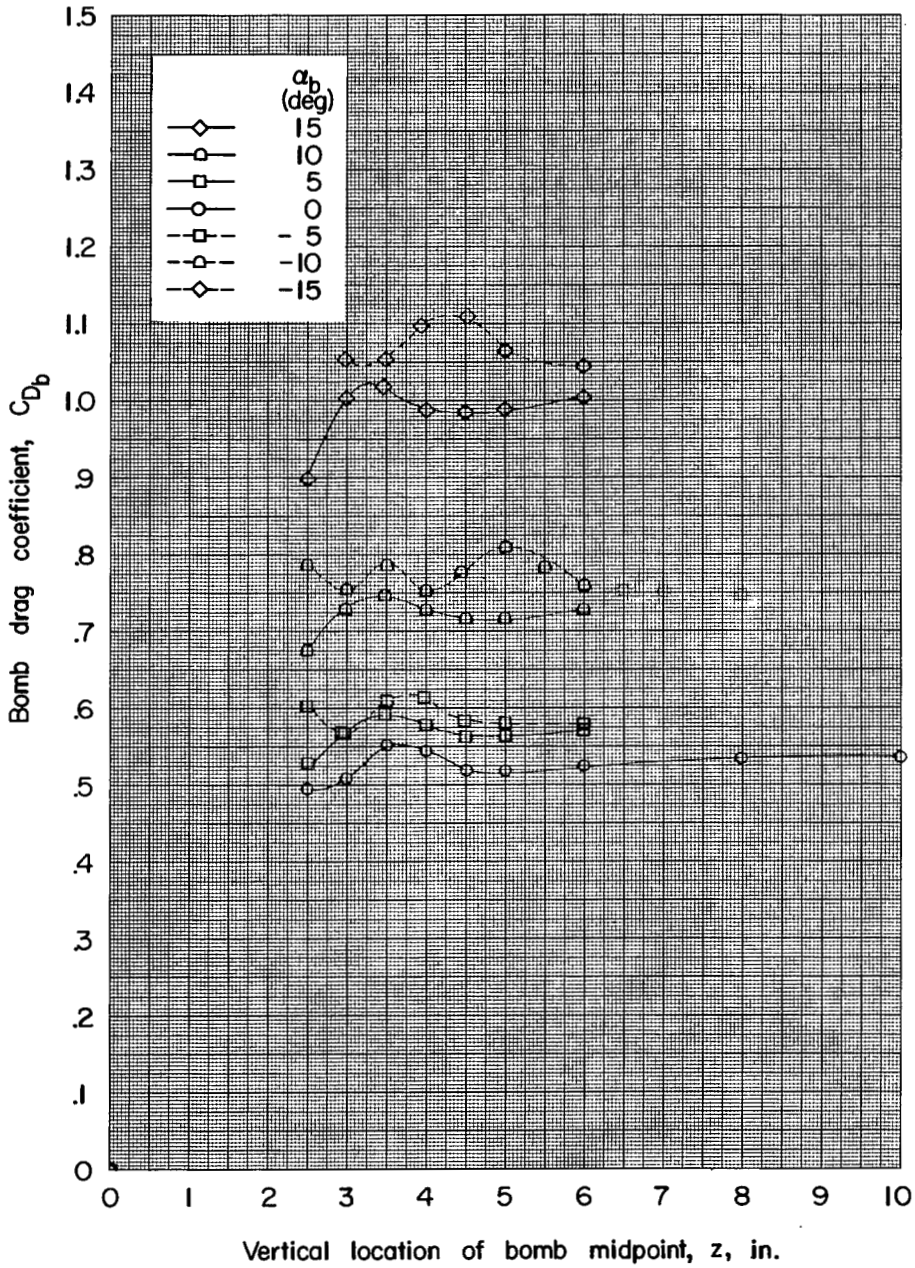

(a) x = -2.55 inches.

Figure 5.- Force and moment data for bomb 2 in presence of the wing-fuselage combination without ejector. $\alpha_{wf} = 4^\circ$.

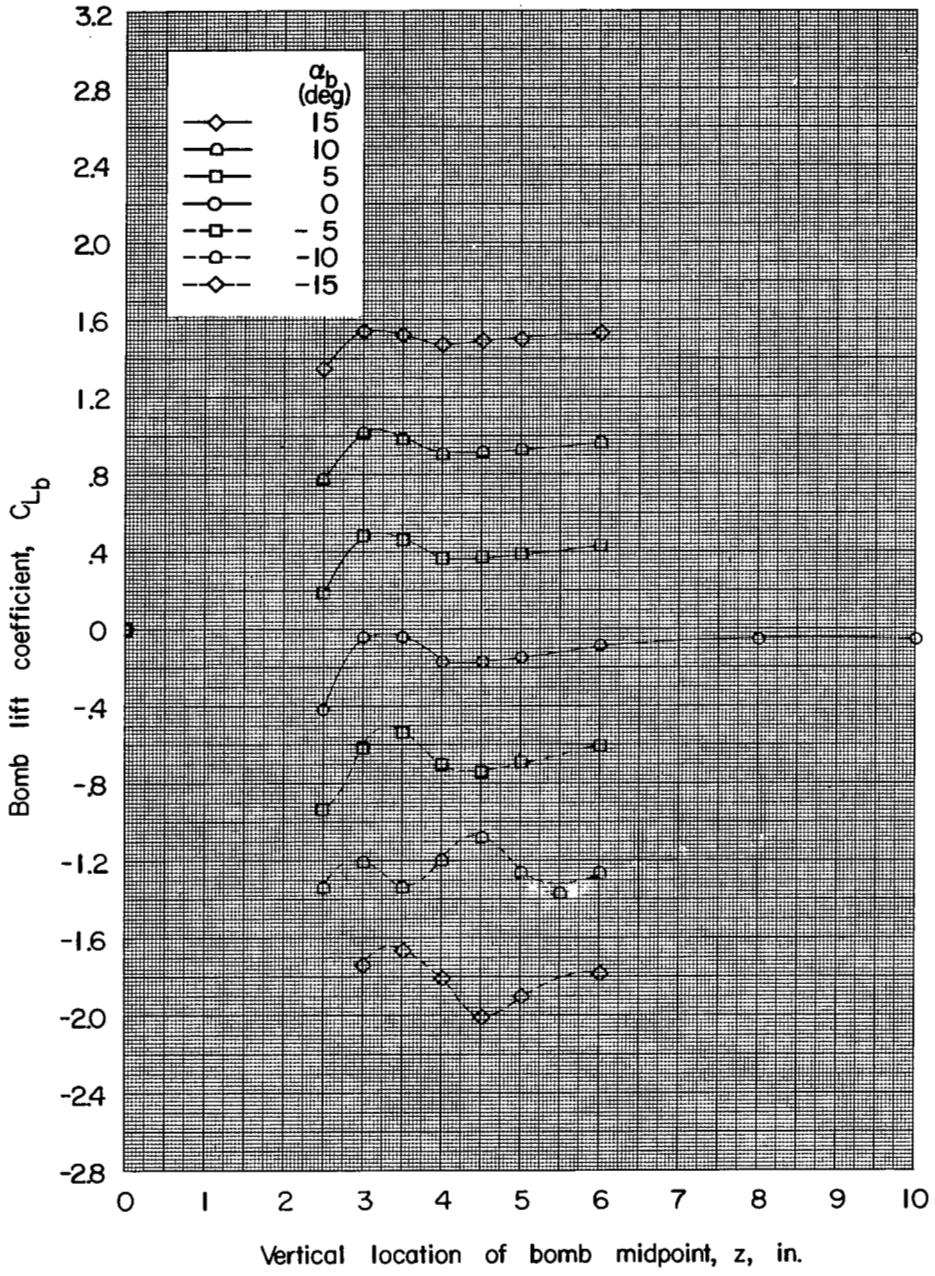

(a) Continued.

Figure 5.- Continued.

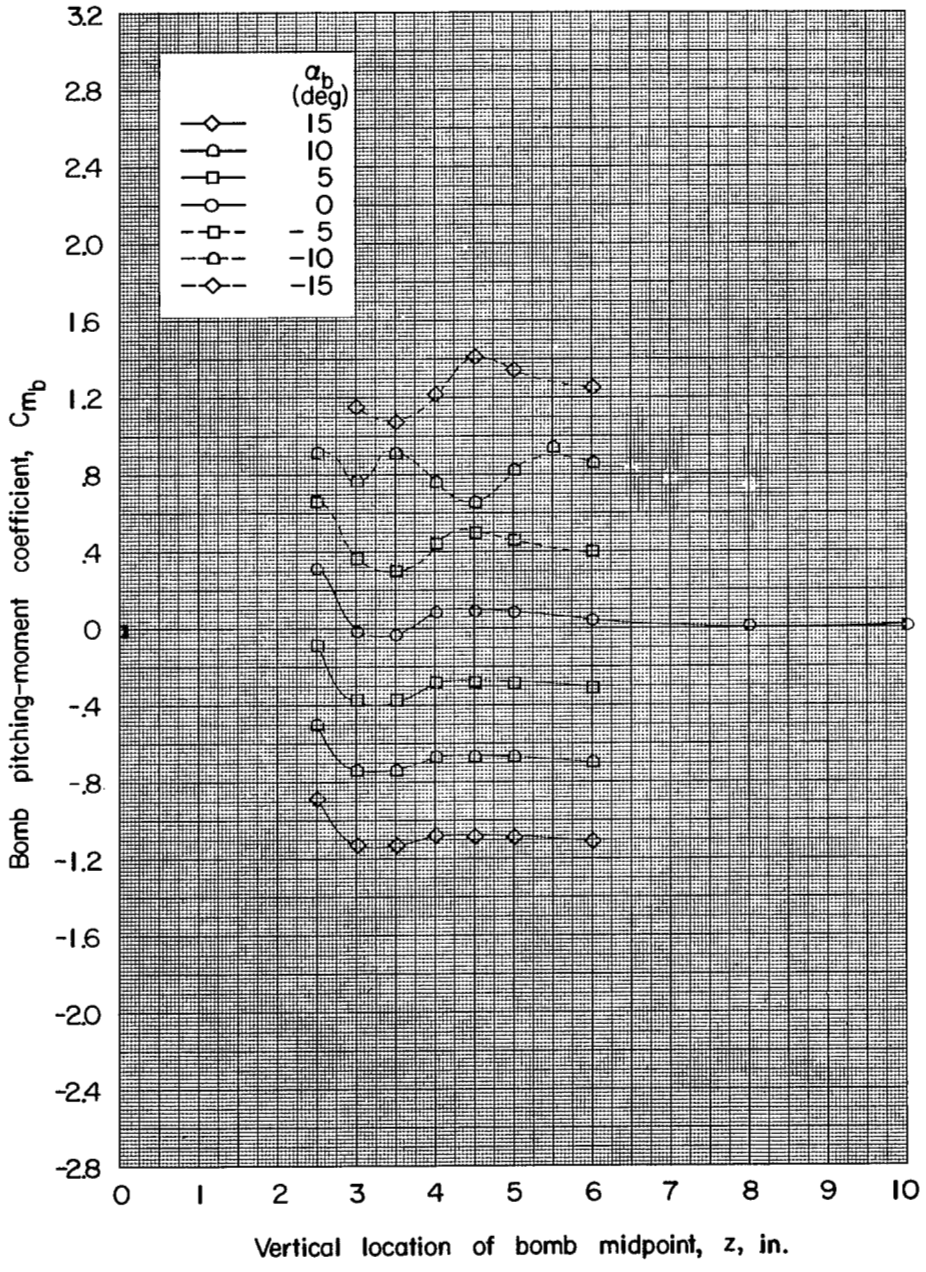

(a) Concluded.

Figure 5.- Continued.

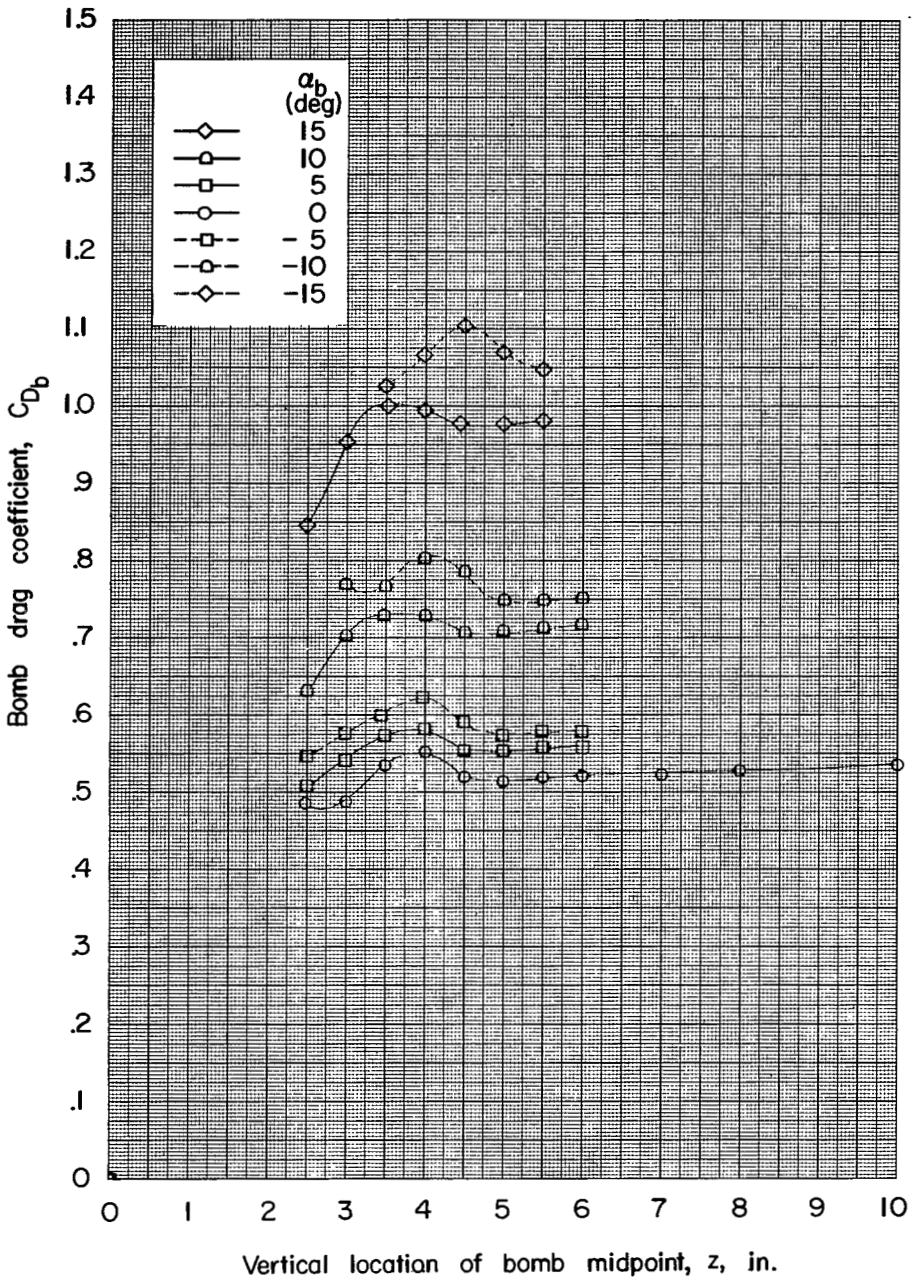

(b) x = -1.05 inches.

Figure 5.- Continued.

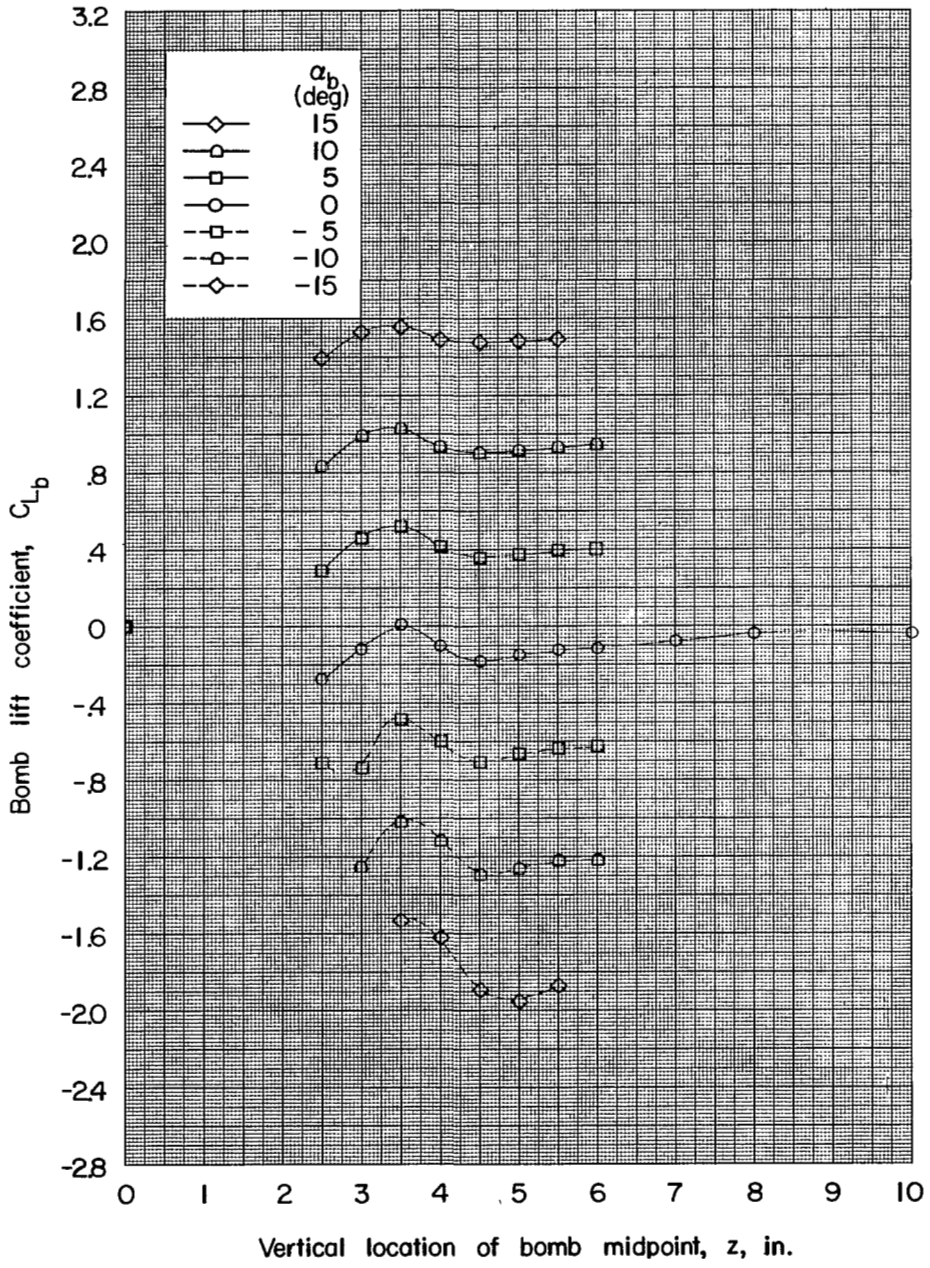

(b) Continued.

Figure 5.- Continued.

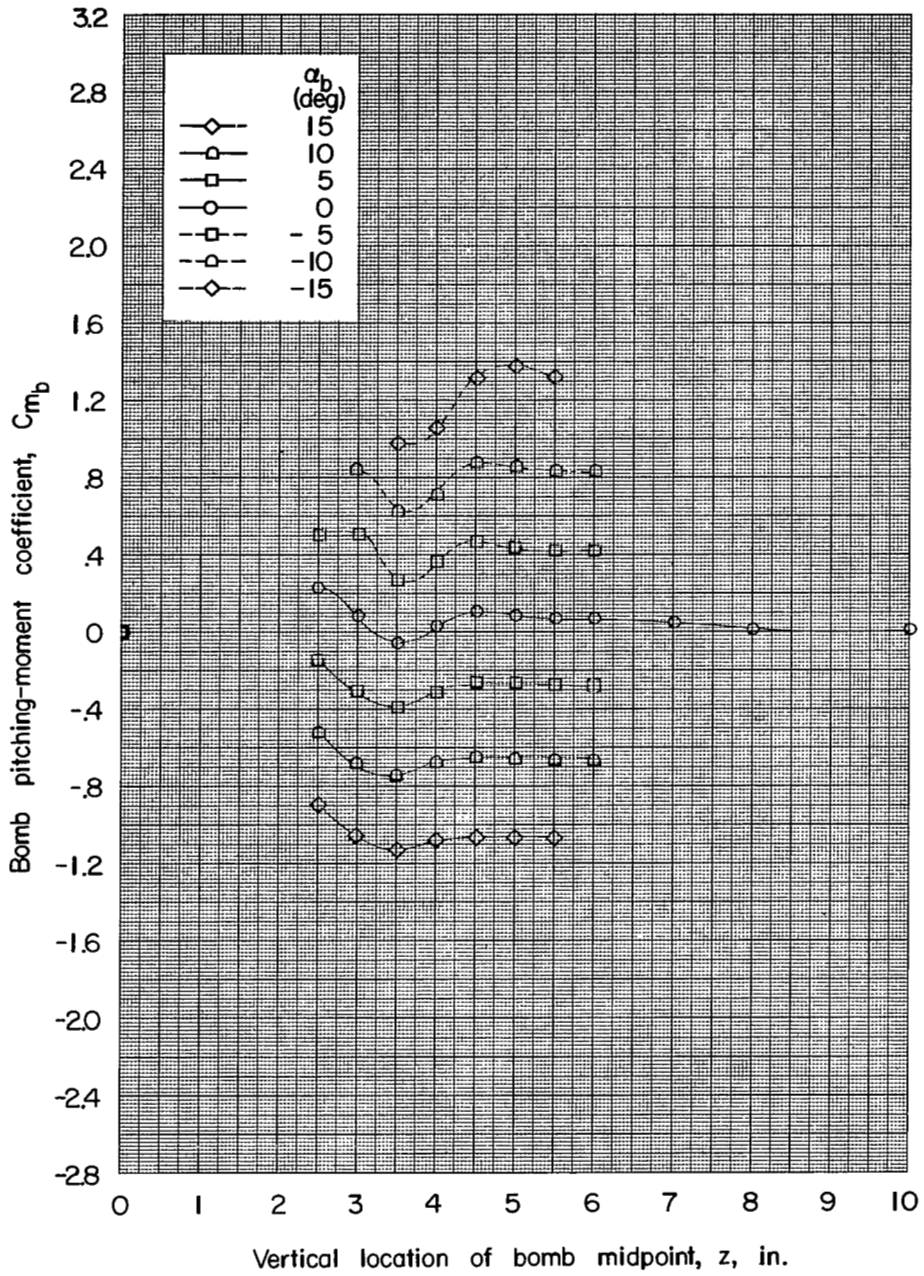

(b) Concluded.

Figure 5.- Continued.

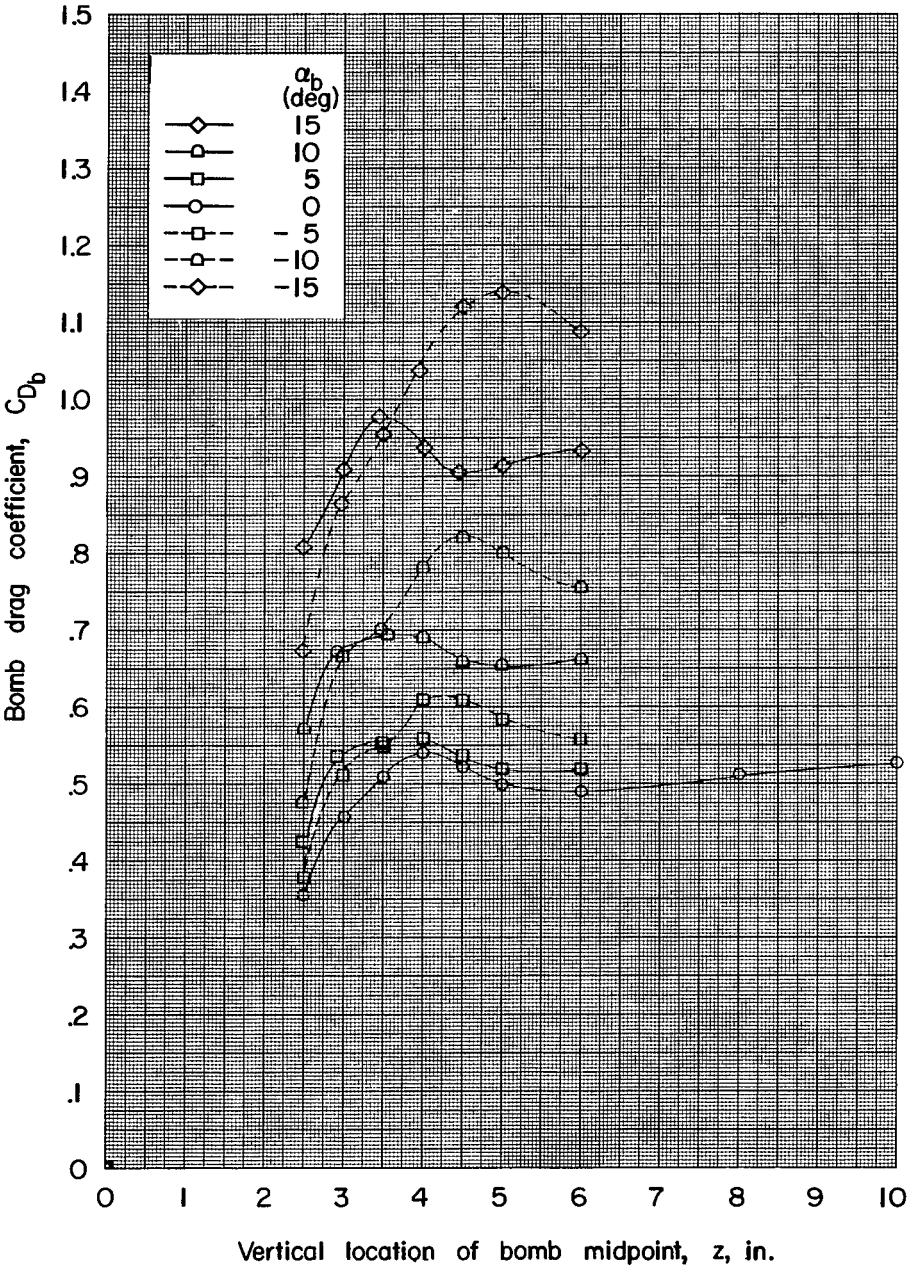

(c) x = 0.95 inch.

Figure 5.- Continued.

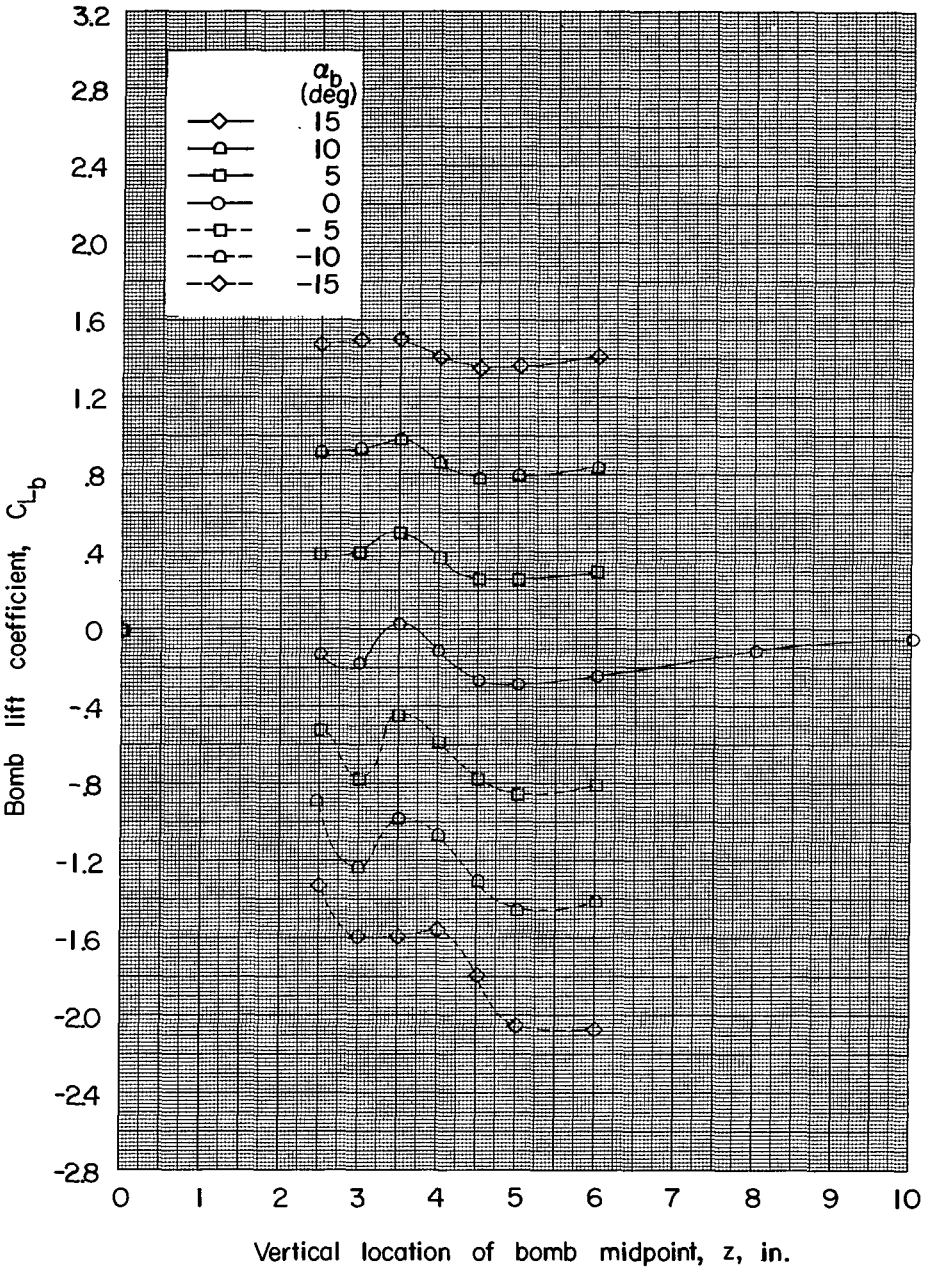

(c) Continued.

Figure 5.- Continued.

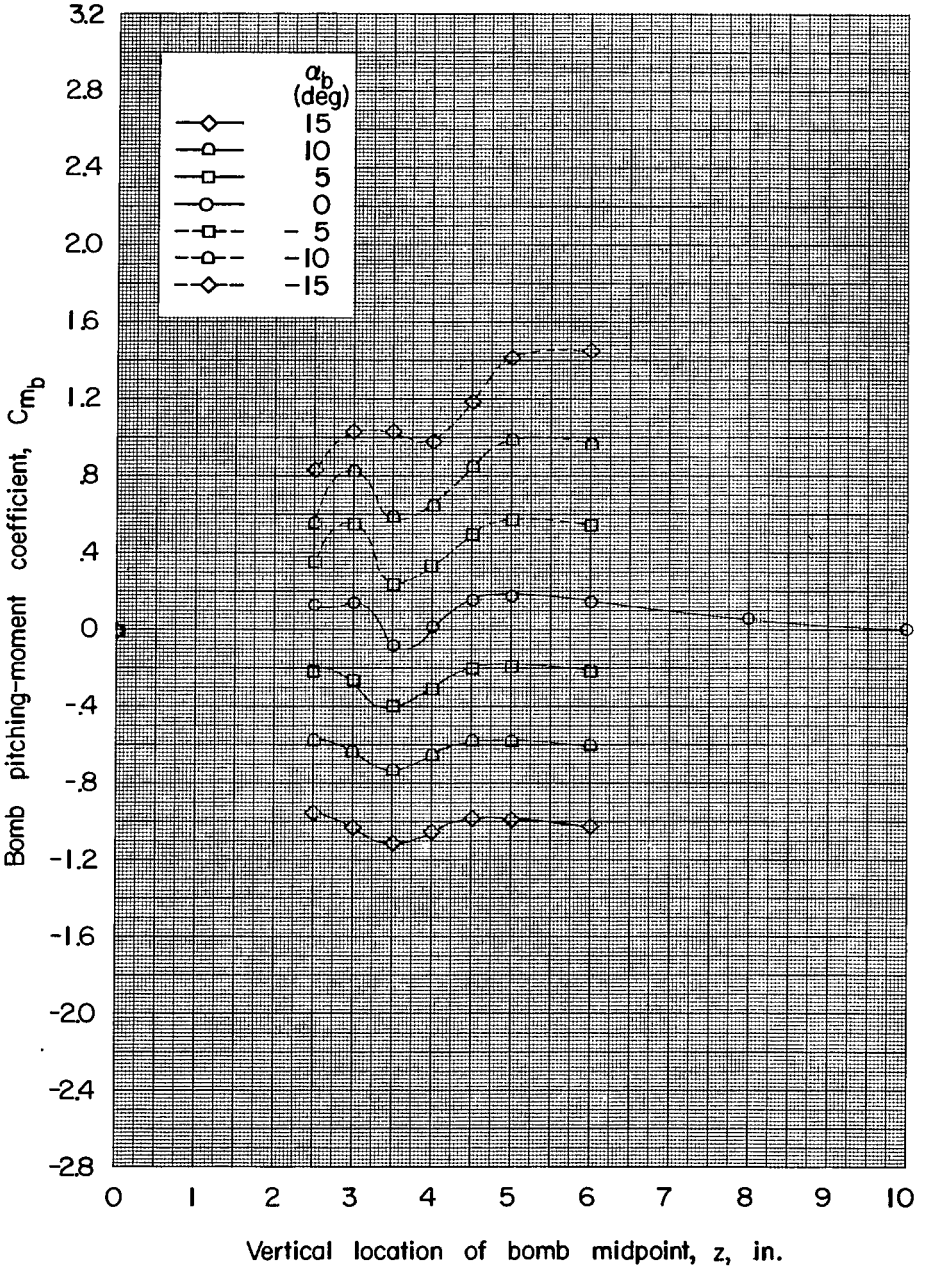

(c) Concluded.

Figure 5.- Continued.

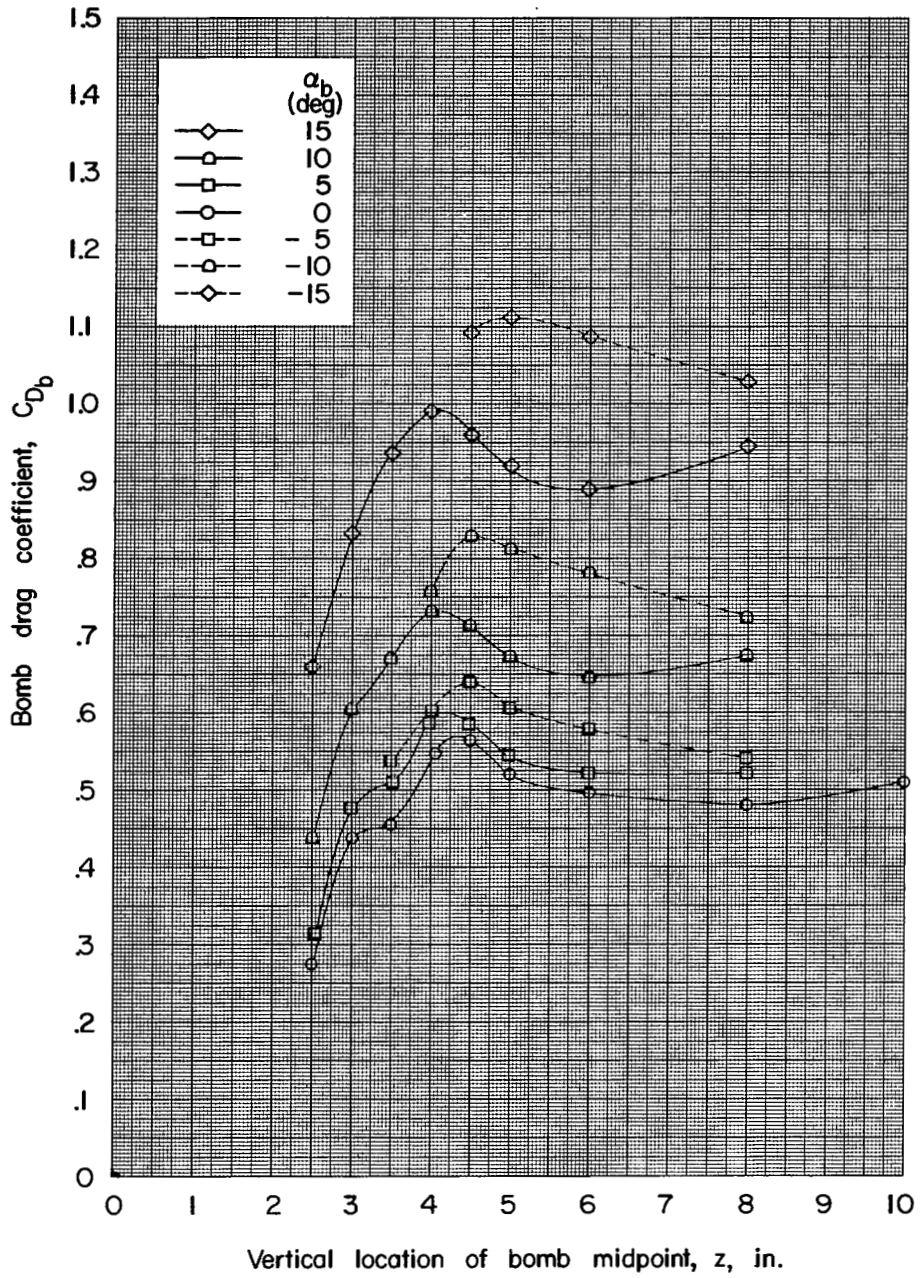

(d) x = 2.95 inches.

Figure 5.- Continued.

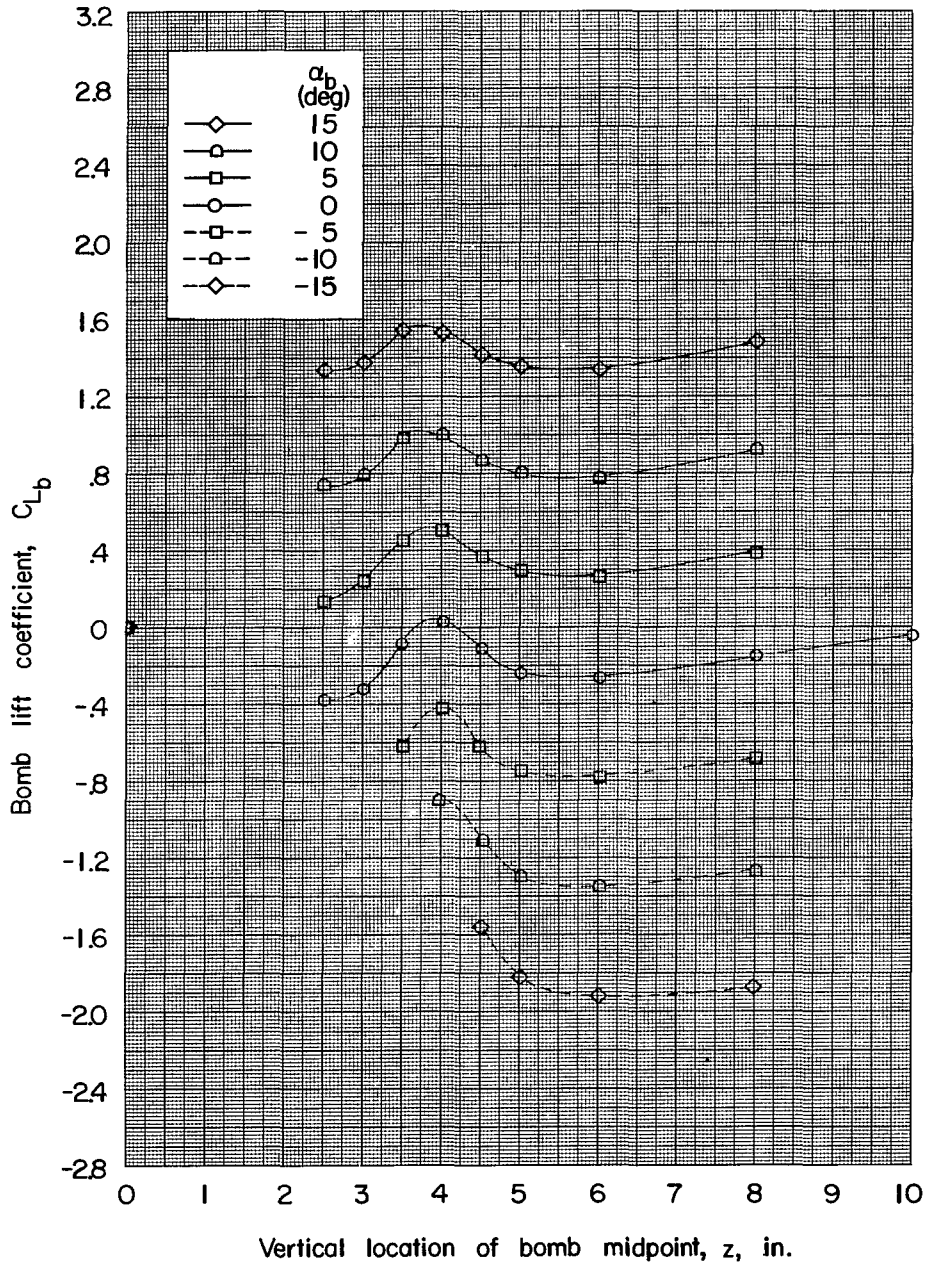

(d) Continued.

Figure 5.- Continued.

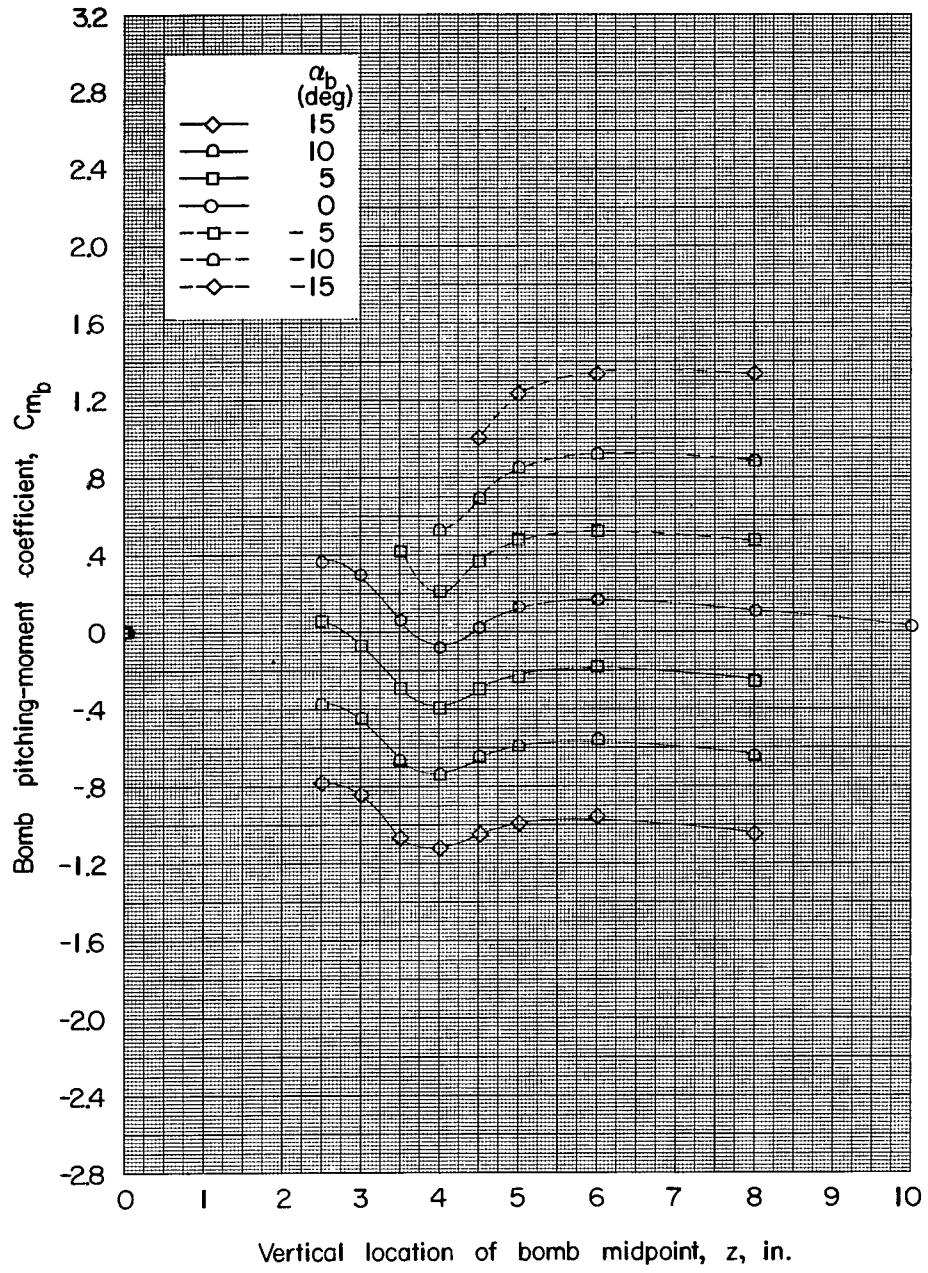

(d) Concluded.

Figure 5.- Continued.

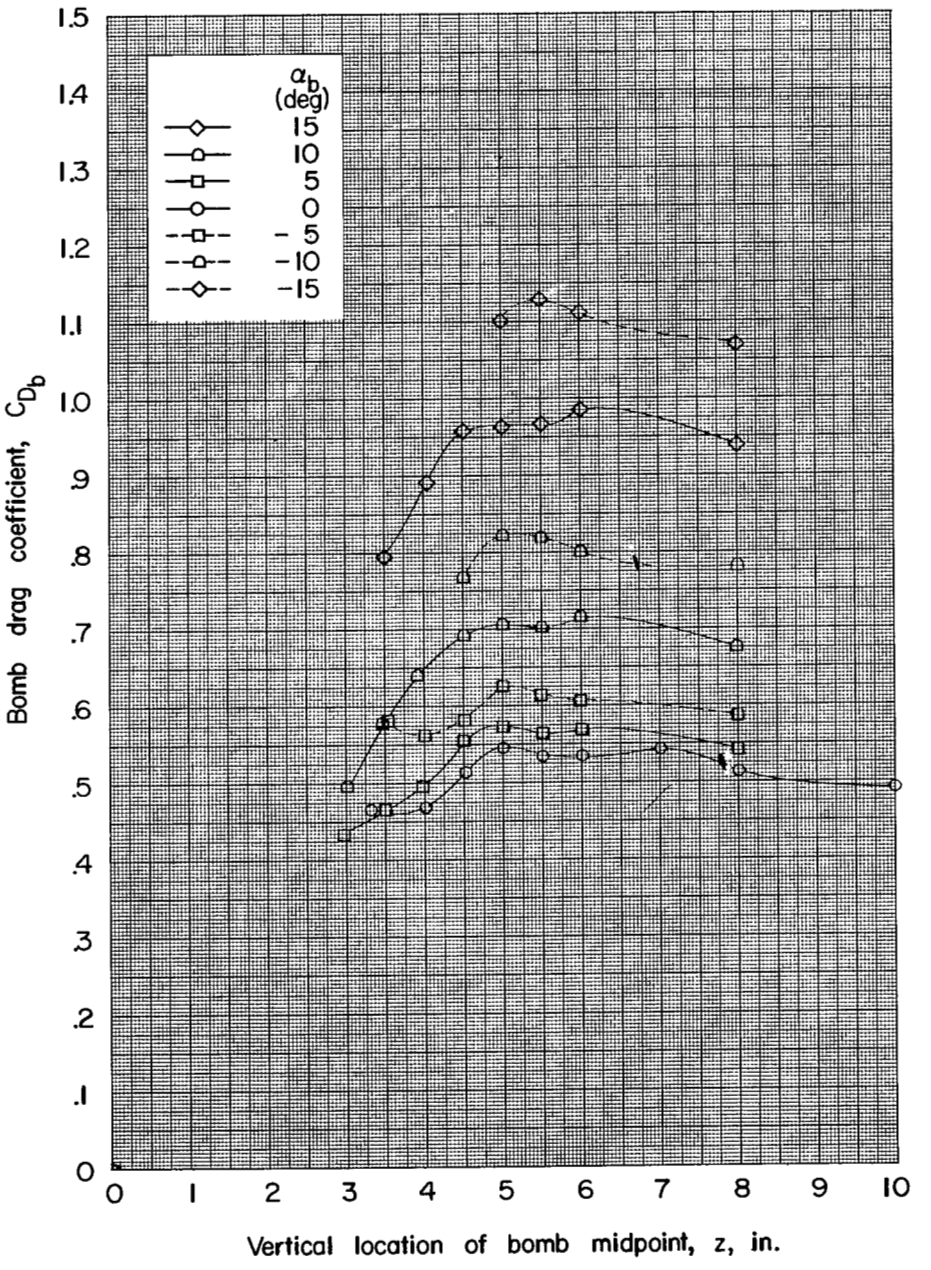

(e) x = 5.95 inches.

Figure 5.- Continued.

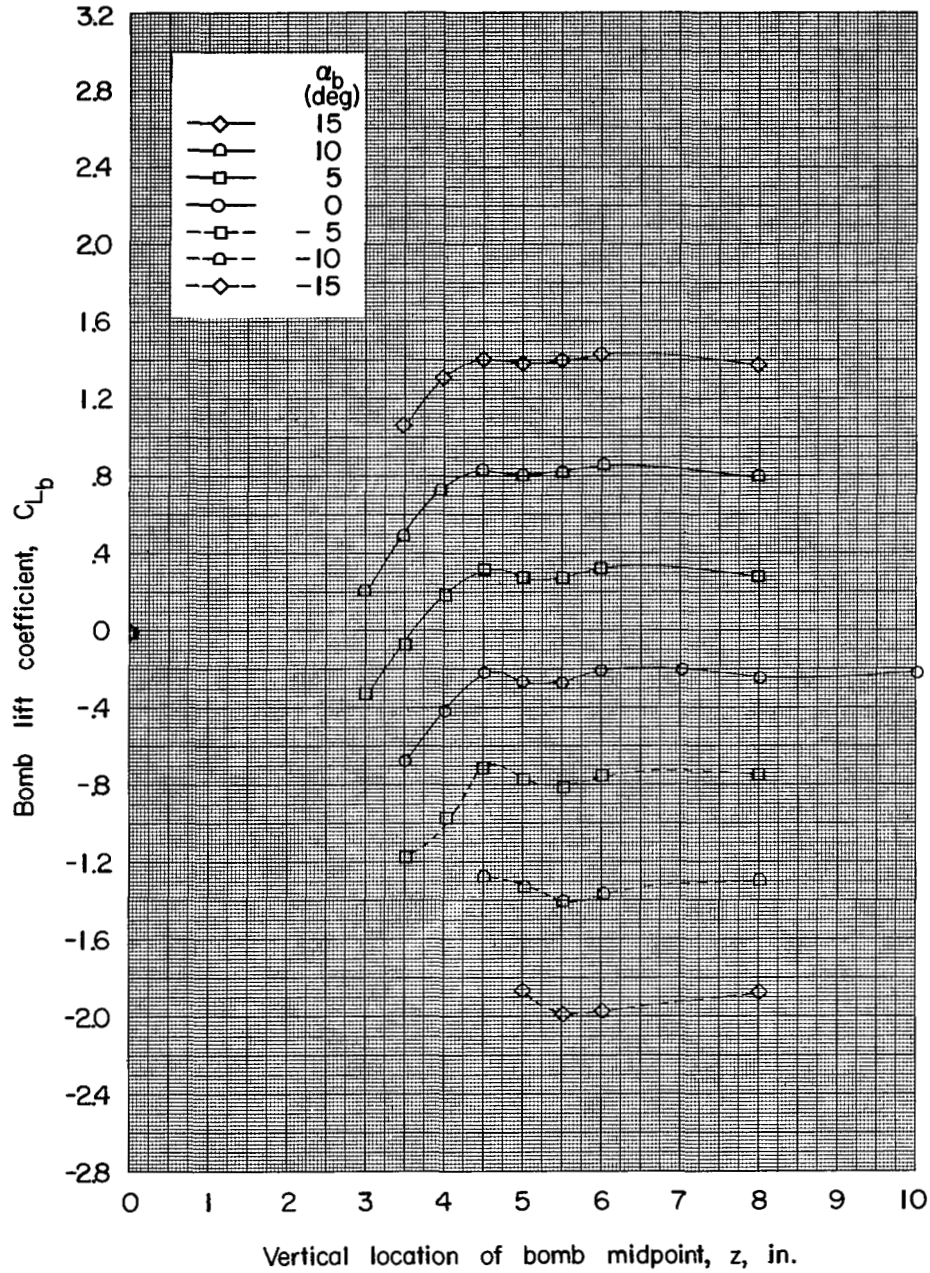

(e) Continued.

Figure 5.- Continued.

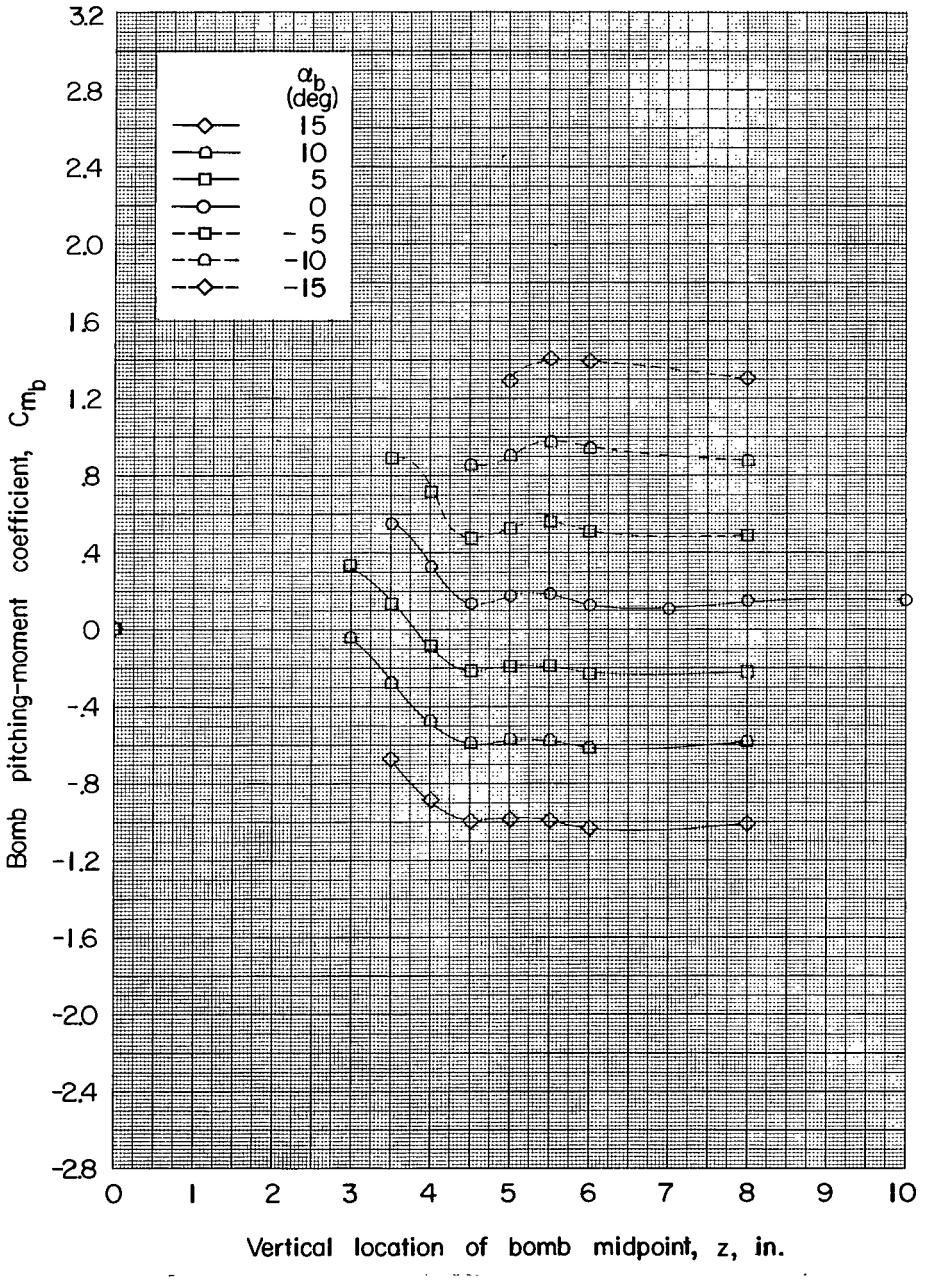

(e) Concluded.

Figure 5.- Concluded.

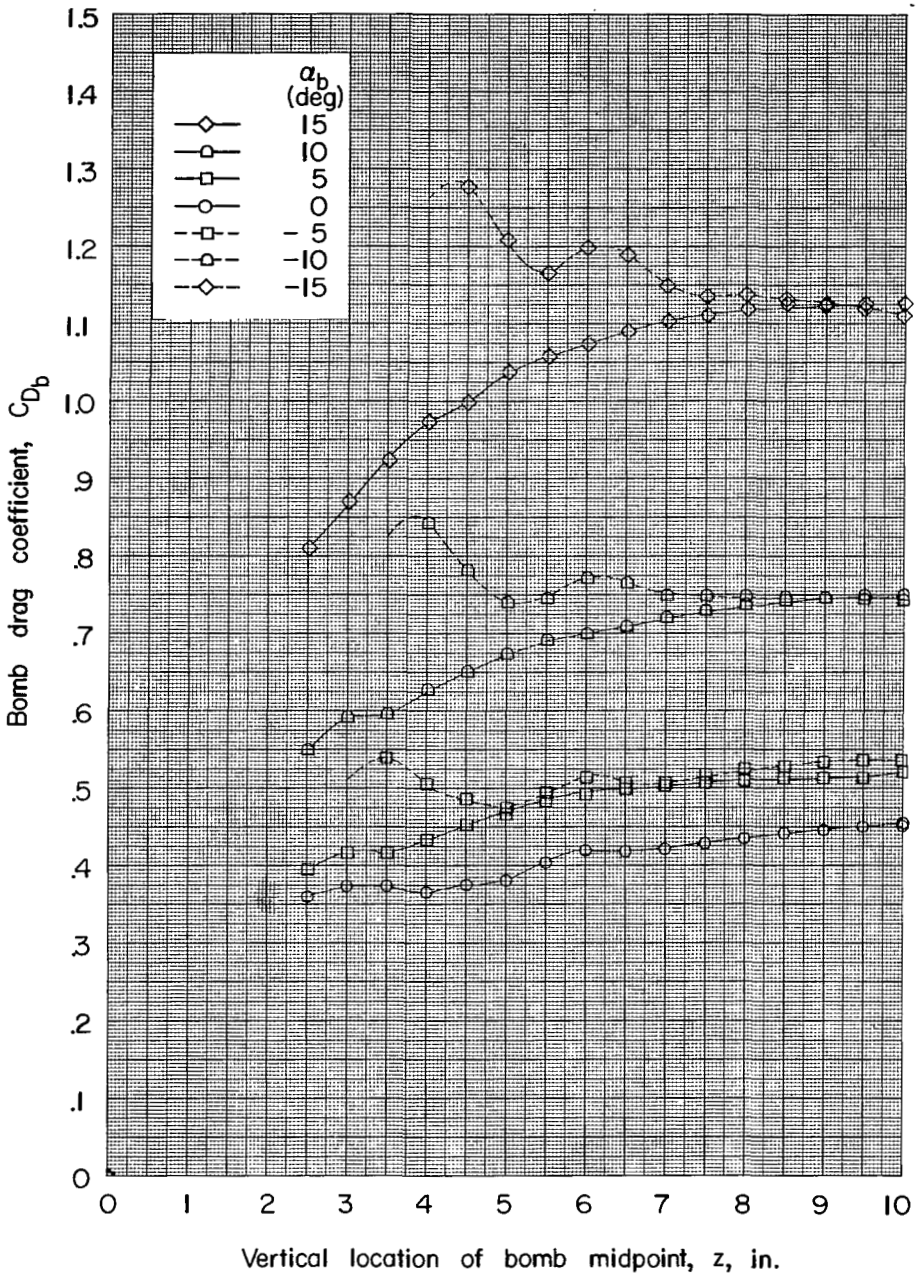

(a) x = -1.65 inches.

Figure 6.- Force and moment data for bomb 3 in presence of the wing-fuselage combination without ejector. $\alpha_{wf} = 4^{\circ}$.

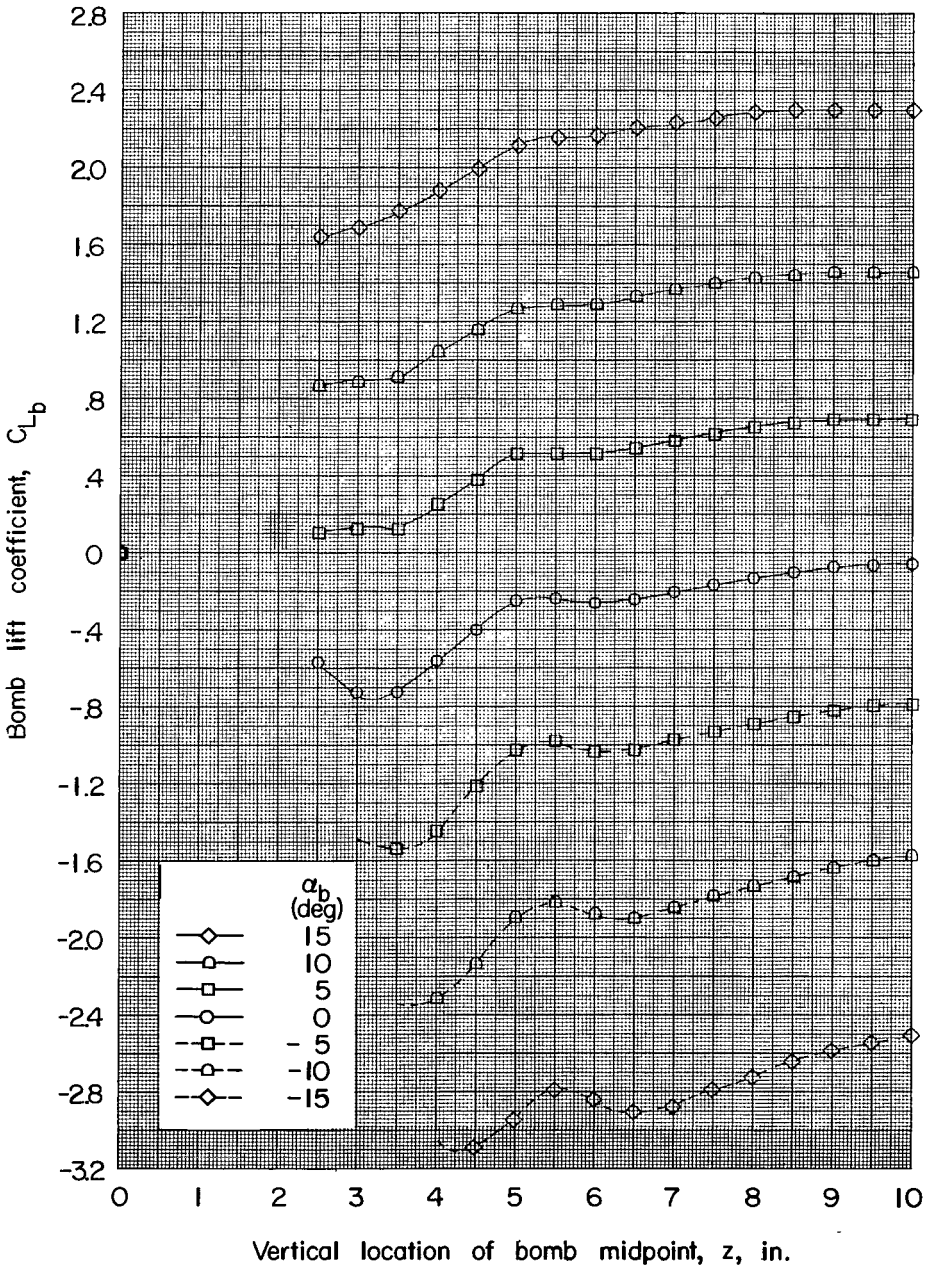

(a) Continued.

Figure 6.- Continued.

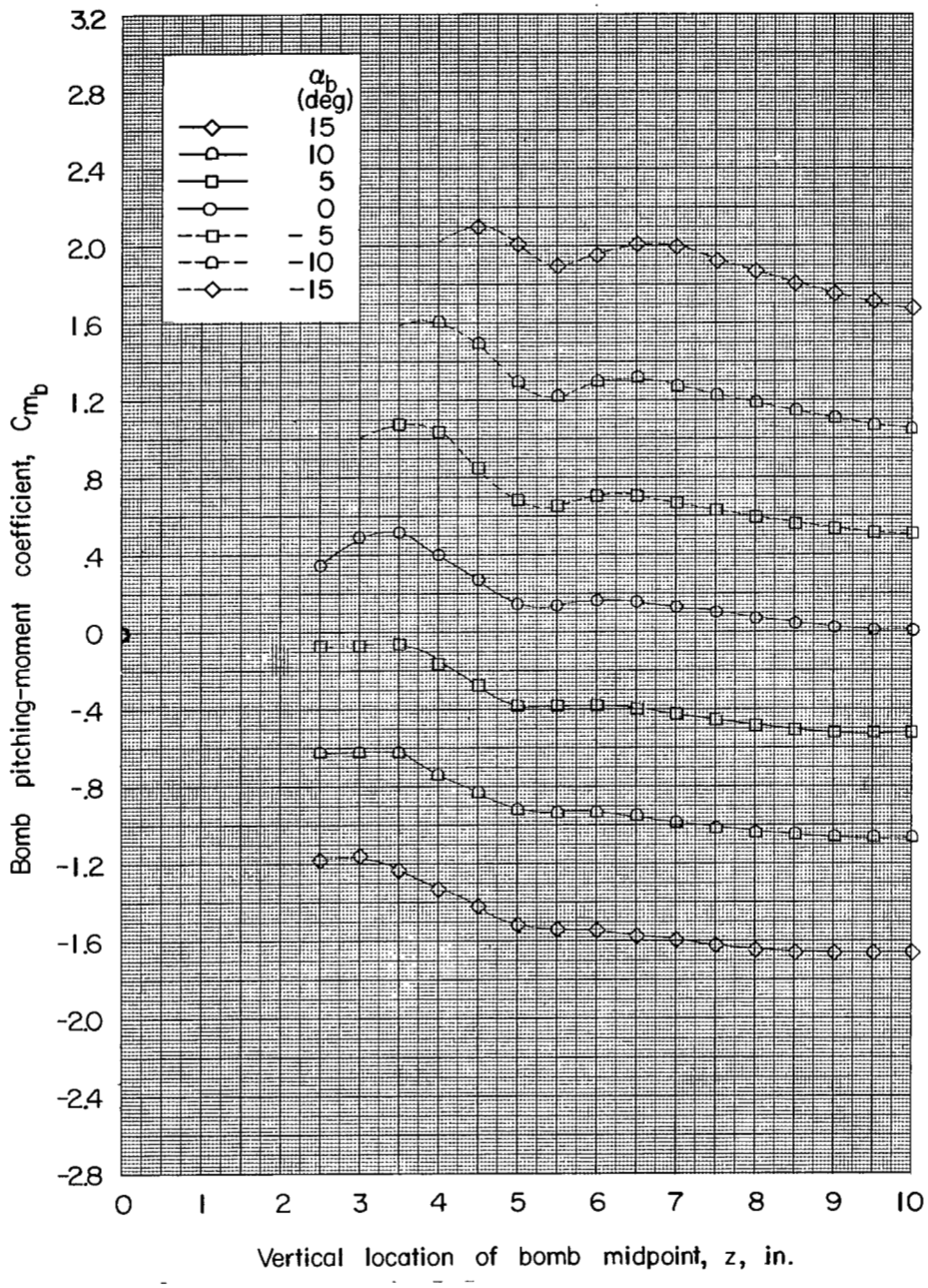

(a) Concluded.

Figure 6.- Continued.

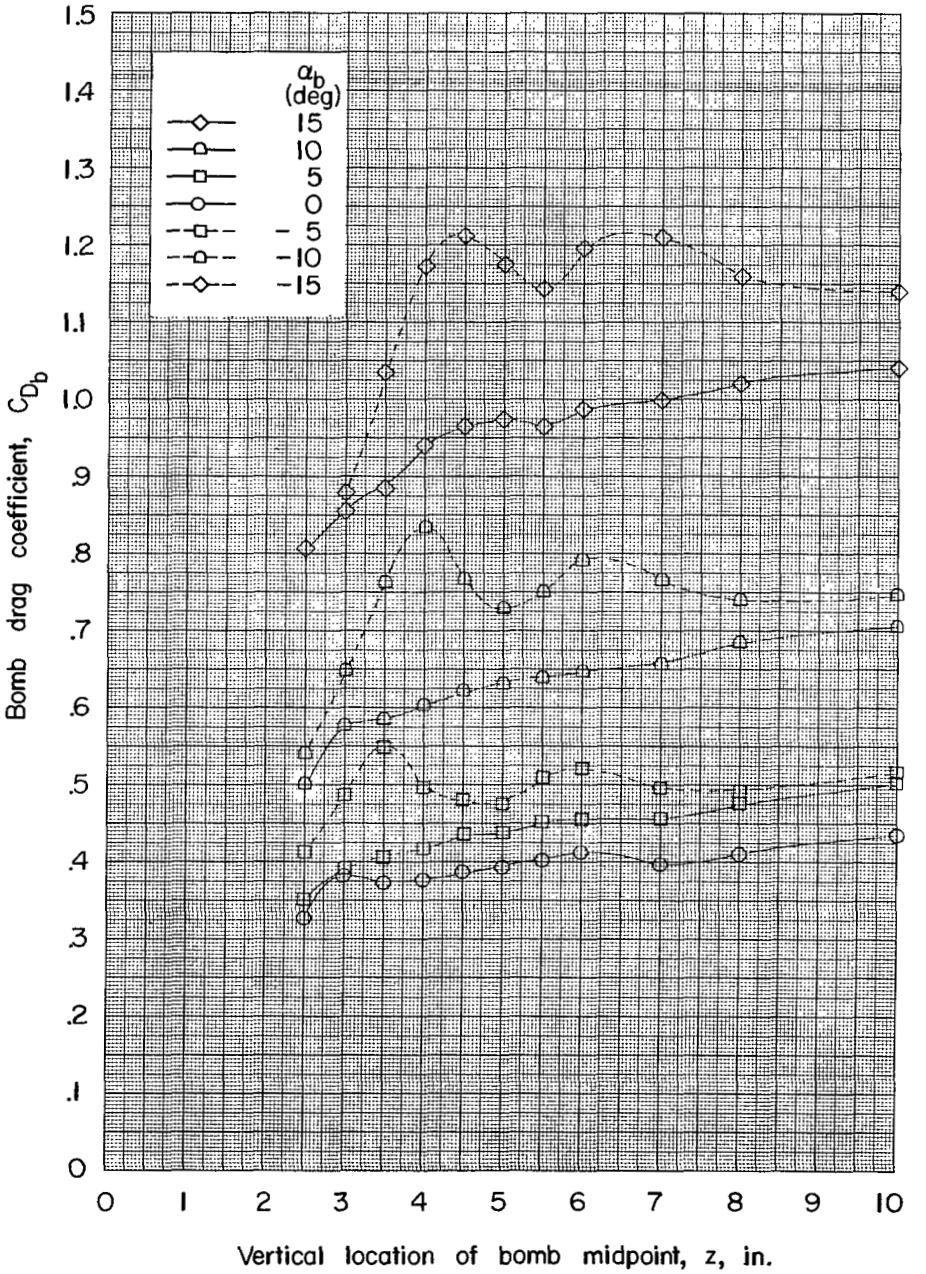

(b) x = -0.15 inch.

Figure 6.- Continued.

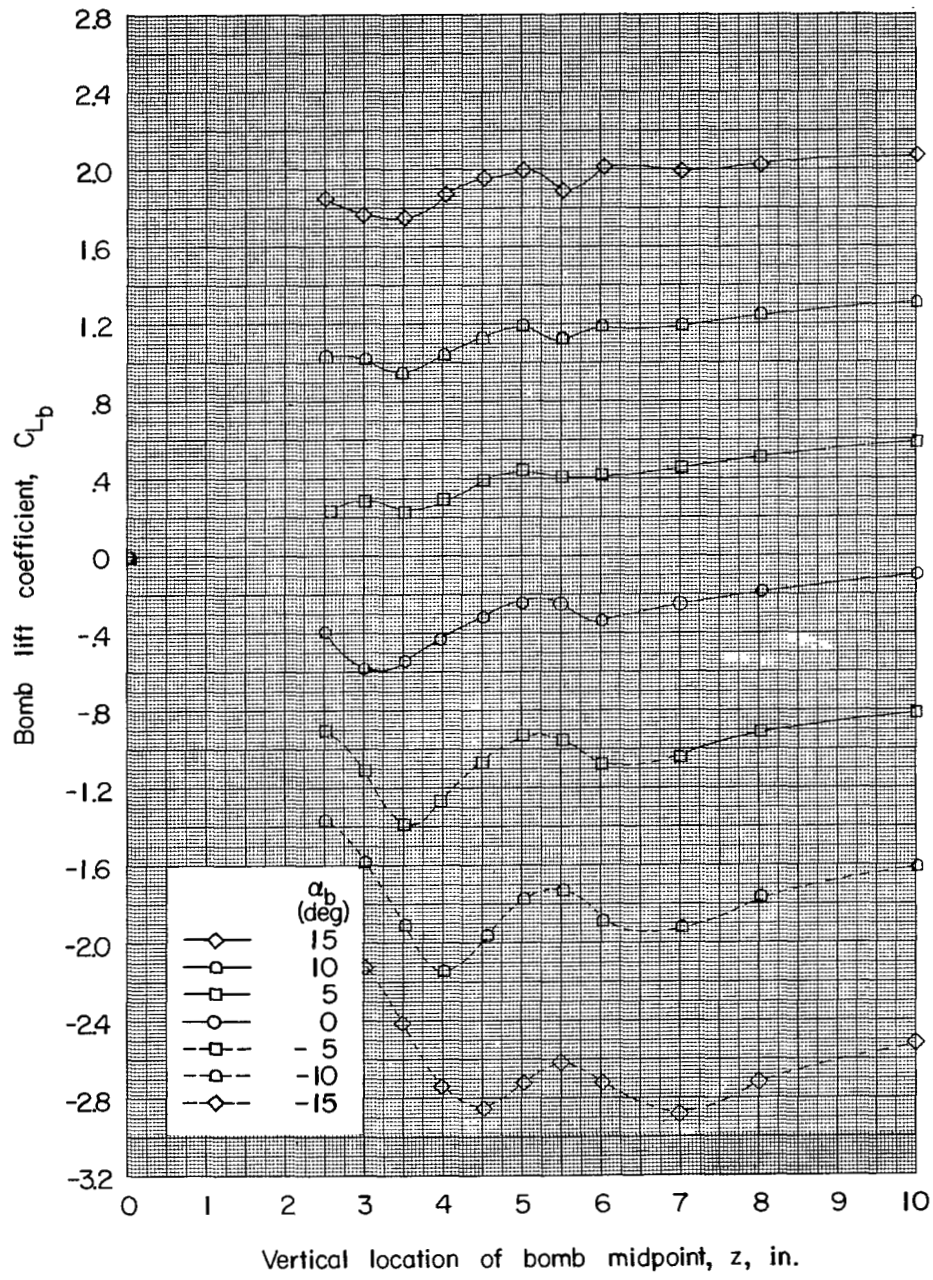

(b) Continued.

Figure 6.- Continued.

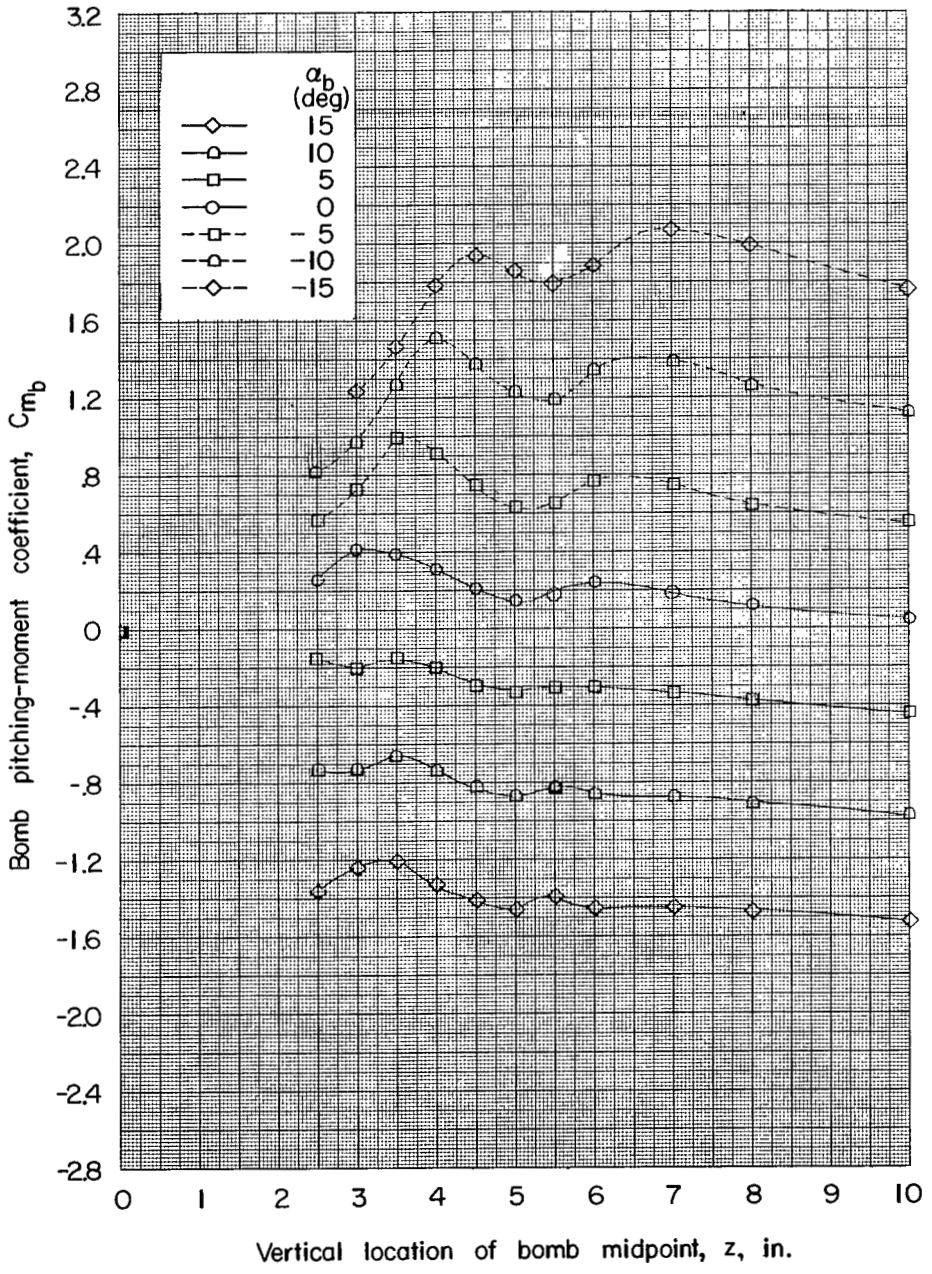

(b) Concluded.

Figure 6.- Continued.

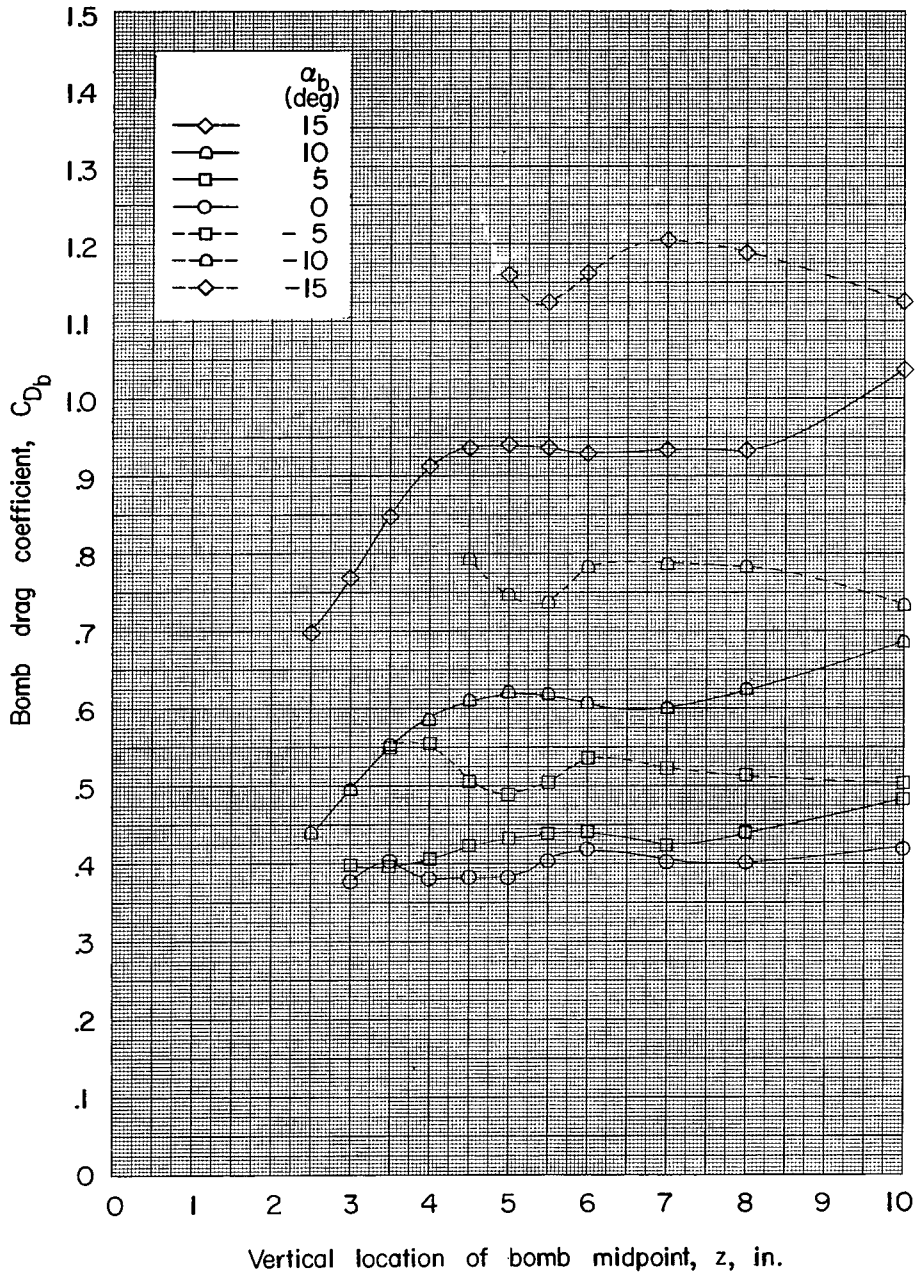

(c) x = 1.85 inches.

Figure 6.- Continued.

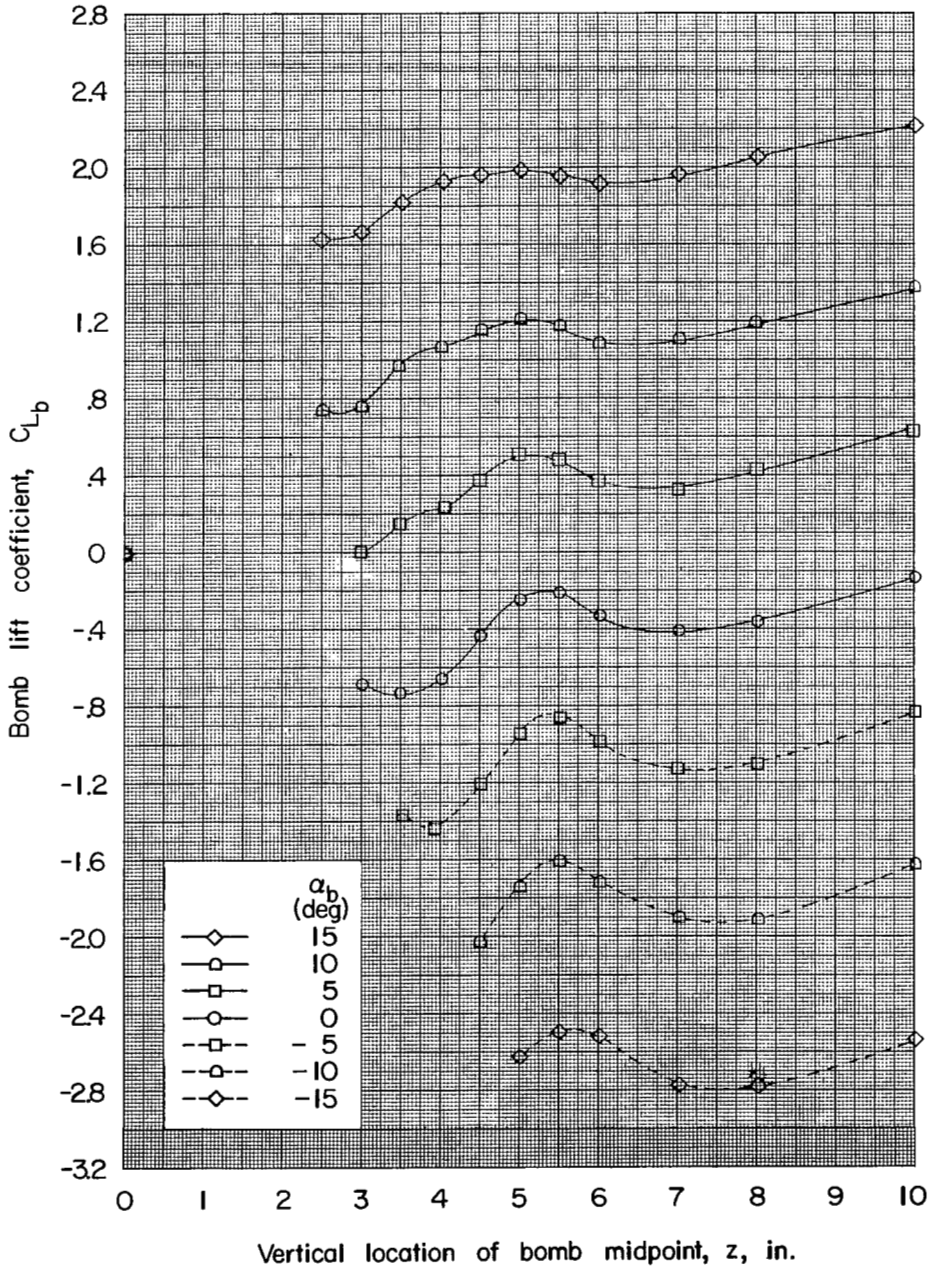

(c) Continued.

Figure 6.- Continued.

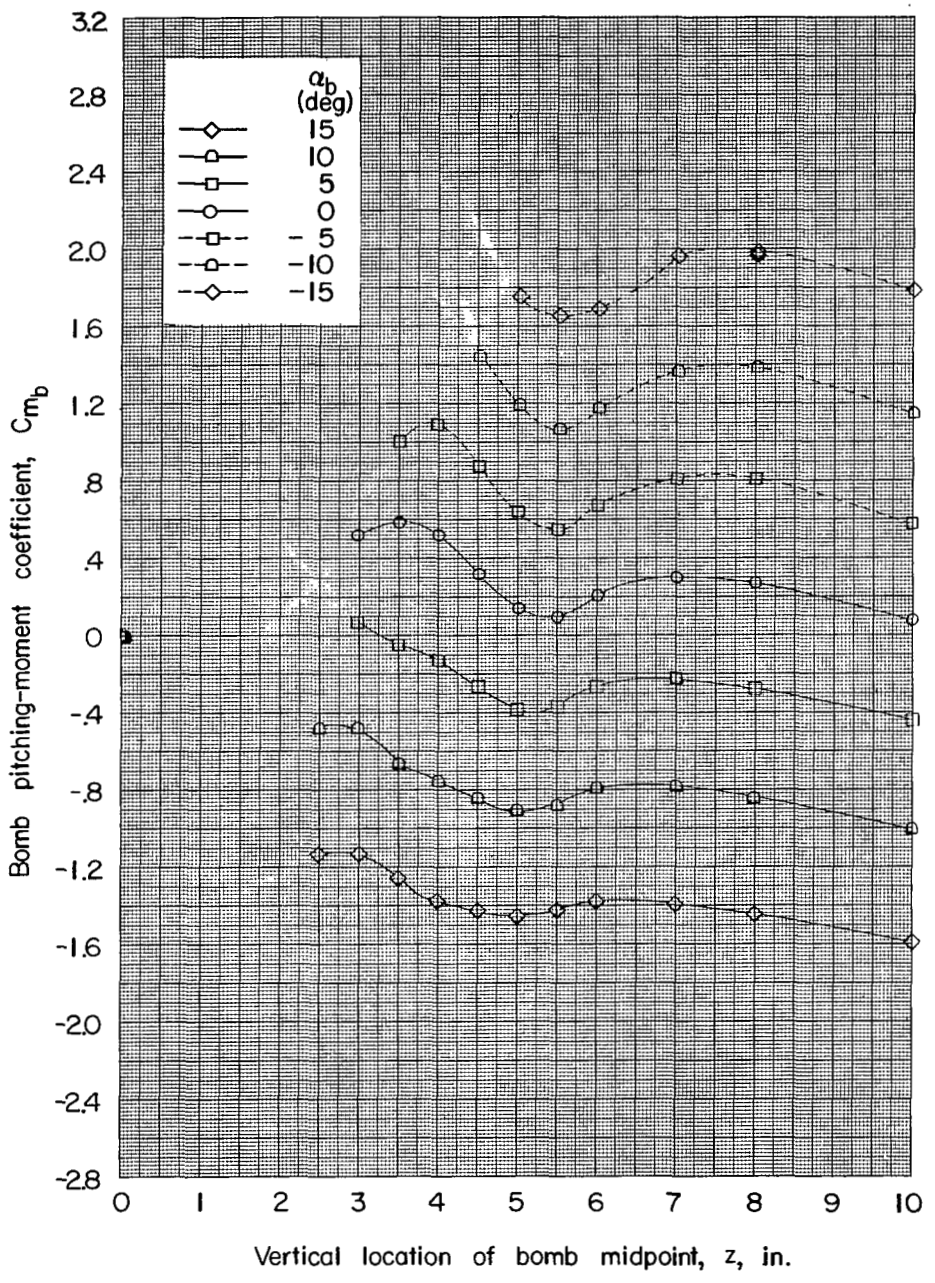

(c) Concluded.

Figure 6.- Continued.

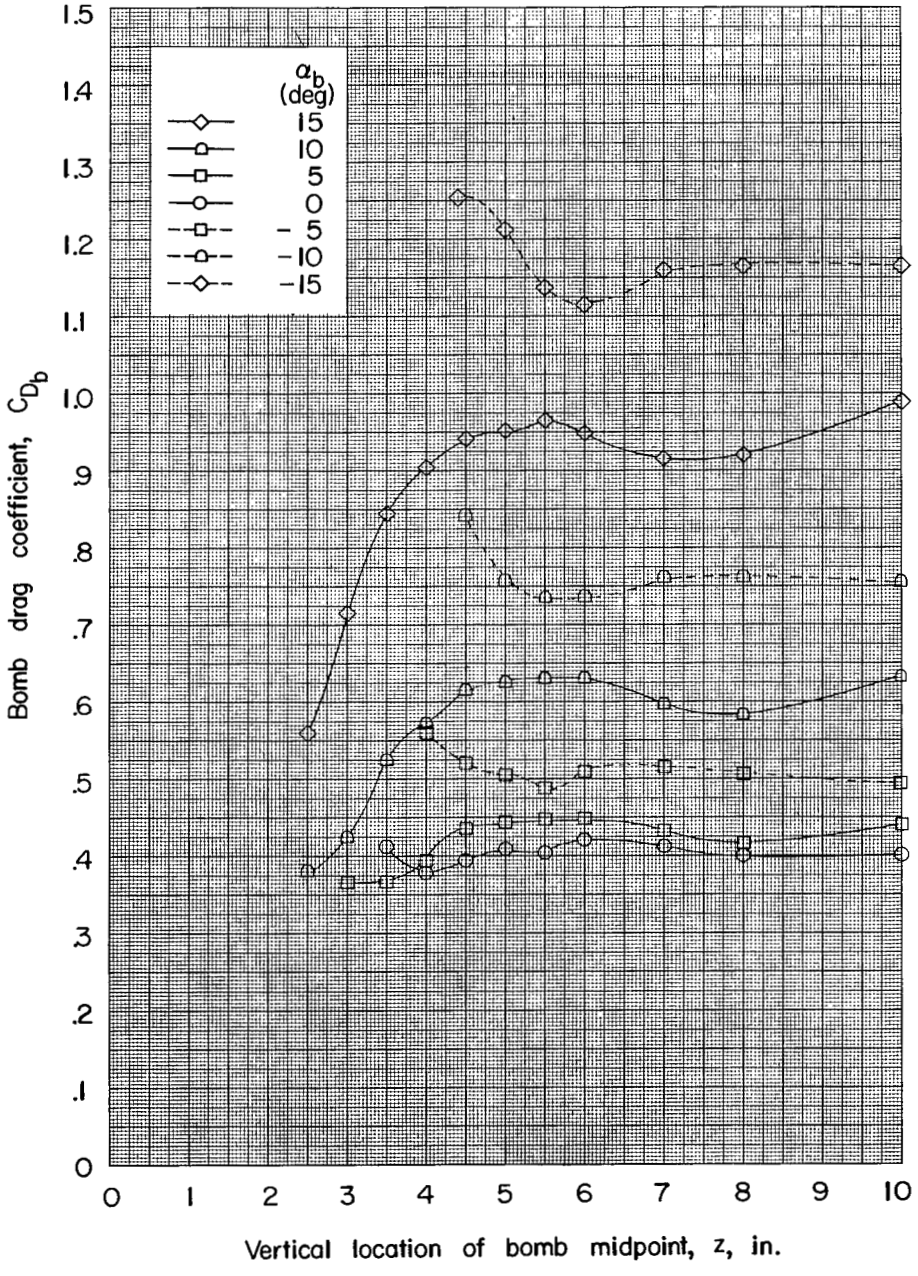

(d) x = 3.85 inches.

Figure 6.- Continued.

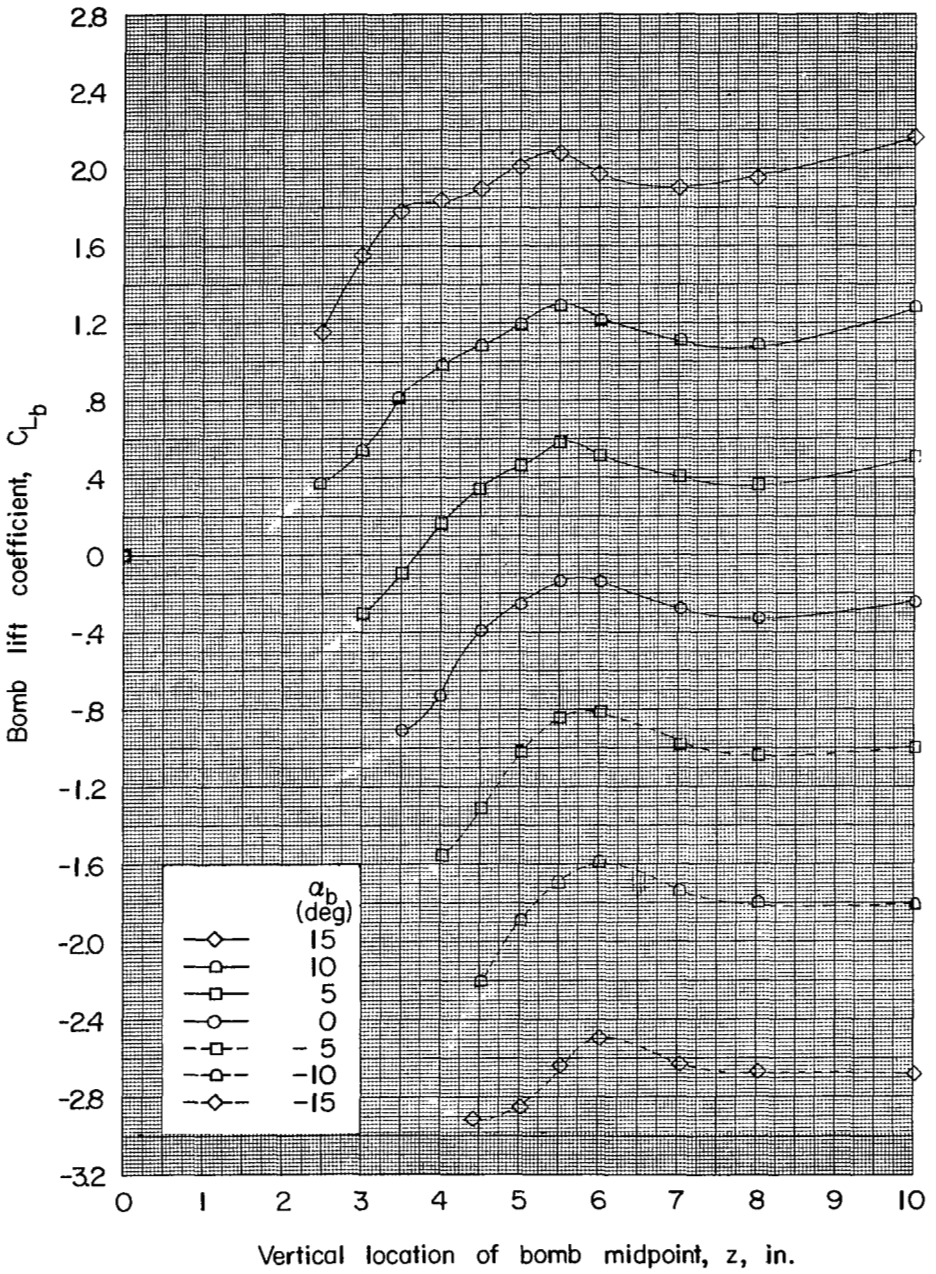

(d) Continued.

Figure 6.- Continued.

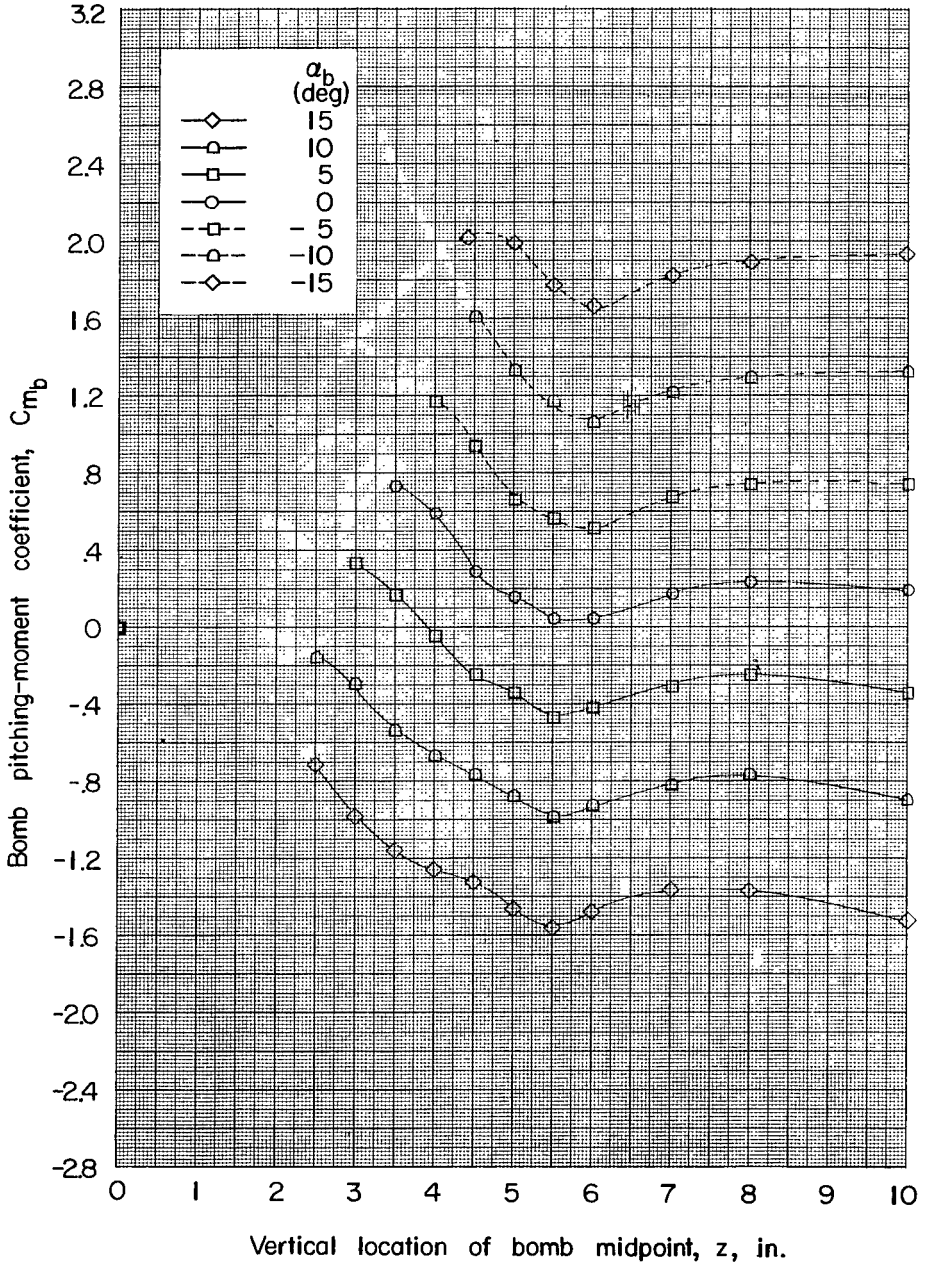

(d) Concluded.

Figure 6.- Concluded.

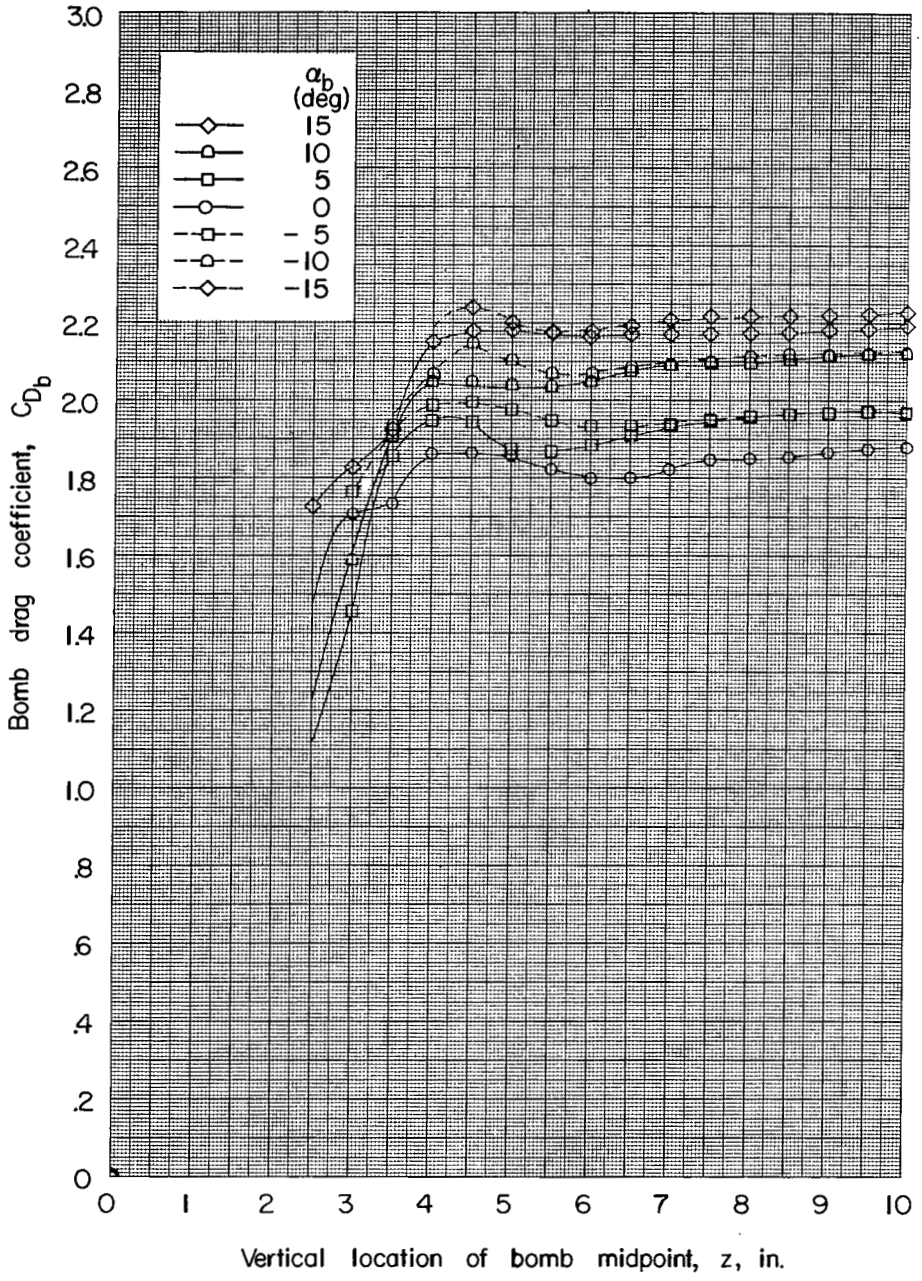

(a) x = -1.50 inches.

Figure 7.- Force and moment data for bomb 1 in presence of the wing-fuselage combination with ejector C. $\alpha_b = 4^\circ$.

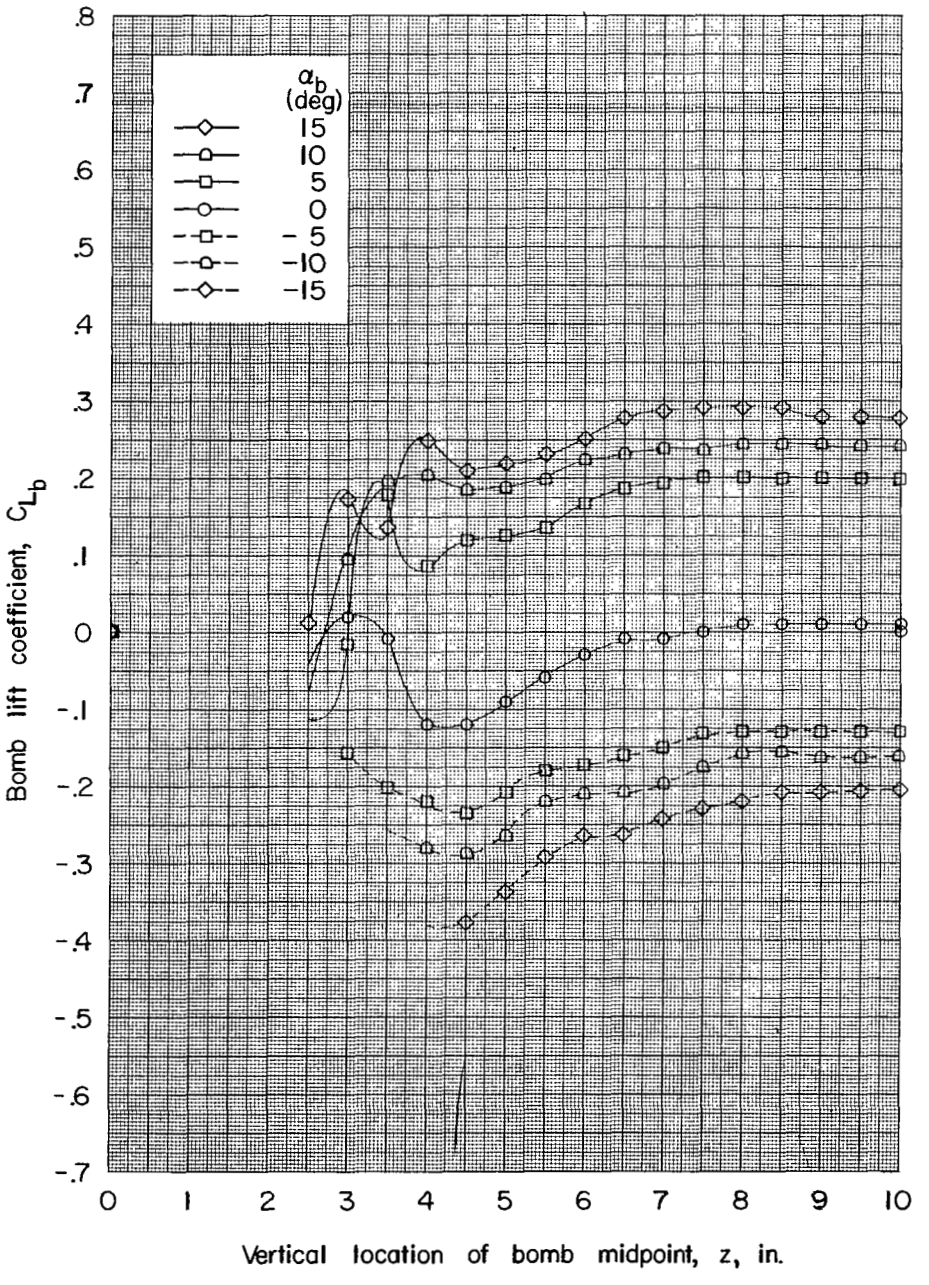

(a) Continued.

Figure 7.- Continued.

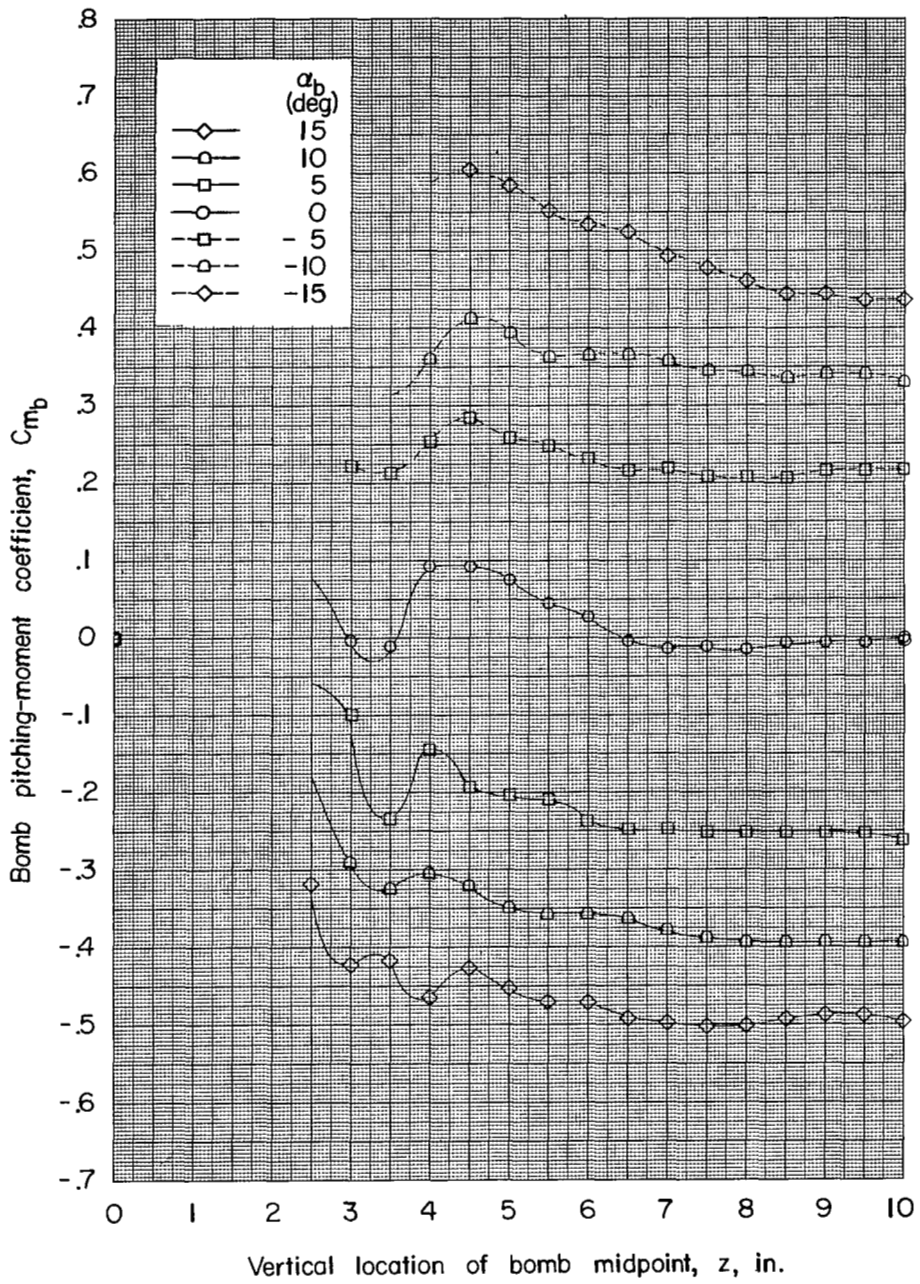

(a) Concluded.

Figure 7.- Continued.

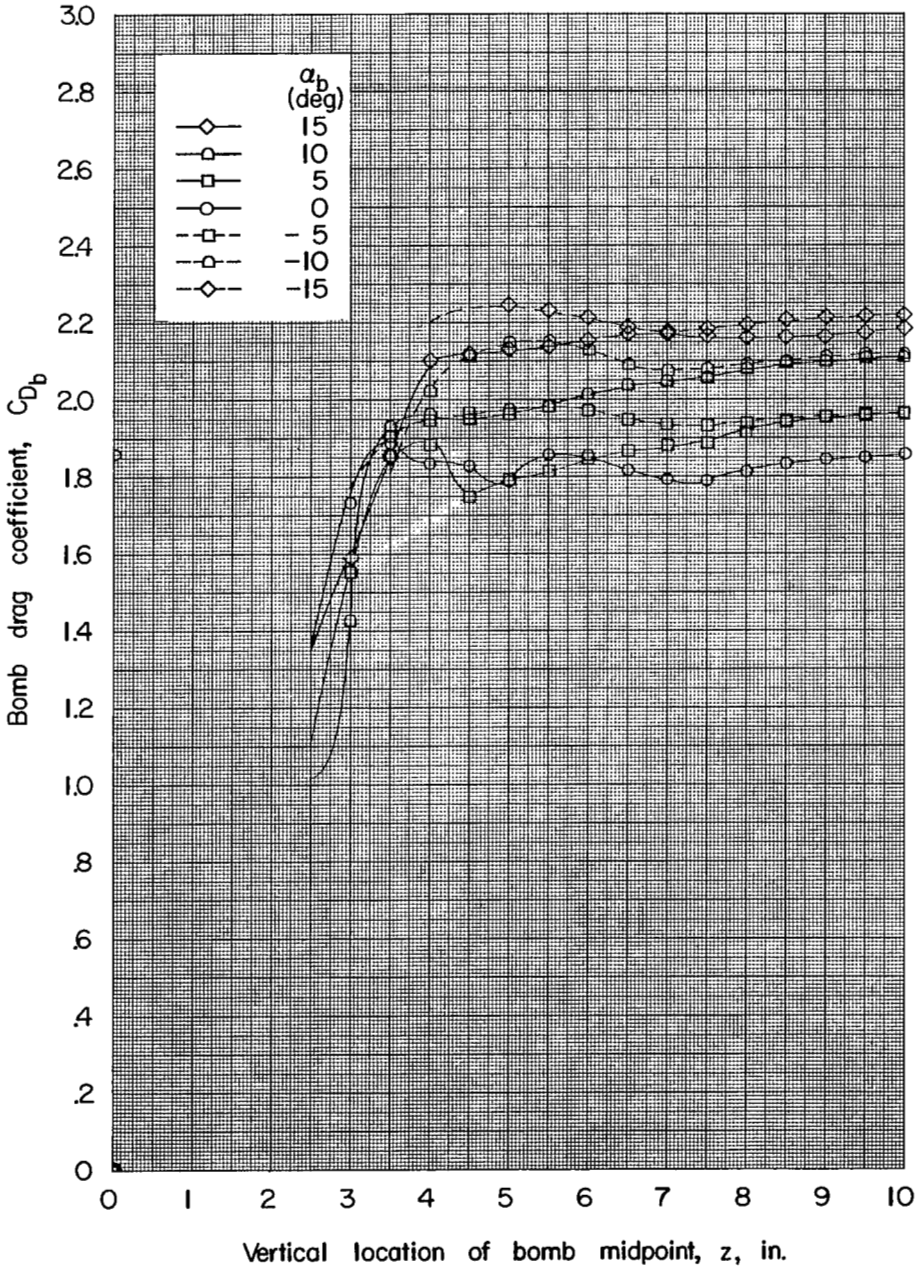

(b) x = -0.37 inch.

Figure 7.- Continued.

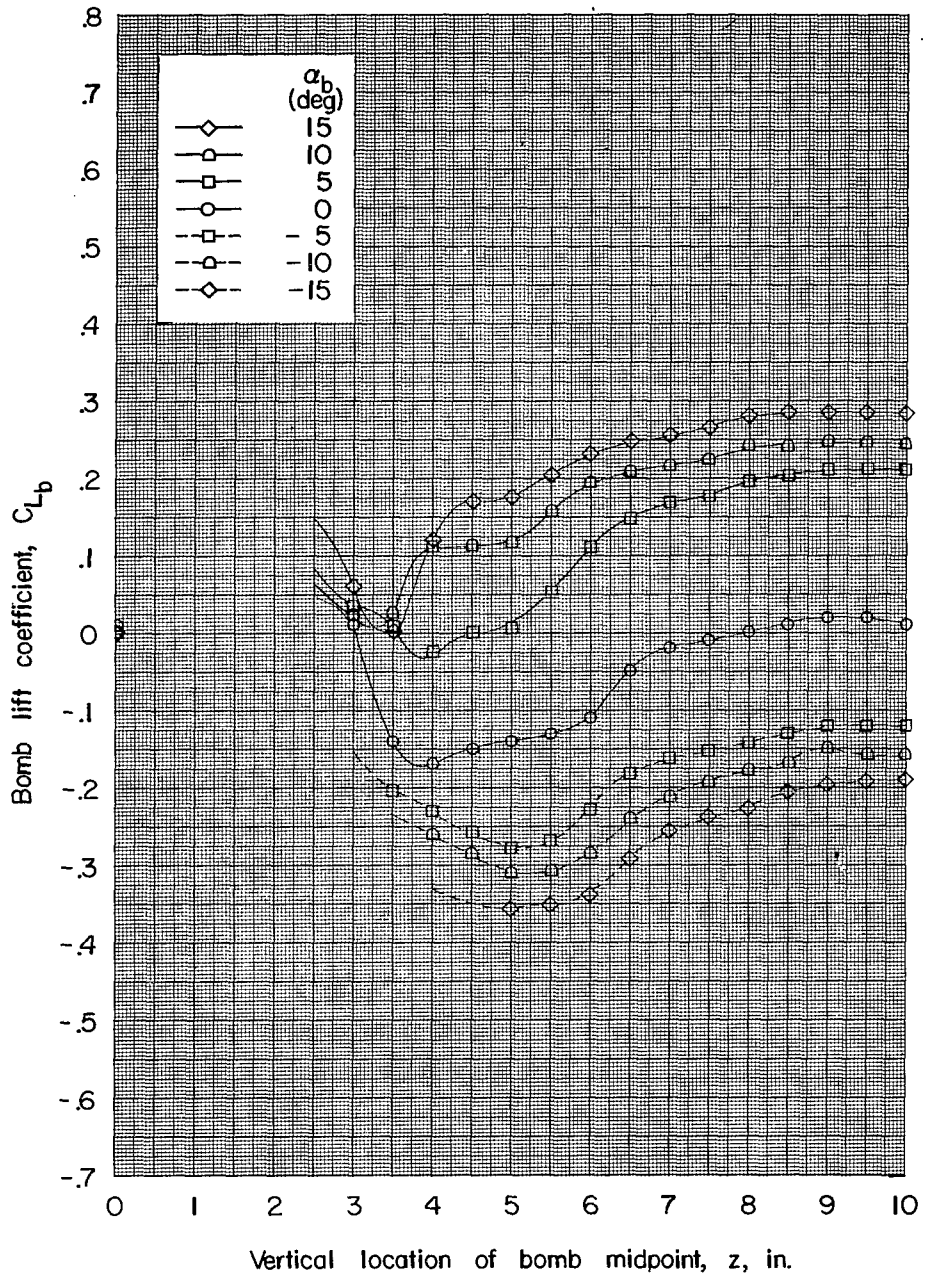

(b) Continued.

Figure 7.- Continued.

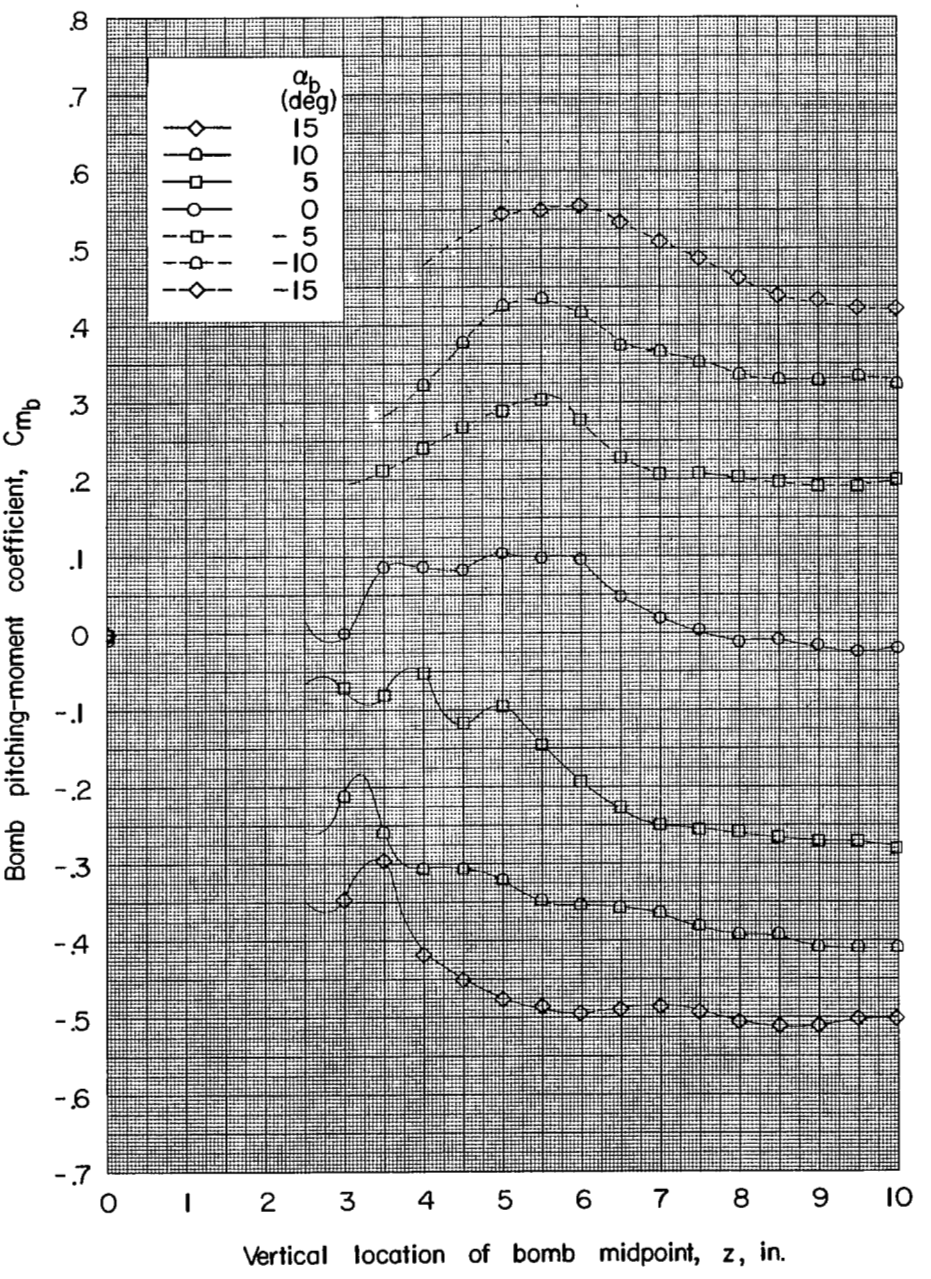

(b) Concluded.

Figure 7.- Continued.

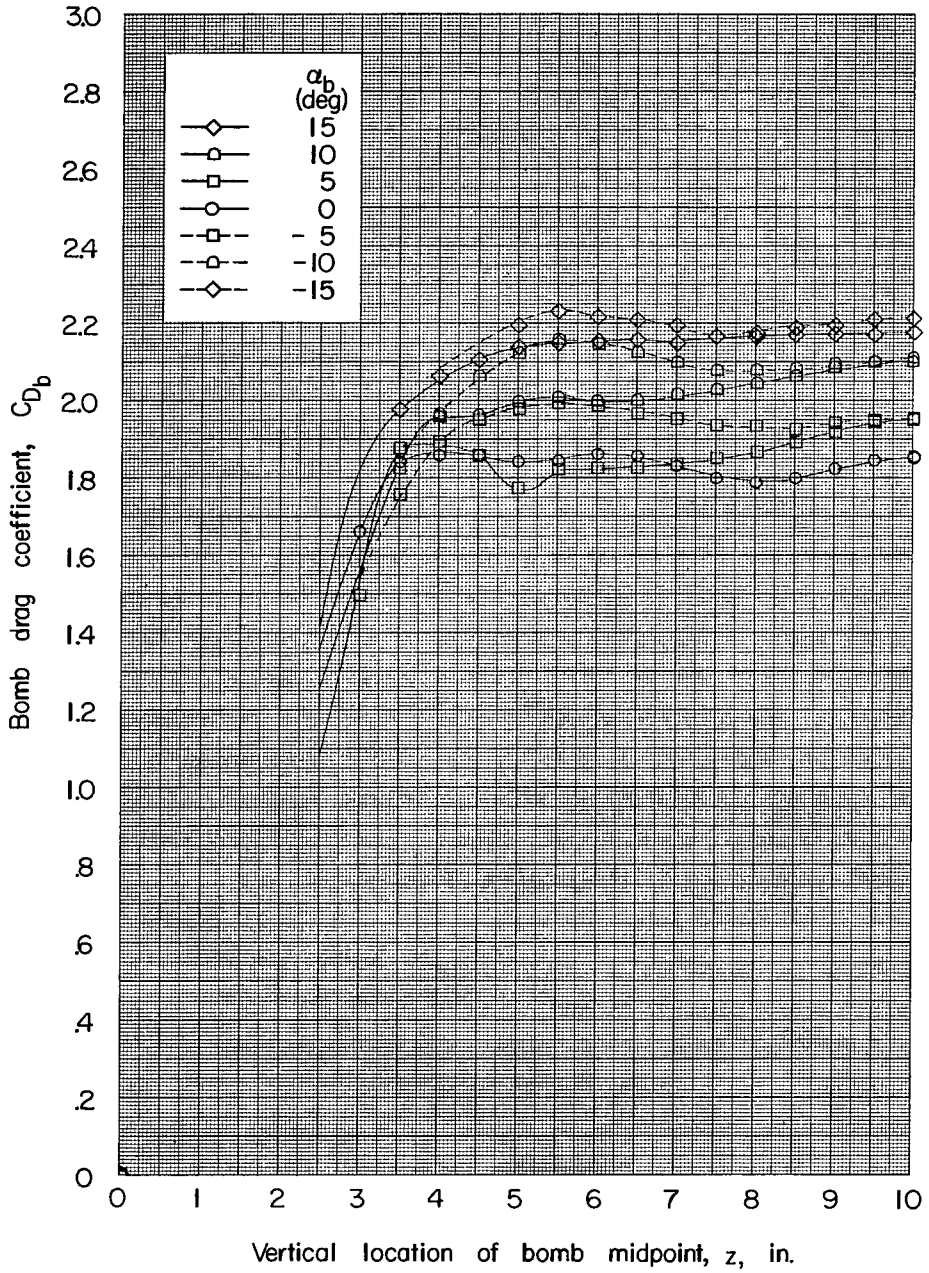

(c) x = 0.50 inch.

Figure 7.- Continued.

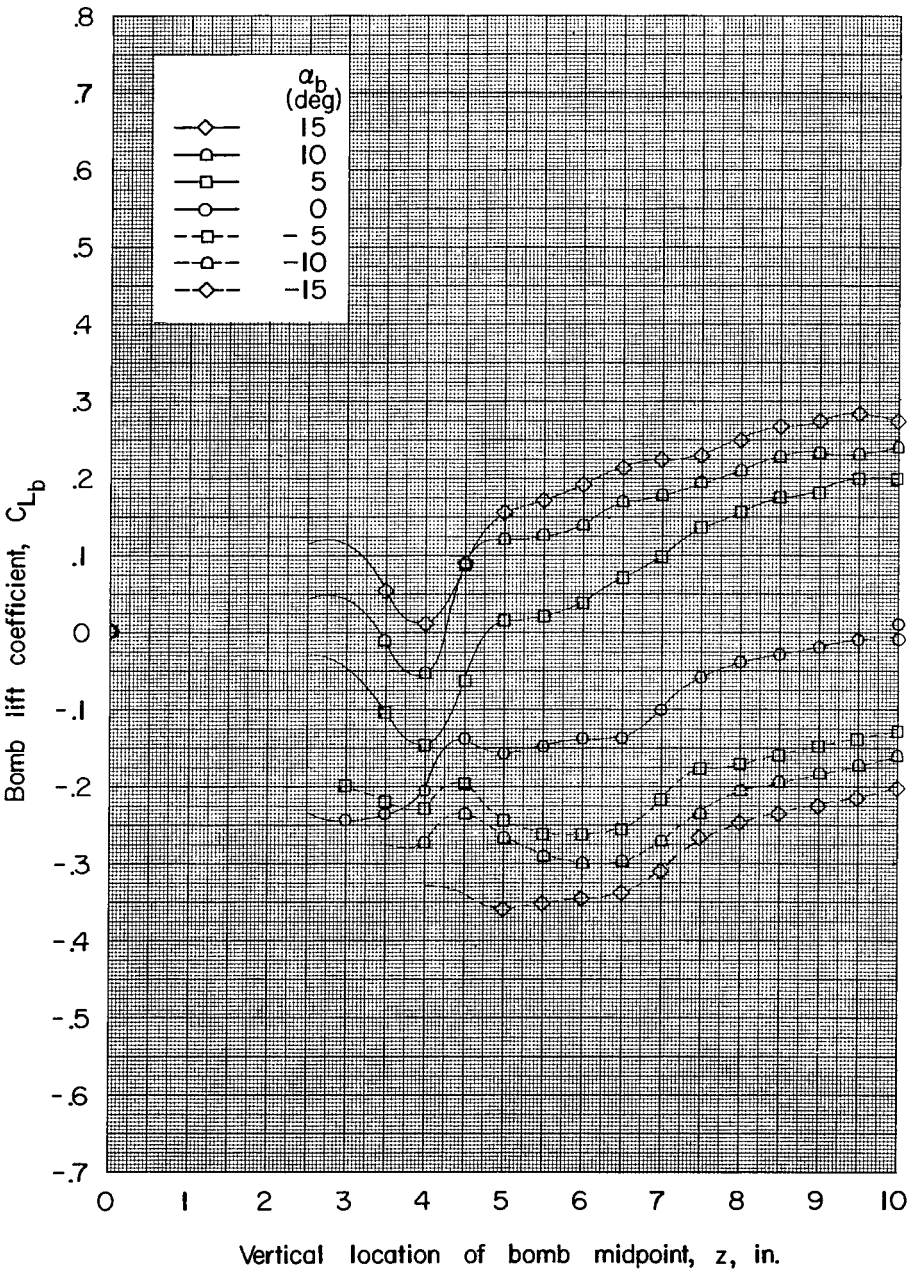

(c) Continued.

Figure 7.- Continued.

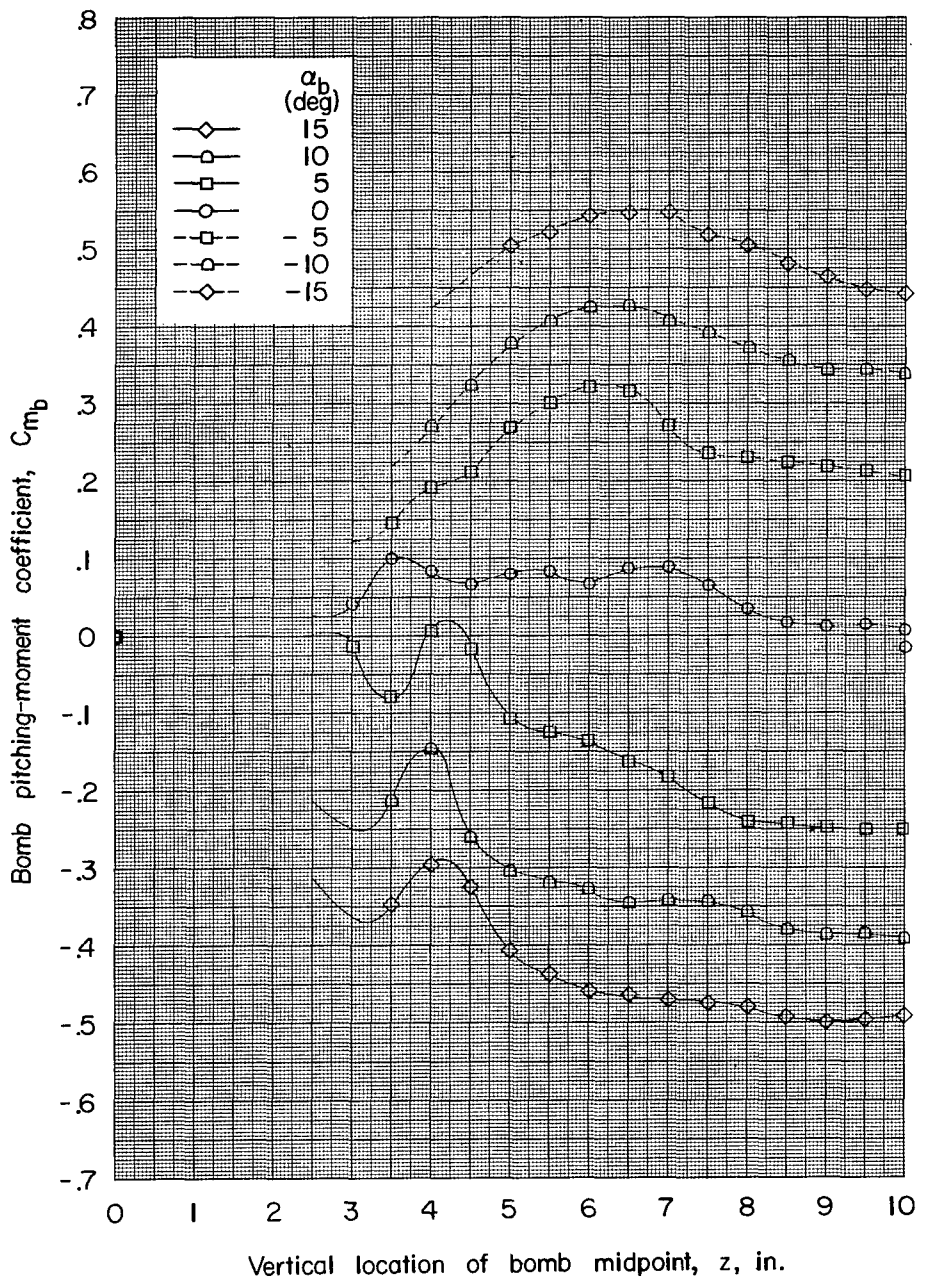

(c) Concluded.

Figure 7.- Continued.

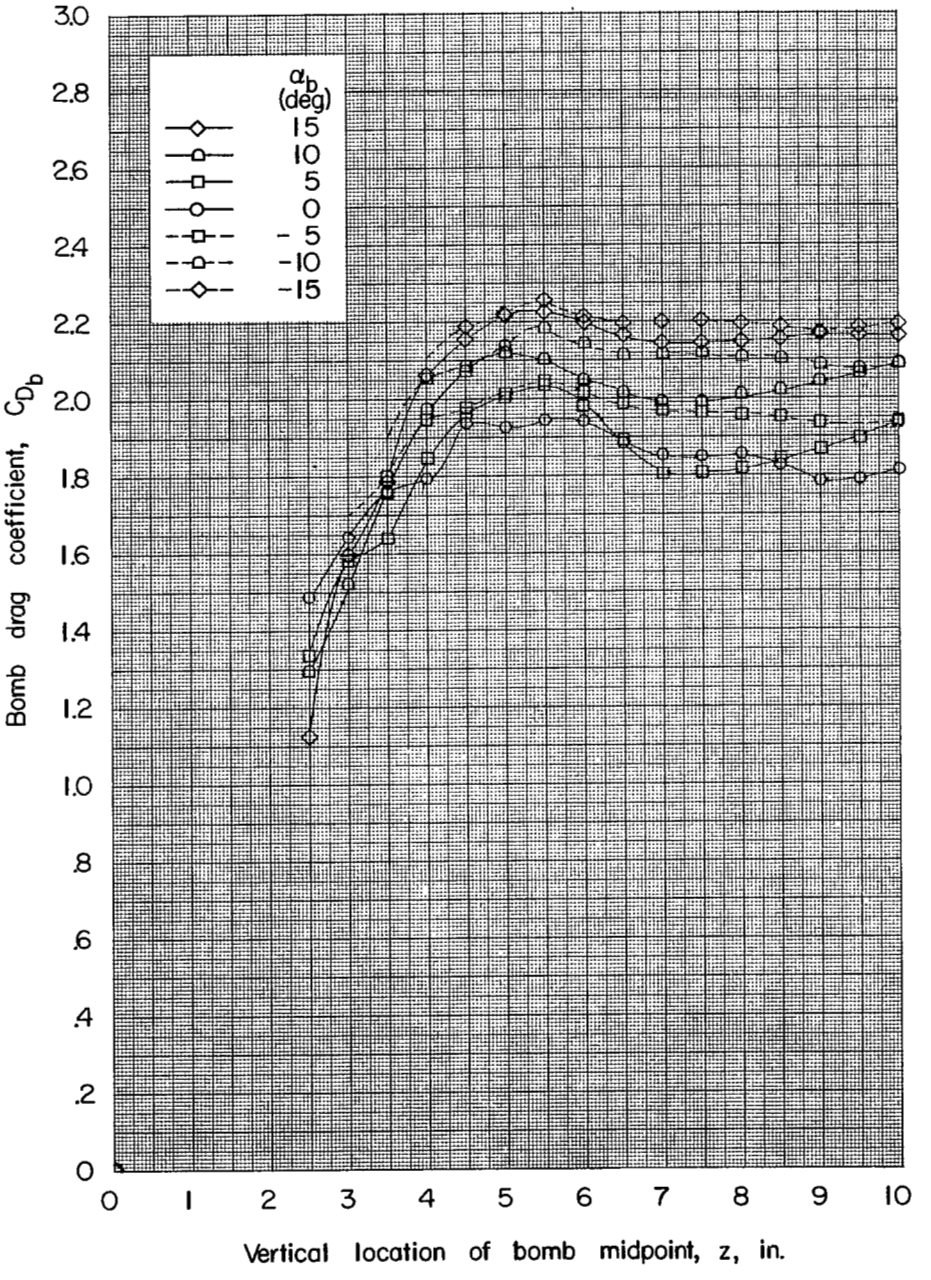

(d) x = 2.00 inches.

Figure 7.- Continued.

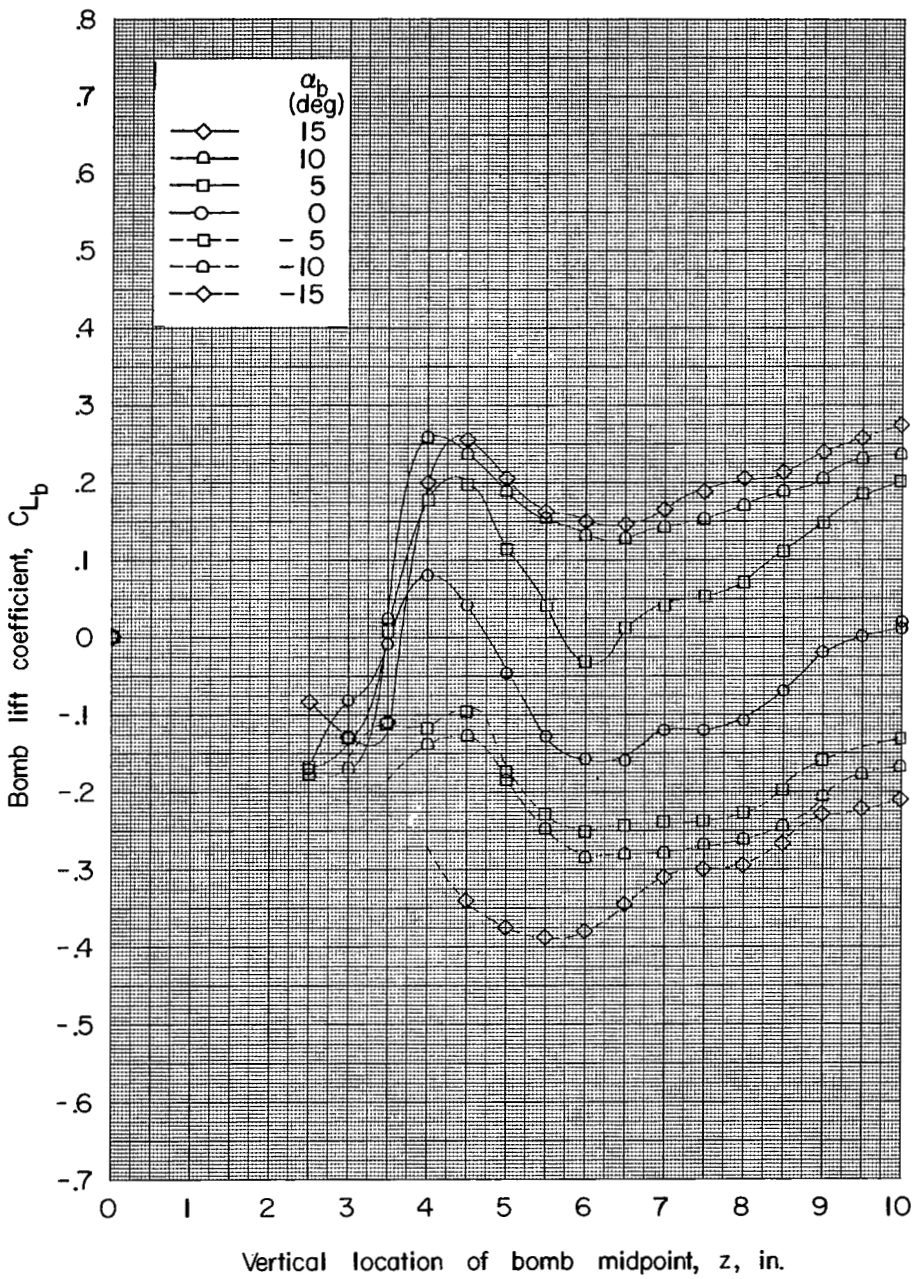

(d) Continued.

Figure 7.- Continued.

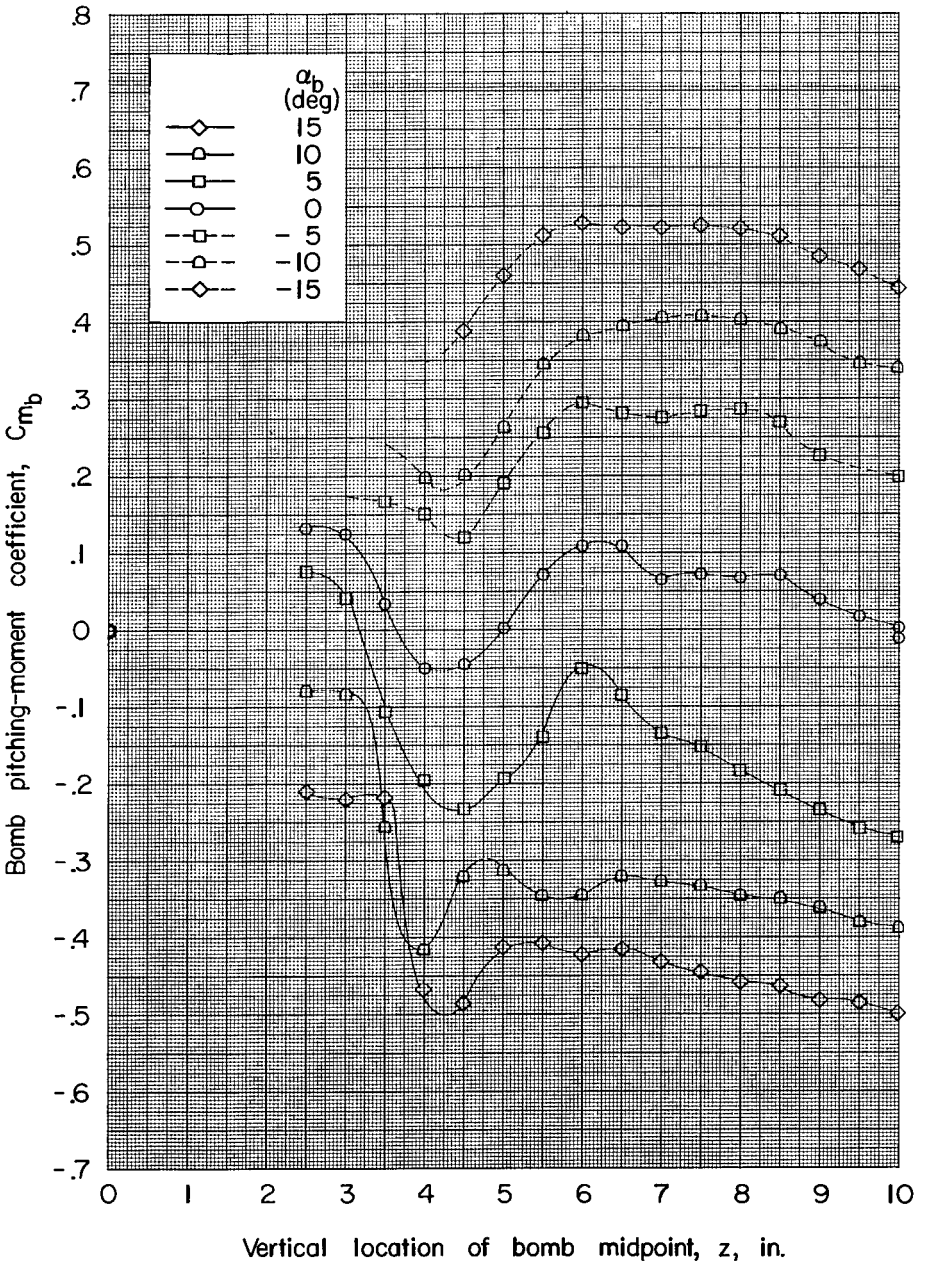

(d) Concluded.

Figure 7.- Continued.

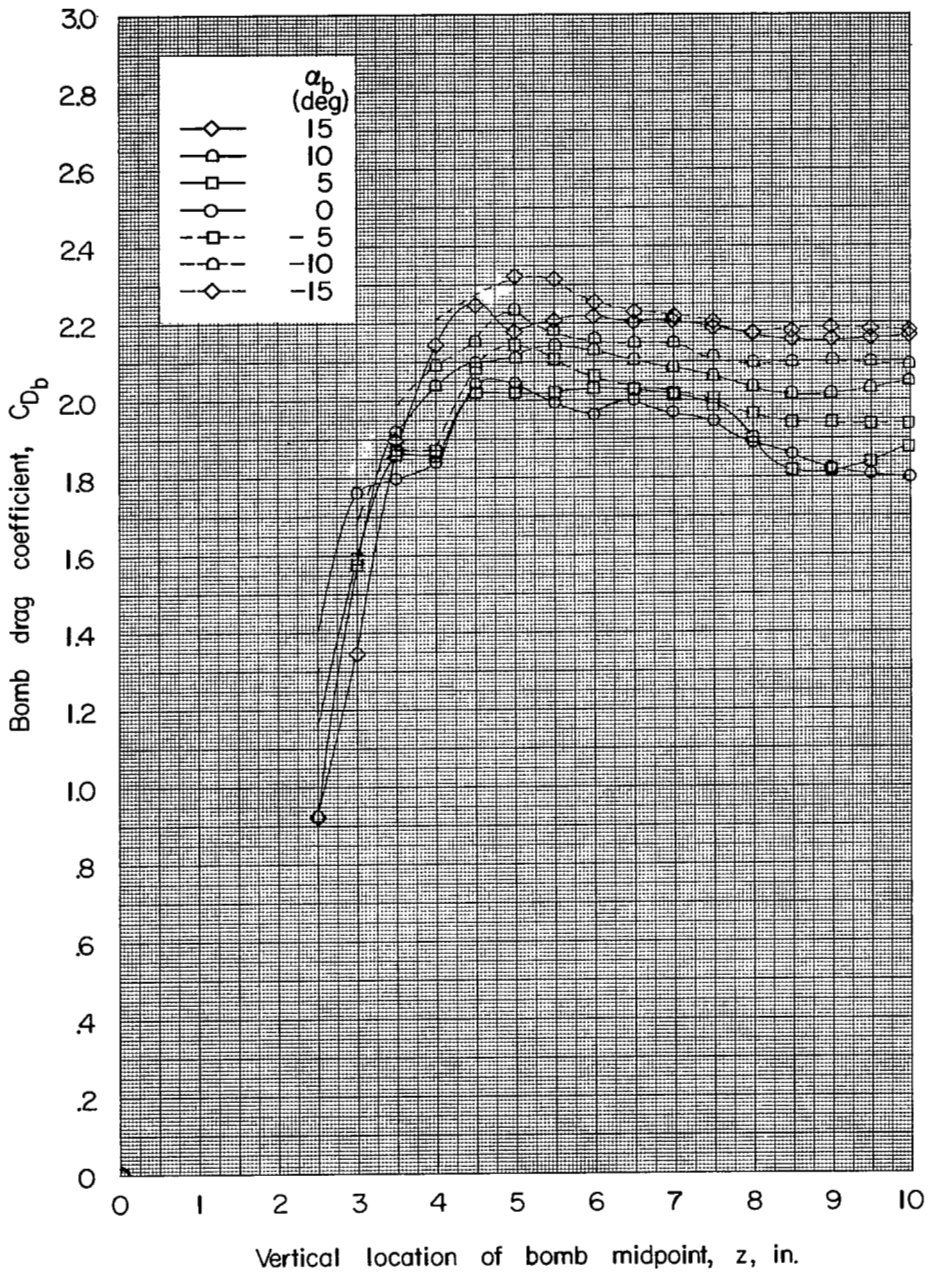

(e) x = 4.00 inches.

Figure 7.- Continued.

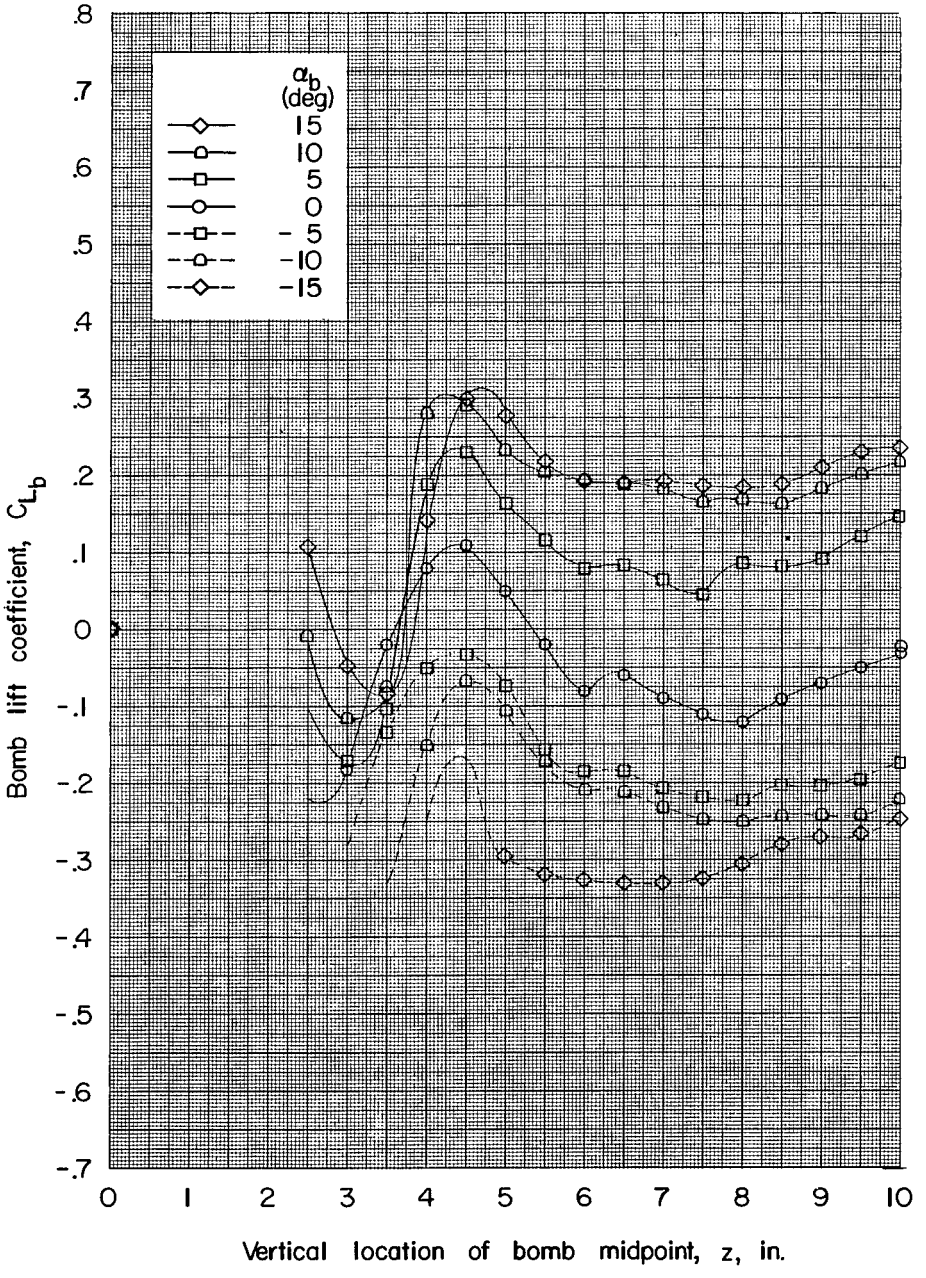

(e) Continued.

Figure 7.- Continued.

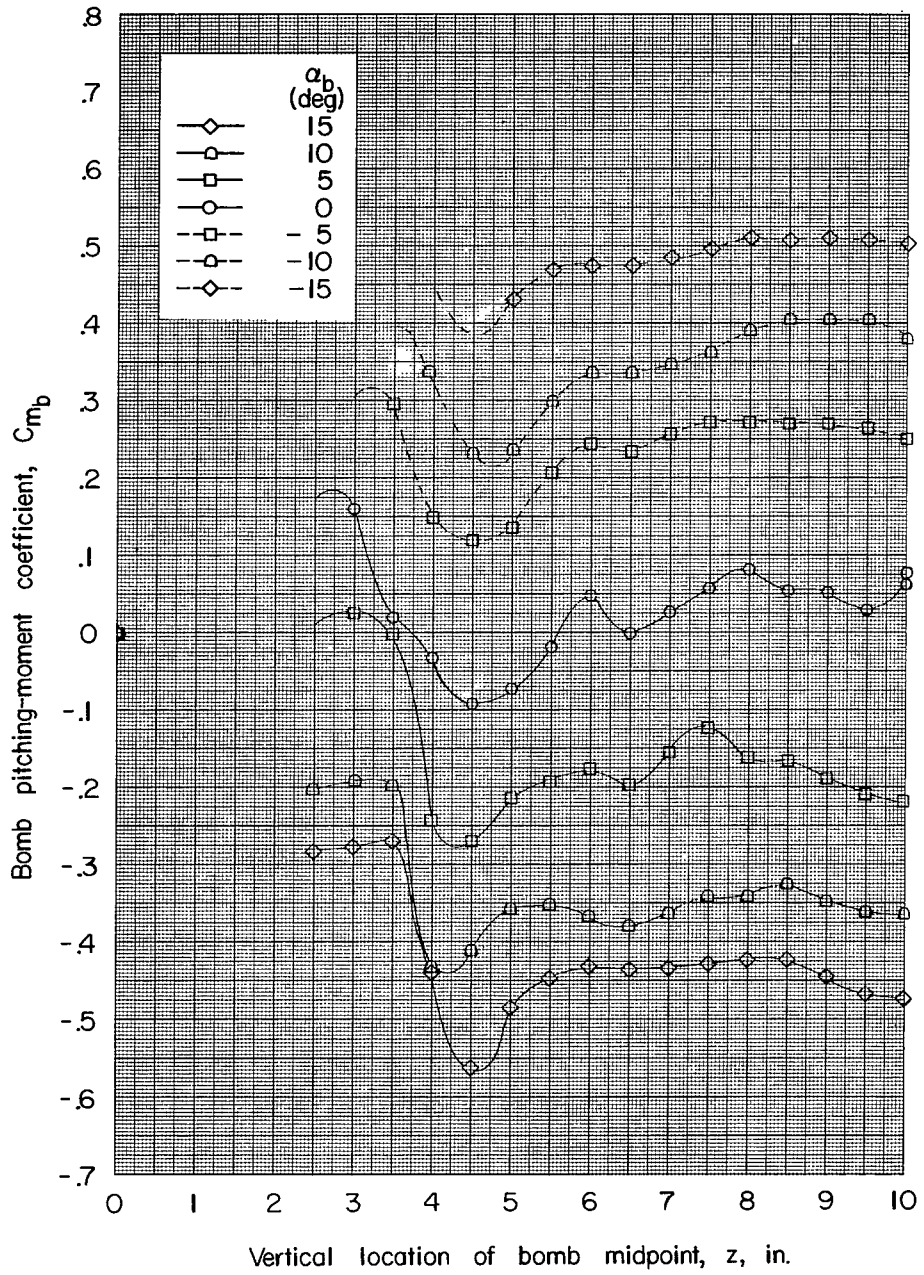

(e) Concluded.

Figure 7.- Continued.

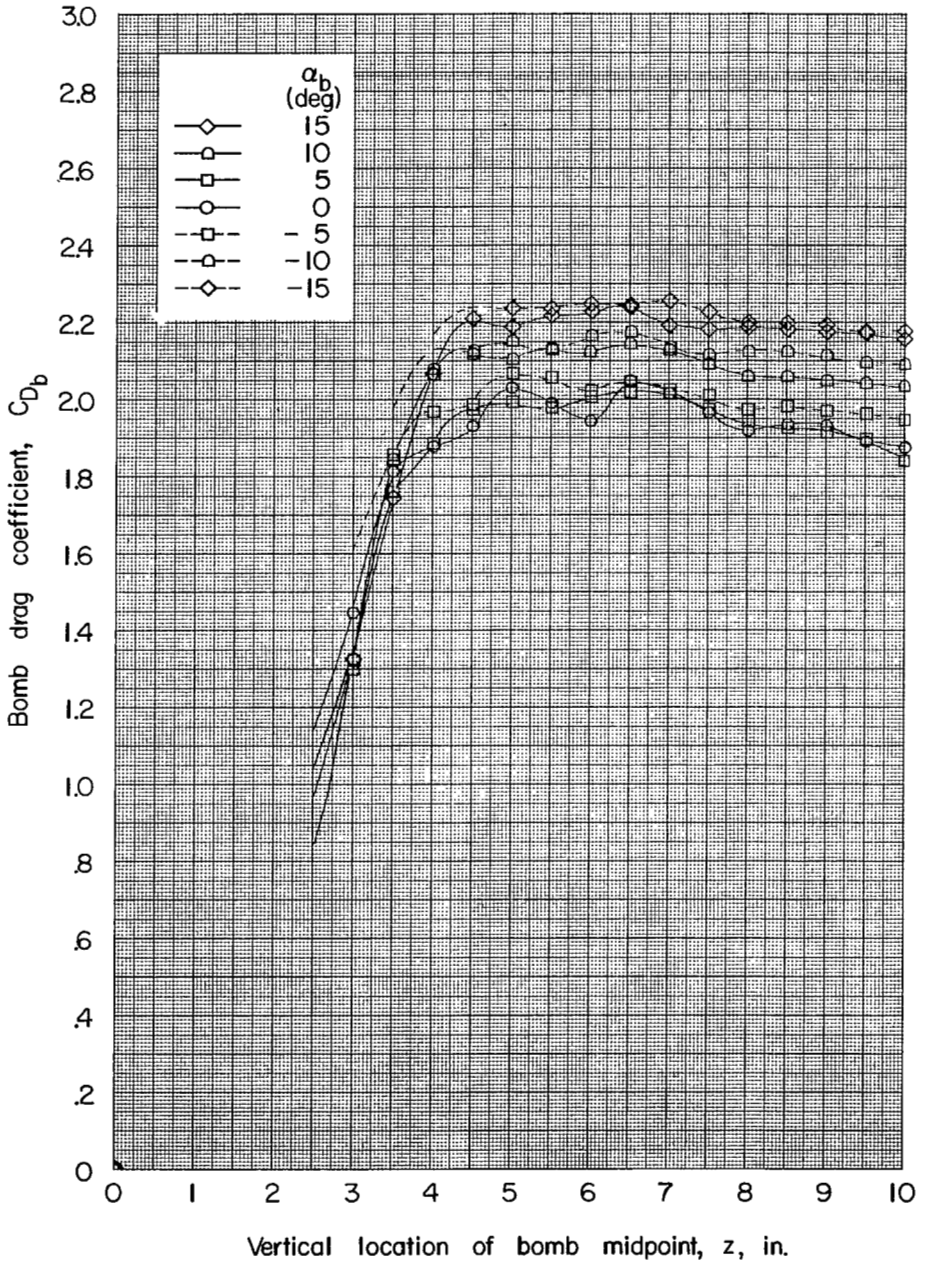

(f) x = 6.00 inches.

Figure 7.- Continued.

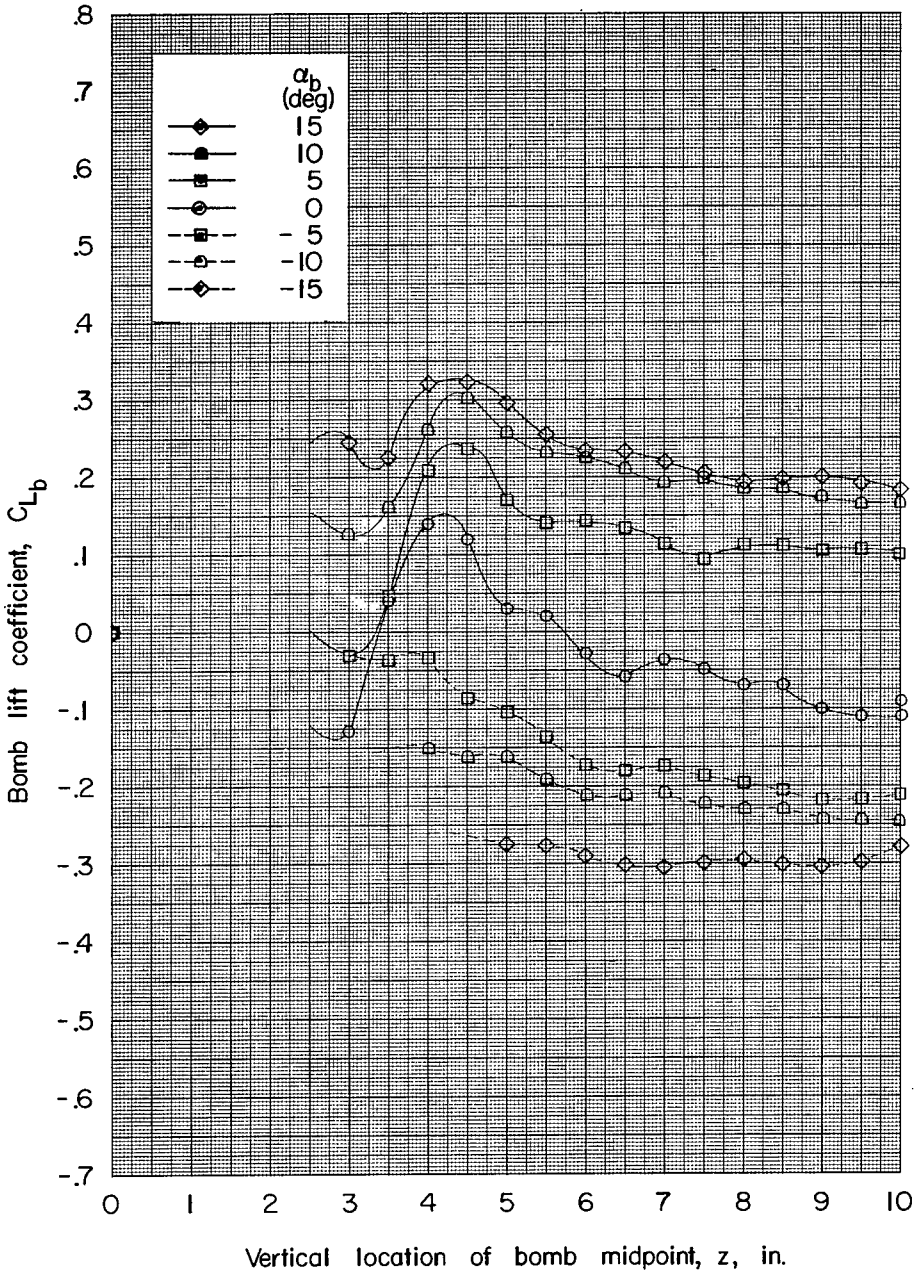

(f) Continued.

Figure 7.- Continued.

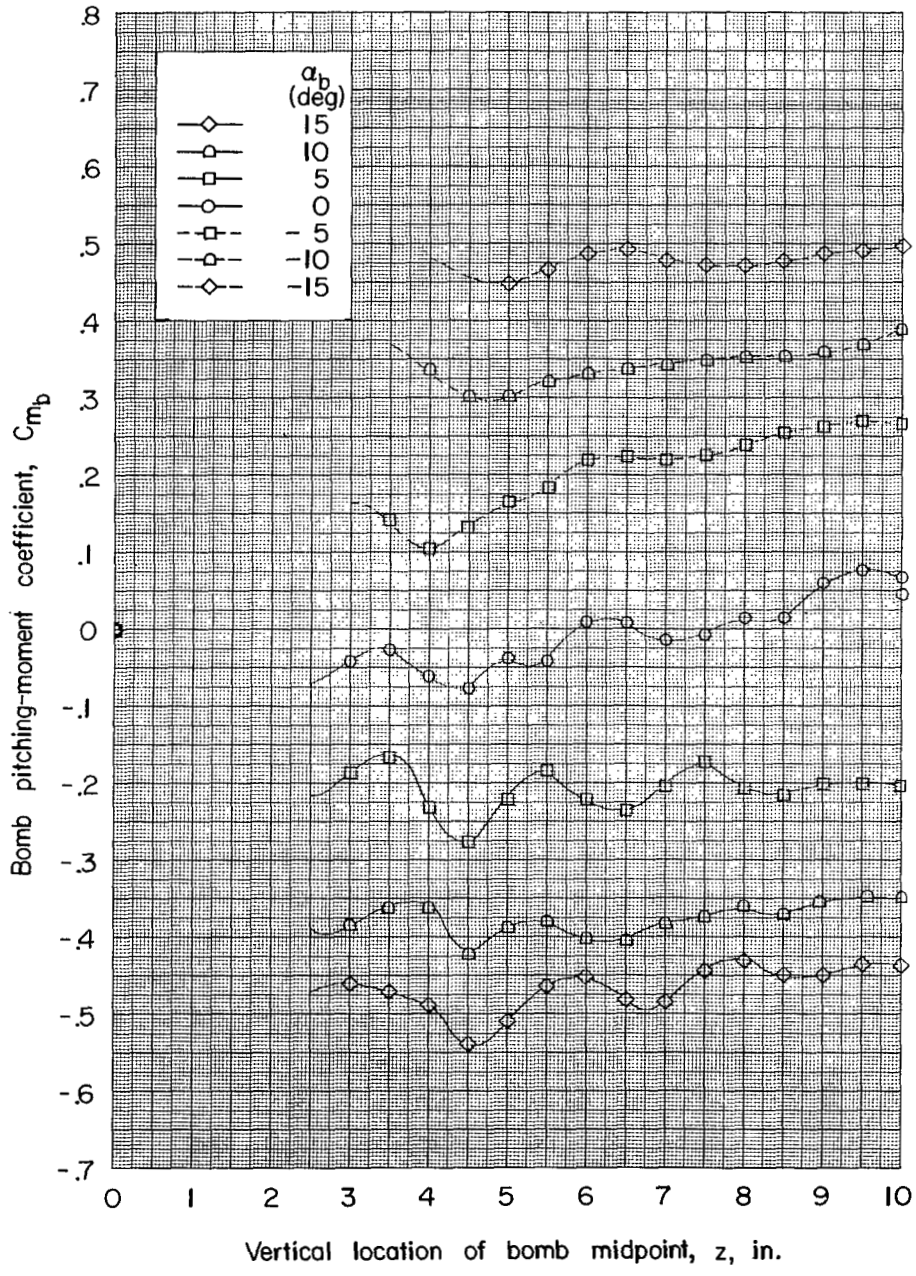

(f) Concluded.

Figure 7.- Continued.

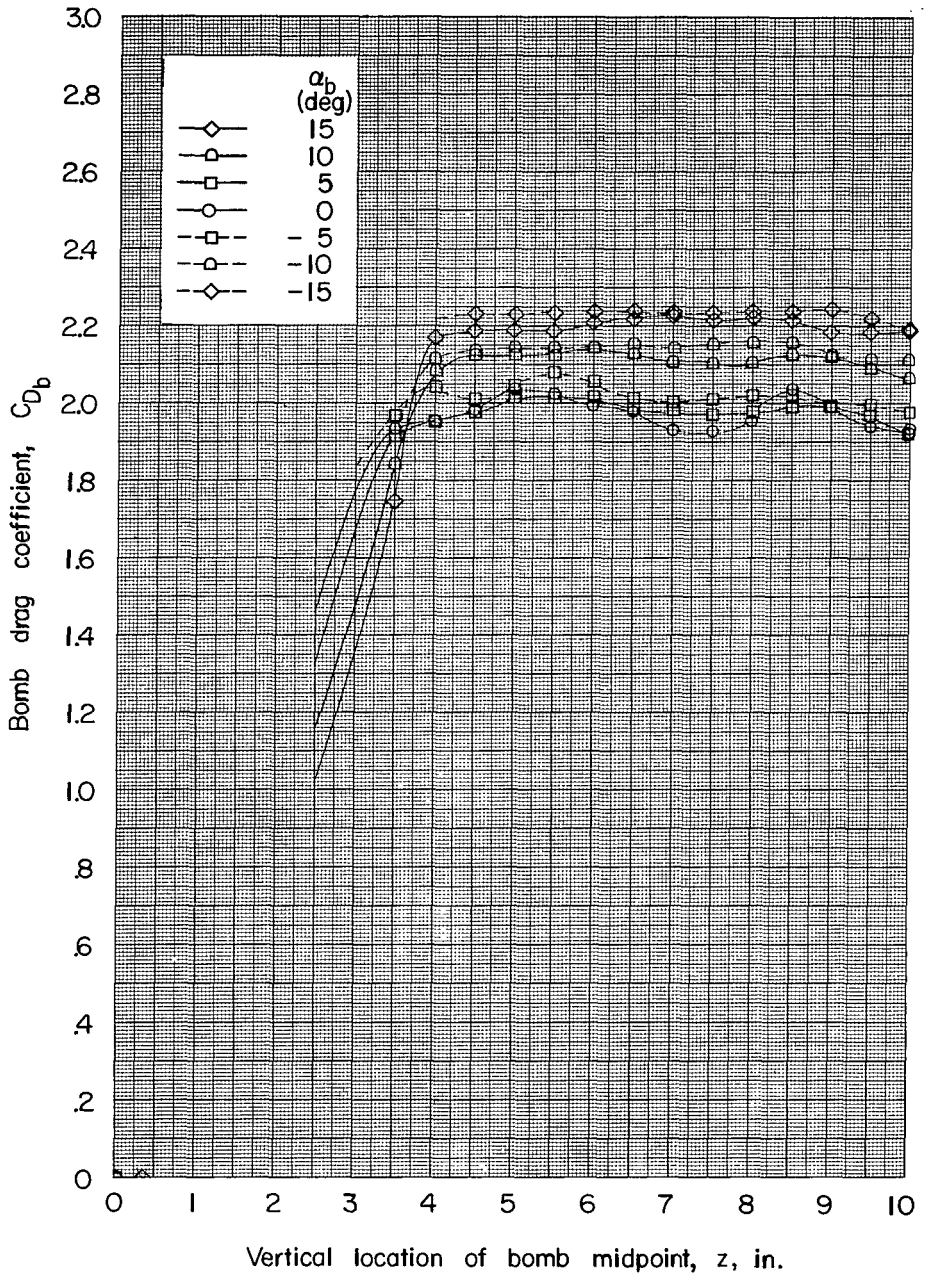

(g) x = 8.00 inches.

Figure 7.- Continued.

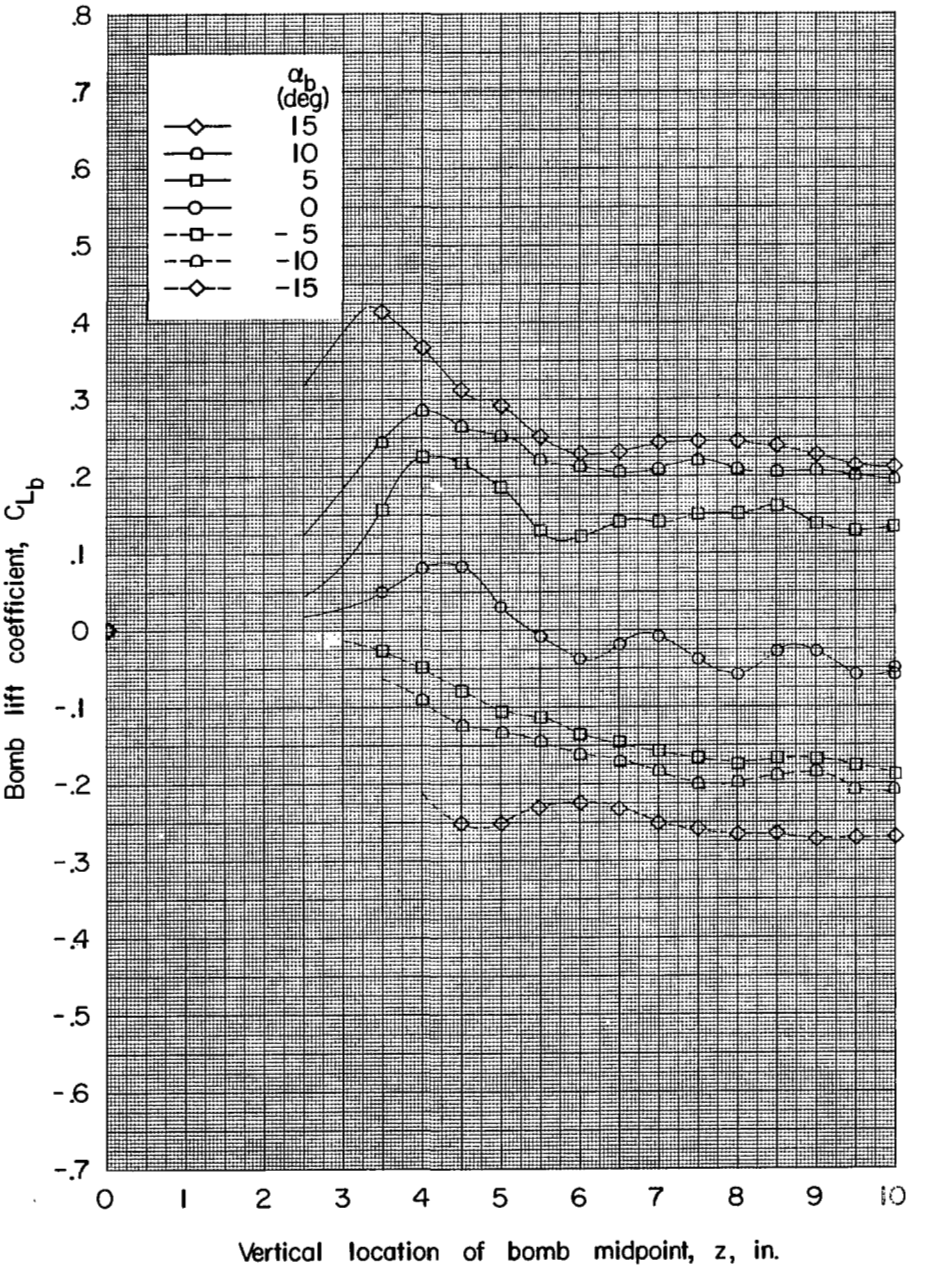

(g) Continued.

Figure 7.- Continued.

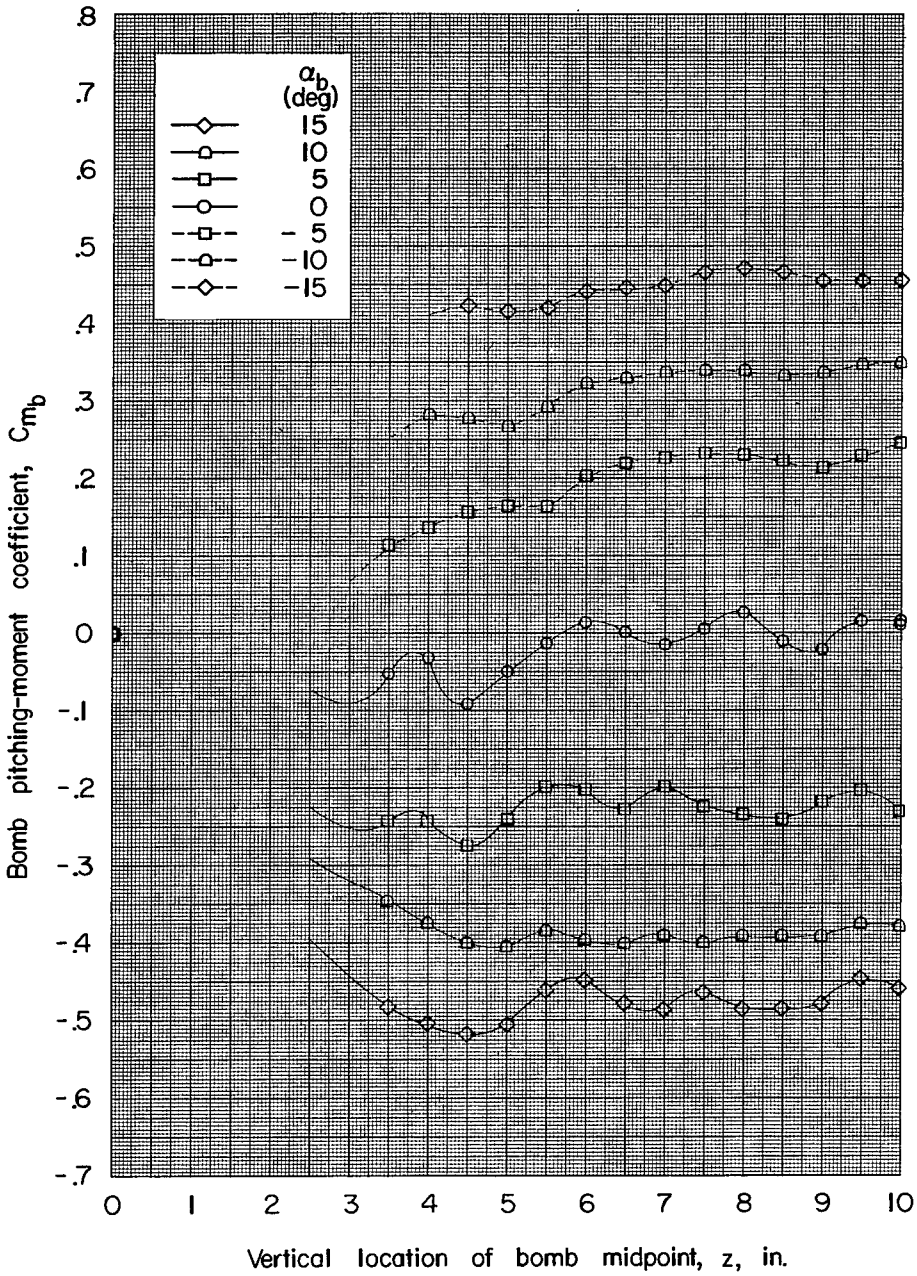

(g) Concluded.

Figure 7.- Concluded.

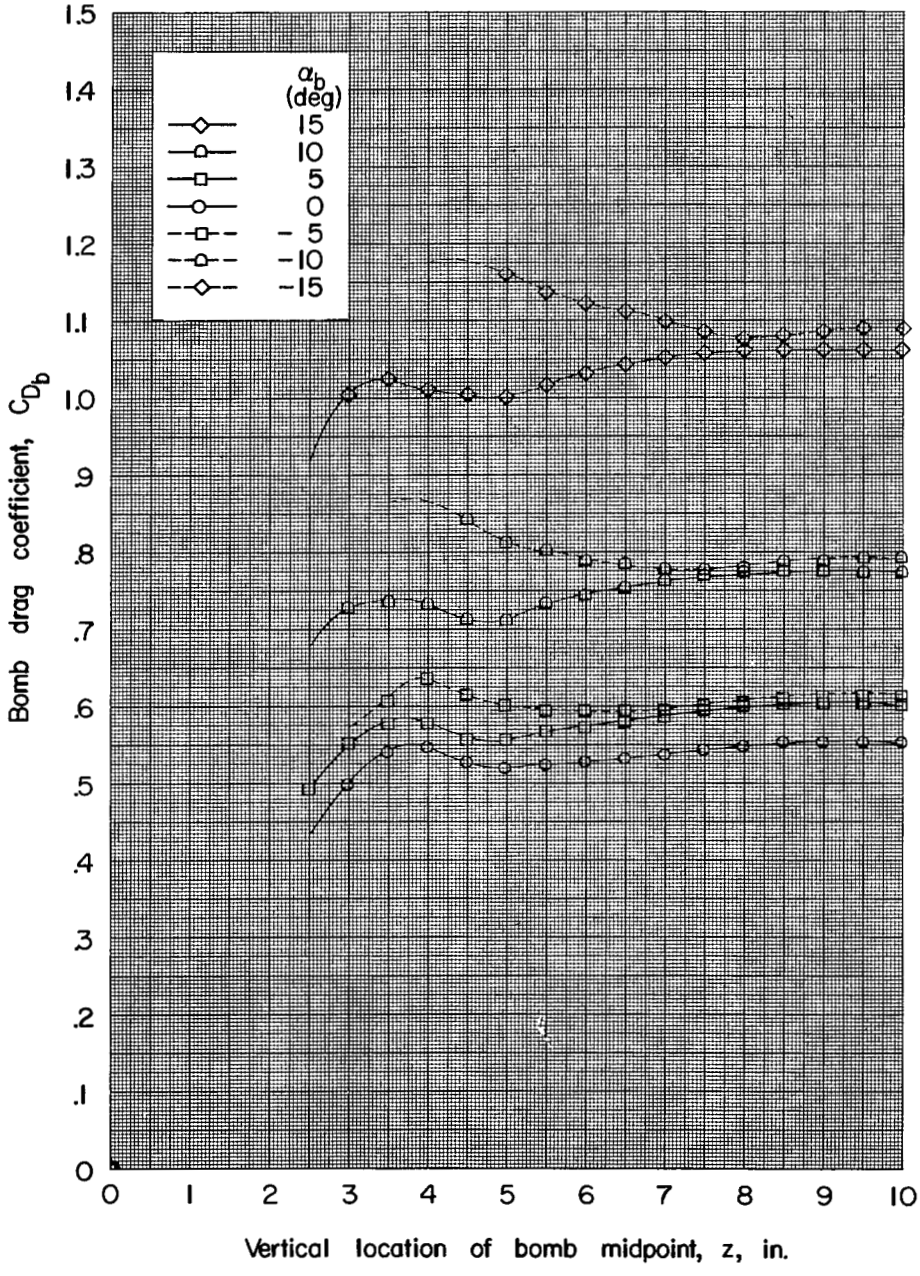

(a) x = -1.50 inches.

Figure 8.- Force and moment data for bomb 2 in presence of the wing-fuselage combination with ejector A. $\alpha_{wf} = 4^{\circ}$.

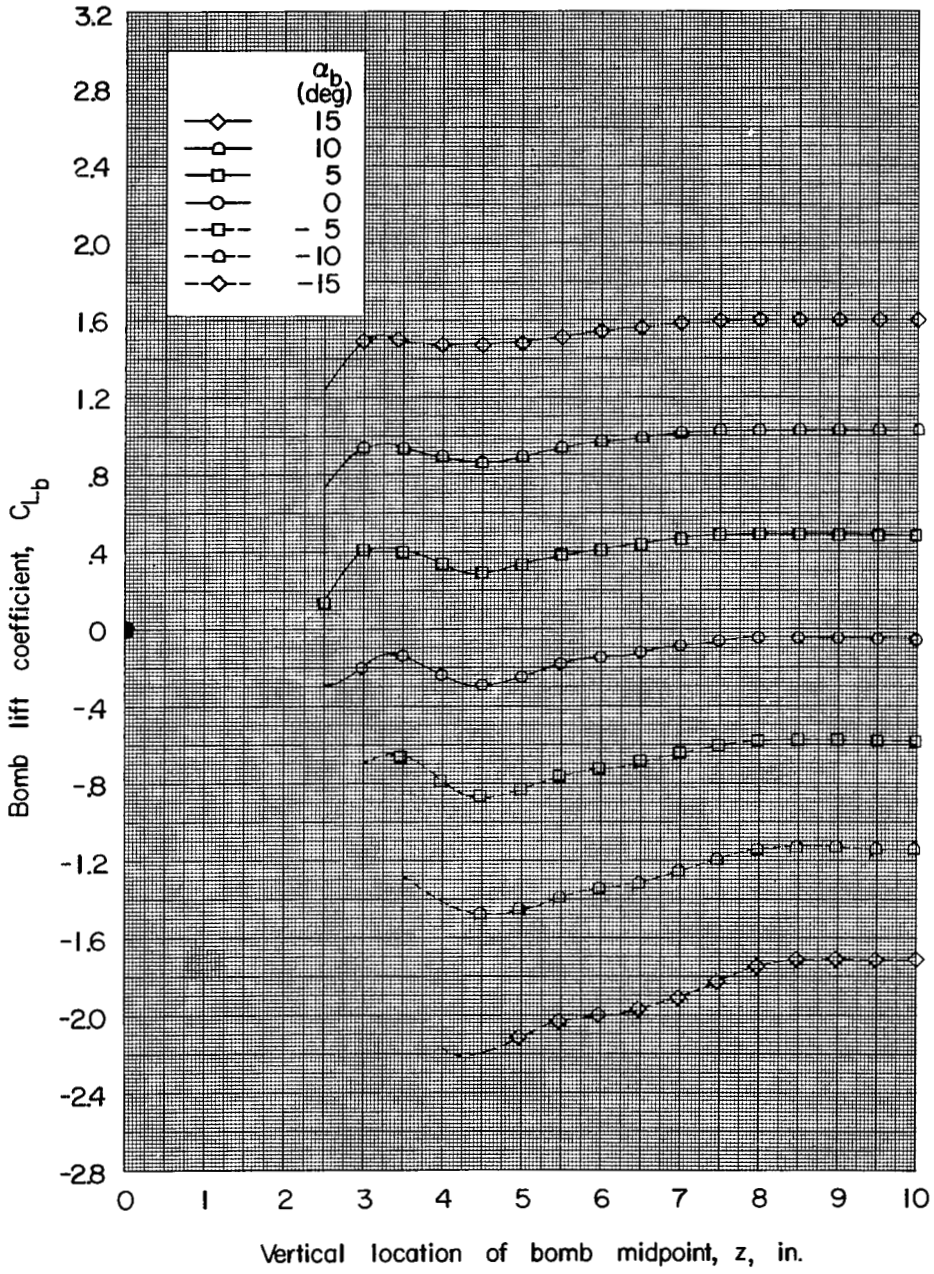

(a) Continued.

Figure 8.- Continued.

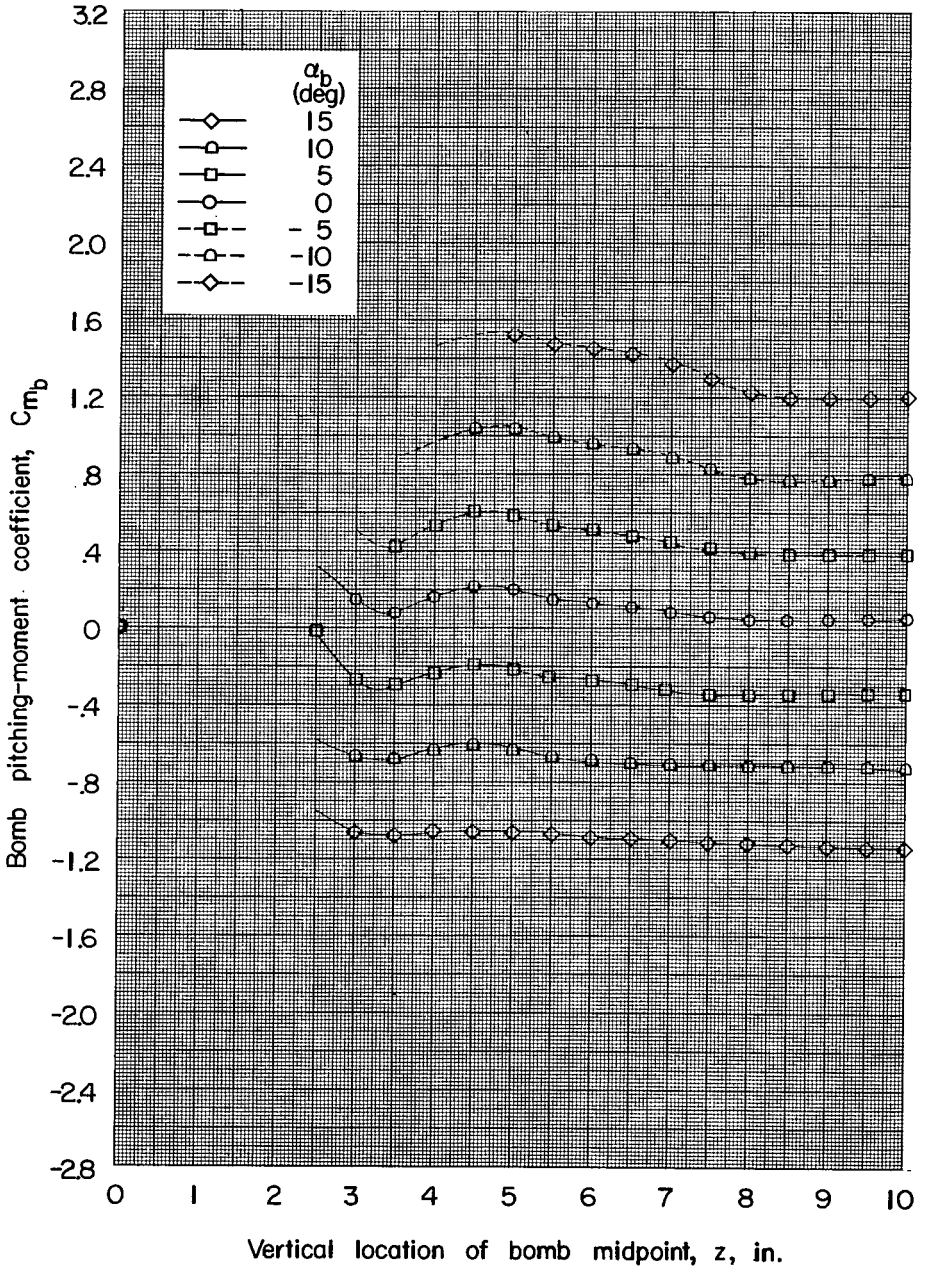

(a) Concluded.

Figure 8.- Continued.

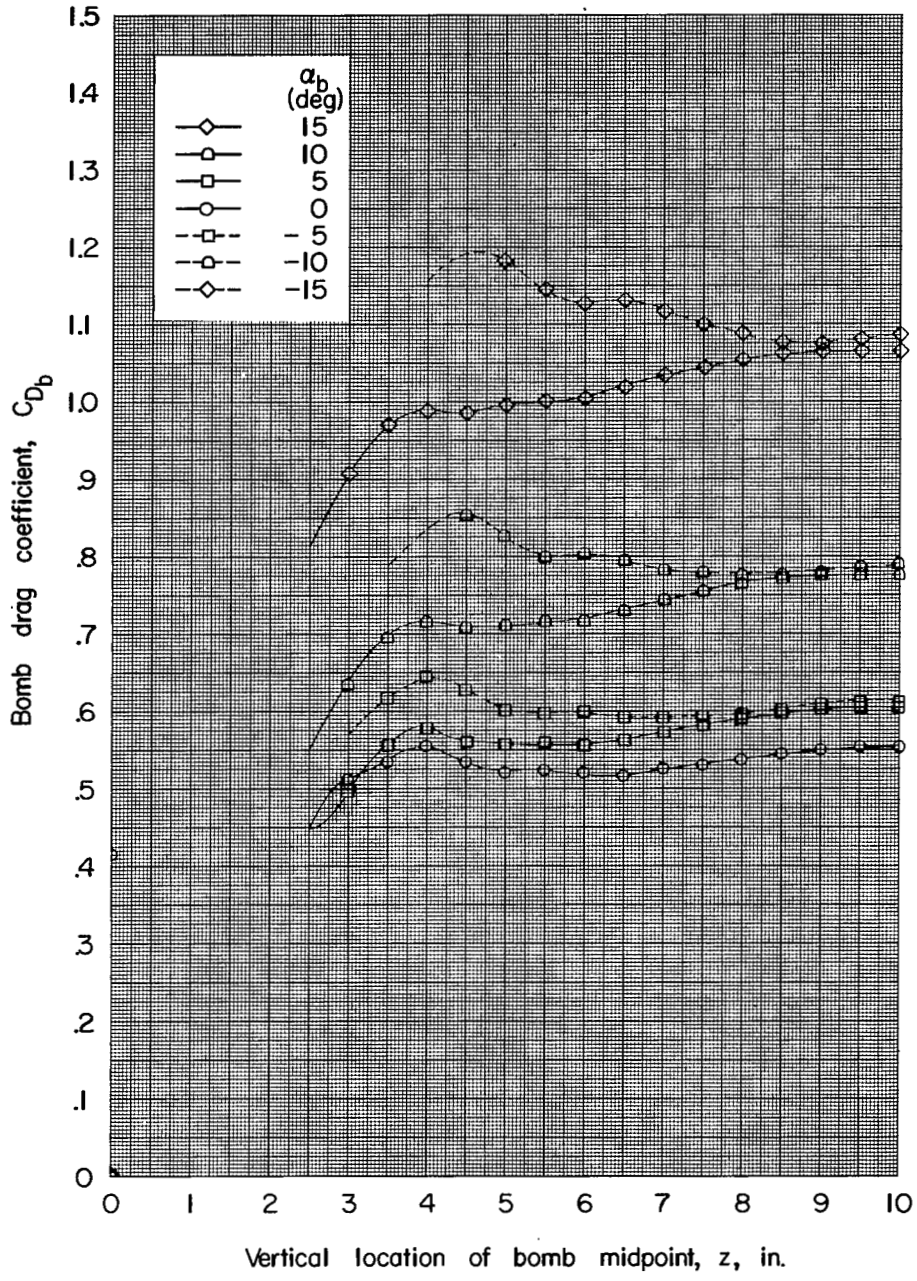

(b) x = -0.50 inch.

Figure 8.- Continued.

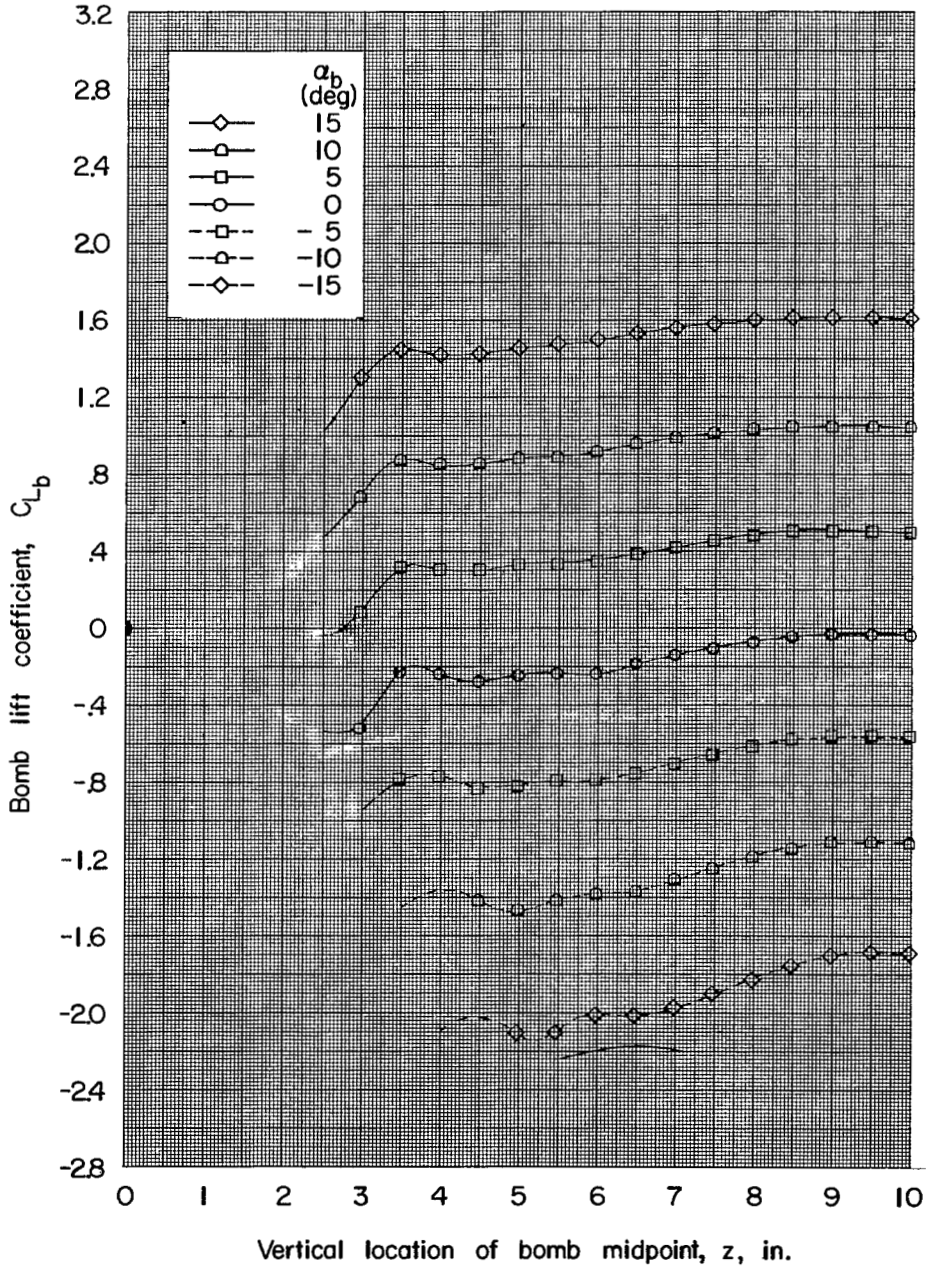

(b) Continued.

Figure 8.- Continued.

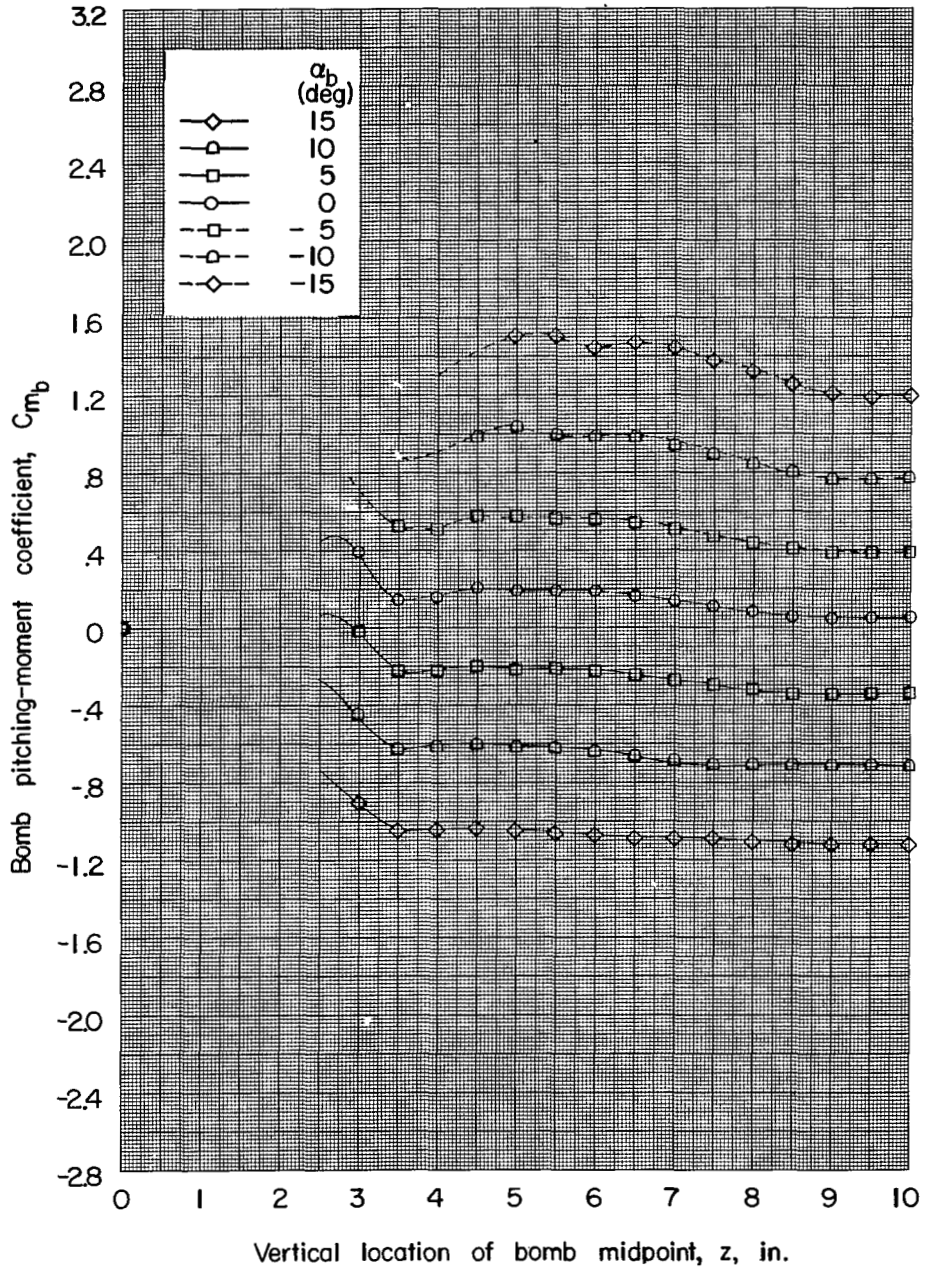

(b) Concluded.

Figure 8.- Continued.

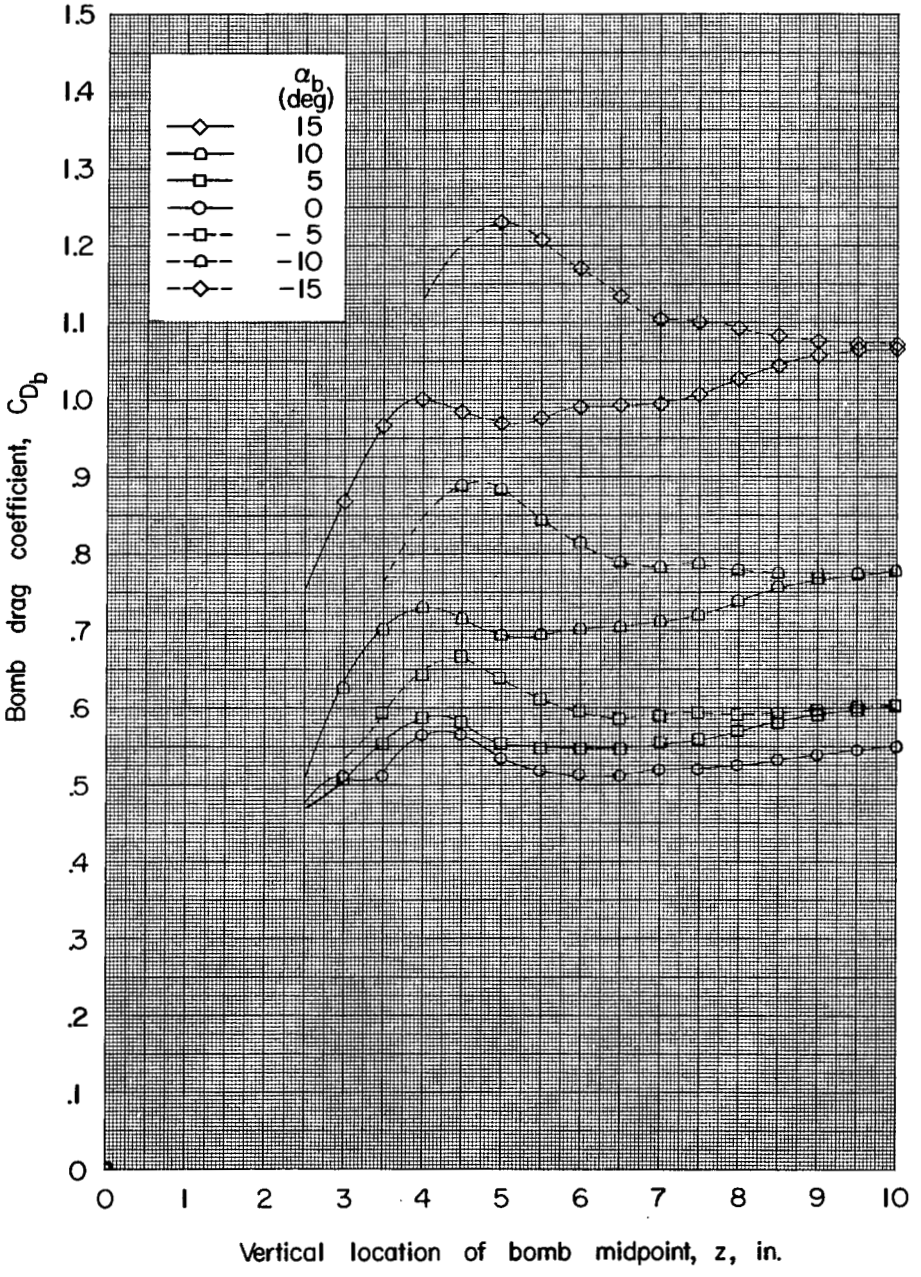

(c) x = 1.00 inch.

Figure 8.- Continued.

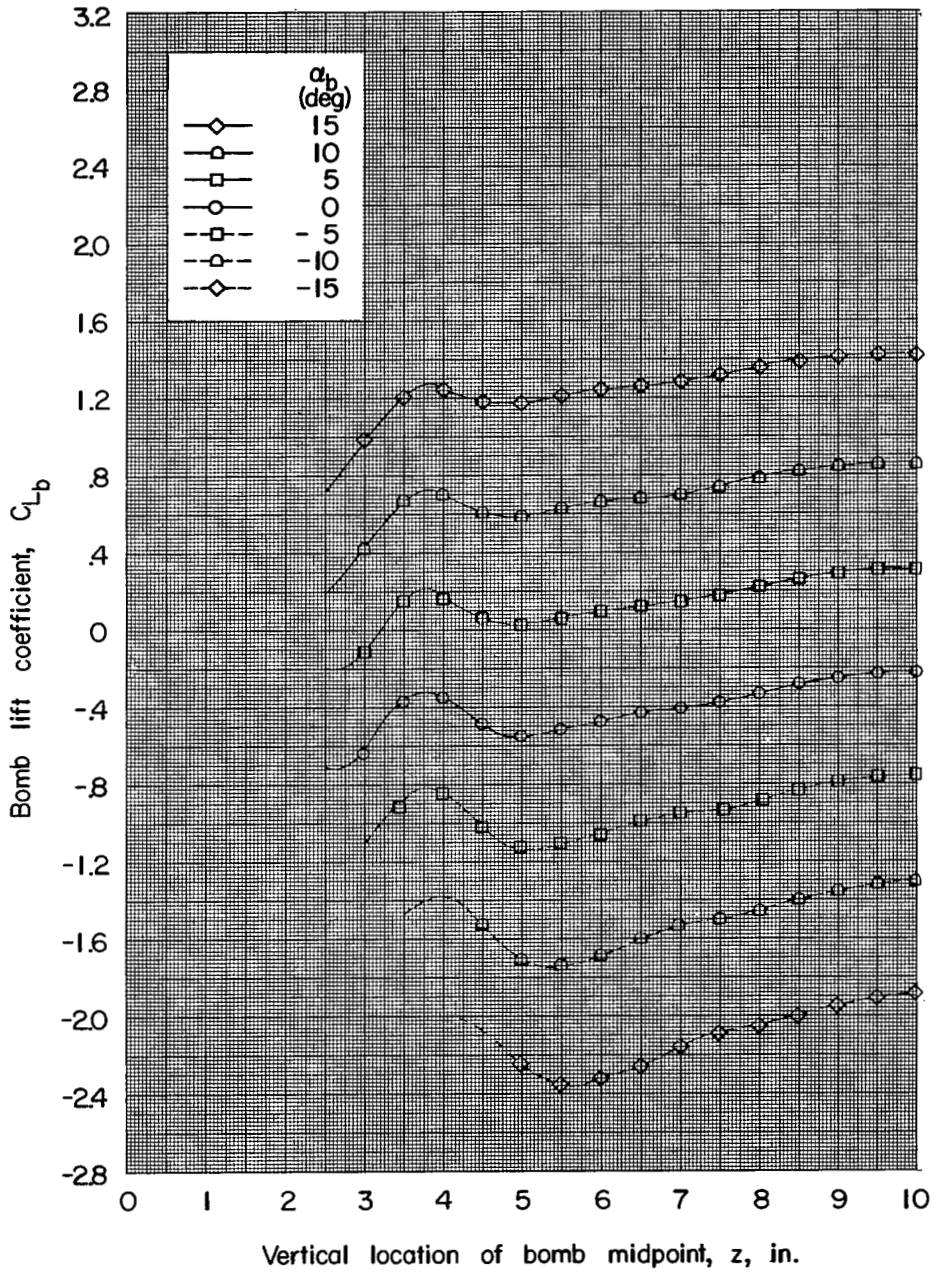

(c) Continued.

Figure 8.- Continued.

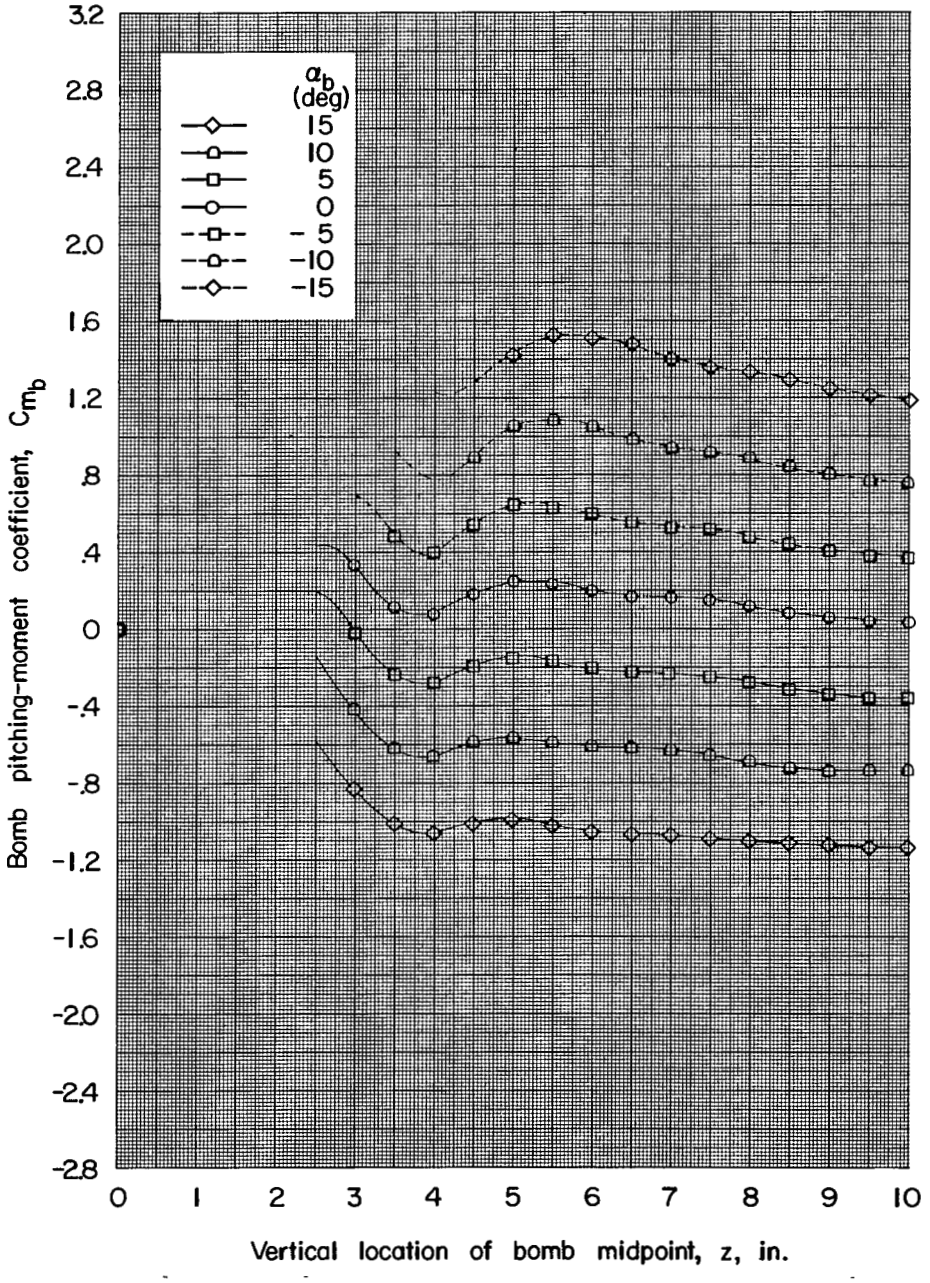

(c) Concluded.

Figure 8.- Continued.

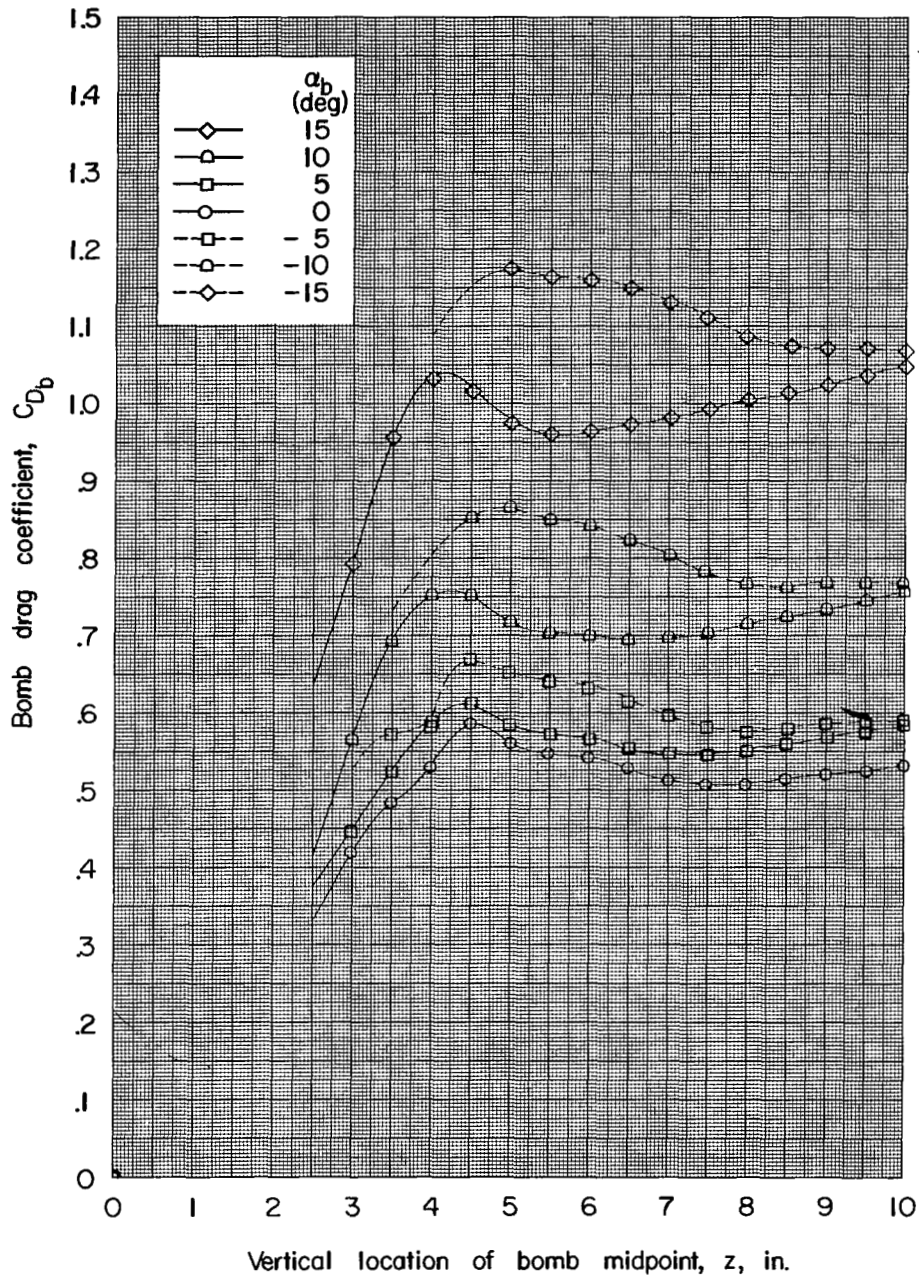

(d) x = 3.00 inches.

Figure 8.- Continued.

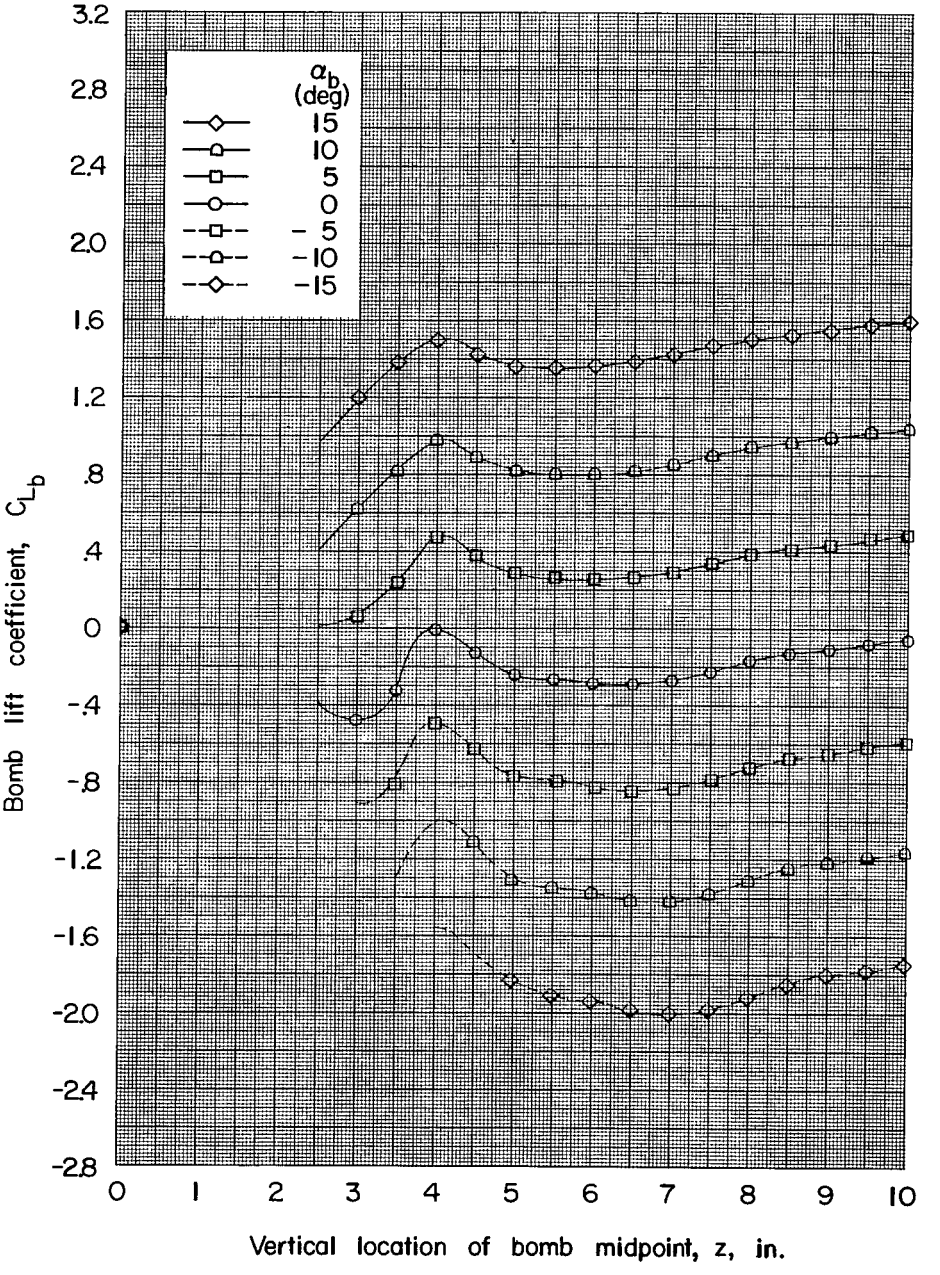

(d) Continued.

Figure 8.- Continued.

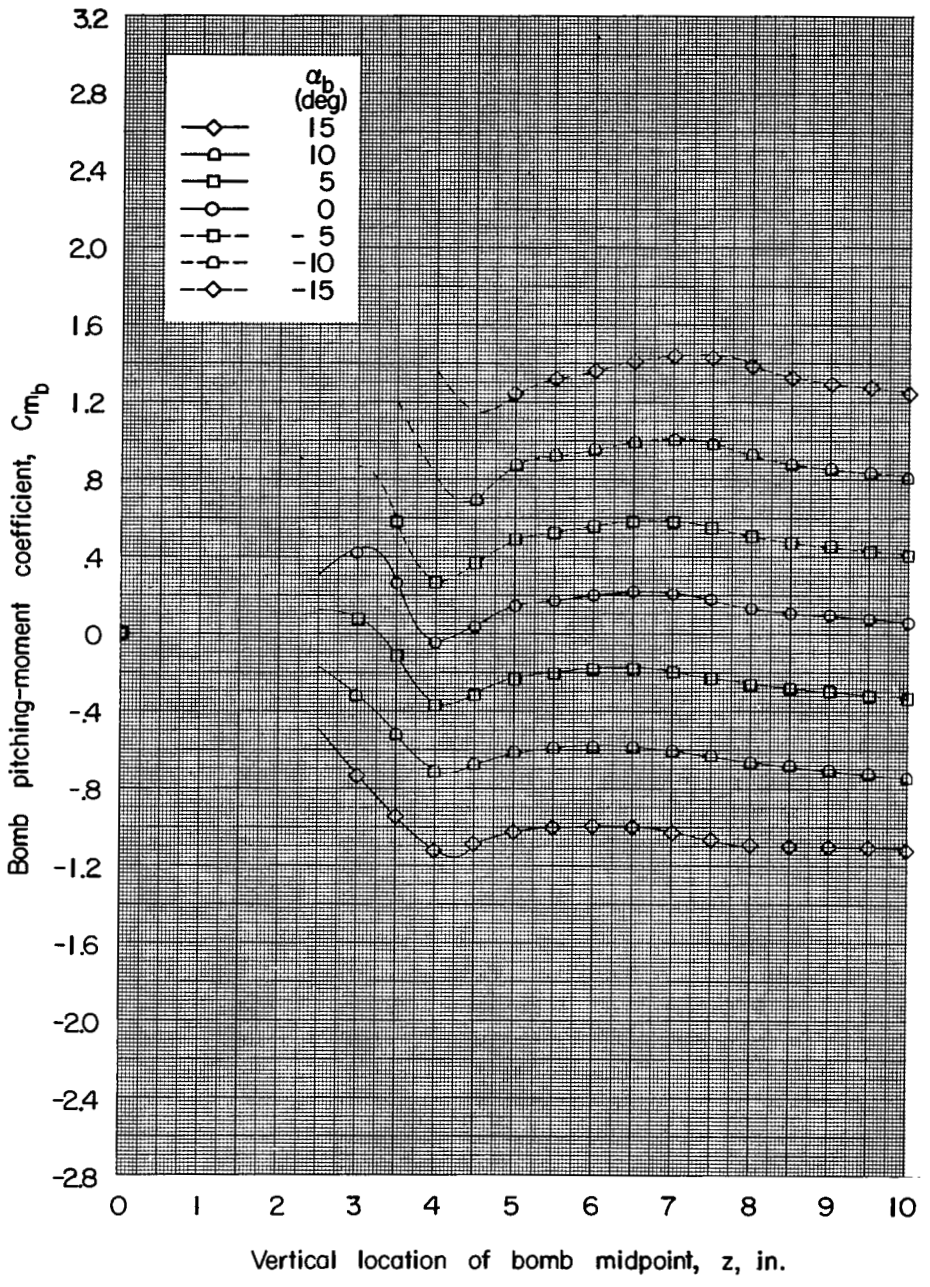

(d) Concluded.

Figure 8.- Continued.

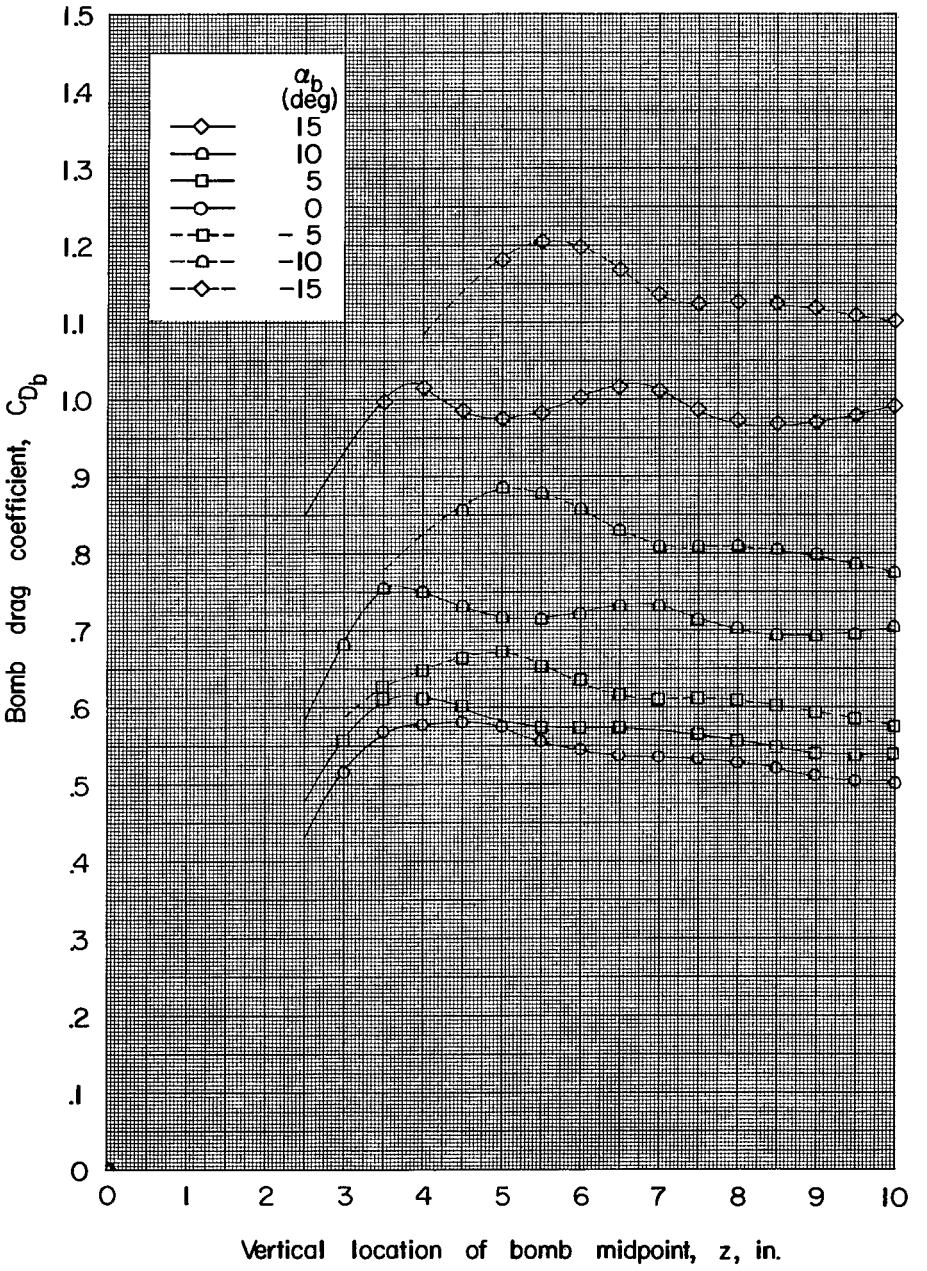

(e) x = 6.00 inches.

Figure 8.- Continued.

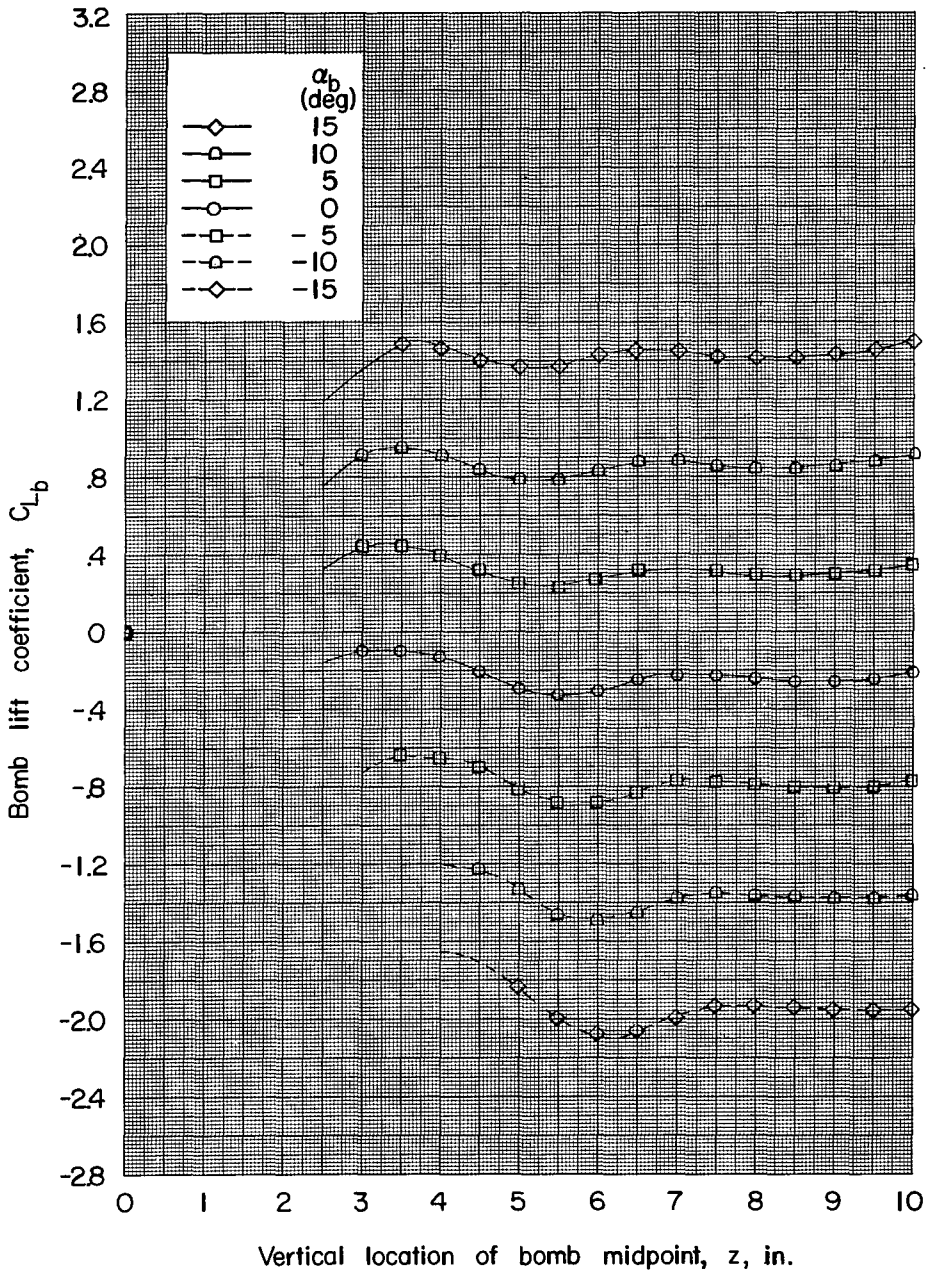

(e) Continued.

Figure 8.- Continued.

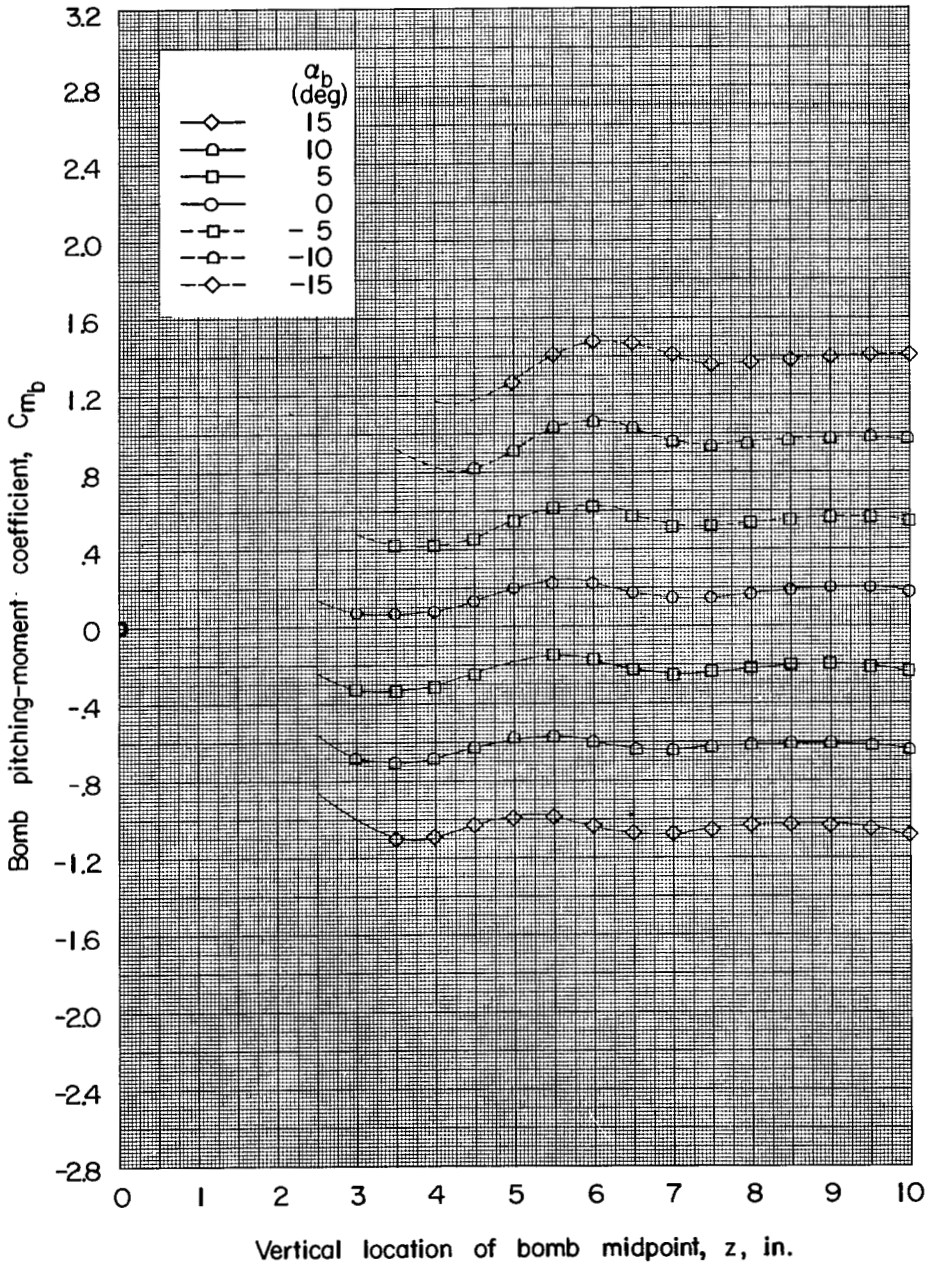

(e) Concluded.

Figure 8.- Concluded.

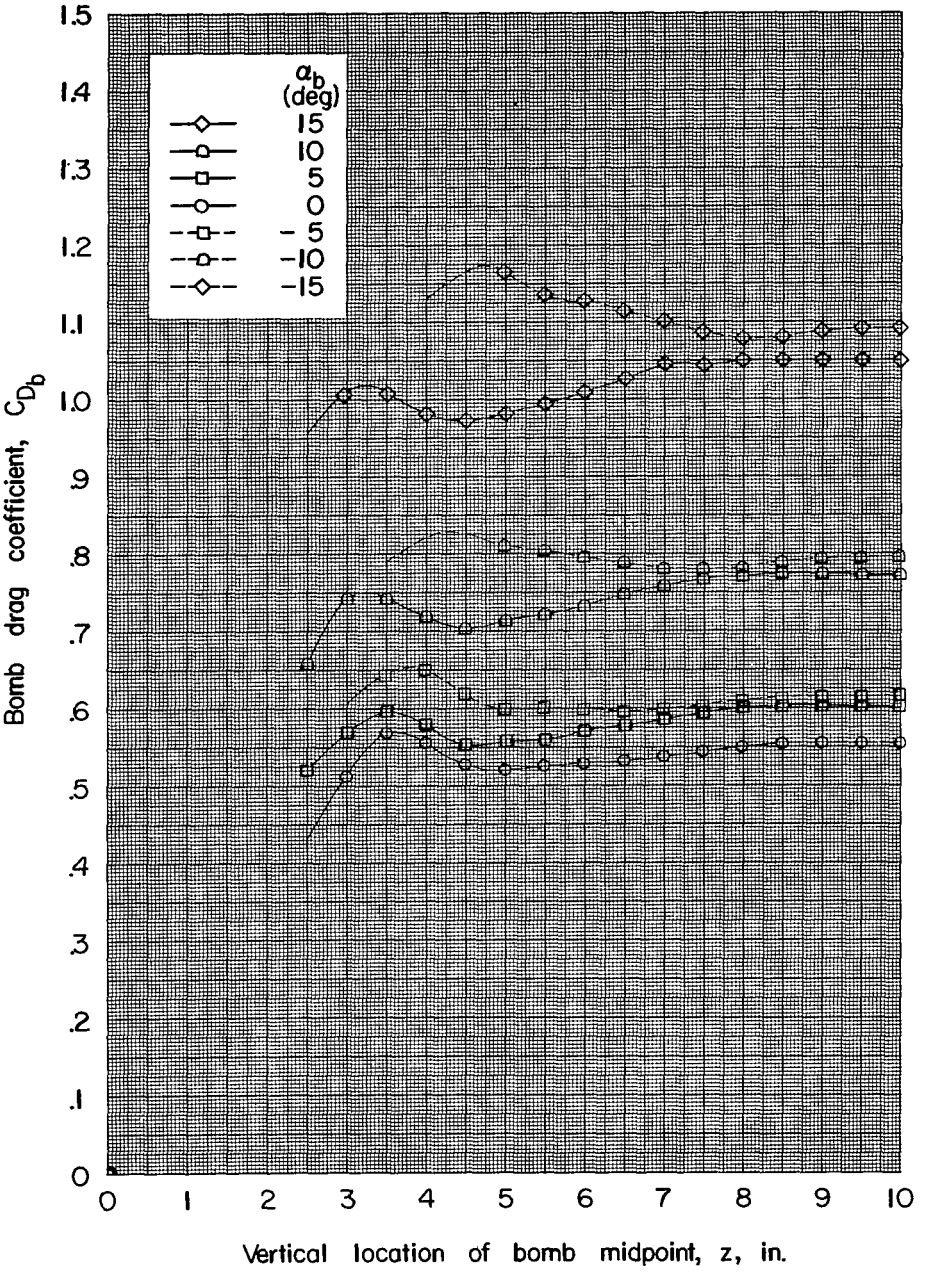

(a) x = -1.50 inches.

Figure 9.- Force and moment data for bomb 2 in presence of the wing fuselage combination with ejector B. $\alpha_{wf} = 4^{o}$.

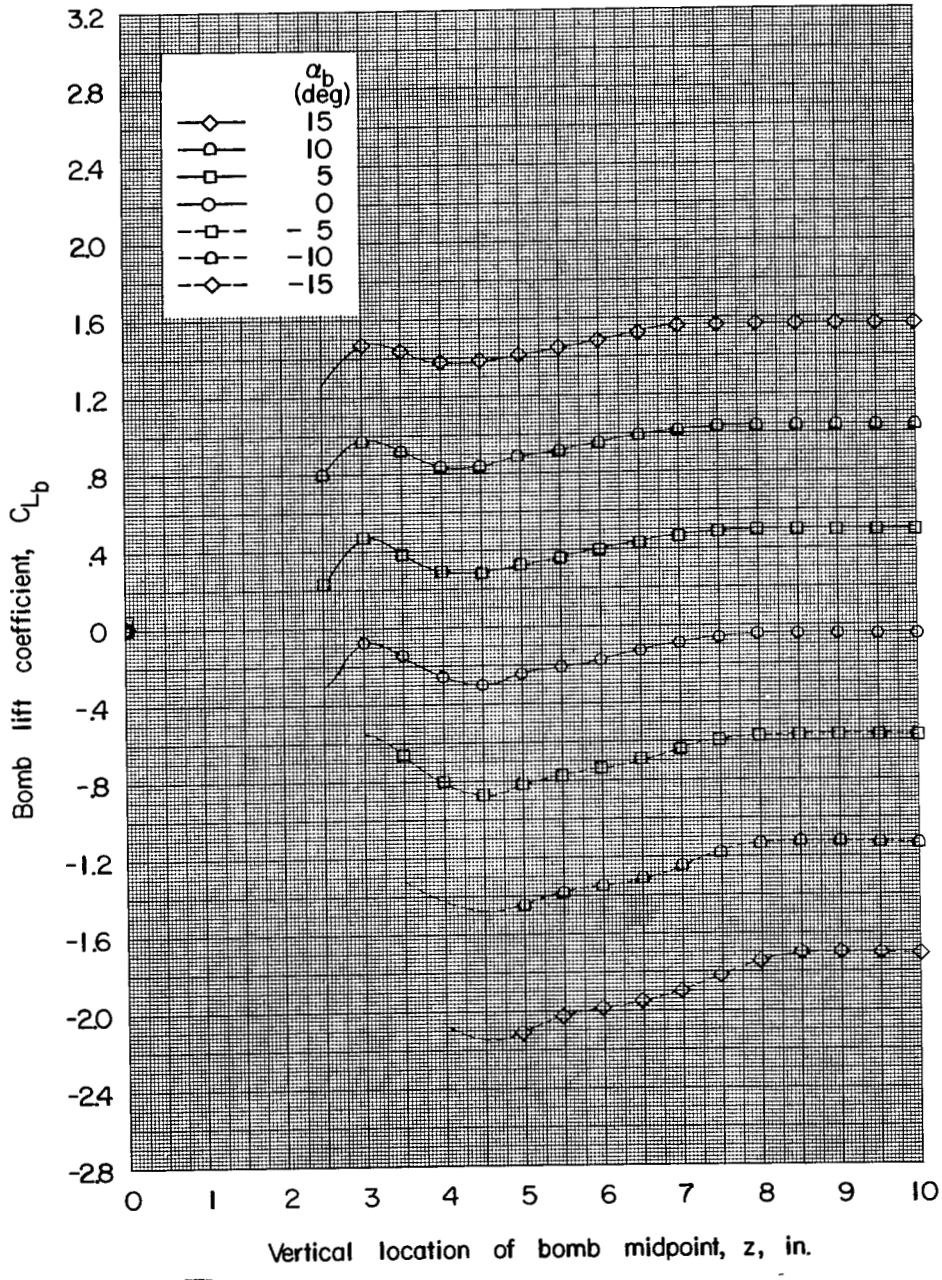

(a) Continued.

Figure 9.- Continued.

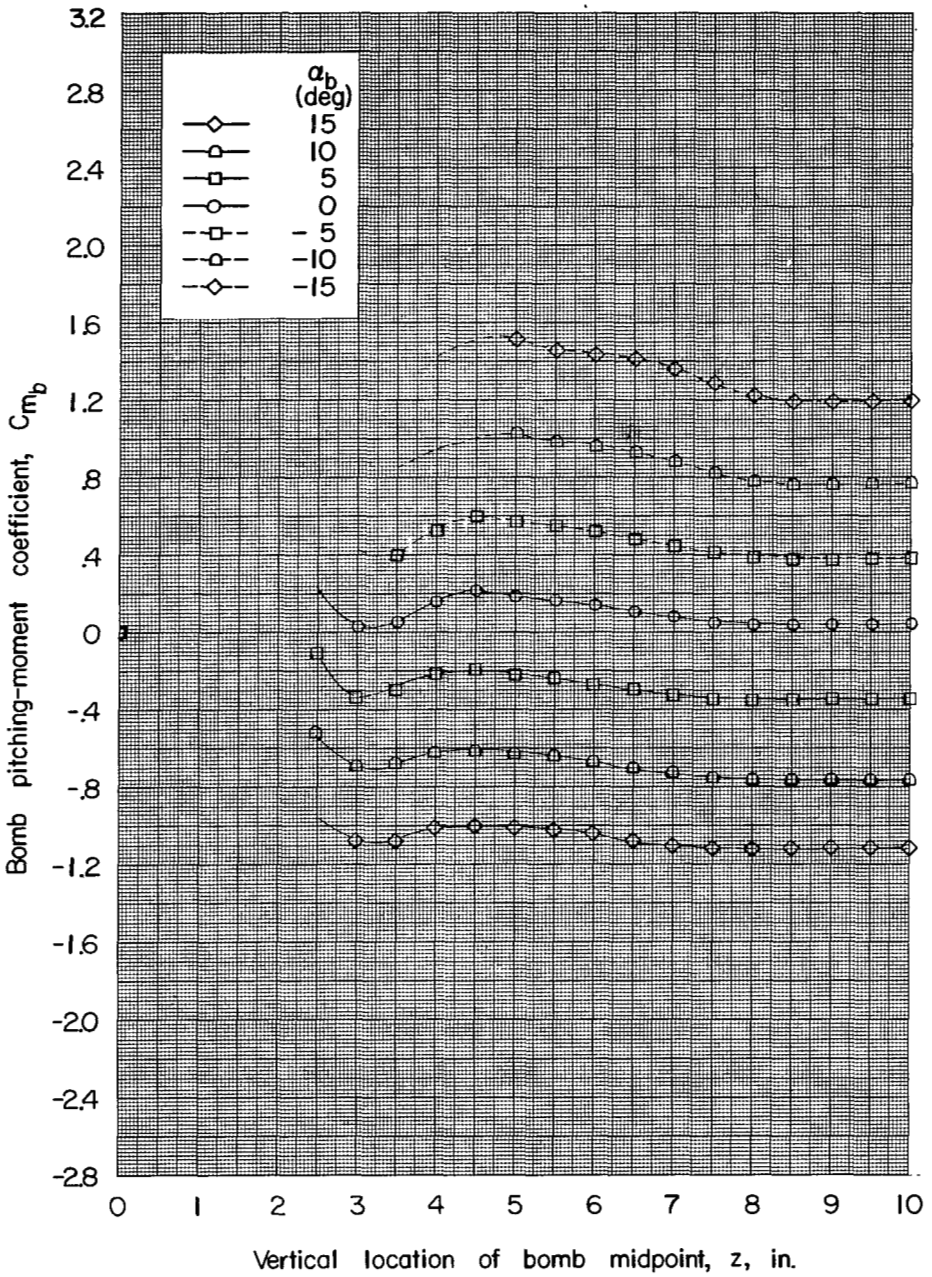

(a) Concluded.

Figure 9.- Continued.

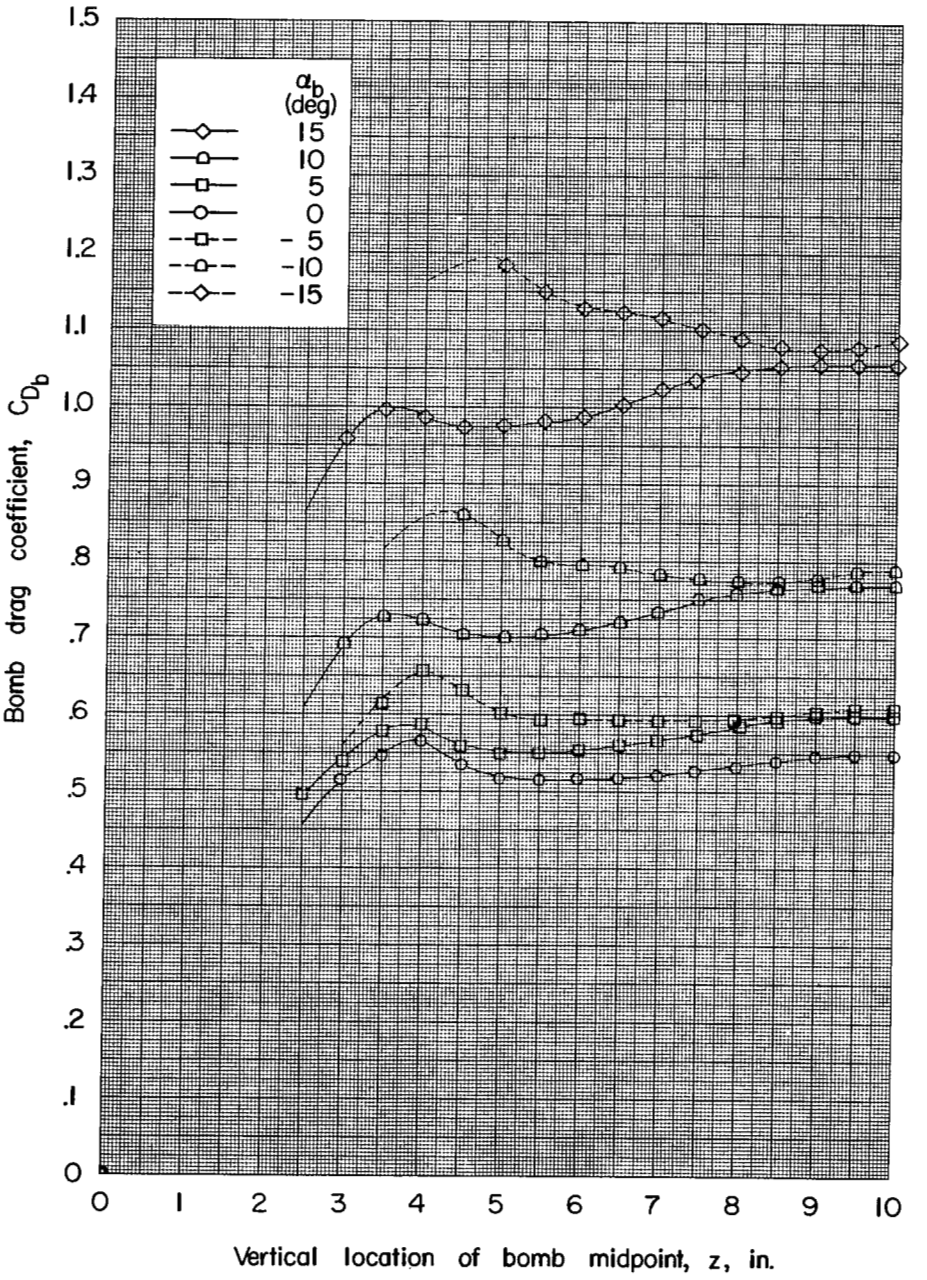

(b) x = -0.50 inch.

Figure 9.- Continued.

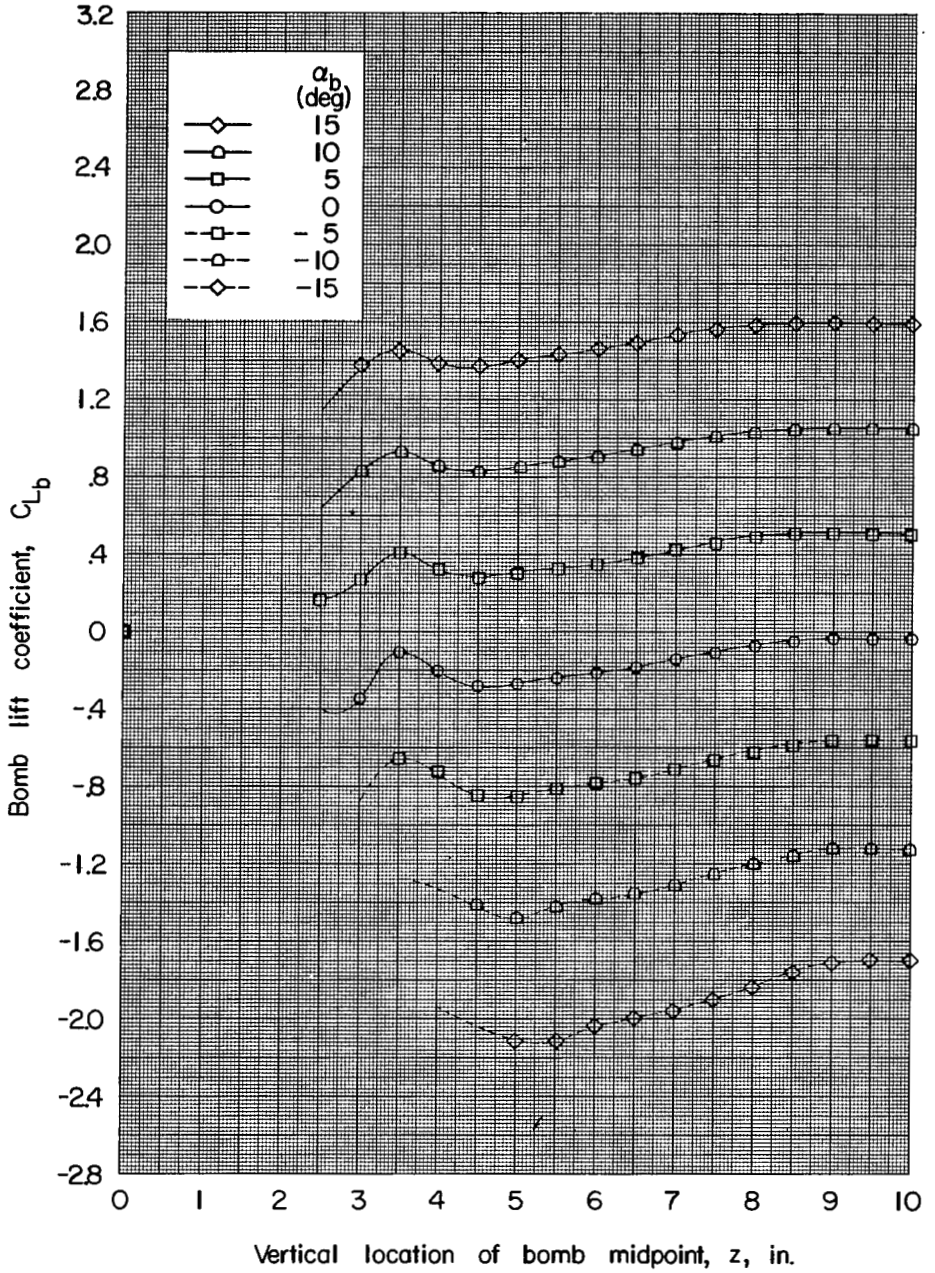

(b) Continued.

Figure 9.- Continued.

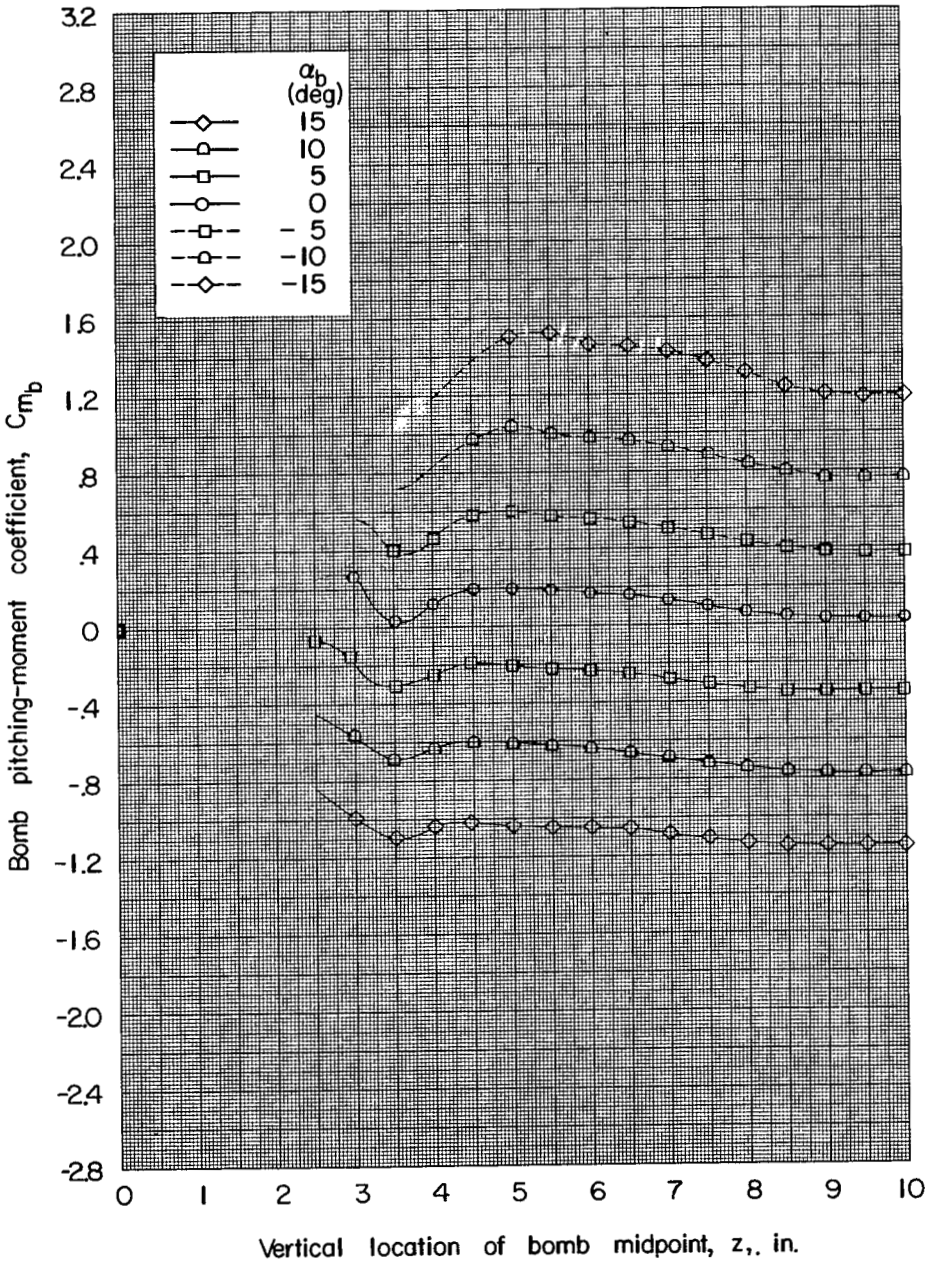

(b) Concluded.

Figure 9.- Continued.

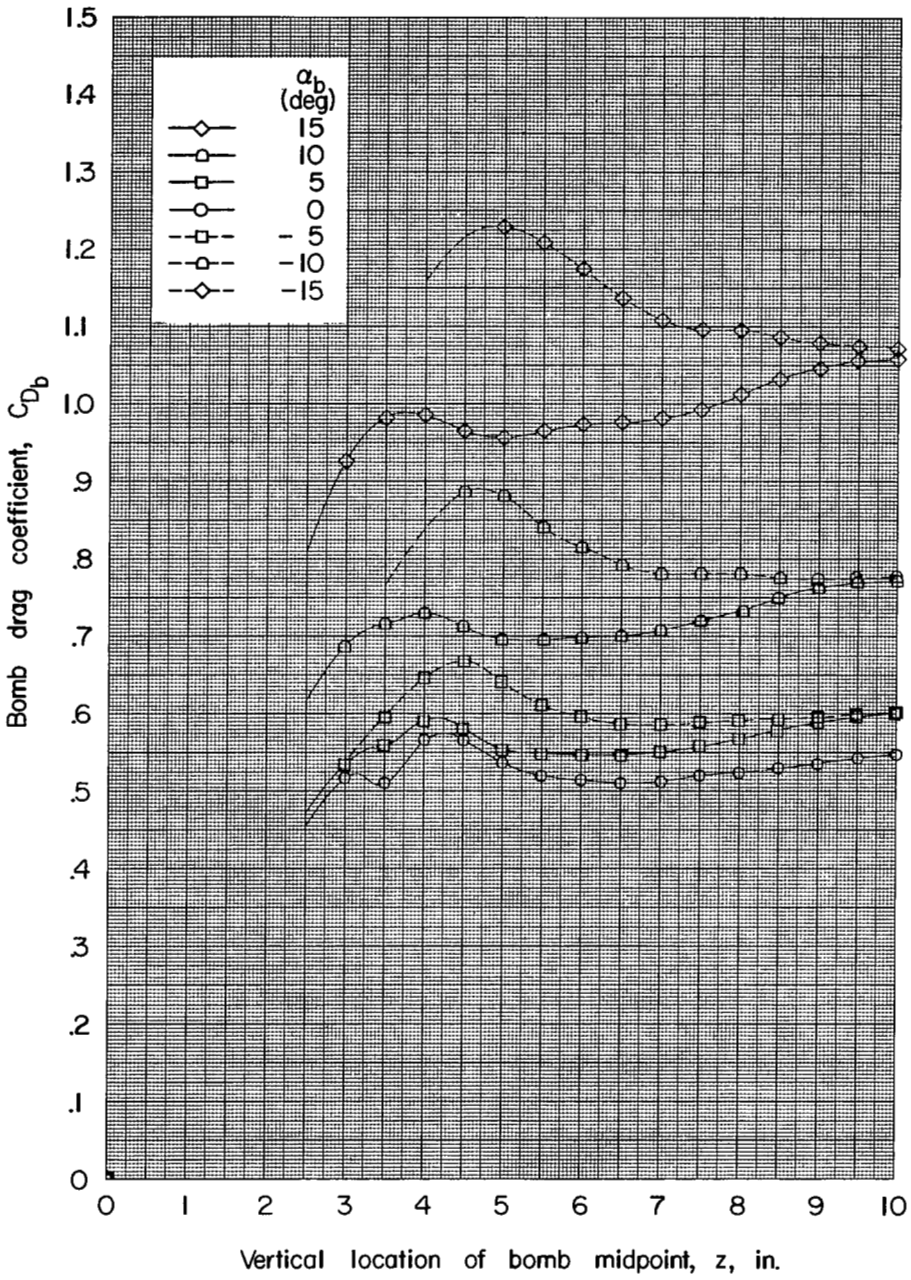

(c) x = 1.00 inch.

Figure 9.- Continued.

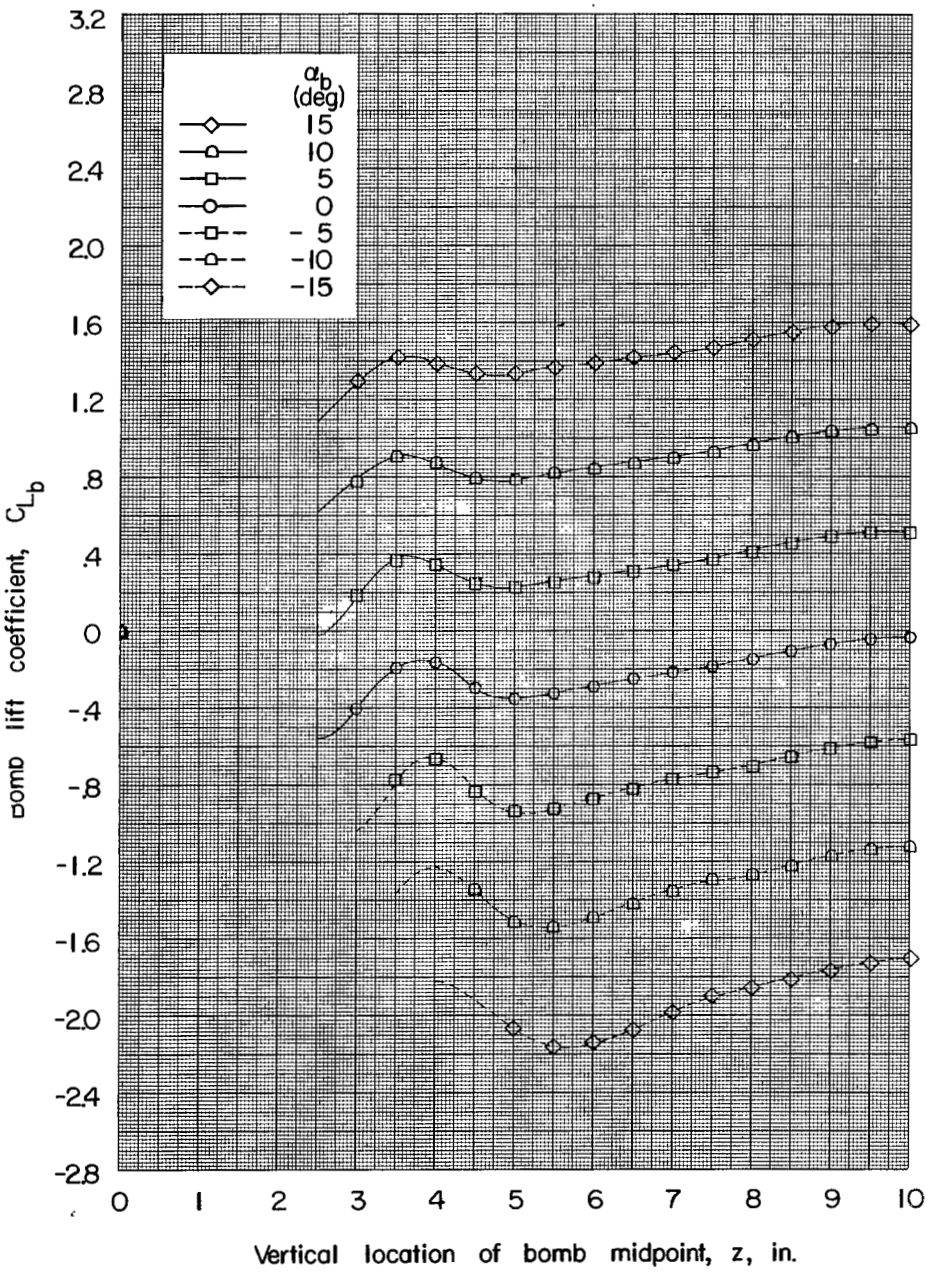

(c) Continued.

Figure 9.- Continued.

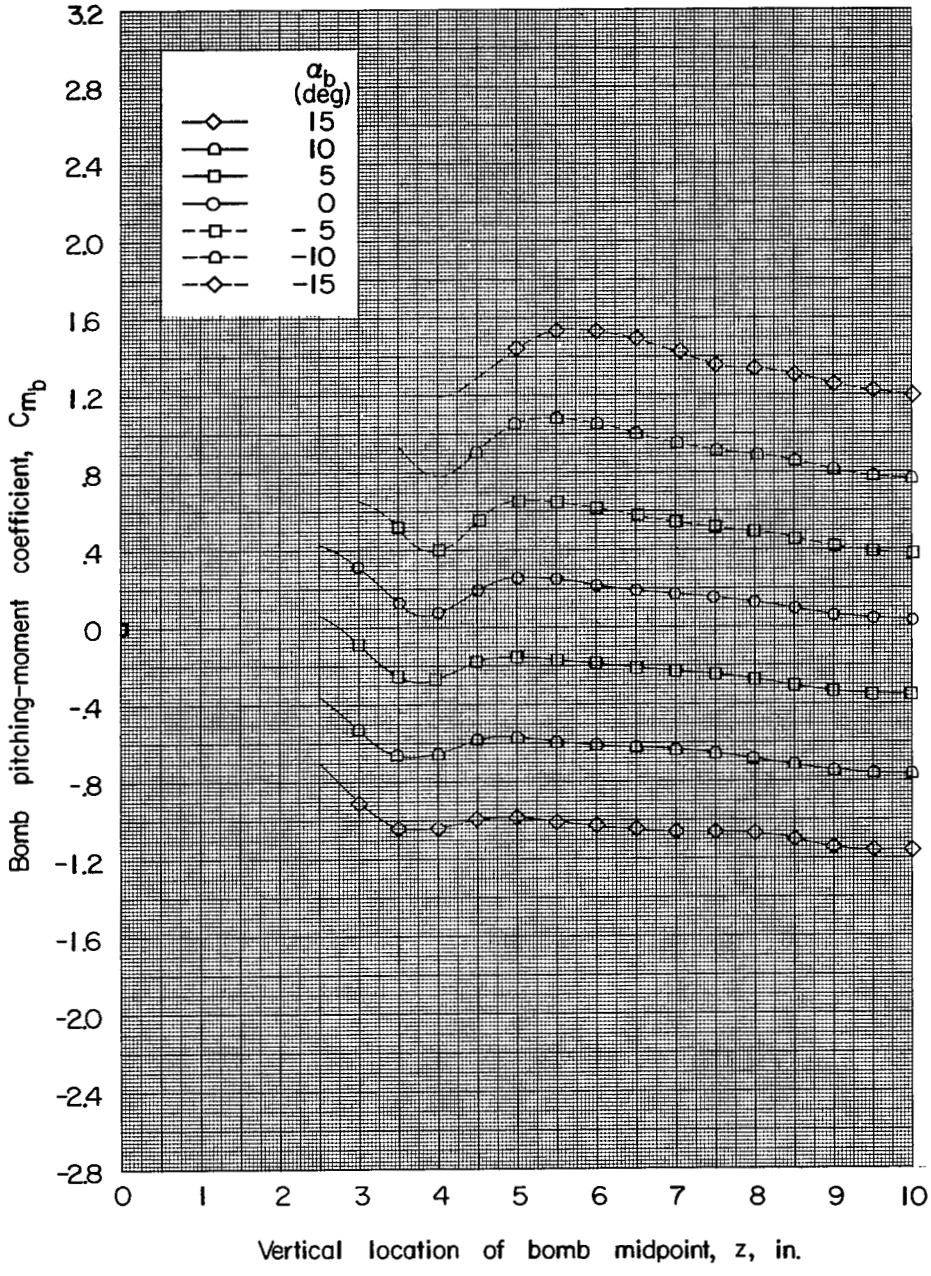

(c) Concluded.

Figure 9.- Continued.

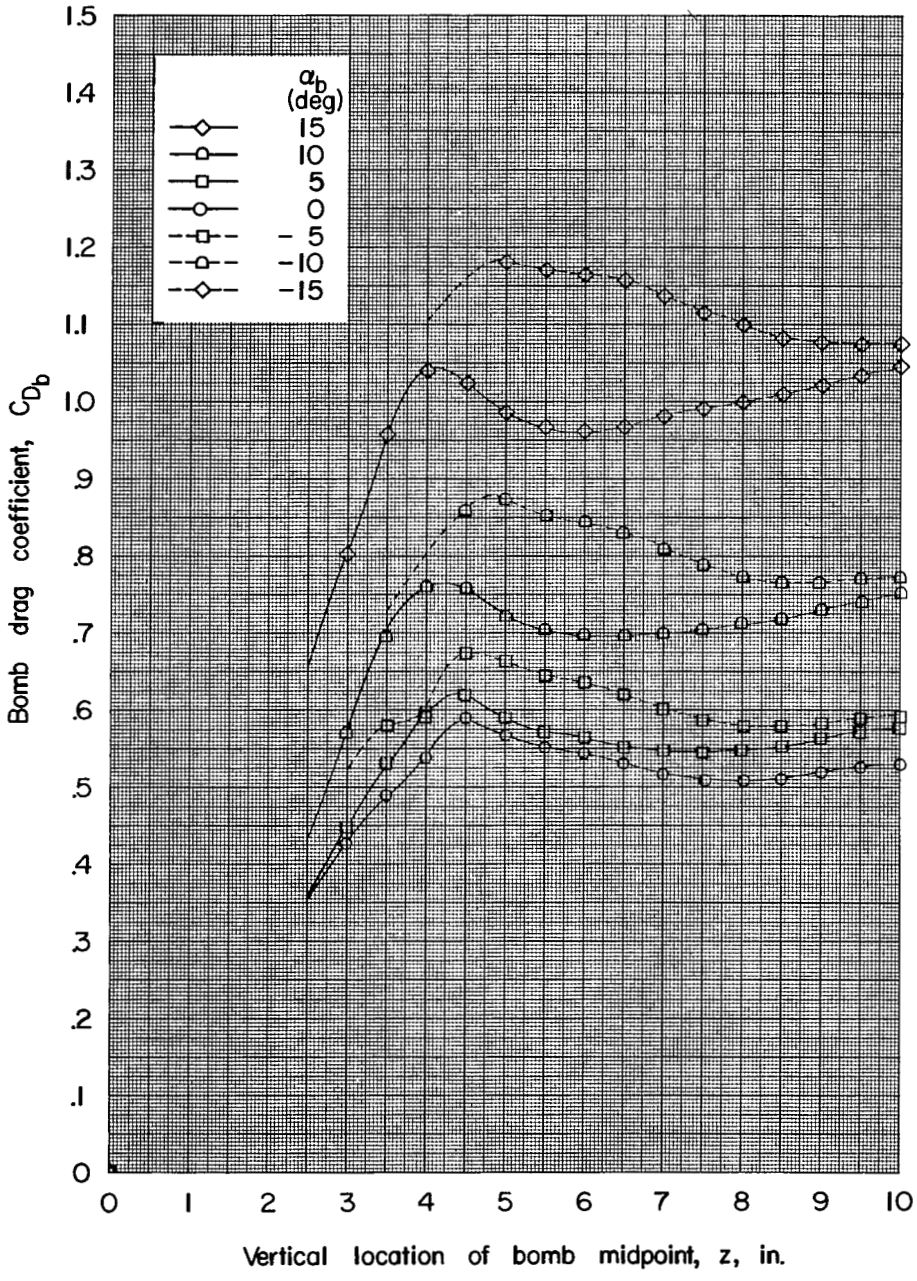

(d) x = 3.00 inches.

Figure 9.- Continued.

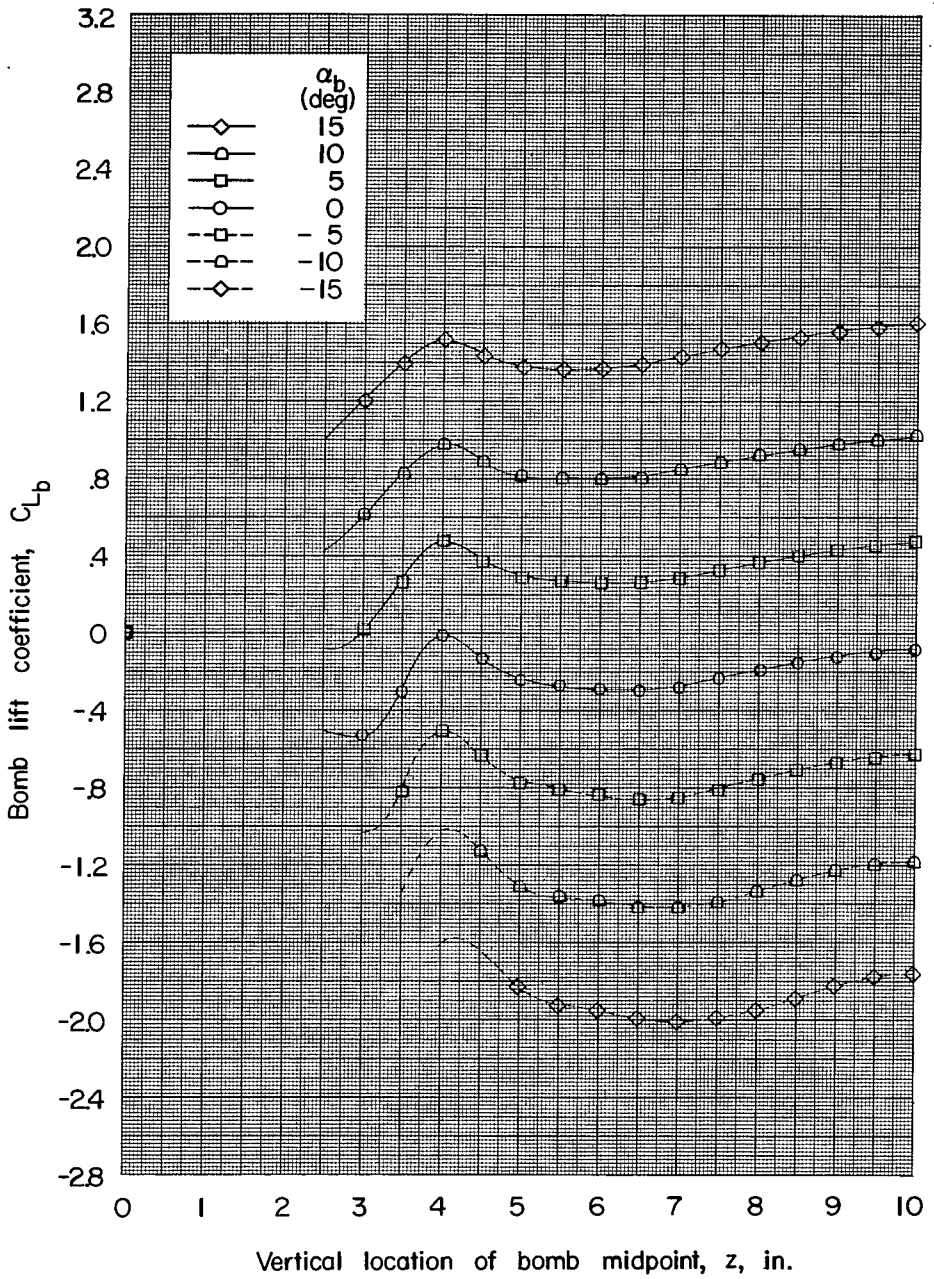

(d) Continued.

Figure 9.- Continued.

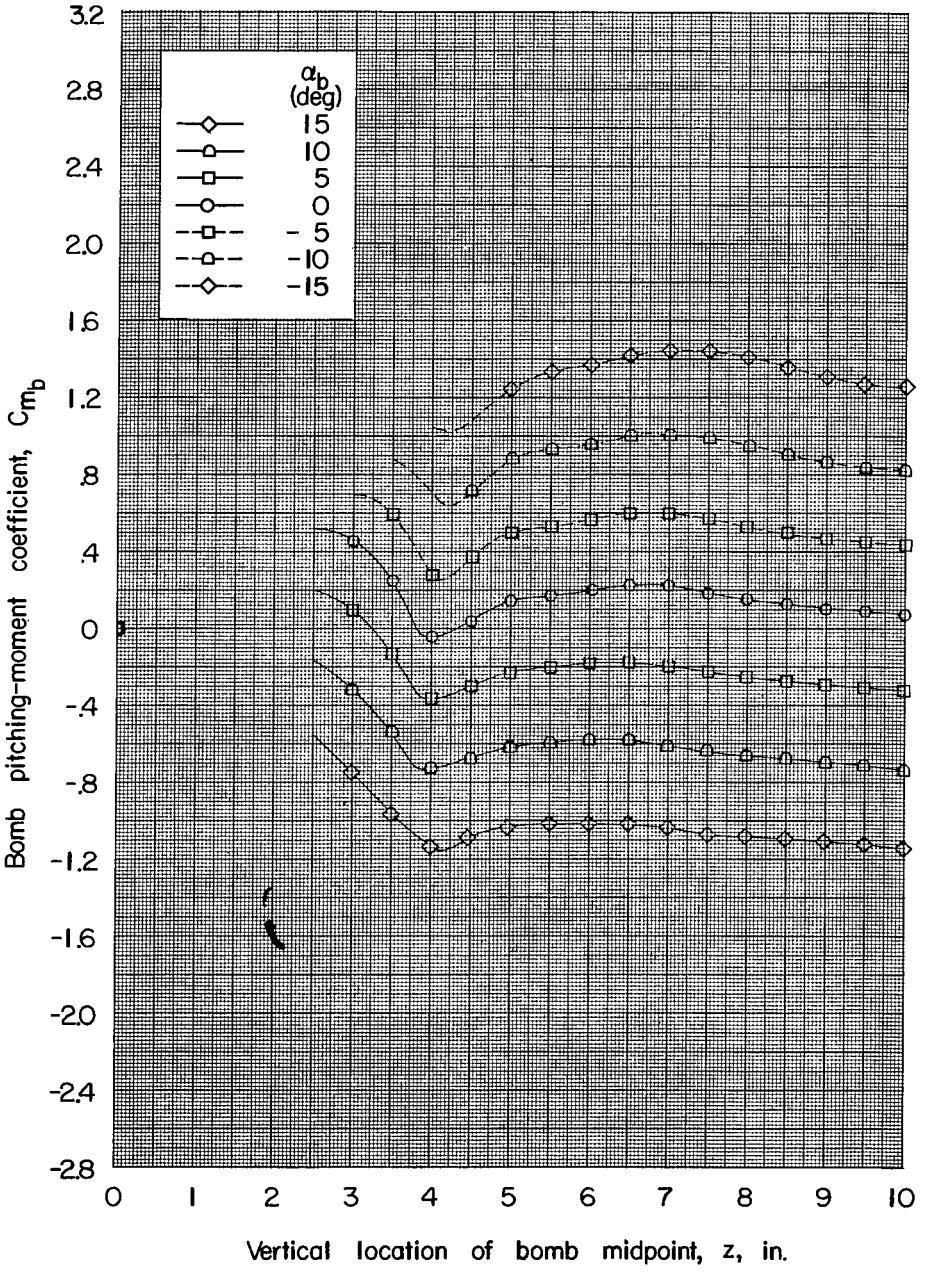

(d) Concluded.

Figure 9.- Continued.

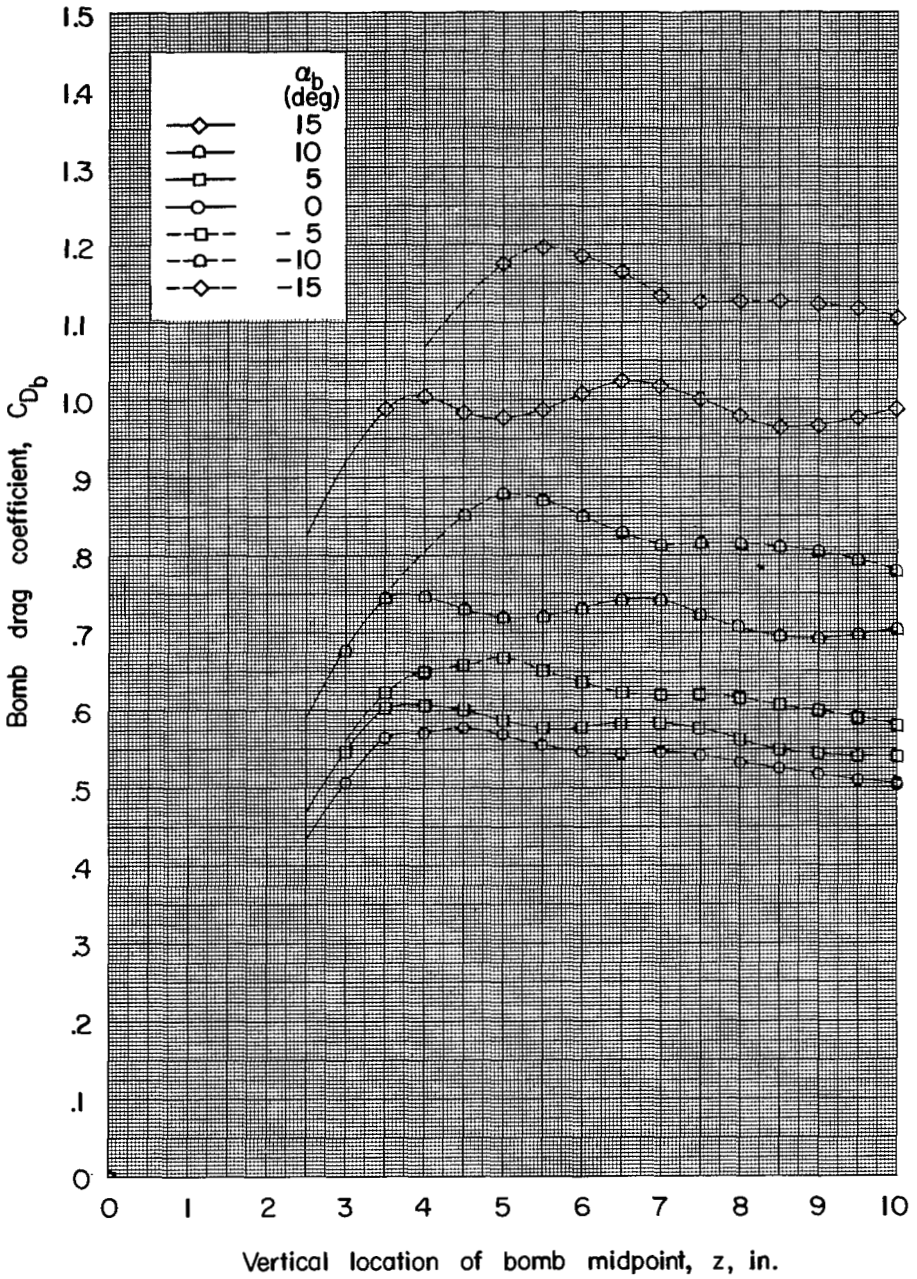

(e) x = 6.00 inches.

Figure 9.- Continued.

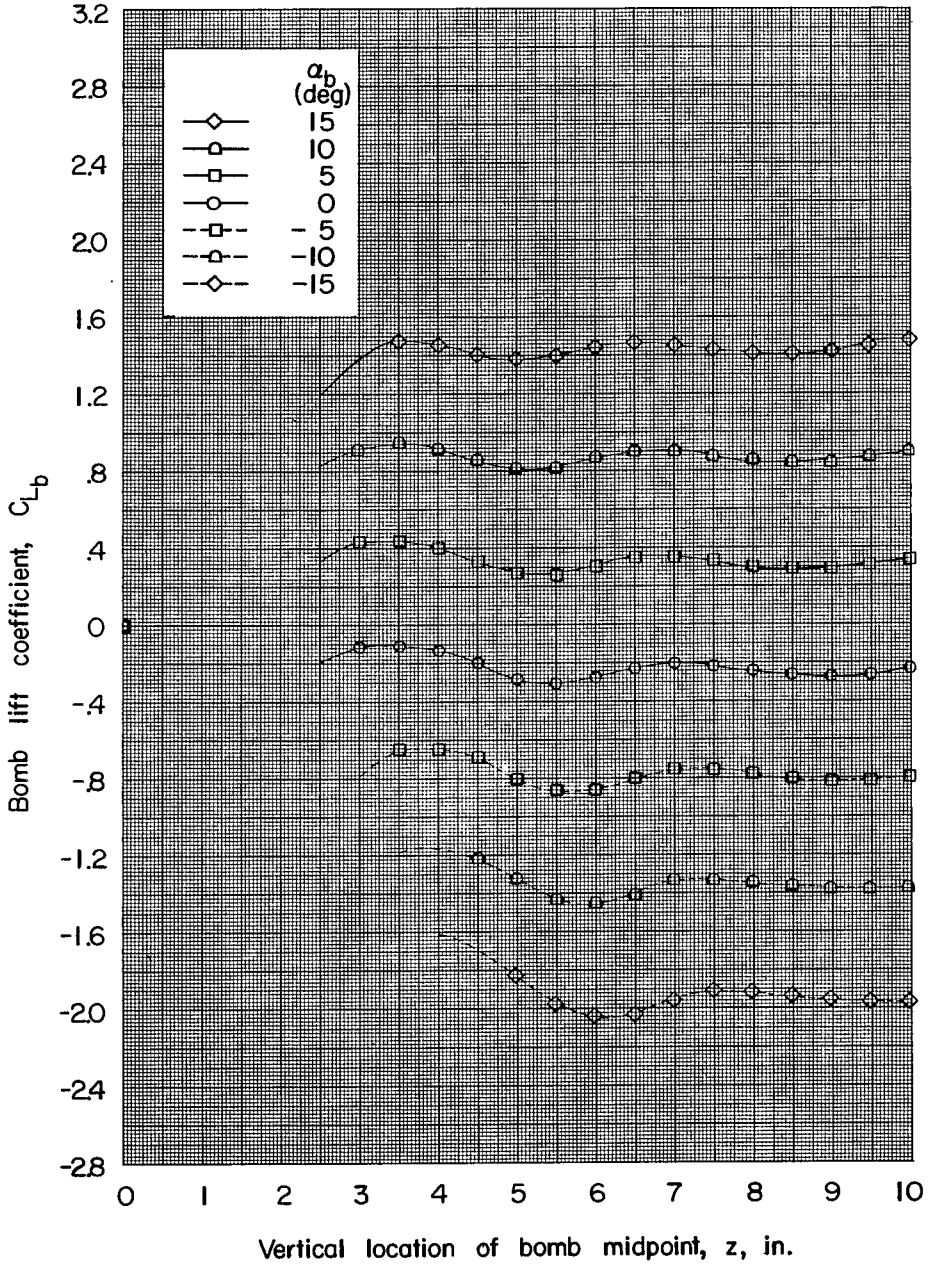

(e) Continued.

Figure 9.- Continued.

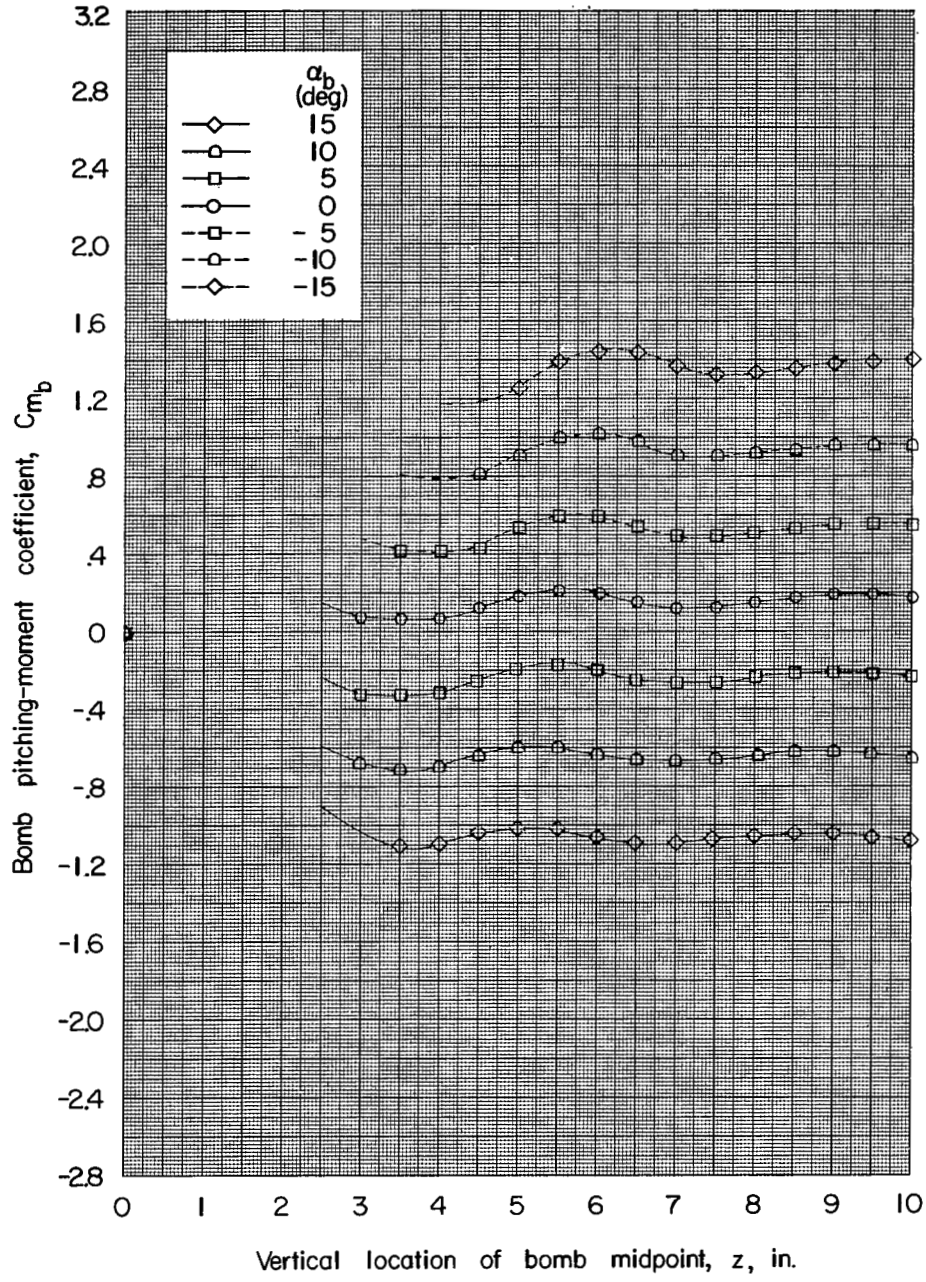

(e) Concluded.

Figure 9.- Concluded.

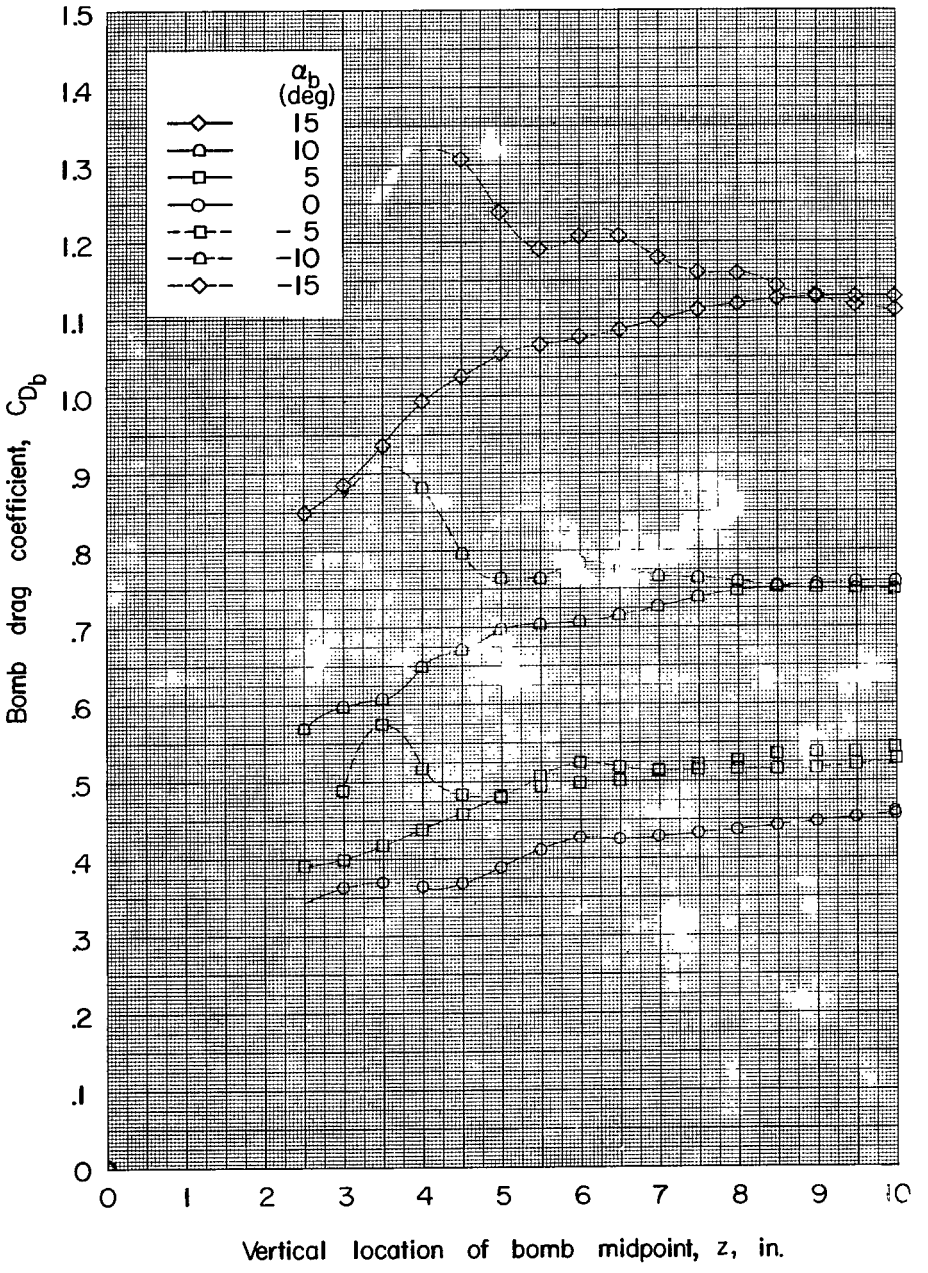

(a) x = -1.65 inches.

Figure 10.- Force and moment data for bomb 3 in presence of the wing-fuselage combination with ejector A. $\alpha_{wf} = 4^\circ$.

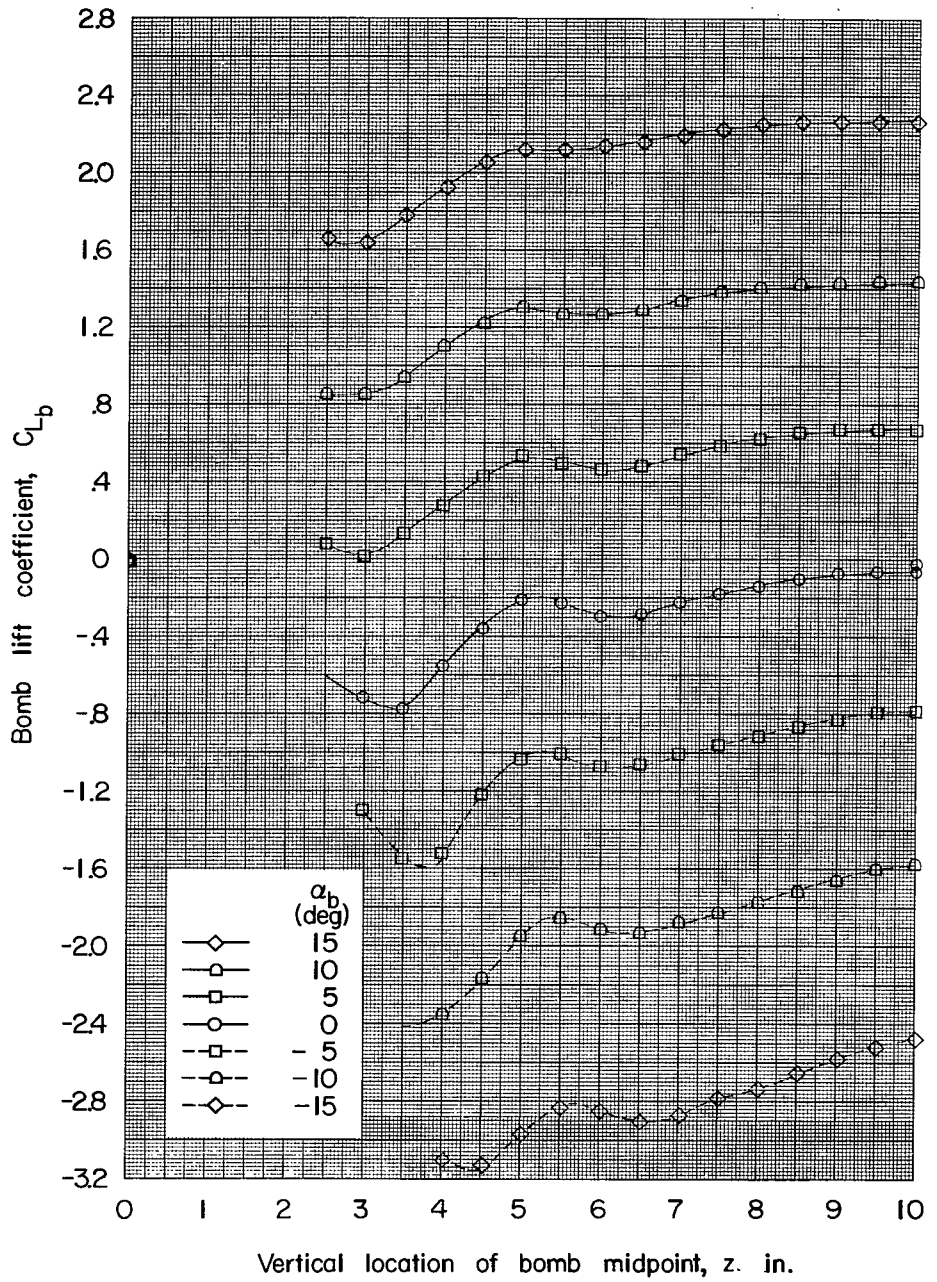

(a) Continued.

Figure 10.- Continued.

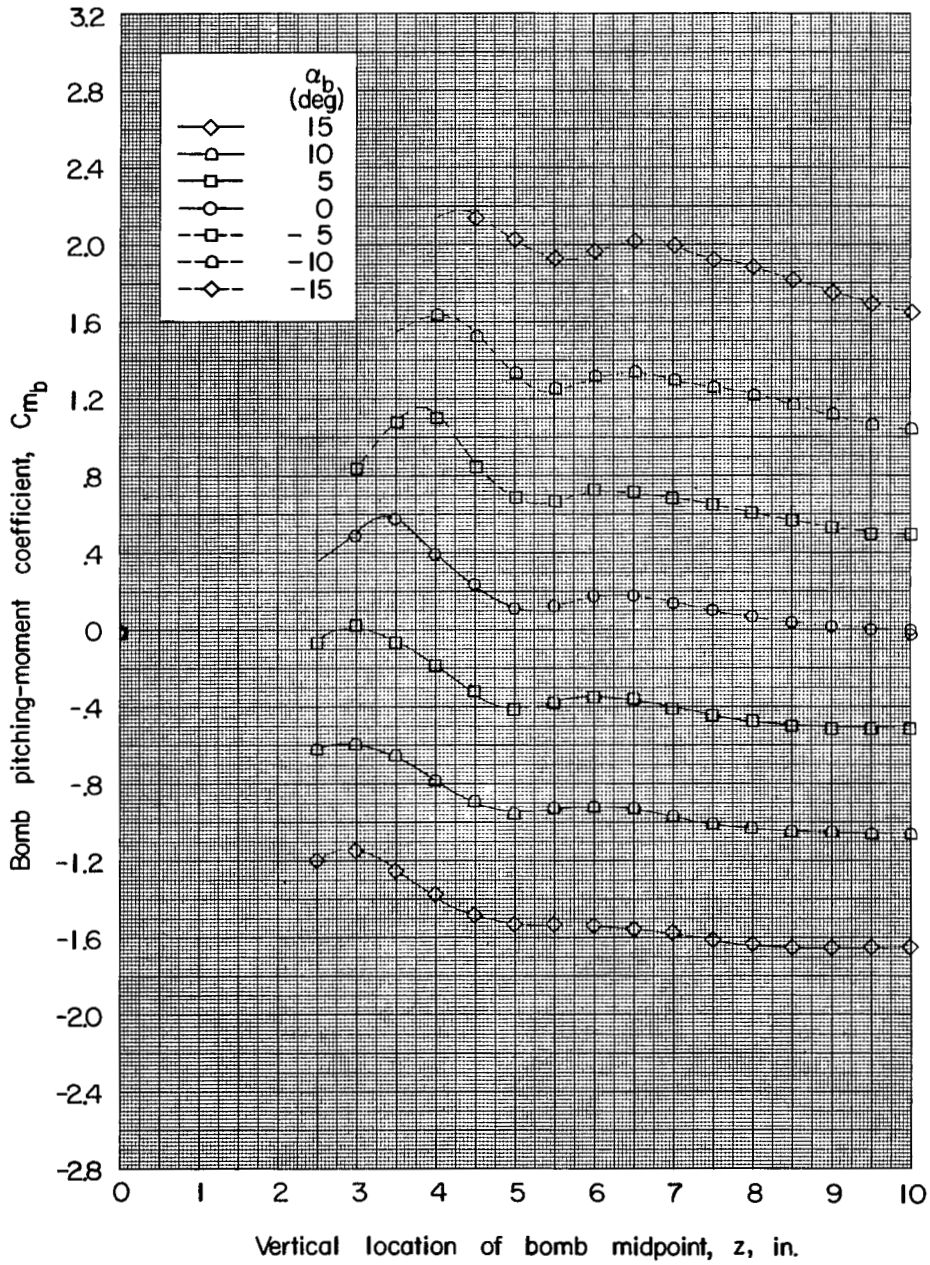

(a) Concluded.

Figure 10.- Continued.

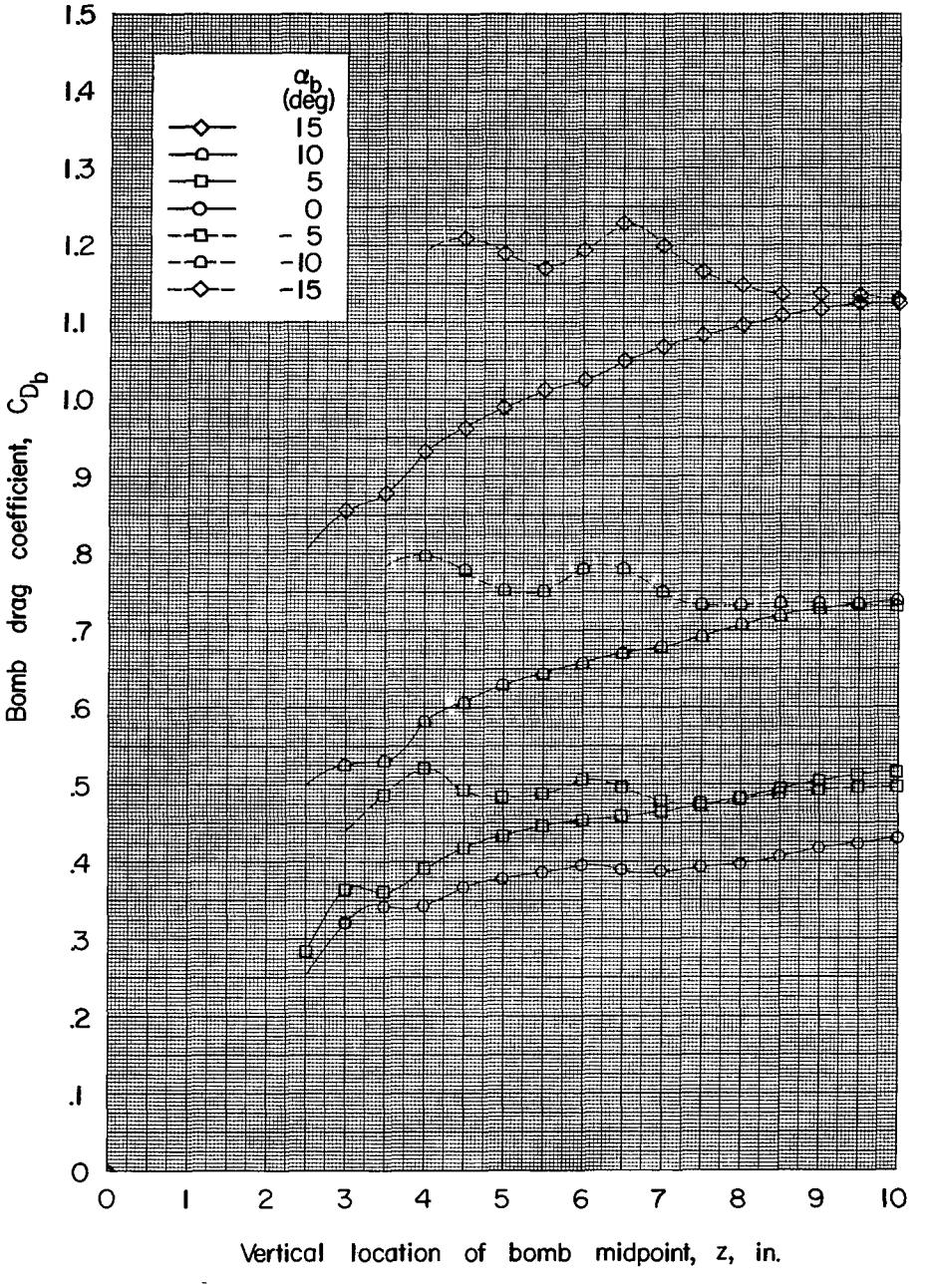

(b) x = -0.15 inch.

Figure 10.- Continued.

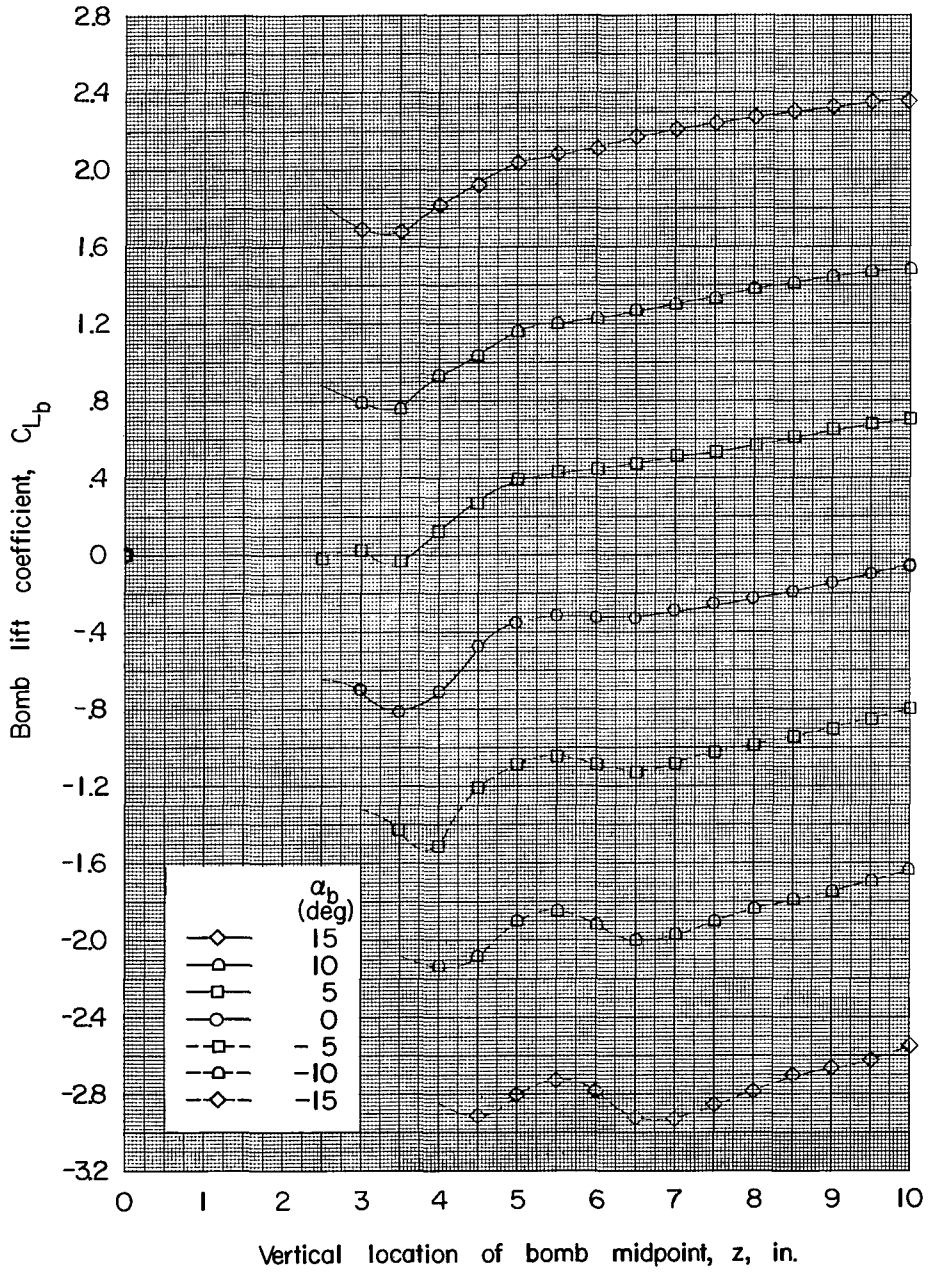

(b) Continued.

Figure 10.- Continued.

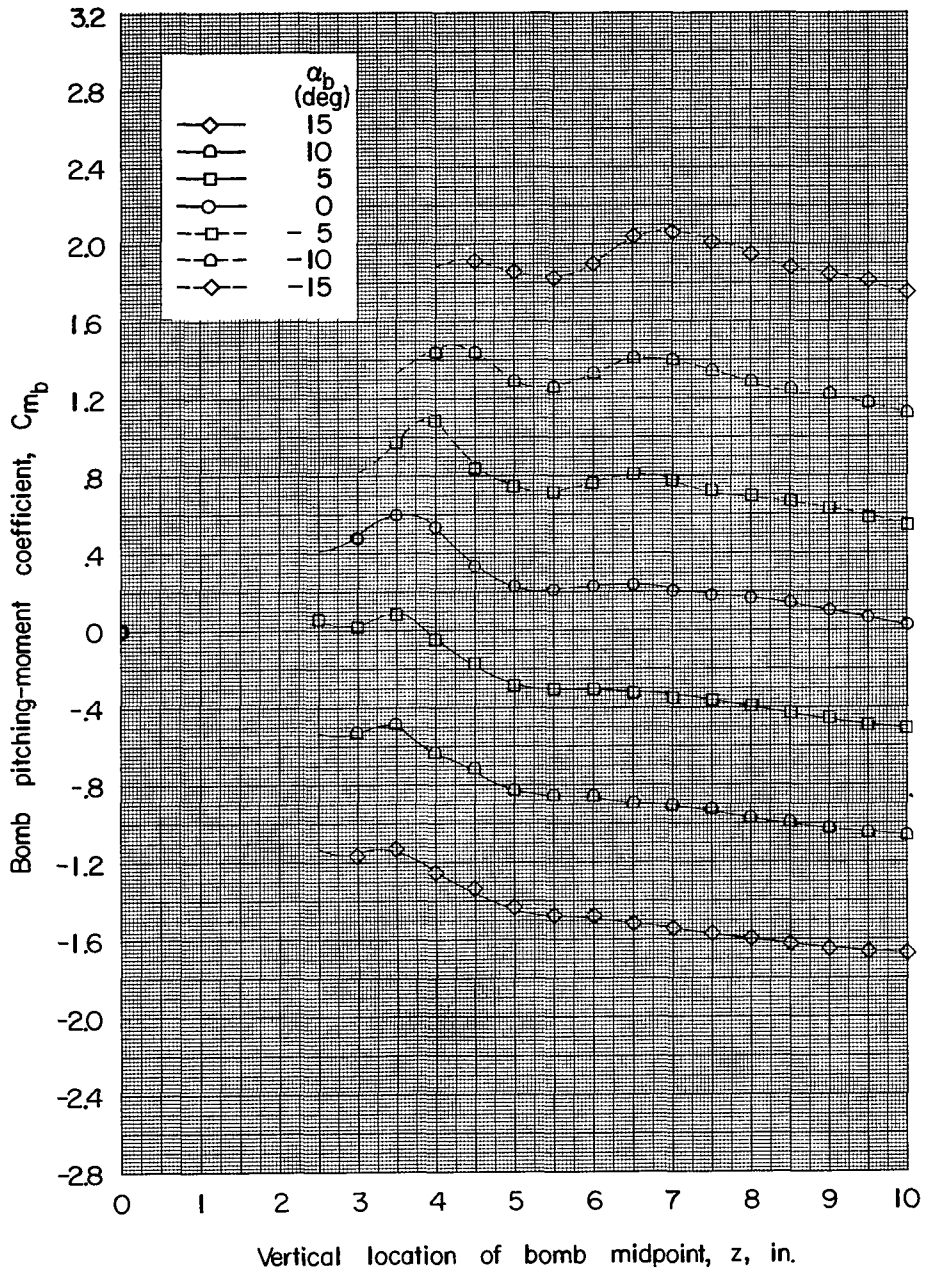

(b) Concluded.

Figure 10.- Continued.

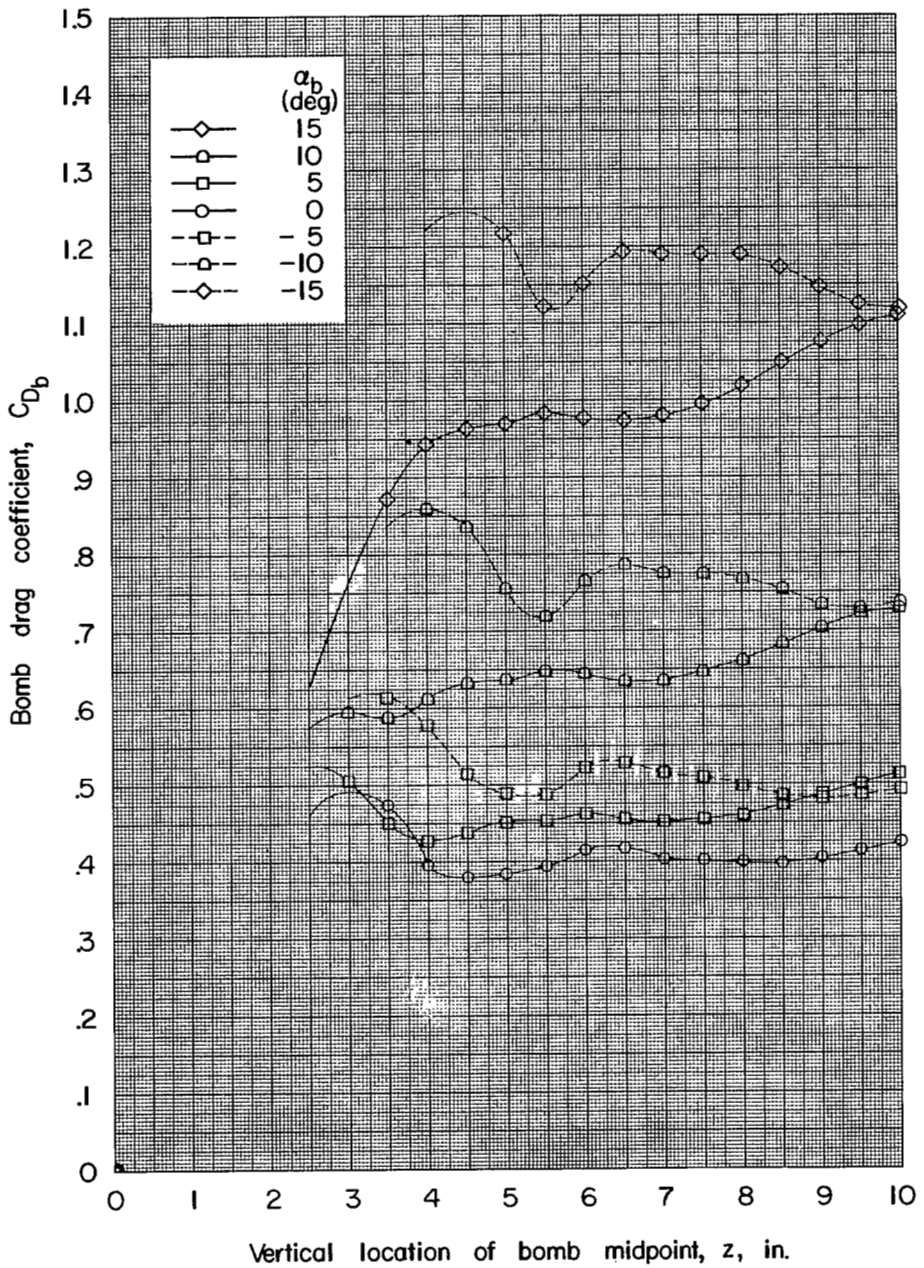

(c) x = 1.85 inches.

Figure 10.- Continued.

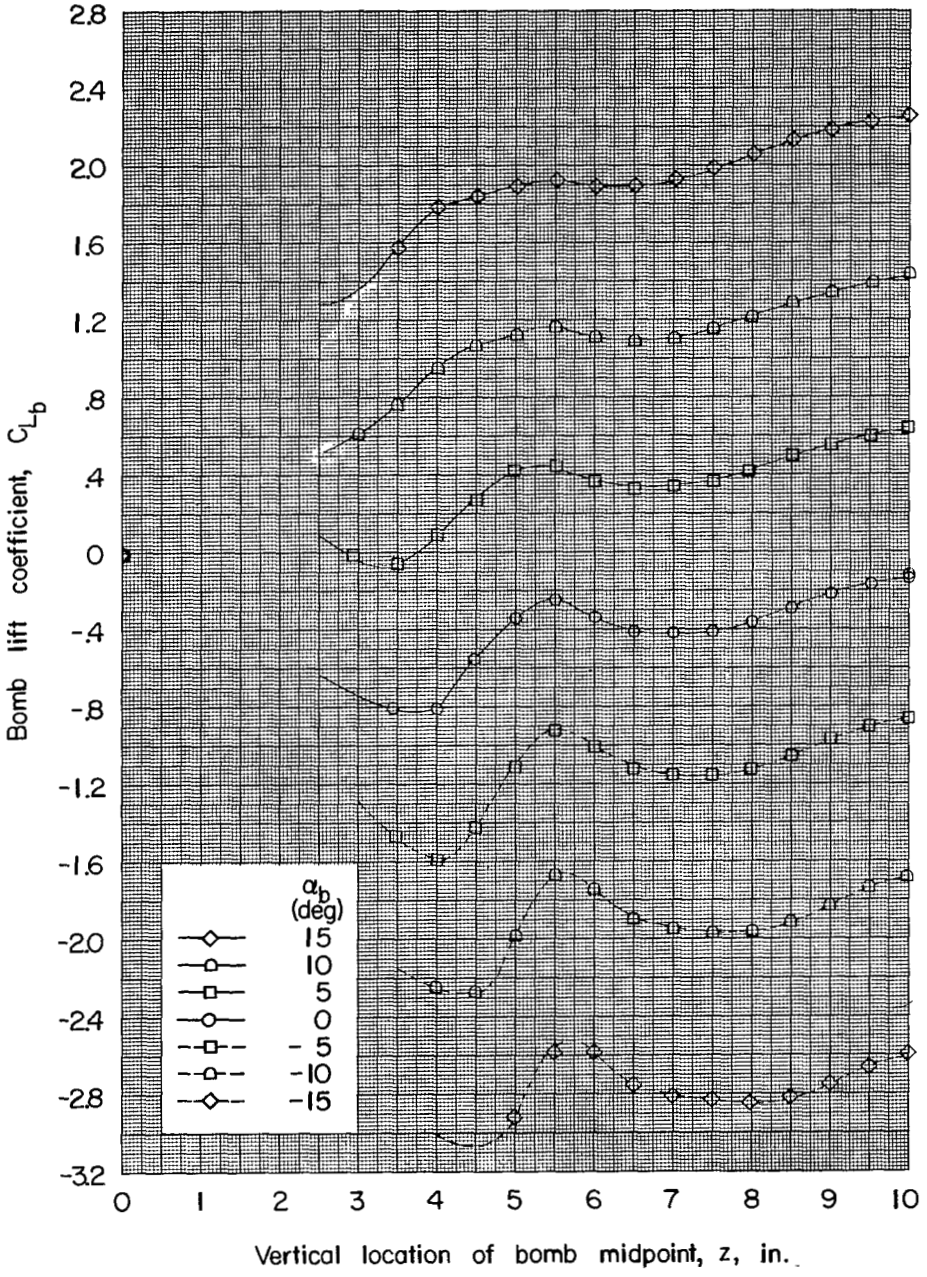

(c) Continued.

Figure 10.- Continued.

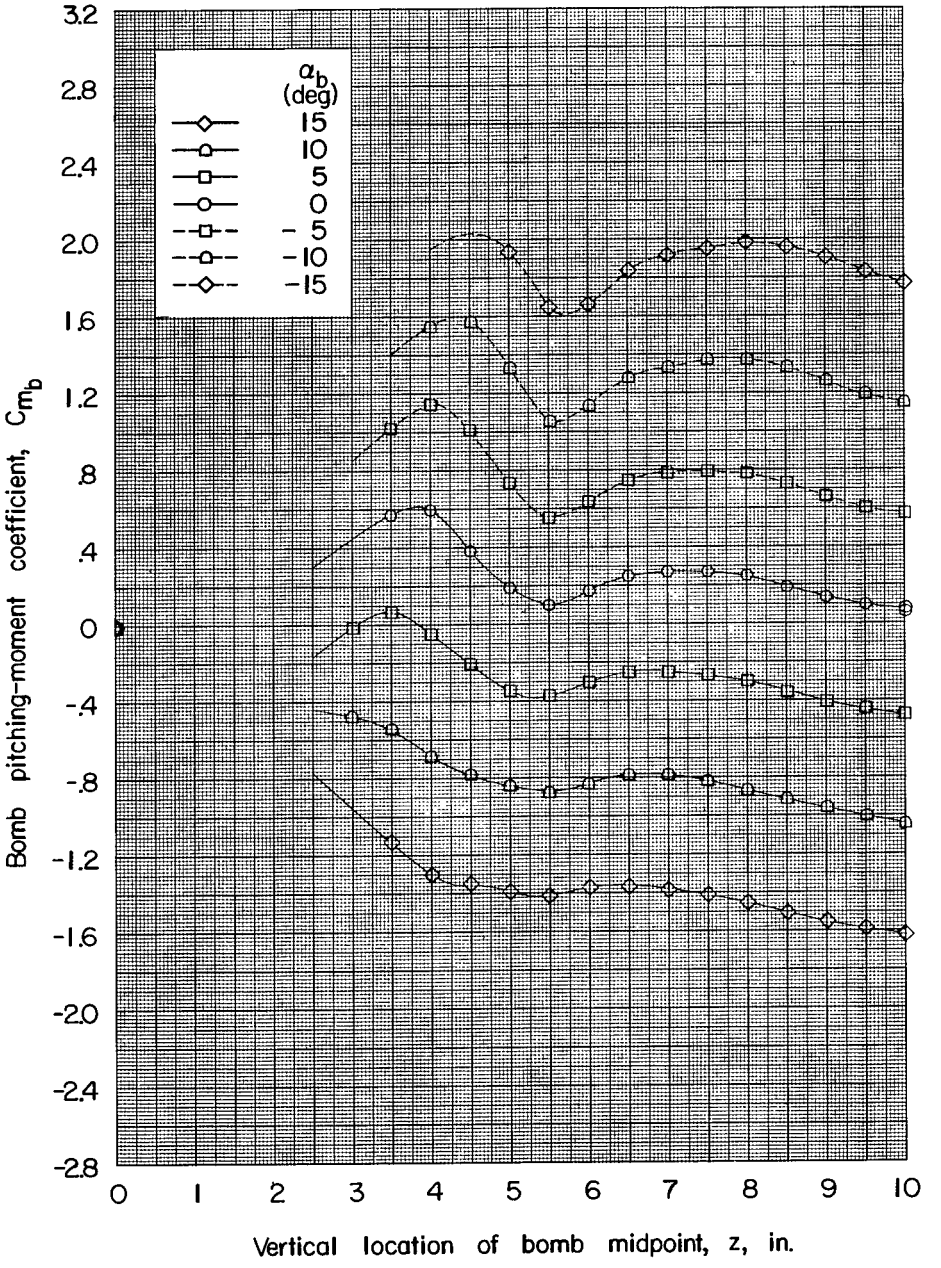

(c) Concluded.

Figure 10.- Continued.

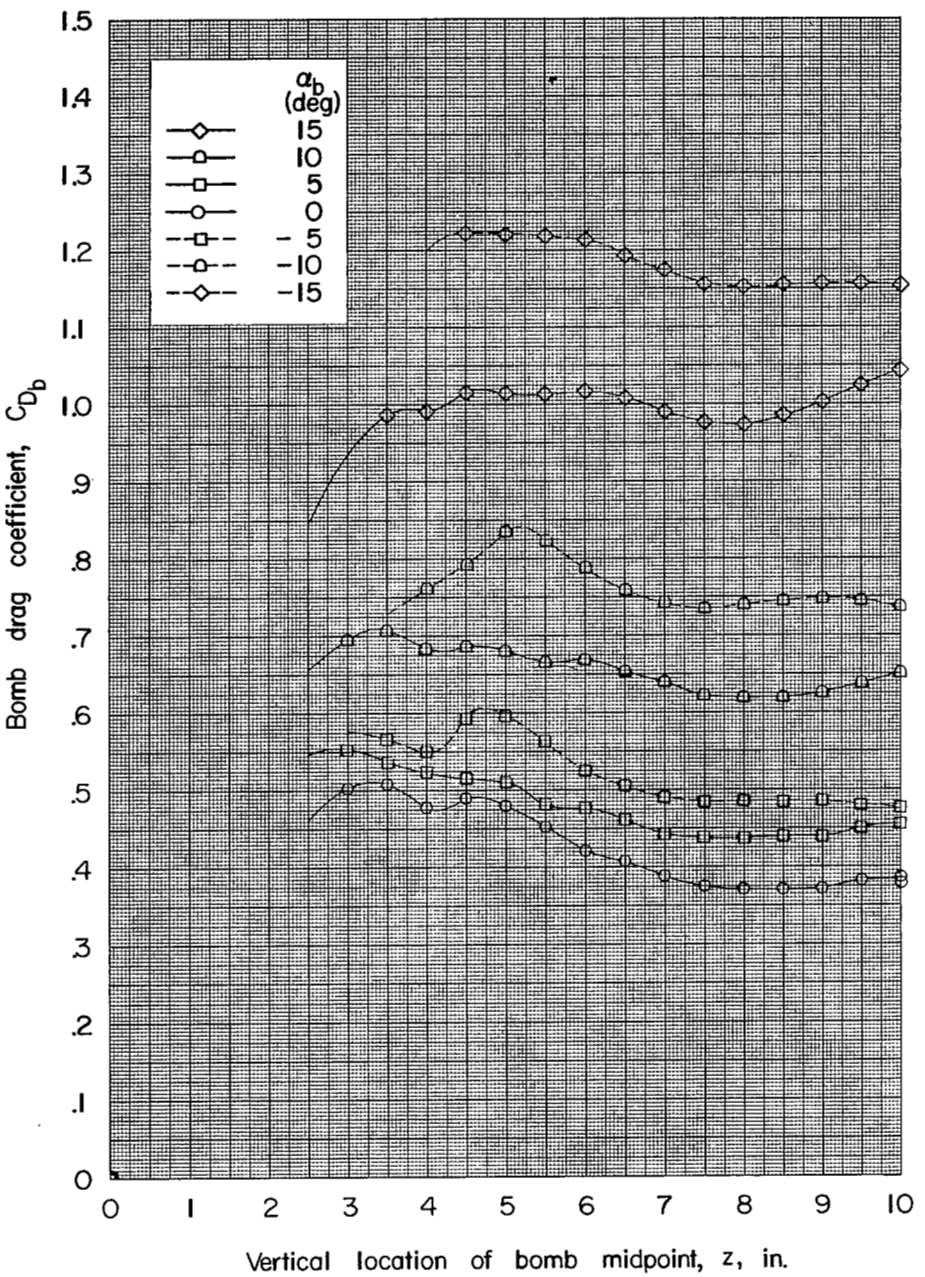

(d) x = 3.85 inches.

Figure 10.- Continued.

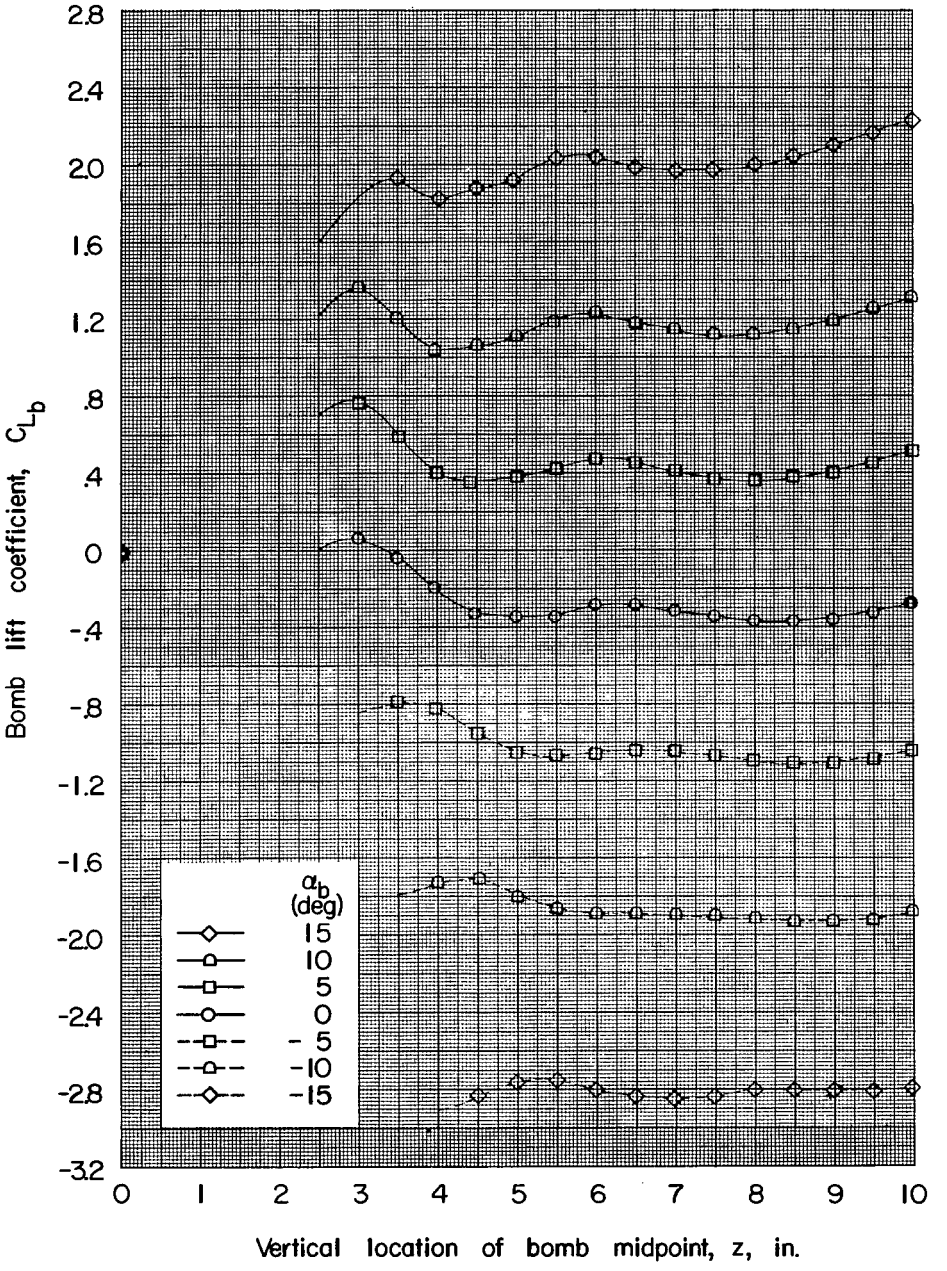

(d) Continued.

Figure 10.- Continued.

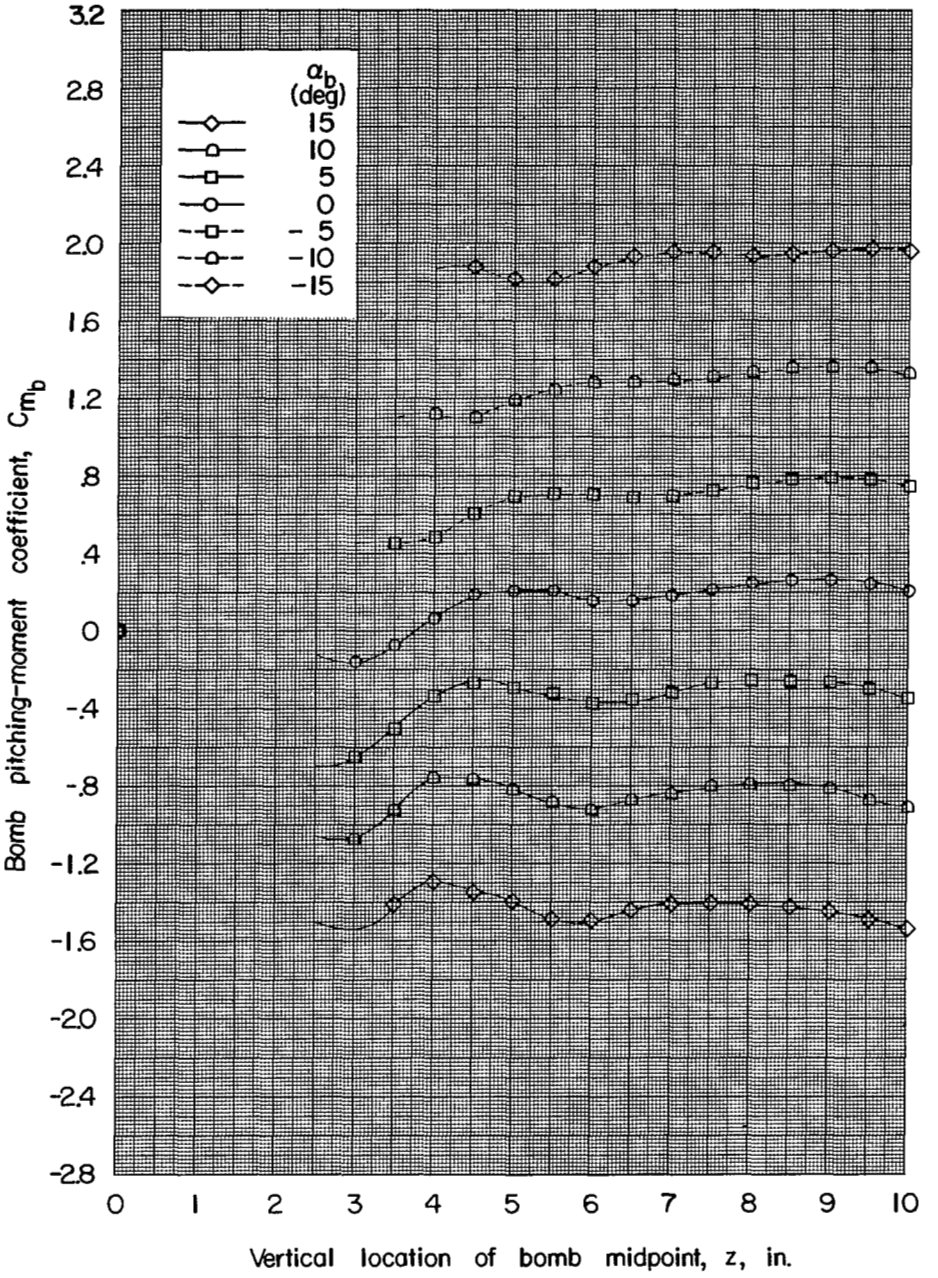

(d) Concluded.

Figure 10.- Concluded.

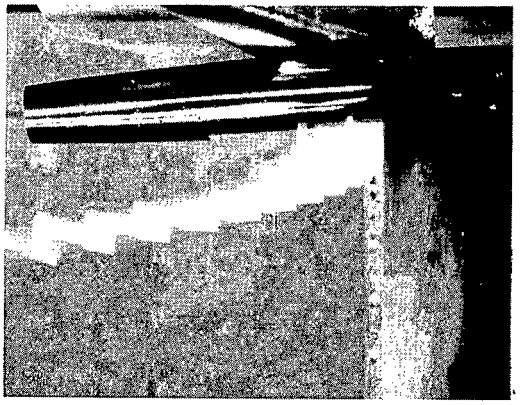

CASE 1

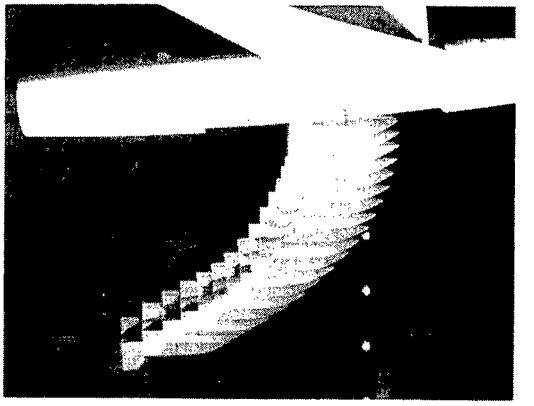

CASE 4

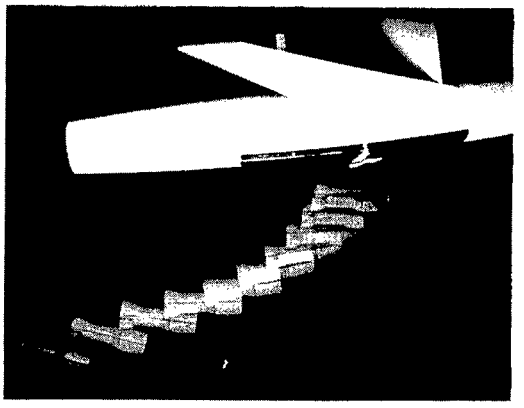

CASE 2

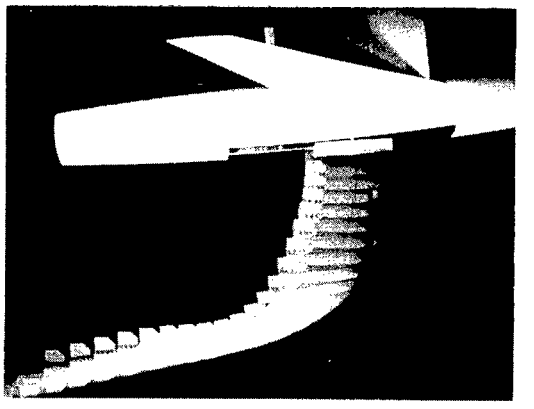

CASE 5

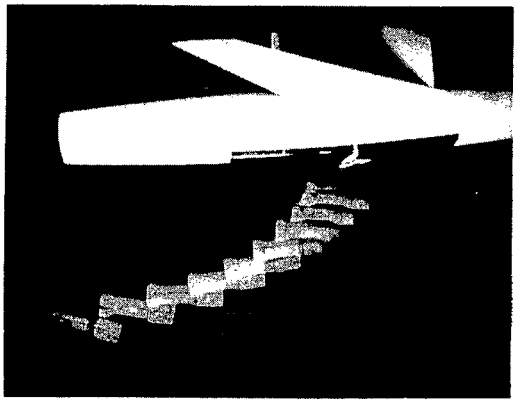

CASE 3

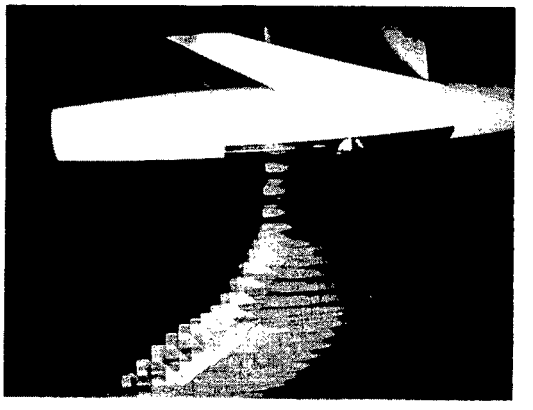

CASE 6

Figure 11.- Stroboscopic photographs of bomb drops. L-57-1648

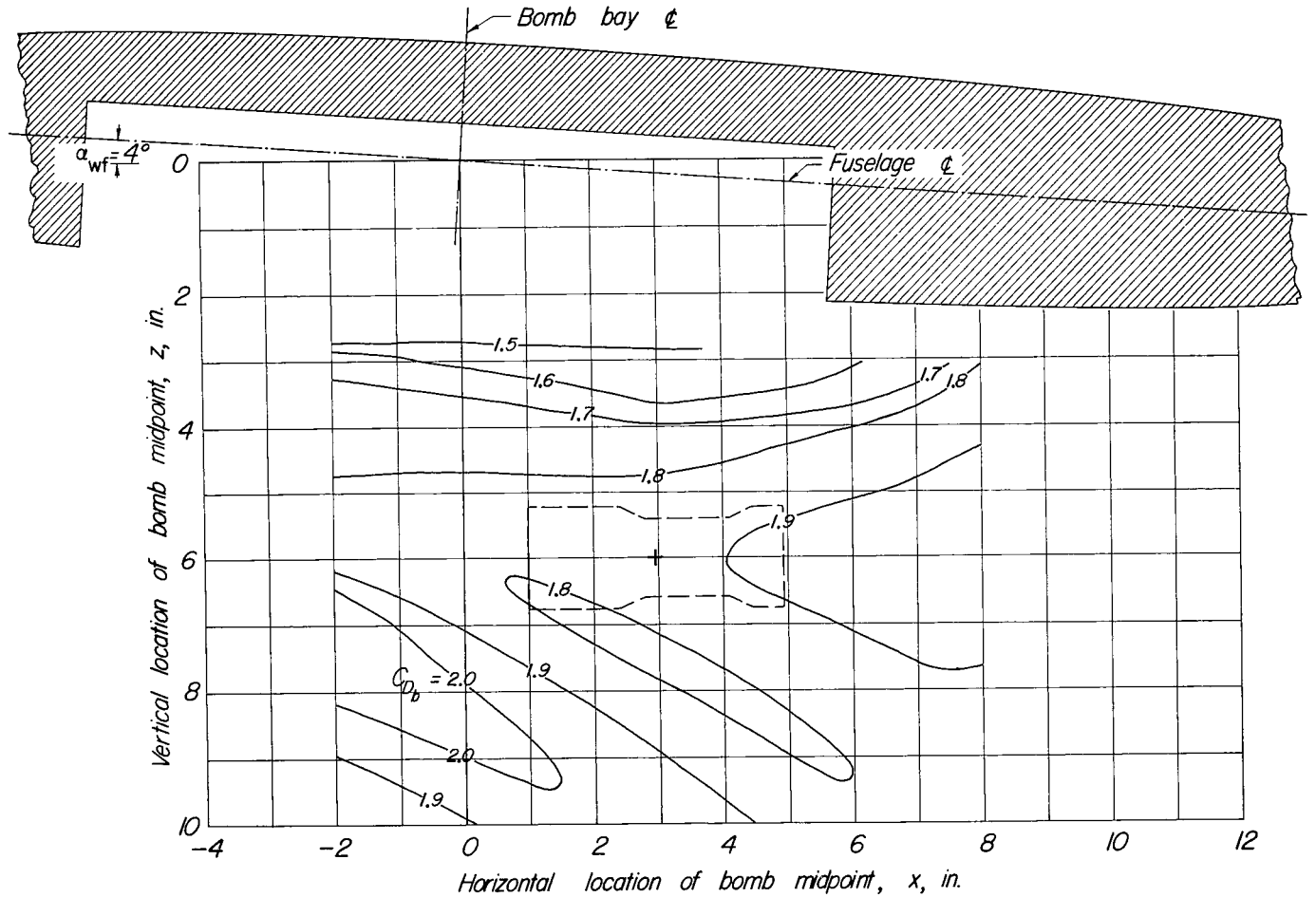

(a) Drag.

Figure 12.- Contour plot of force and moment data of bomb 1 in presence of the wing-fuselage combination without ejector. $\alpha_b = 0°$.

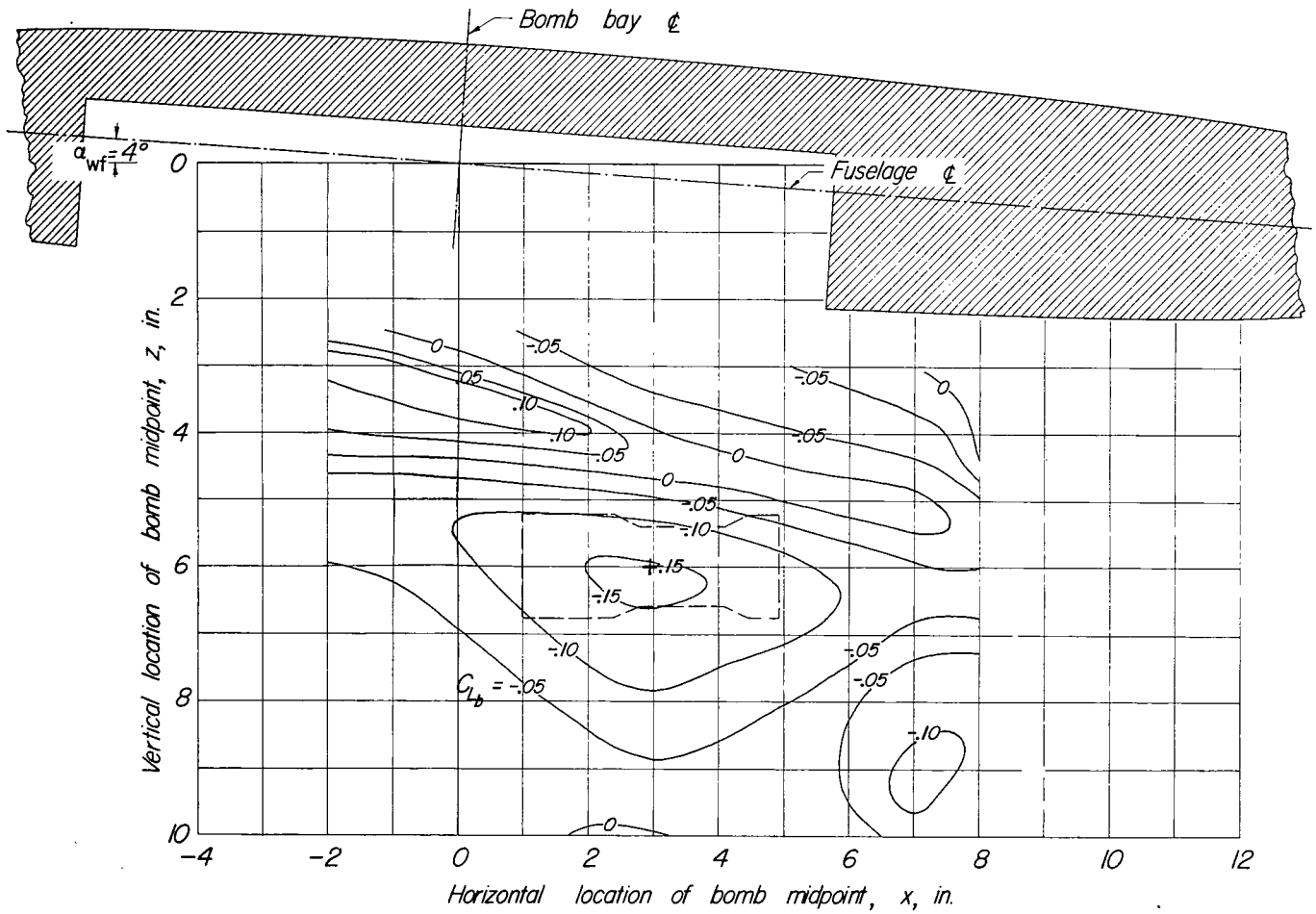

(b) Lift.

Figure 12.- Continued.

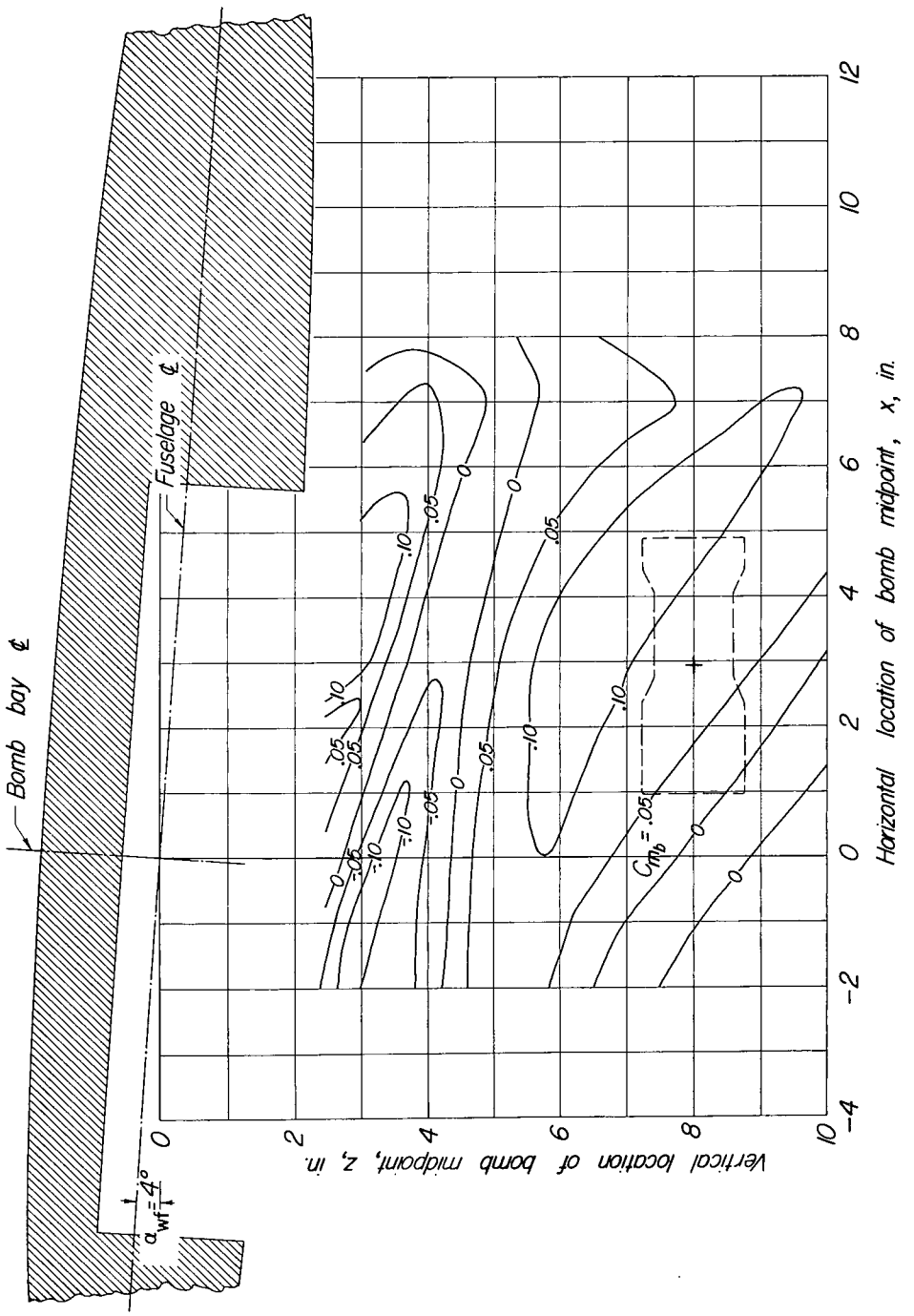

(c) Pitching moment.

Figure 12.- Concluded.

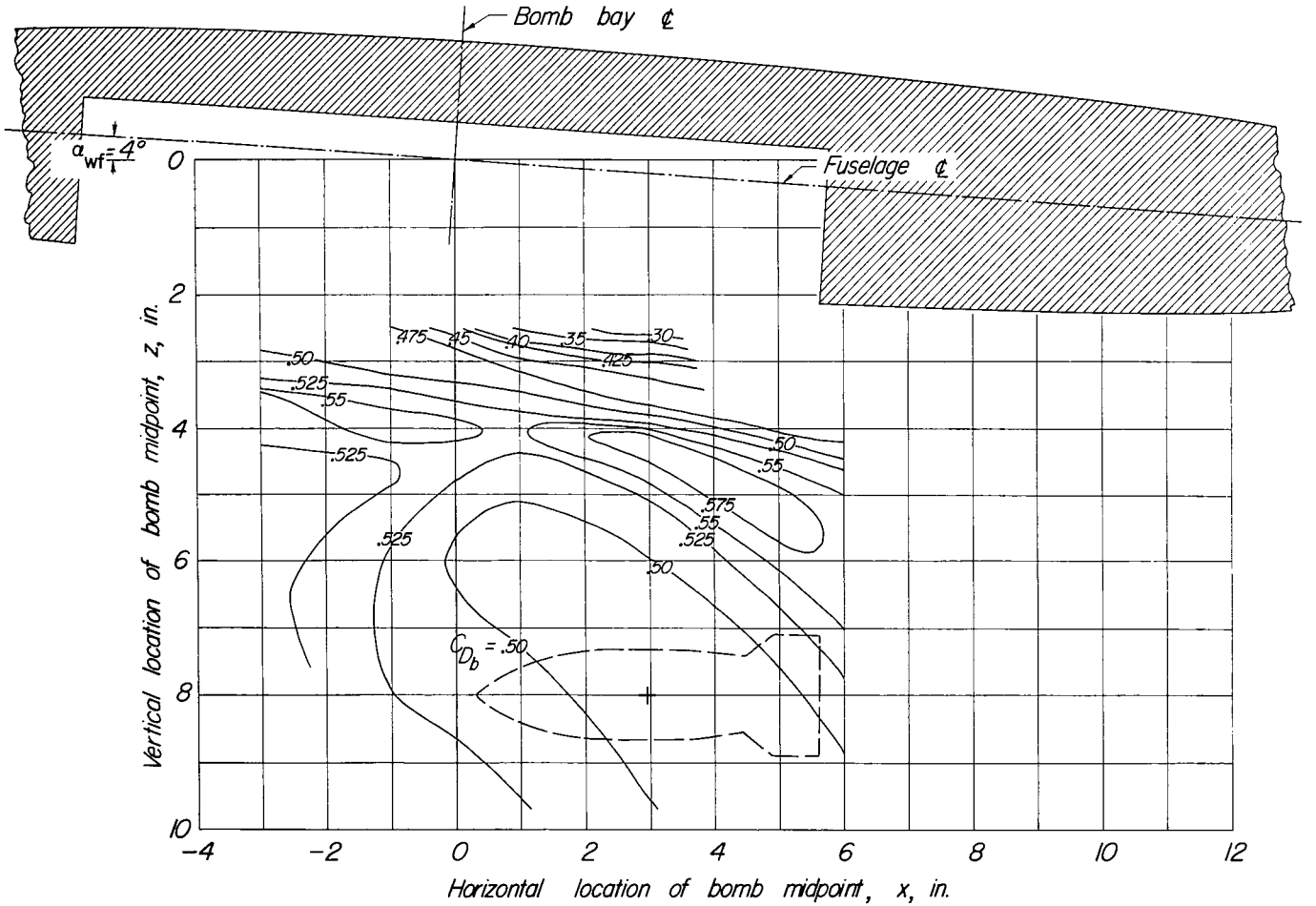

(a) Drag.

Figure 13.- Contour plot of force and moment data of bomb 2 in presence of the wing-fuselage combination without ejector. $\alpha_b = 0°$.

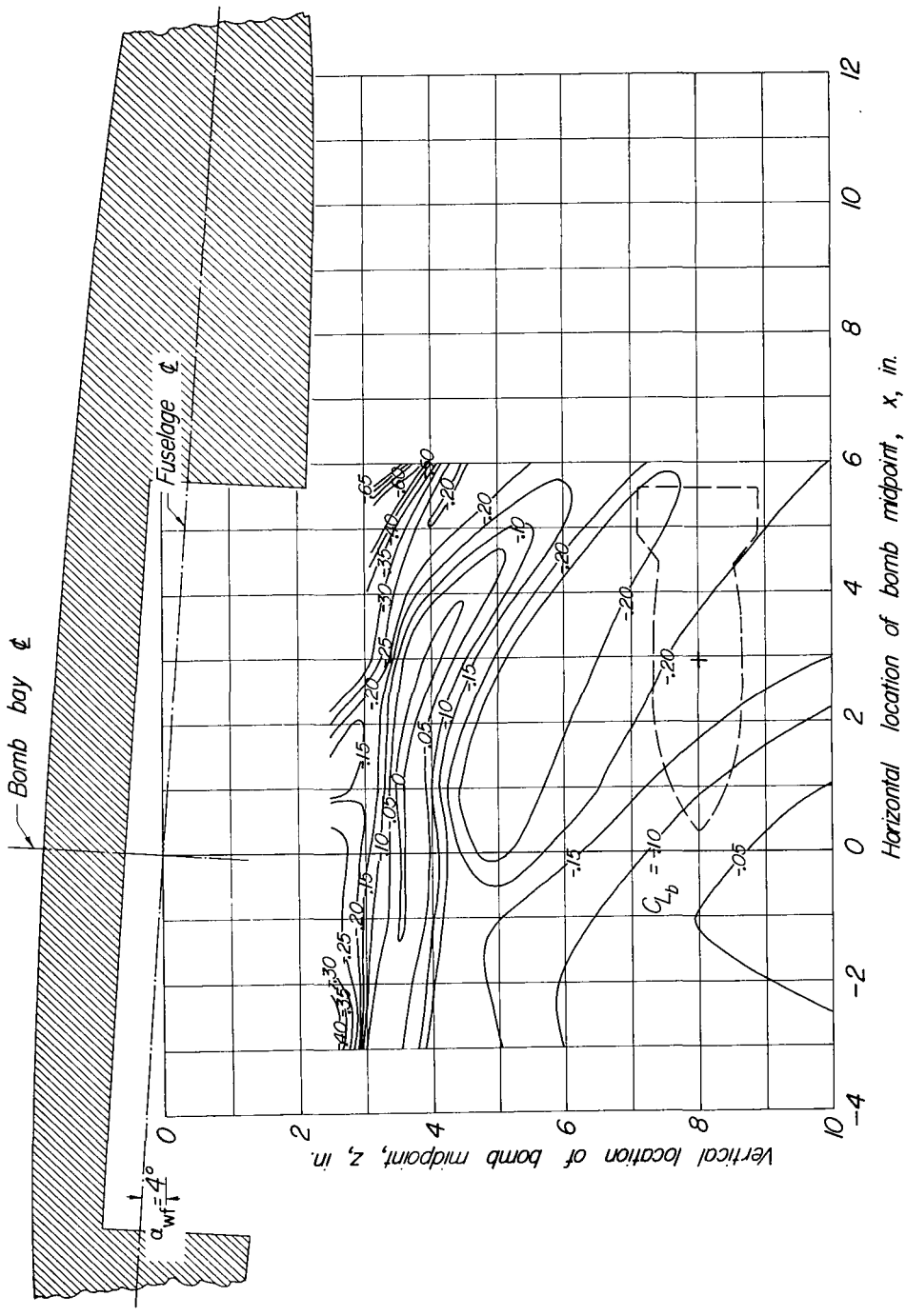

(b) Lift.

Figure 13.- Continued.

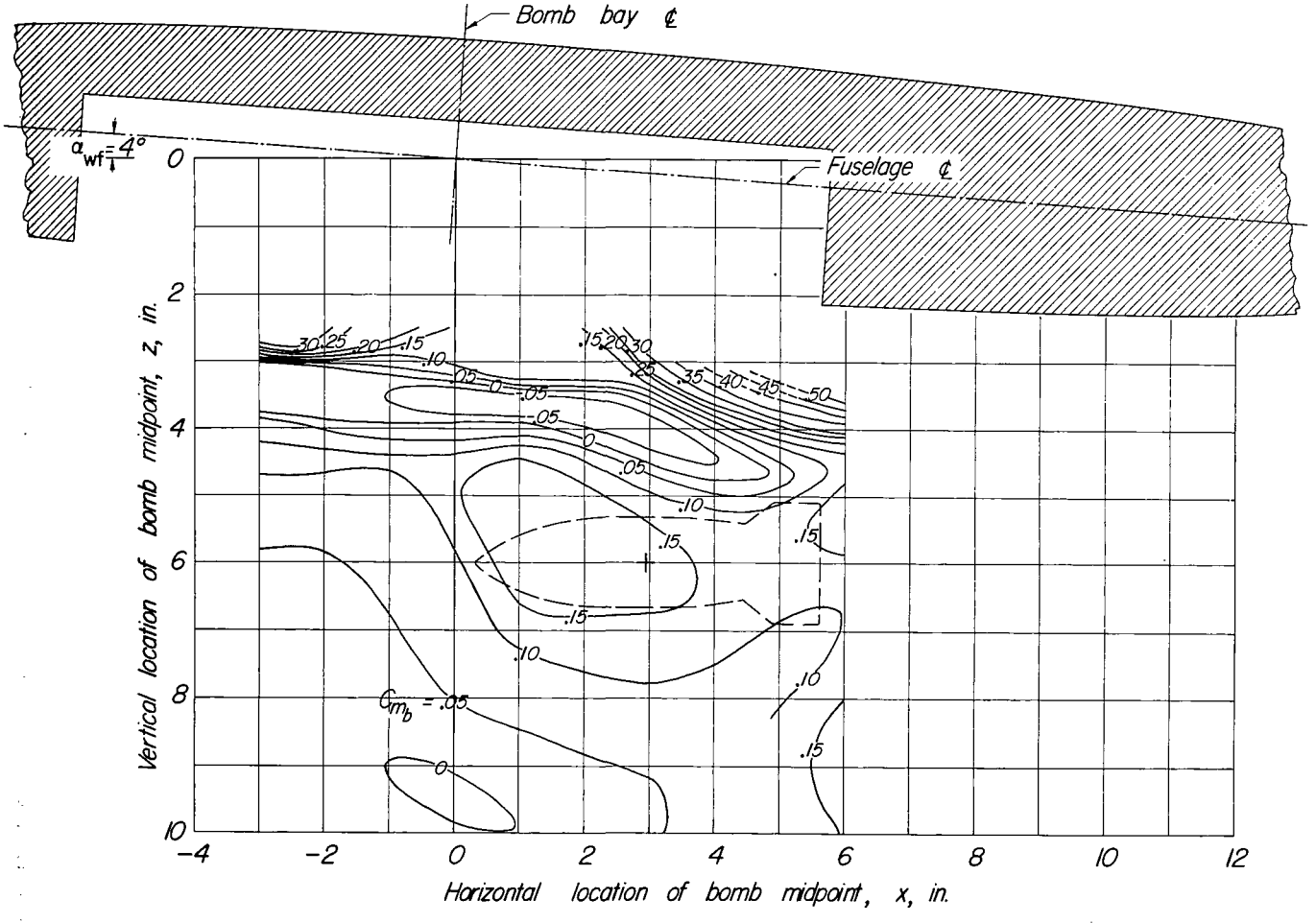

(c) Pitching moment.

Figure 13.- Concluded.

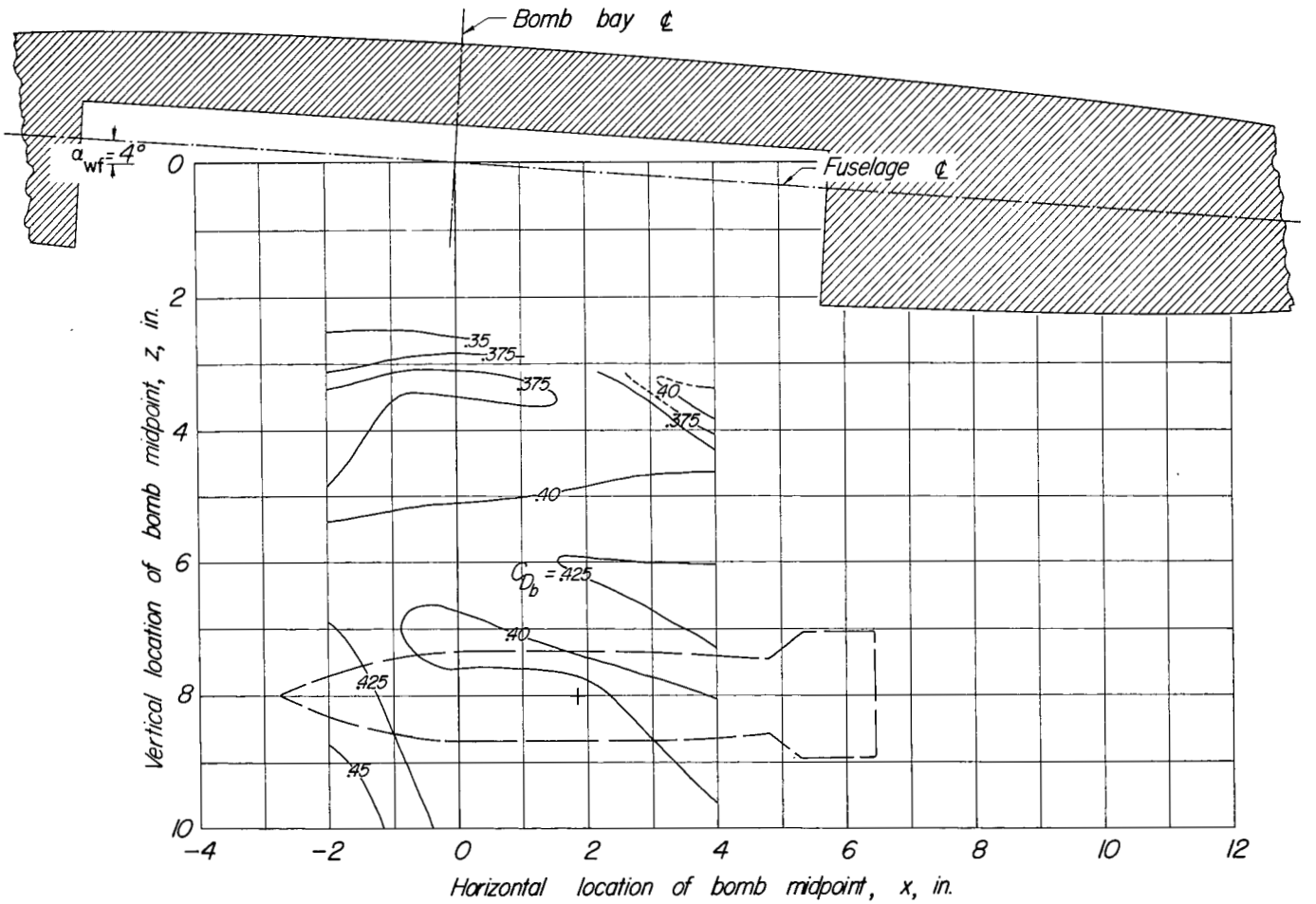

(a) Drag.

Figure 14.- Contour plot of force and moment data of bomb 3 in presence of the wing-fuselage combination without ejector. $\alpha_b = 0°$.

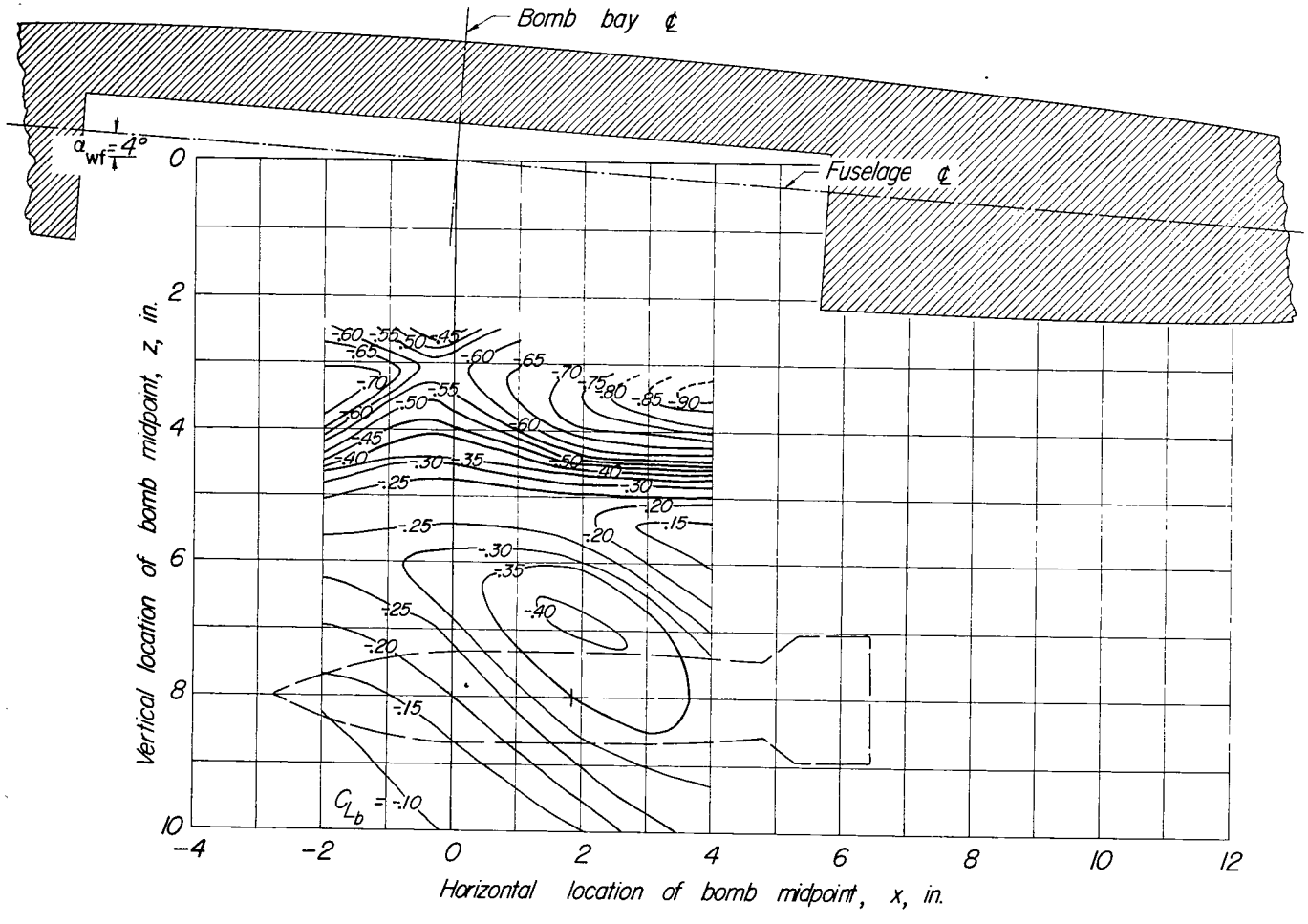

(b) Lift.

Figure 14.- Continued.

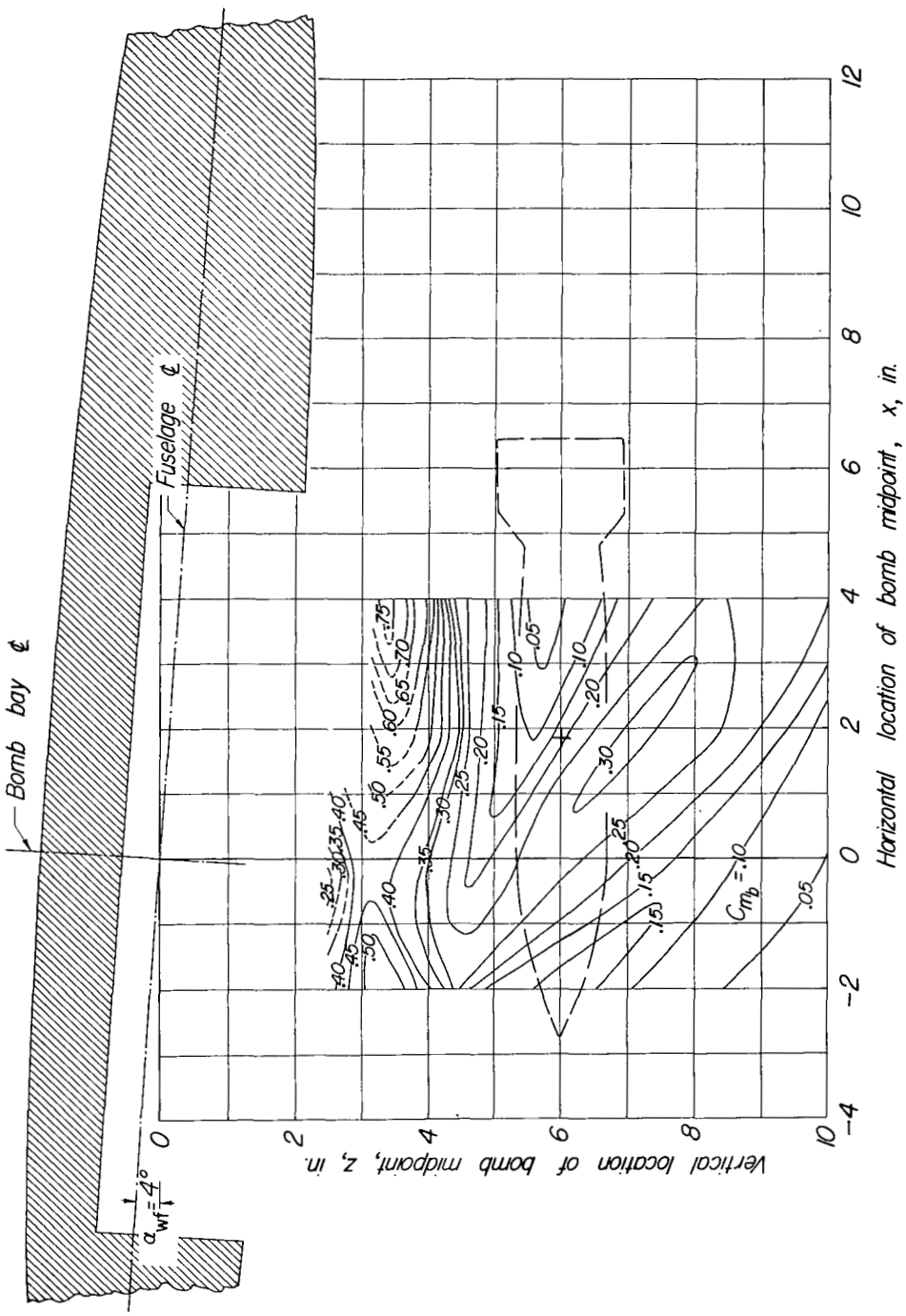

(c) Pitching moment.

Figure 14.- Concluded.

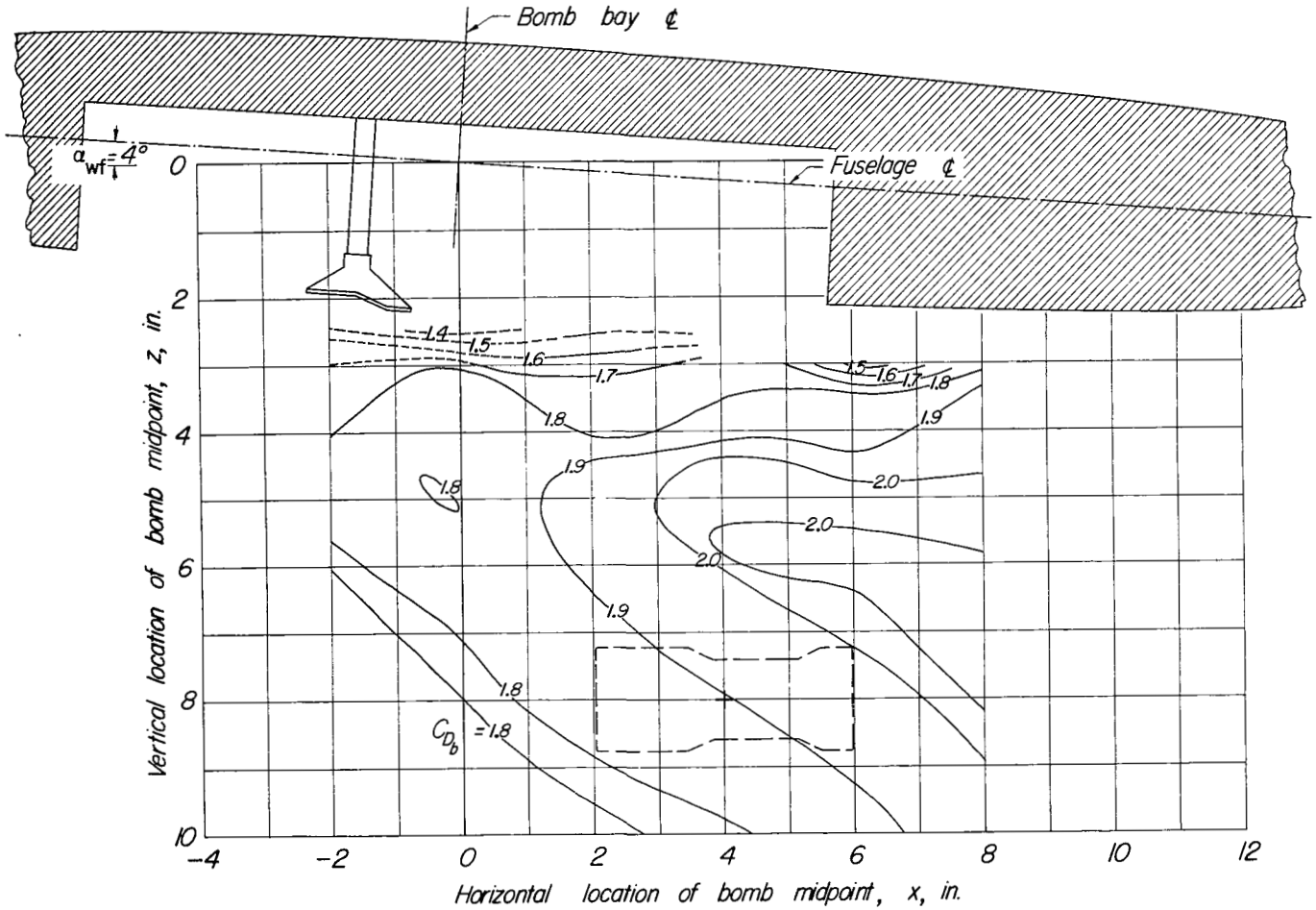

(a) Drag.

Figure 15.- Contour plots of force and moment data of bomb 1 in presence of the wing-fuselage combination with ejector C. $\alpha_b = 0^\circ$.

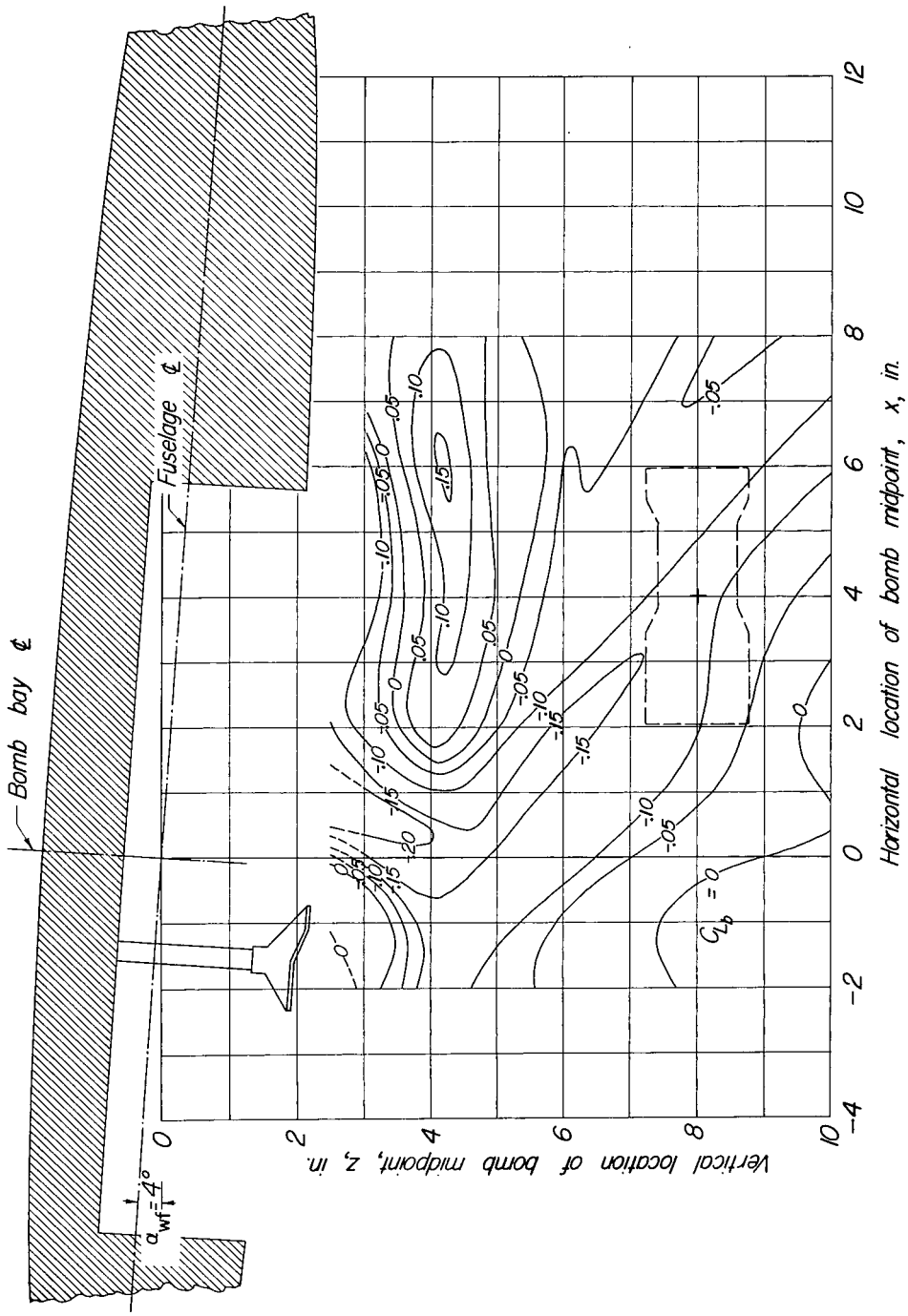

(b) Lift.

Figure 15.- Continued.

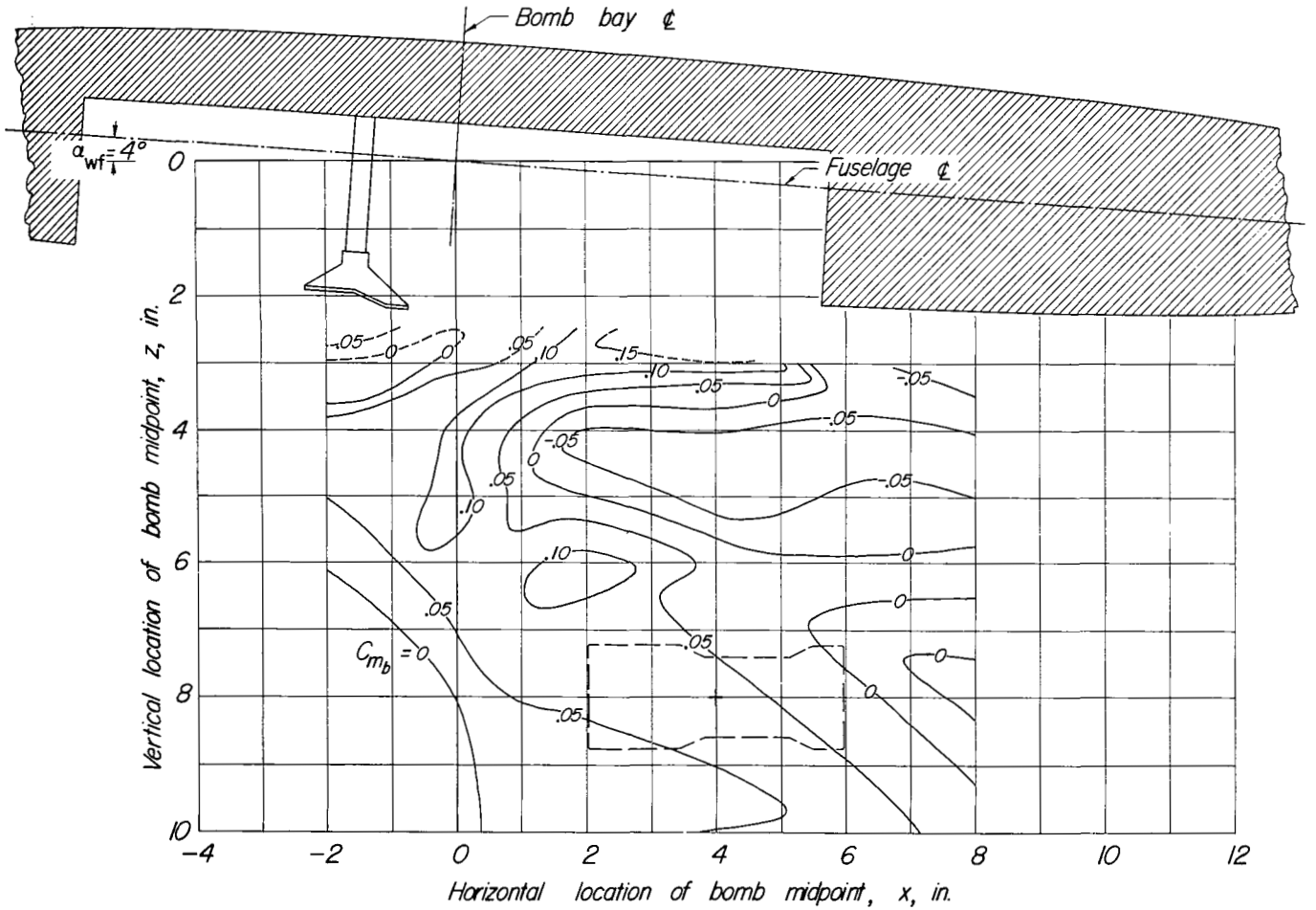

(c) Pitching moment.

Figure 15.- Concluded.

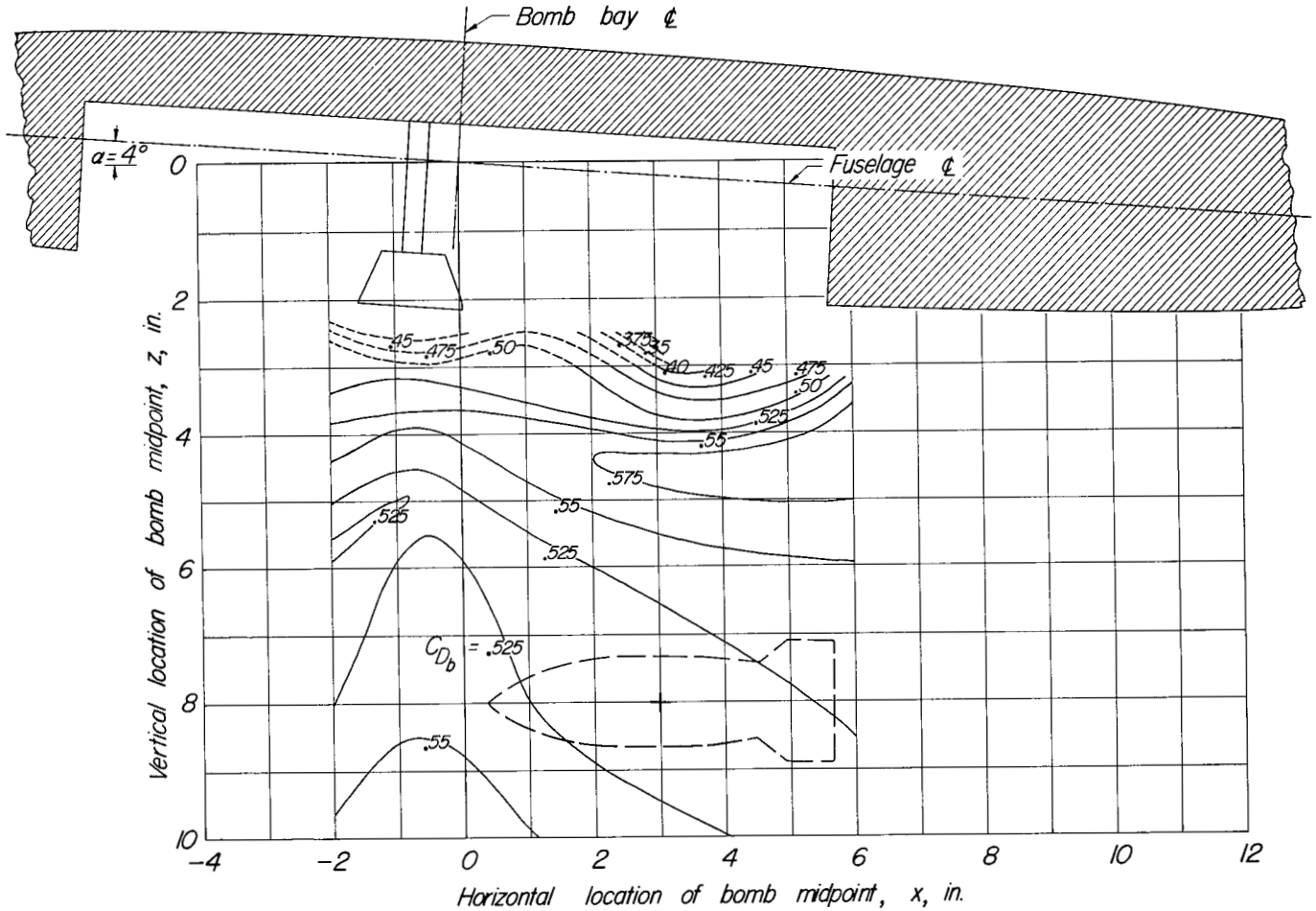

(a) Drag.

Figure 16.- Contour plots of force and moment data of bomb 2 in presence of the wing-fuselage combination with ejector A. $\alpha_b = 0^o$.

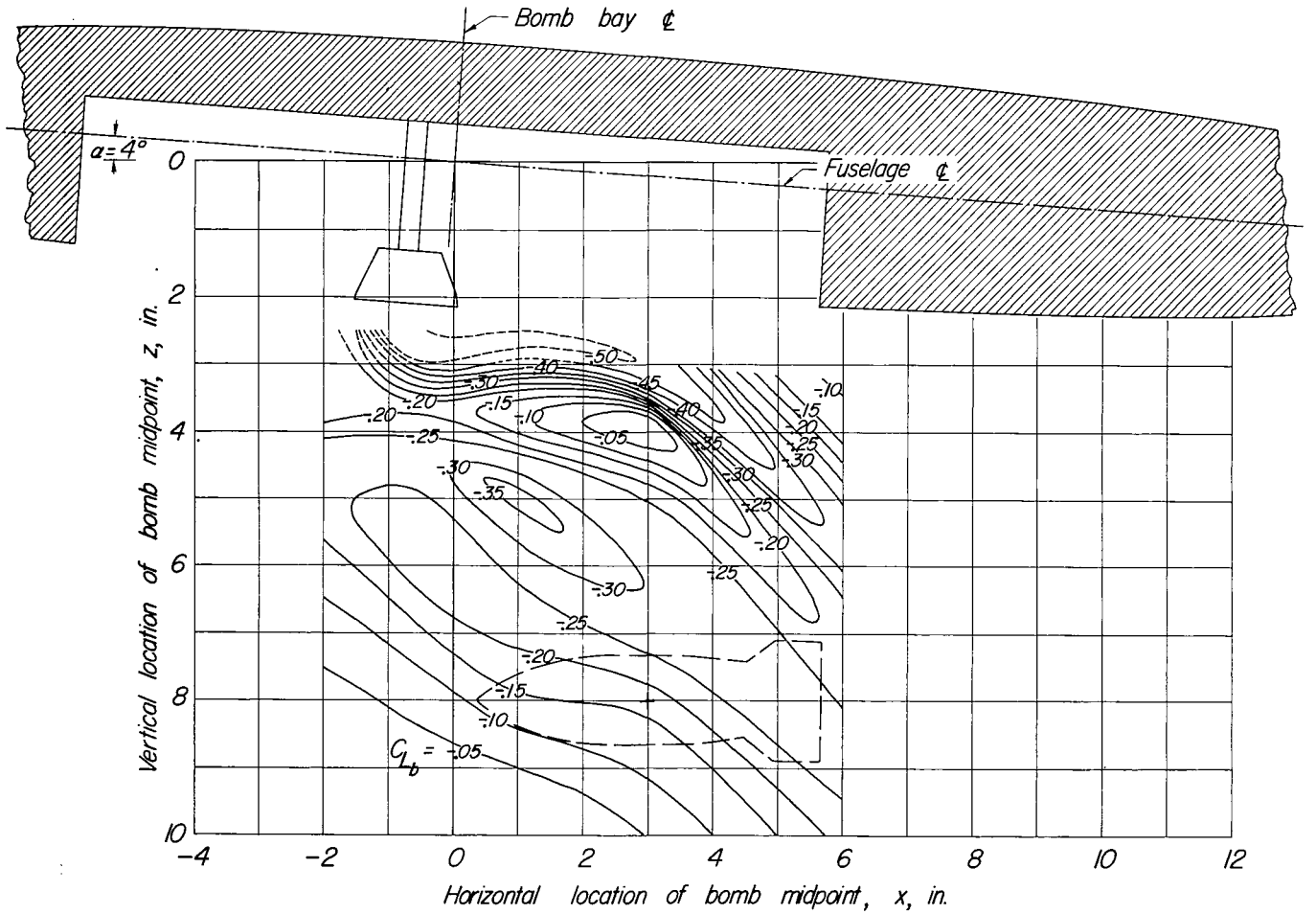

(b) Lift.

Figure 16.- Continued.

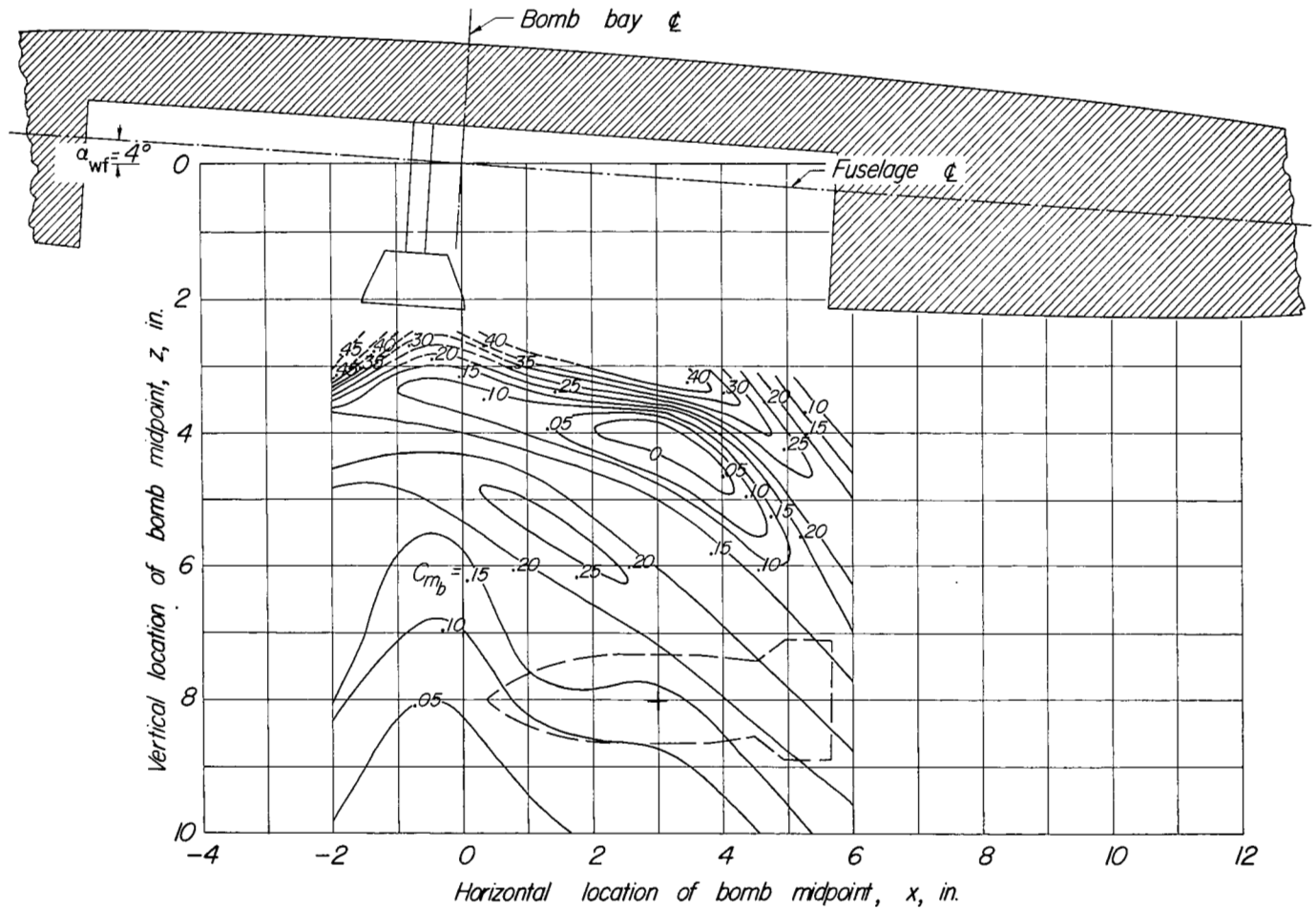

(c) Pitching moment.

Figure 16.- Concluded.

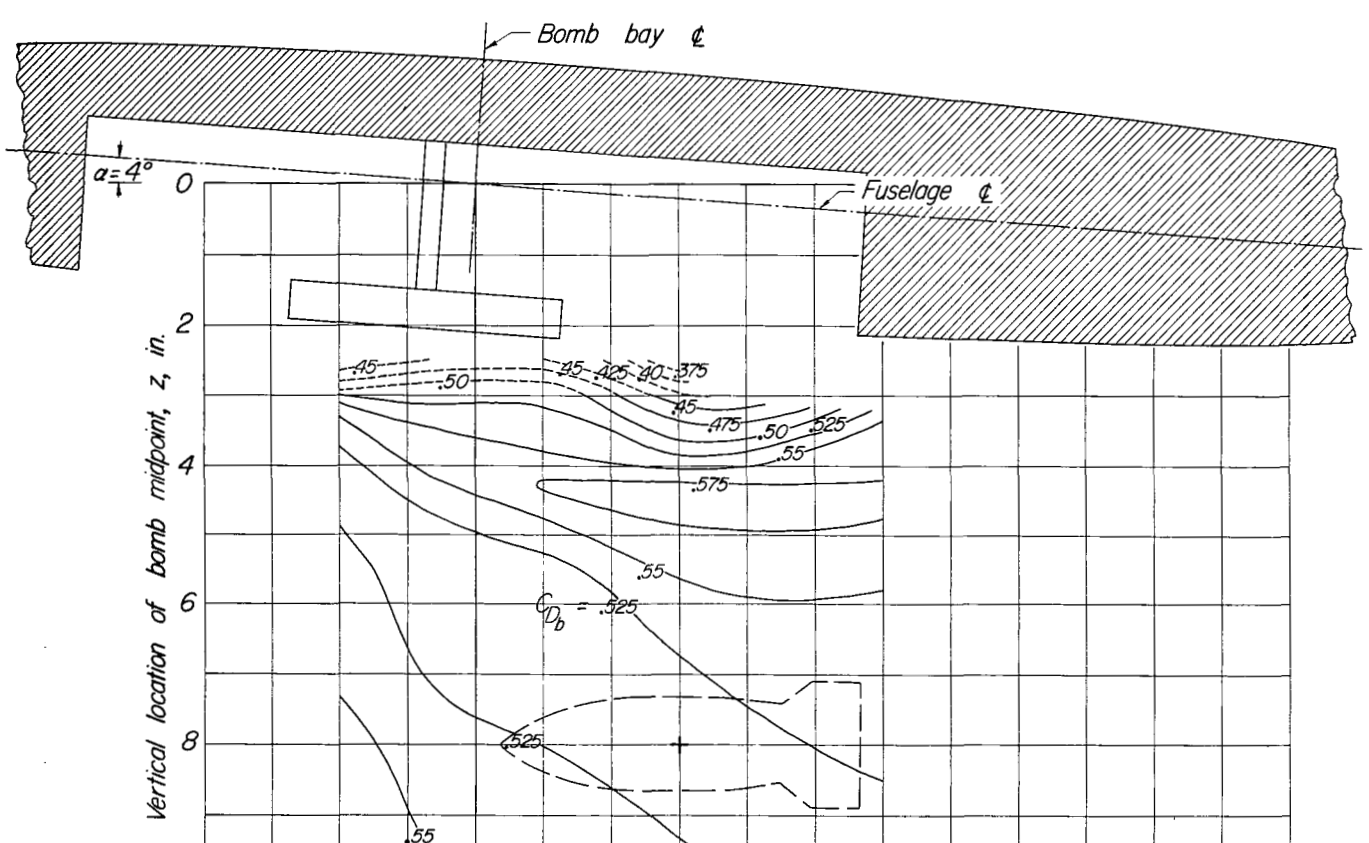

(a) Drag.

Figure 17.- Contour plots of force and moment data of bomb 2 in presence of the wing-fuselage combination with ejector B. $\alpha_b = 0^\circ$.

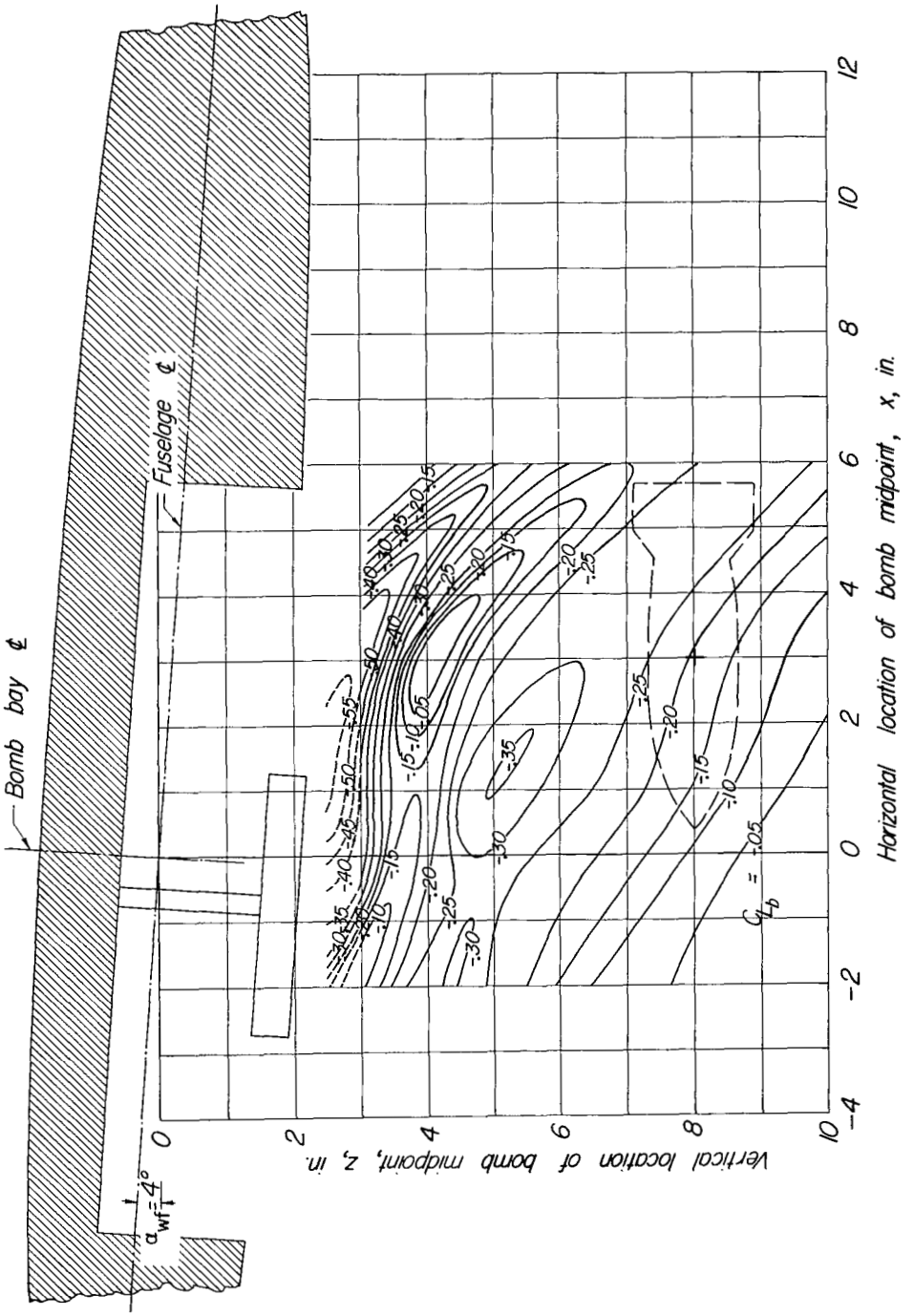

(b) Lift.

Figure 17.- Continued.

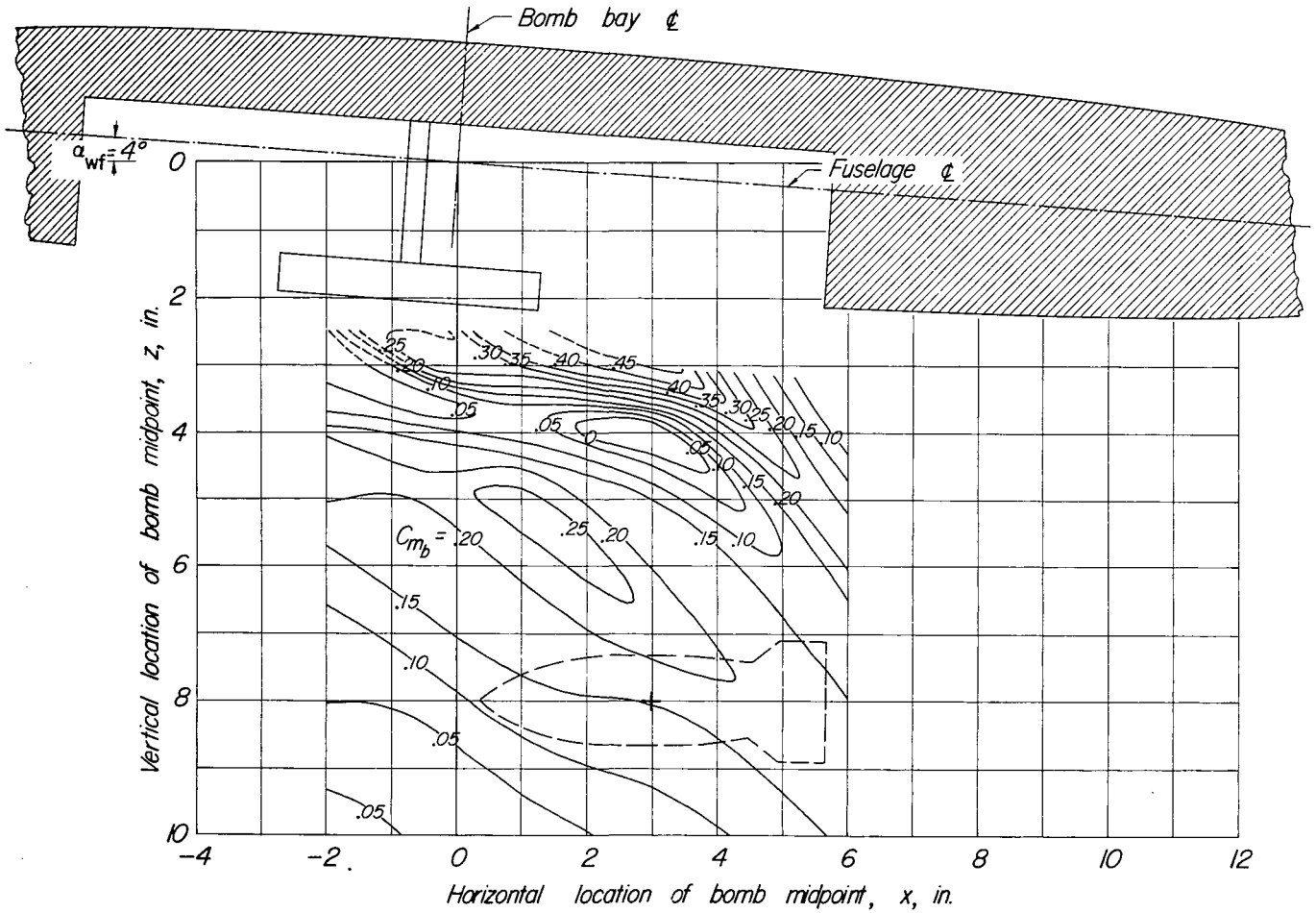

(c) Pitching moment.

Figure 17.- Concluded.

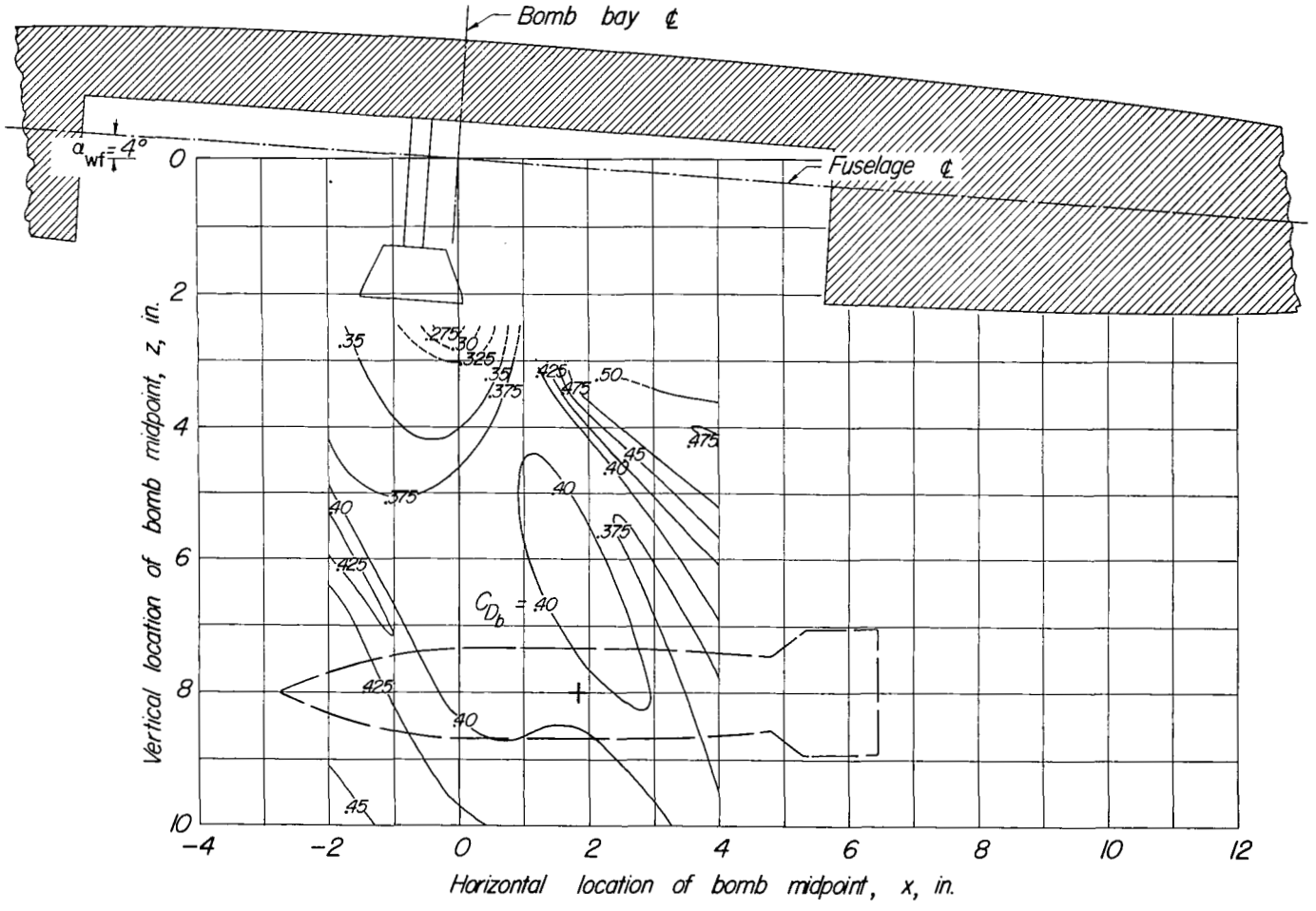

(a) Drag.

Figure 18.- Contour plots of force and moment data of bomb 3 in presence of the wing-fuselage combination with ejector A. $\alpha_b = 0°$.

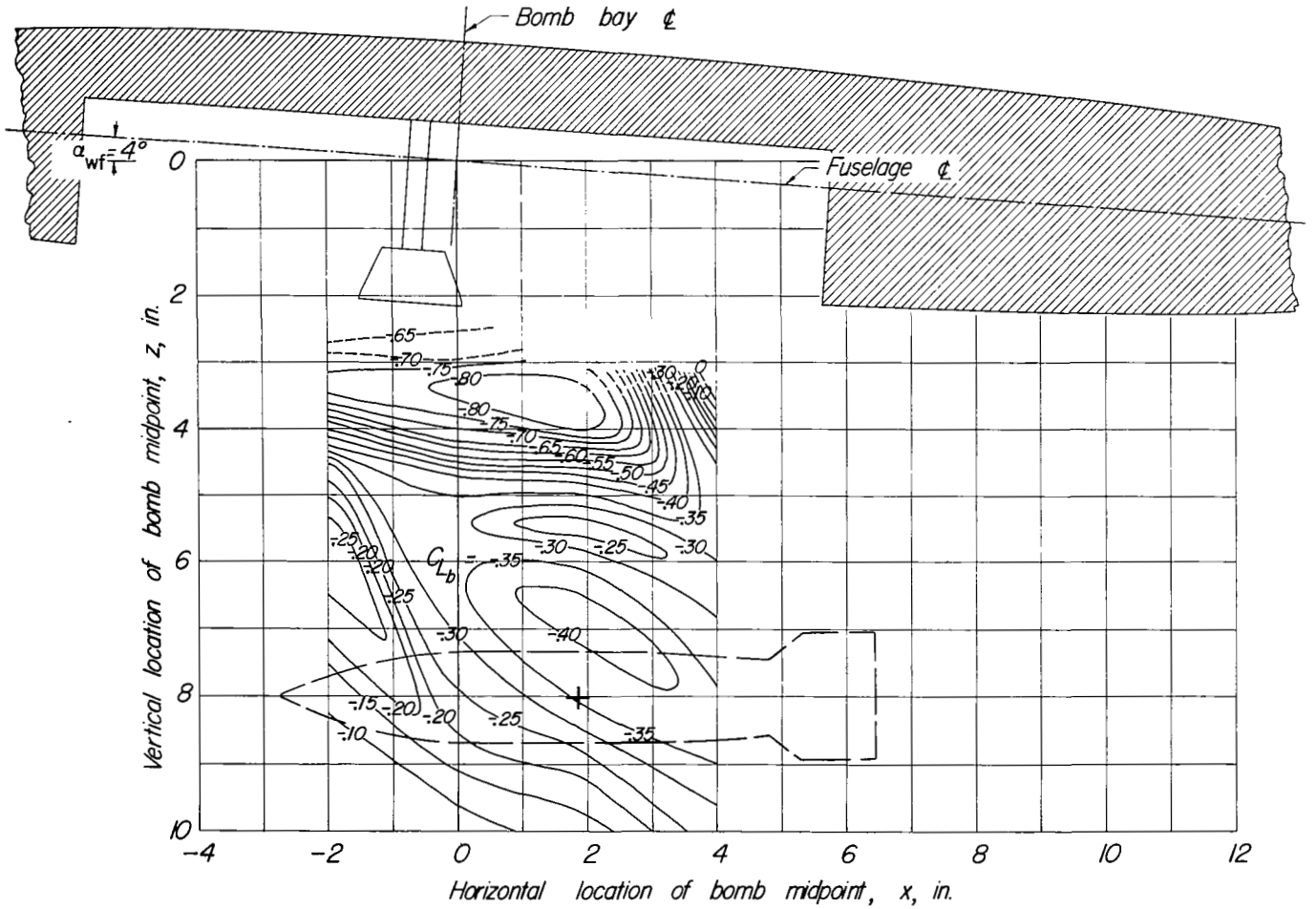

(b) Lift.

Figure 18.- Continued.

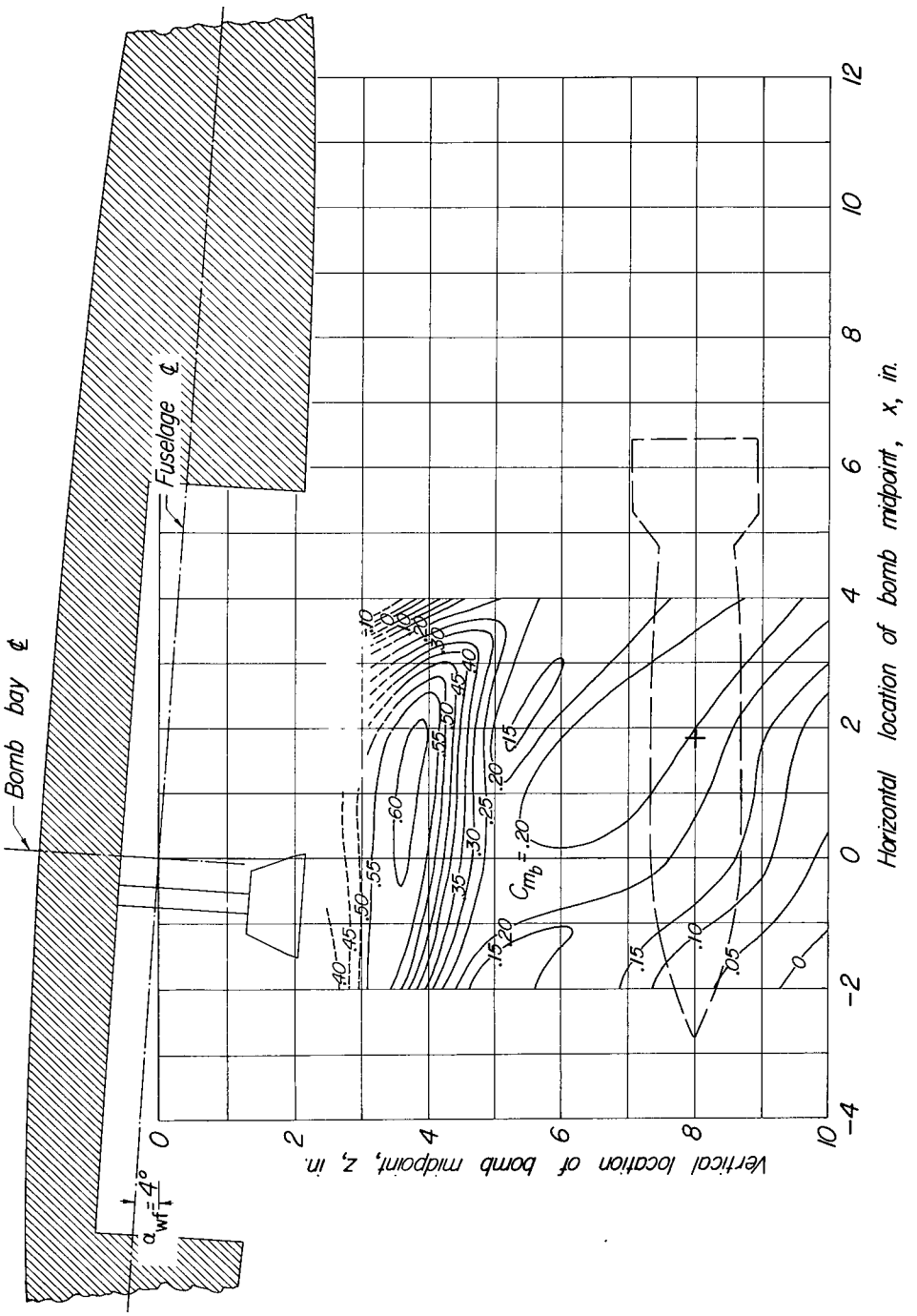

(c) Pitching moment.

Figure 18.- Concluded.

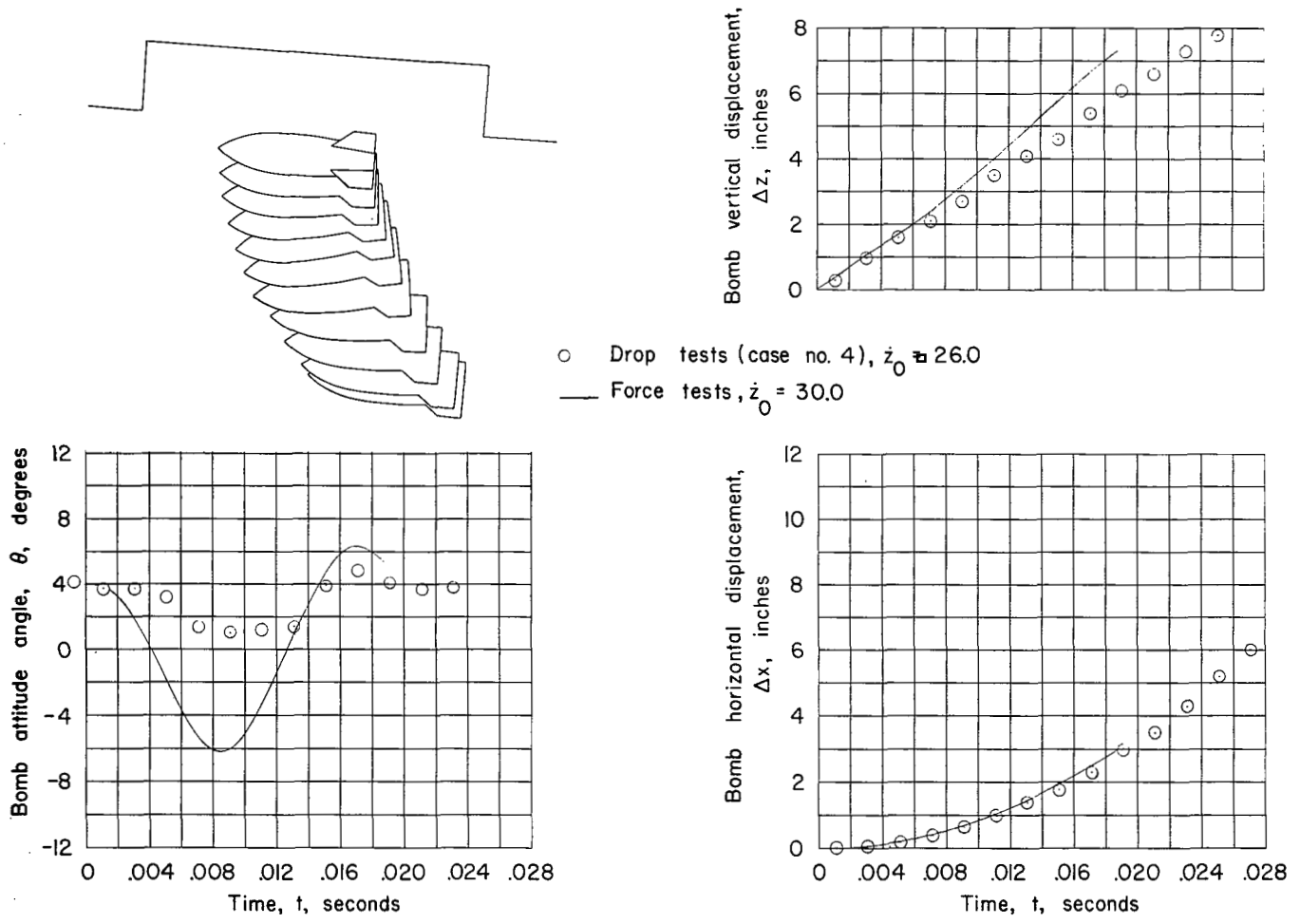

(a) Without ejector.

Figure 19.- Comparison of dynamic model drop with drops calculated from force data measured with and without an ejector in the bomb bay. Bomb 2 released with high ejection velocity.

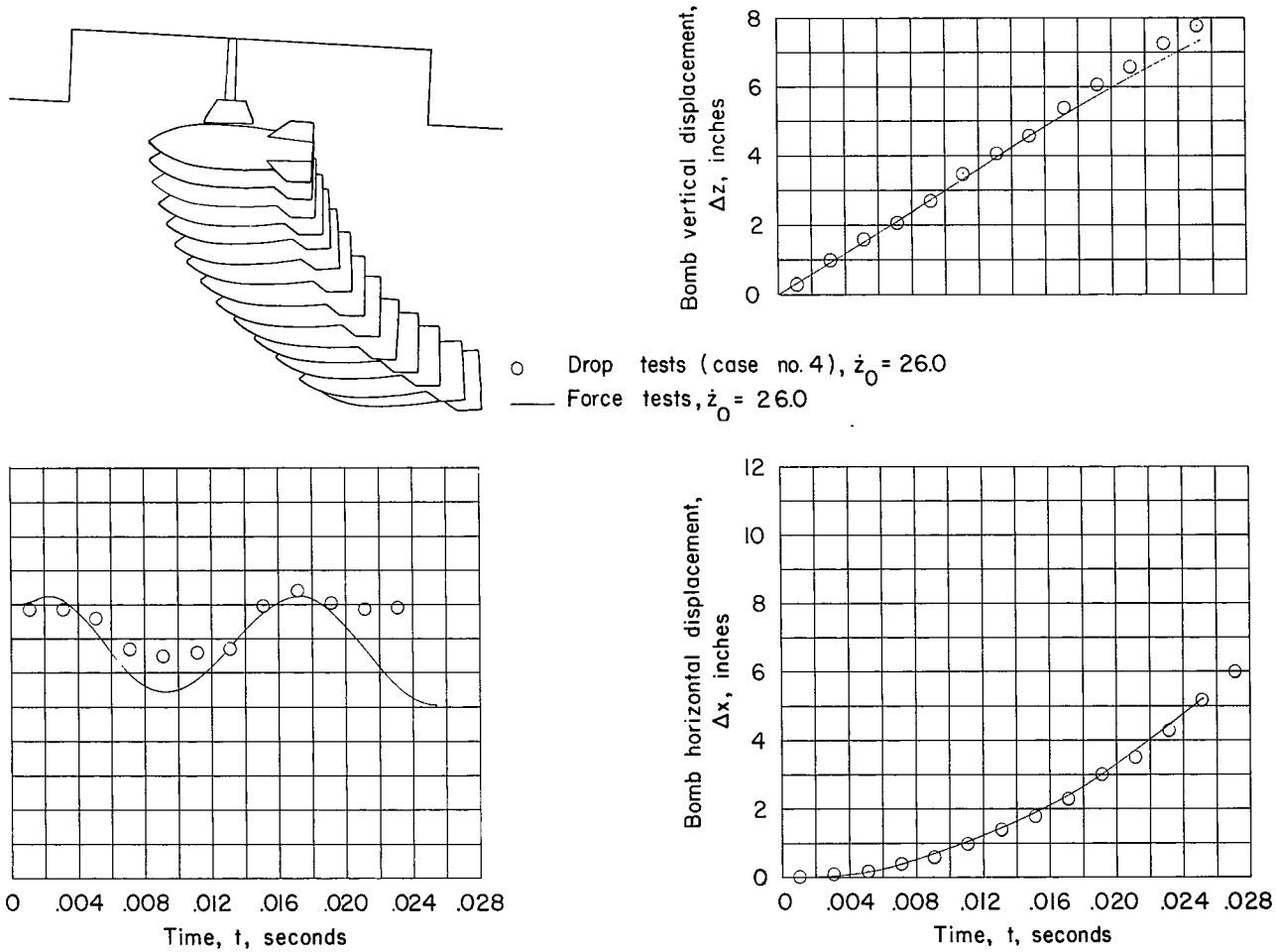

(b) With ejector.

Figure 19.- Concluded.

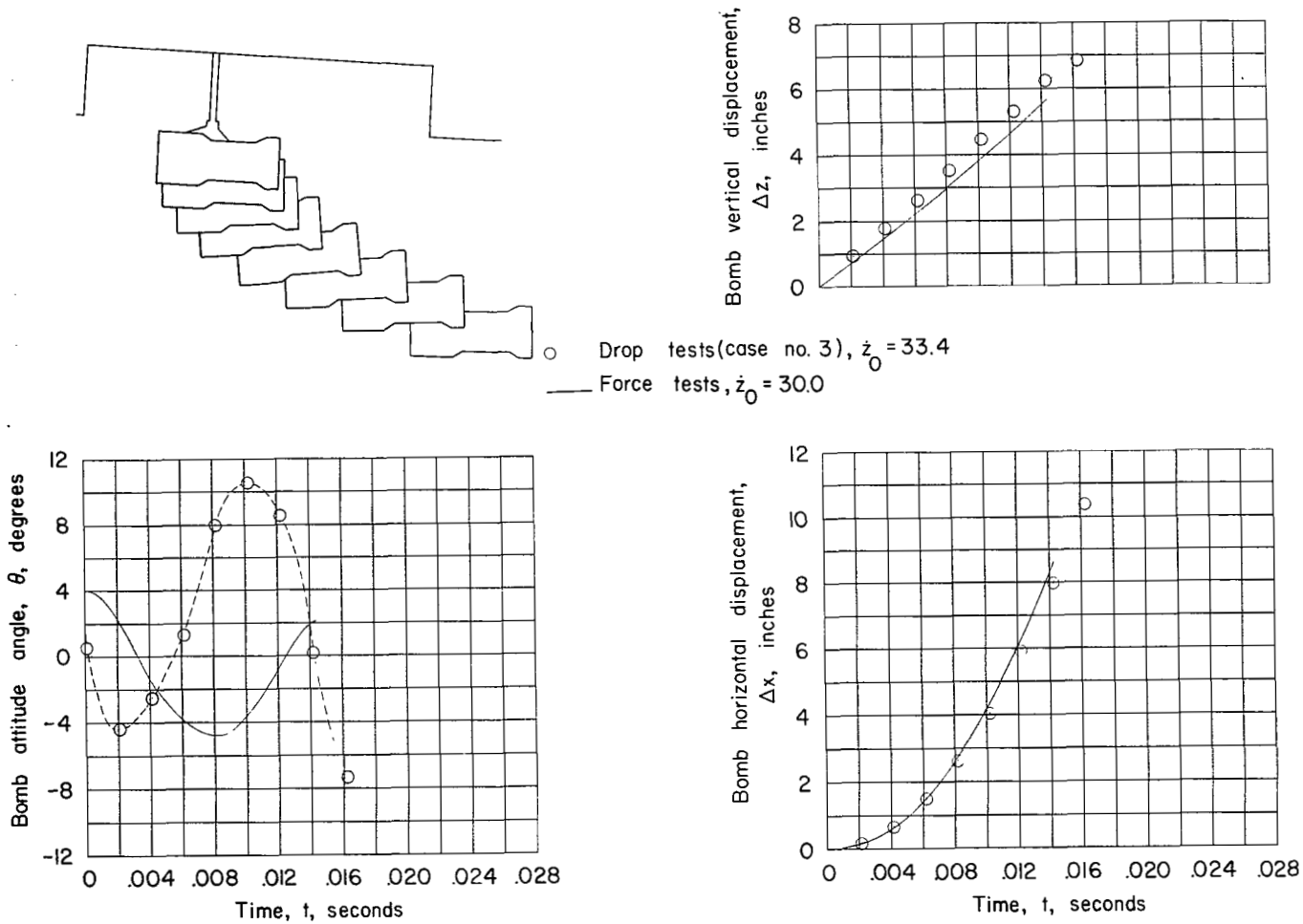

(a) Nominal initial conditions specified for drop tests.

Figure 20.- Effect of initial release conditions on the correlation of calculated drops with dynamic model drops for bomb 1 released with high ejection velocity.

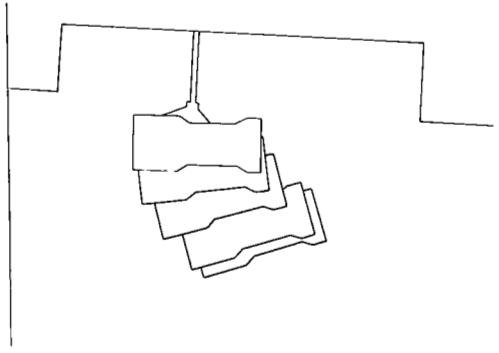

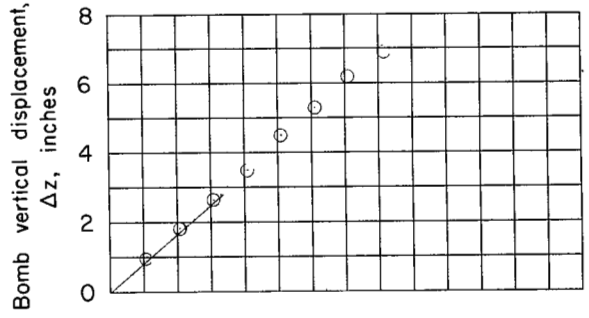

○ Drop tests (case no. 3), $\dot{z}_0 = 33.4$

— Force tests, $\dot{z}_0 = 33.4$

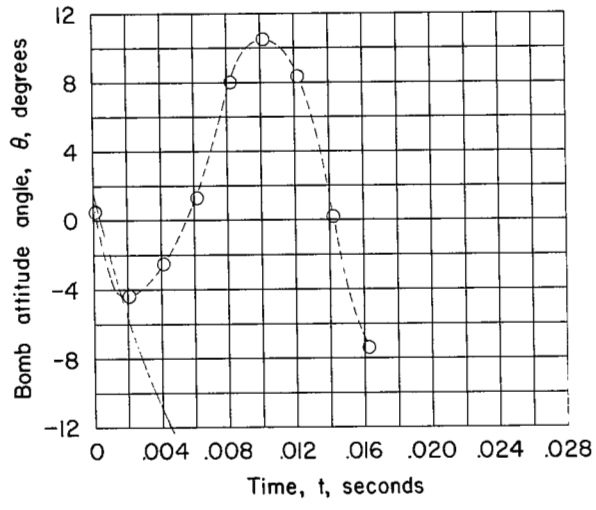

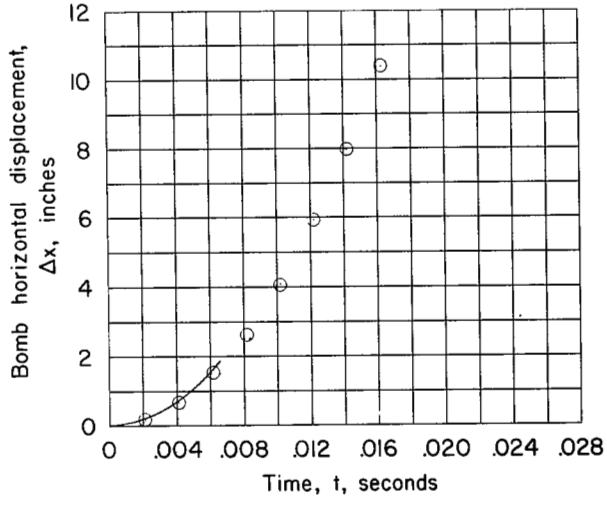

(b) Actual initial conditions derived from results of single drop test.

Figure 20.- Continued.

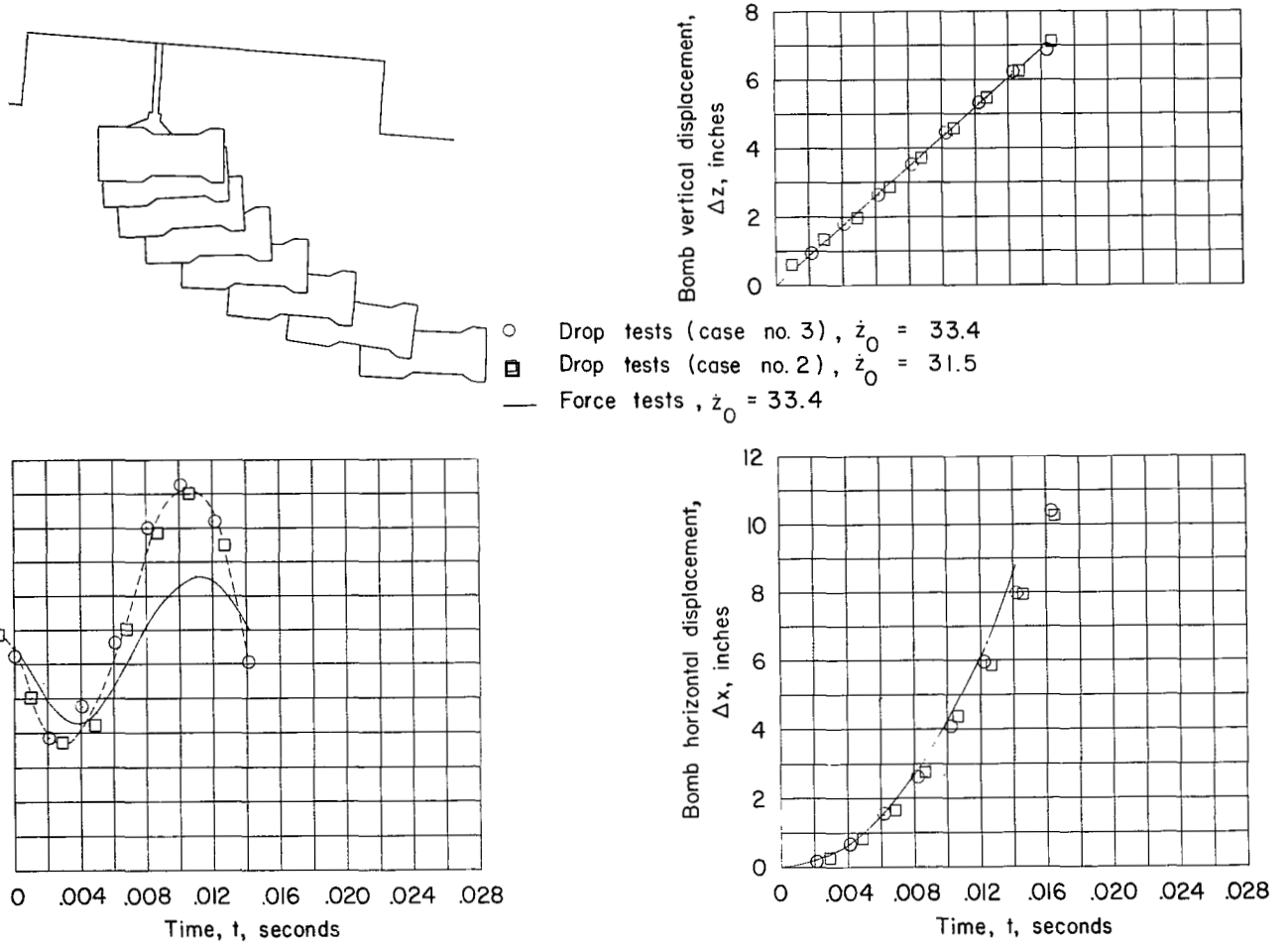

(c) Actual initial conditions derived from results of two drop tests.

Figure 20.- Concluded.

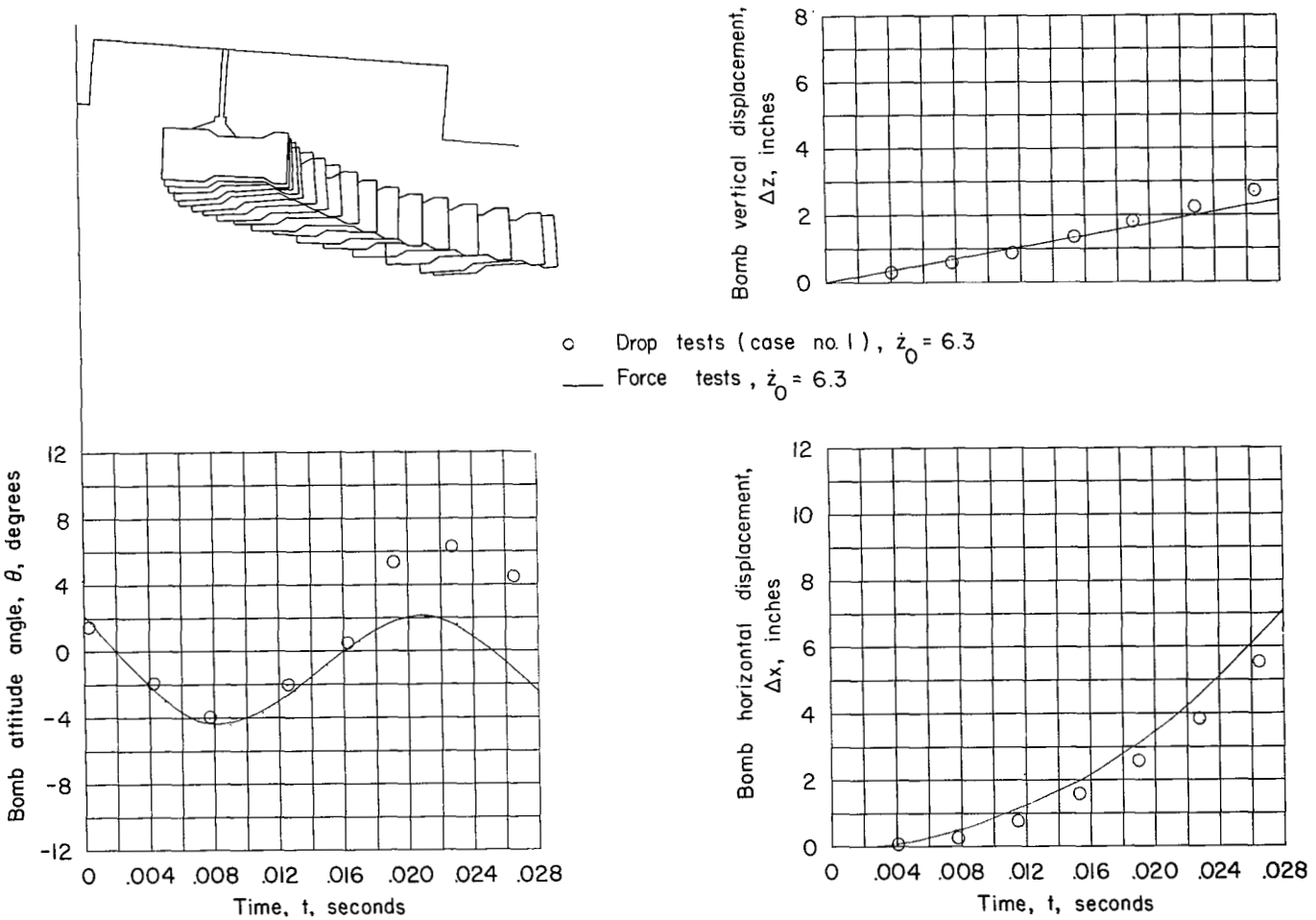

Figure 21.- Comparison of calculated drops with dynamic model drops for bomb 1 released with low ejection velocity of 6.3 feet per second.

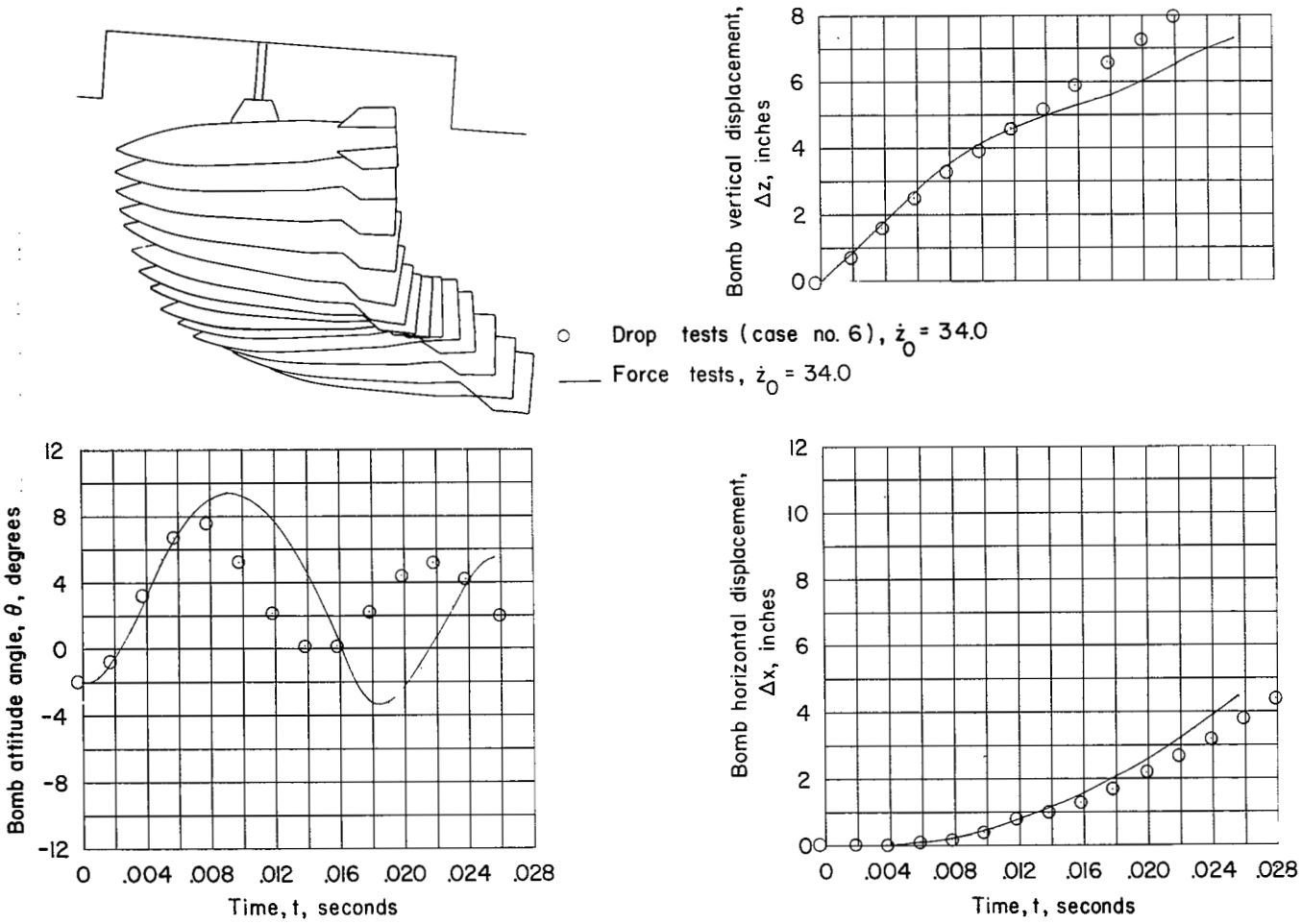

Figure 22.- Comparison of calculated drops with dynamic model drops for bomb 3 released with high ejection velocity of 36 feet per second.

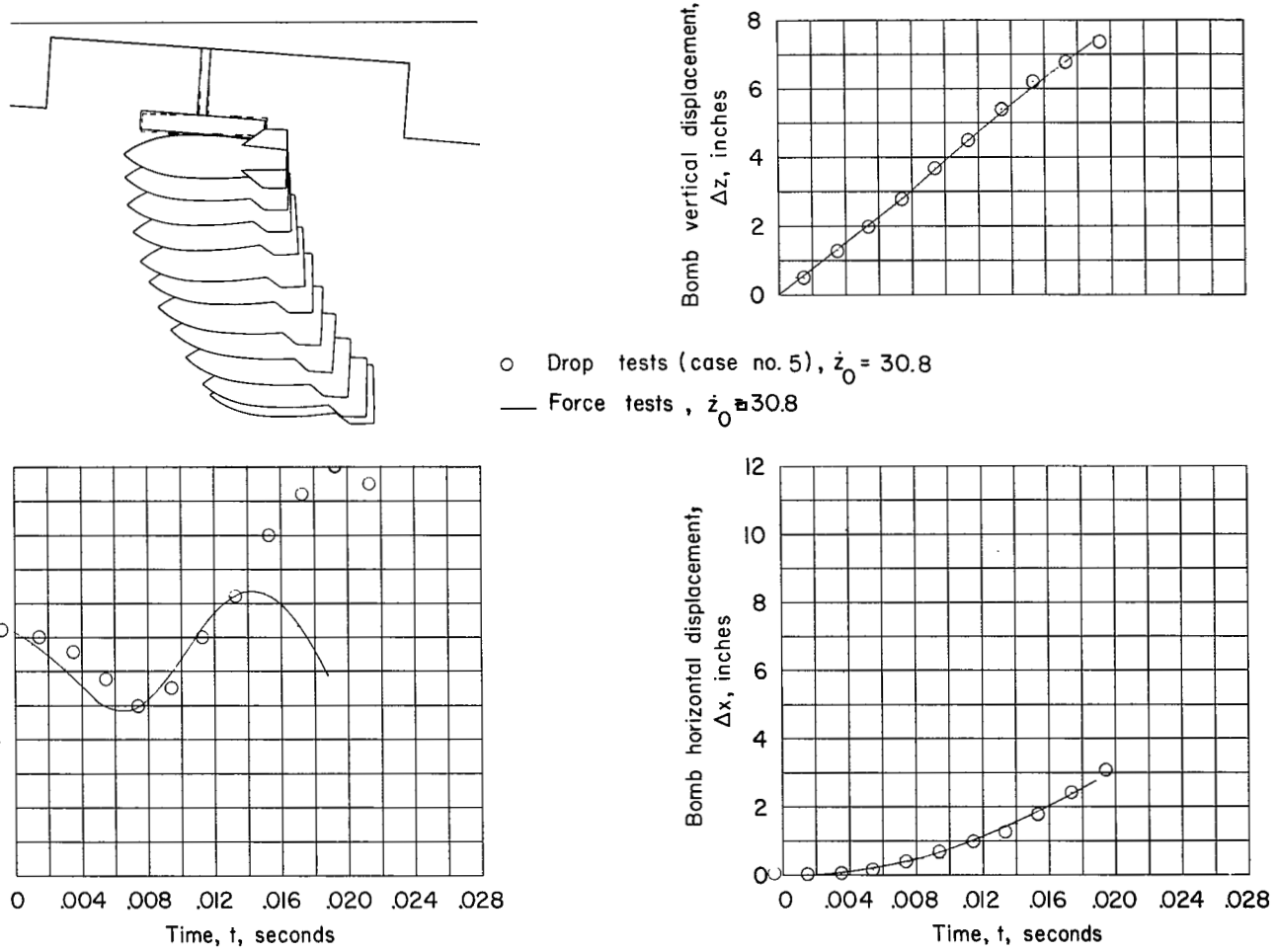

Figure 23.- Comparison of calculated drops with dynamic model drops for bomb 2 released with high ejection velocity from a streamlined ejector.

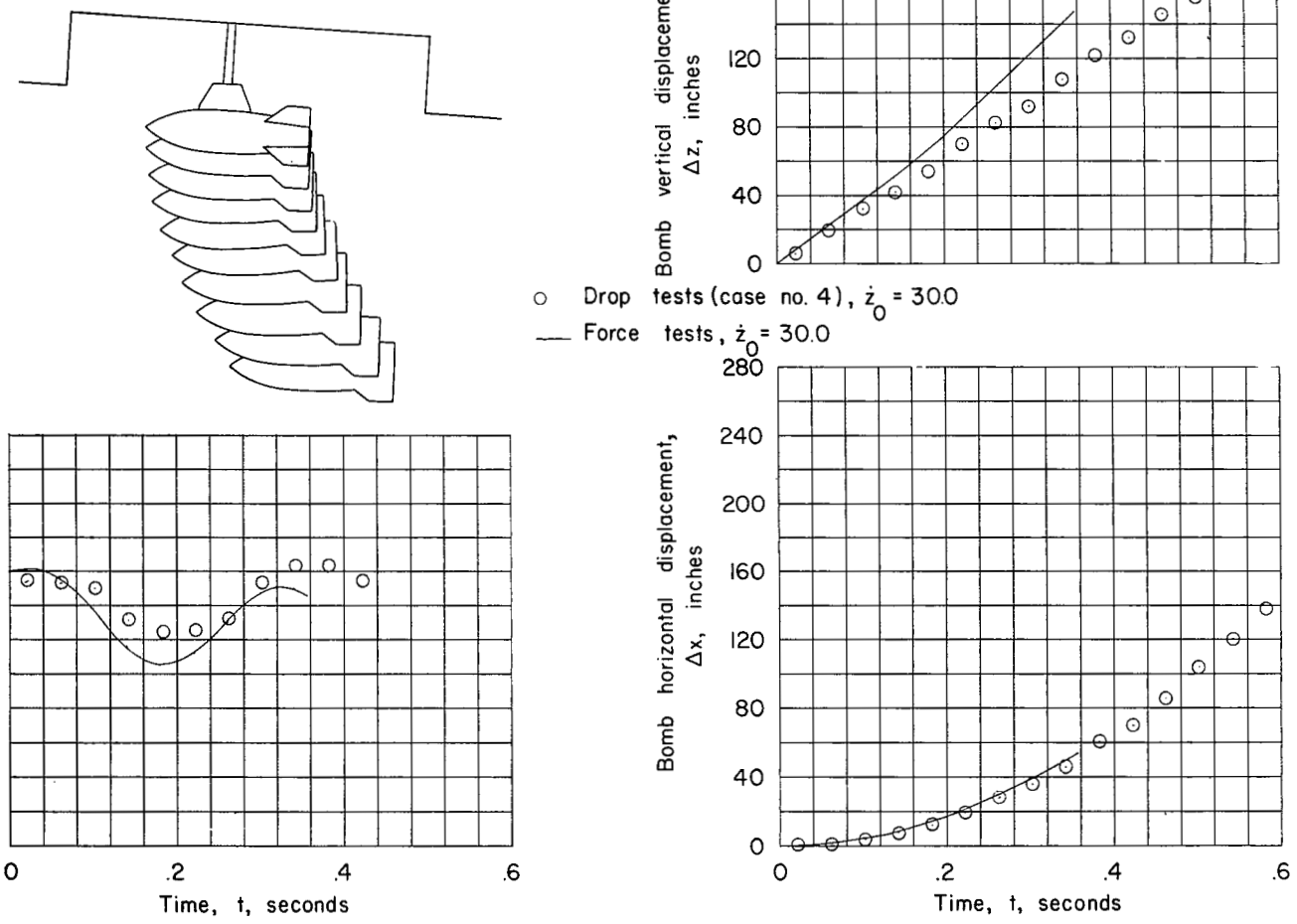

(a) 1,000-pound bomb; 30,000 feet; p = 8.880 lb/sq in. abs.

Figure 24.- Comparison of calculated full-scale drops with scaled dynamic model drops for bomb 2 released with high ejection velocity.

(b) 2,000-pound bomb; 14,000 feet; p = 17.57 lb/sq in. abs.

Figure 24.- Continued.

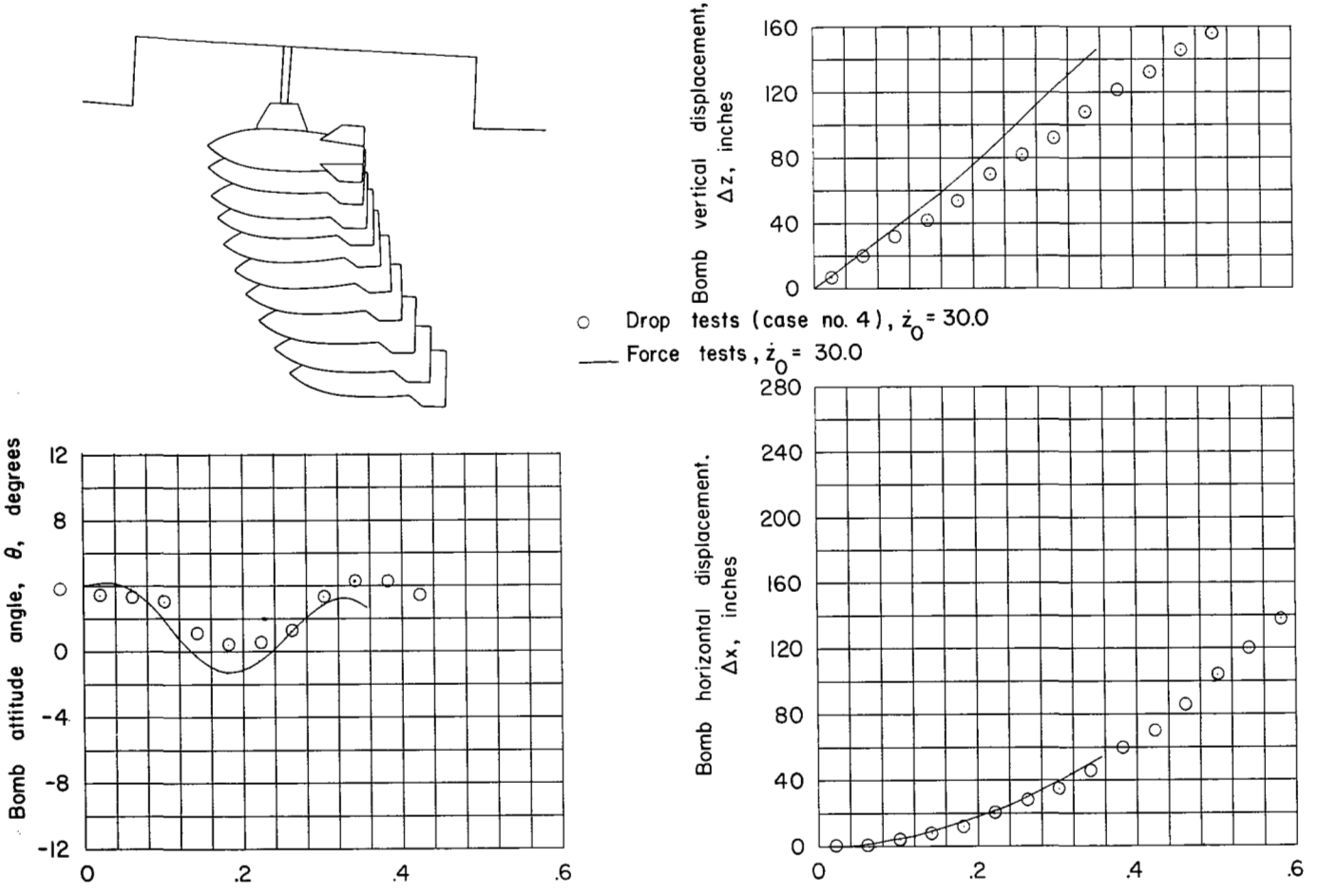

(c) 3,000-pound bomb; 3,000 feet; p = 26.33 lb/sq in. abs.

Figure 24.- Concluded.